NACA TN 3208

NATIONAL ADVISORY COMMITTEE FOR AERONAUTICS

TECHNICAL NOTE 3208

HEAT, MASS, AND MOMENTUM TRANSFER FOR FLOW OVER A FLAT PLATE WITH BLOWING OR SUCTION

By H. S. Mickley, R. C. Ross, A. L. Squyers, and W. E. Stewart

Massachusetts Institute of Technology

NACA

Washington

July 1954

ERRATUM

NACA TECHNICAL NOTE 3208

By H. S. Mickley, R. C. Ross, A. L. Squyers,
and W. E. Stewart
July 1954

Since TN 3208 was published, additional work by Professor Mickley with the same equipment as used for the tests reported therein established that significant errors were present in the experimental work as reported.

For this test program, a woven fiberglas-nichrome wire heater cloth was attached directly to the back side of the porous test wall in order to insure exact and known temperature profiles for the injected air. As best as can be determined, this heating layer became separated from the porous wall while the tunnel was being moved. The data obtained during this period were not in complete agreement with the data obtained by other investigators; however, these data were consistent, and since all logical sources of error had been checked there was no reason to suspect erroneous test results. The trouble was finally located following unsuccessful efforts to obtain proper mass balances in the main stream when helium was injected through the porous wall. Careful checks of the flow in the boundary layer then indicated that the flow velocity was not approaching zero at the wall but rather at some point some 0.07 inch behind the surface of the porous wall. Although the wall was only 0.04 inch thick and the air space between the heater cloth and the wall was not over 0.03 inch, it is apparent that there was sufficient longitudinal flow behind the porous wall to invalidate all test results obtained between the time the tunnel was moved and the time the gap was discovered. After this trouble was discovered, the heater cloth was removed and the air cavity behind the porous wall was filled with very fine glass beads. This eliminated all trouble and the boundary layer behaved properly with no indication of flow within or behind the wall.

It appears that the local friction coefficients reported in TN 3208 were 15 to 30 percent higher than correct values and that, in general, the experimental data presented in this report should not be used. There is no reason, however, to doubt the validity of the theoretical analysis included in this report.

The correct experimental data will be reported in a later paper.

NACA - Langley Field, Va.

TABLE OF CONTENTS

NATIONAL ADVISORY COMMITTEE FOR AERONAUTICS

TECHNICAL NOTE 3208

HEAT, MASS, AND MOMENTUM TRANSFER FOR FLOW OVER A FLAT PLATE WITH BLOWING OR SUCTION

By H. S. Mickley, R. C. Ross, A. L. Squyers, and W. E. Stewart

SUMMARY

The effect on the boundary layer of sucking or blowing air through a porous flat plate into or out of a main air stream flowing parallel to the plate was studied theoretically and experimentally.

Laminar-boundary-layer theory was used to calculate velocity, temperature, and concentration profiles and friction, heat, and mass transfer coefficients as a function of the Prandtl or Schmidt modulus and the mass transfer rate for the case of laminar, zero Euler number flow with a mass transfer rate varying as $1/\sqrt{x}$, where x is the axial distance from the leading edge of the plate. For turbulent flow film theory was expanded to provide a prediction of the effect of mass transfer on the friction, heat, and mass transfer coefficients.

Experimental measurements of velocity and temperature profiles and of friction and heat transfer coefficients were carried out over a range of flow conditions. Main-stream velocity was varied between 5 and 60 fps, a length Reynolds number range of 6,500 to 3,300,000 was covered, and the mass transfer velocity ranged from -0.3 to 0.26 fps and included constant axial mass transfer velocity and $1/\sqrt{x}$ and $1/x^{0.2}$ distributions. One test was made with a positive Euler number; all other results apply to zero Euler number flow.

INTRODUCTION

The Massachusetts Institute of Technology has completed one phase of a theoretical and experimental study of the effect of the bulk exchange of material between a fluid stream and its boundaries on the fluid boundary layer. This report covers the work carried out under the sponsorship and with the financial assistance of the National Advisory Committee for Aeronautics and a coordinated parallel program supported by industrial fellowships.

When mass crosses a boundary layer in a direction perpendicular to the main motion of the fluid, the magnitude and direction of the mass transfer affect the properties of the boundary layer. The boundary-layer thickness and stability and the velocity, temperature, and concentration profiles are altered. At the same time, the heat, mass, and momentum transfer coefficients are changed. In general, mass transfer from the fluid to the wall ("suction") increases the magnitude of the transfer coefficients, while mass transfer from the wall to the fluid ("blowing") decreases the magnitude of the transfer coefficients. The exploitation of these effects has important applications to the cooling of gas-turbine blades, the development of high-lift airfoils, the improvement of certain atomic-energy processes, and in the industrially important techniques of drying, absorption, extraction, distillation, and adsorption.

The effects of mass transfer on the various transfer coefficients have been predicted by many investigators. Stefan (ref. 1), Lewis and Chang (ref. 2), Sherwood (ref. 3), Colburn and Drew (ref. 4), and others have integrated the Stefan-Maxwell diffusion equations for various cases of mass transfer through a one-dimensional film of fluid, obtaining results which indicate that the mass transfer coefficient as ordinarily defined is a function of the rate of mass transfer. Ackermann (ref. 5), Colburn and Drew (ref. 4), and Friedman (ref. 6) have presented one-dimensional treatments of heat transfer in the presence of mass transfer and predicted analogous relations for the heat transfer coefficient as a function of the rate of mass transfer.

Various results of mass transfer have been investigated theoretically for the case of laminar flow over flat plates and airfoils, using aerodynamic boundary-layer theory. The effect of mass transfer on fluid flow has been treated by Prandtl (ref. 7), Griffith and Meredith (unpublished note; see ref. 8), Damkohler (ref. 9), Schlichting and Bussmann (ref. 10), Schlichting (refs. 11 and 12), Schuh (ref. 13), Thwaites (ref. 14), Yuan (ref. 15), Eckert and Lieblein (ref. 16), Ulrich (ref. 17), Lew (ref. 18), Ringleb (ref. 19), Iglisch (ref. 20), and Brown and Donoughe (ref. 21). The effect on heat transfer has been studied by Yuan (ref. 15), Lew (ref. 18), and Brown and Donoughe (ref. 21). The effect on diffusion has been studied by Eckert and Lieblein (ref. 16) and Schuh (ref. 13).

Experimental measurements of the effect of mass transfer on laminar flat-plate velocity profiles have been reported by Libby, Kaufman, and Harrington (ref. 22) and measurements of the cooling obtained by the injection of a fluid through the porous wall of a round tube and into a hot gas stream have been made by Duwez and Wheeler (ref. 23).

The publications of Colburn and Drew (ref. 4), Blasius (ref. 24), Pohlhausen (ref. 25), Schlichting and Bussmann (ref. 10), Iglish

(ref. 20), Brown and Donoughe (ref. 21), and Libby, Kaufman, and Harrington (ref. 22) are particularly pertinent to the present study. The treatment of film theory given here is an extension of the development of Colburn and Drew (ref. 4). The work of Blasius, Pohlhausen, and Schlichting and Bussmann forms the basis for the boundary-layer treatment presented in this report. Subsequent to the completion of the theoretical calculations reported here, Brown and Donoughe (ref. 21) have published tables giving the effect of a suction or blowing velocity which varies as $x^{\frac{Eu-1}{2}}$ on the velocity and temperature profiles of the laminar boundary layer. Their work includes the effect of a pressure gradient and variation in the fluid properties due to temperature gradients when the fluid is air.

Iglisch (ref. 20) has calculated the laminar velocity profiles and friction factors which result from the application of a uniform suction velocity normal to a flat plate. His results have been compared with the experimental measurements of this investigation.

Libby, Kaufman, and Harrington (ref. 22) have carried out an experimental study of the isothermal laminar velocity boundary layer on a porous flat plate with uniform suction or blowing. They measured laminar velocity profiles and determined the transition Reynolds numbers for various rates of suction and blowing. They compared their measured laminar velocity profiles with those predicted by Yuan (ref. 15) and found good agreement. The Reynolds number at which transition to turbulent flow began was found to be a pronounced function of the injection rate. At a blowing rate of $v_o/u_1 = 0.008$, transition occurred at $R_x \approx 50{,}000$. The transition Reynolds number gradually increased as the blowing rate decreased, reaching a value of $R_x \approx 70{,}000$ at $v_o/u_1 = 0.001$, and then rose sharply, passing through $R_x \approx 150{,}000$ at $v_o/u_1 = 0$ and going to $R_x \approx 300{,}000$ at very low suction rates. The values of transition Reynolds numbers are the only measurements reported by Libby, Kaufman, and Harrington (ref. 22) in the turbulent region.

In this work two theoretical approaches have been used. The first, designated "film theory," predicts transfer coefficients under mass transfer conditions from known (by experimental observation or theory) coefficients in the absence of mass transfer. This method is of general application but rests on crude physical assumptions and is to be considered primarily as a qualitative guide in correlating data and in treating cases not amenable to more exact analysis. The second approach, designated "boundary-layer theory," consists of exact numerical solution of Prandtl's equations for the laminar boundary layer with uniform fluid properties under certain restricted conditions of mass transfer, to yield not only transfer coefficients but also velocity, temperature, and concentration profiles in the boundary layer for a range of Prandtl or Schmidt numbers.

The experimental program was designed to test the theory and to investigate cases where theoretical analysis is not possible. A wind tunnel was constructed to simulate the boundary conditions of the theoretical analysis but with sufficient flexibility to investigate a range of conditions not considered in the theory.

The physical model used in both theory and experiment is a flat plate immersed in an infinite fluid.

This work was a cooperative effort of the Department of Chemical Engineering and the Gas Turbine Laboratory at M.I.T. The counsel and cooperation of the staff of both the Chemical Engineering Department and the Gas Turbine Laboratory were most helpful. Approximately one-half the funds expended were supplied by the National Advisory Committee for Aeronautics. The remainder of the financial support was in the form of graduate fellowships given to the junior authors and provided by the William S. Knudsen Memorial Fund, Standard Oil Co. of Indiana, Proctor & Gamble Co., Humble Oil & Refining Co., E. I. Du Pont de Nemours & Co., Inc., American Cyanamid Co., and Arthur D. Little, Inc.

The assistance of Messrs. John Feyk, Robert McMurtrie, John Forgrieve, David Dudley, David Hacker, and Sven Hultin was most helpful.

SYMBOLS

The units reported are those directly measured in the experimental work and do not necessarily give consistent results if used directly in the equations.

A	area of a panel of test wall surface, sq ft
C	dimensionless mass transfer parameter in laminar-boundary-layer theory, $\frac{-2v_o}{u_1}\sqrt{\frac{u_1 x \rho}{\mu}}$
c_f	friction coefficient, $\frac{2\tau_o}{\rho_1 u_1^2}$
c_p	specific heat at constant pressure, Btu/(lb)($^\circ$F)
D_{im}	diffusivity of species i through mixture, sq ft/sec

Eu	Euler number, $\frac{-x\frac{dP}{dx}}{\rho_1 u_1^2}$
f	dimensionless stream function, $\frac{\psi}{\sqrt{\frac{u_1 x \mu}{\rho}}}$
f',f'',f'''	derivatives of f with respect to η
g	local acceleration due to gravity, ft/sec^2
H	height above a datum plane, ft
h	local heat transfer coefficient, $\frac{(q/A)_o}{T_o - T_1}$, Btu/(hr)(sq ft)(^{o}F)
K_i	mass transfer coefficient, moles/(hr)(sq ft)(unit mole fraction change)
k	thermal conductivity, Btu/(hr)(ft)(^{o}F)
l	dimensionless number
M	molecular weight
m	dimensionless y-coordinate defined by equations (17)
N	total mass transfer intensity, summed over all molecular species, moles/(hr)(sq ft)
N_i	mass transfer intensity for species i, from wall into fluid, moles/(hr)(sq ft)
P	static pressure, in. Hg
Pr	Prandtl number
q	rate of heat flow, Btu/hr
R	resistance factor defined by equation (28) and figure 2
R_x	Reynolds number, $u_1 x\rho/\mu$ for test surface
T	temperature, ^{o}F

u local velocity parallel to plate, fps

u_1 main-stream velocity parallel to plate, fps

v local velocity normal to plate, fps

W air flow rate through a test-wall panel, lb/hr

X_i mole fraction of species i

x distance downstream from leading edge of plate measured parallel to plate, in.

y normal distance from plate, in.

Z dimensionless physical property group; 1 for momentum transfer, $c_p\mu/k$ for heat transfer, and $\mu/\rho D_{im}$ for mass transfer

z coordinate normal to x- and y-coordinates, in.

β generalized profile factor; $\beta_F = u/u_1$, $\beta_H = \frac{T_o - T}{T_o - T_1}$, and $\beta_D = \frac{X_{io} - X_i}{X_{io} - X_{il}}$

Γ dimensionless measure of mass transfer rate, defined by equations (16); related to ϕ by equations (23b)

Δ "film thickness" for a given transfer process, in.

δ^* displacement thickness of boundary layer, in.

η dimensionless coordinate in laminar-boundary-layer theory, $\frac{y}{2x}\sqrt{R_x}$

θ correction factor for transfer coefficients

ϑ momentum thickness of boundary layer, in.

ϑ' momentum thickness corrected for mass blown or sucked through wall, in.

μ absolute viscosity, lb/(sec)(ft)

ν	kinematic viscosity, μ/ρ, sq ft/sec
ξ	enthalpy thickness of boundary layer, in.
ξ'	enthalpy thickness corrected for mass blown or sucked through wall, in.
ρ	fluid density, lb/cu ft
τ_o	shear stress at wall, poundals/sq ft
ϕ	dimensionless mass tranfer rate, defined by equations (23b) and in figures 1 and 2
ψ	stream function, $d\psi = u\,dy - v\,dx$

Subscripts:

B	conditions at a baffle behind test wall
D	process of diffusion
E	electrical
F	friction or momentum transfer
H	heat transfer
i	species i in a diffusing system
L	laminar
m	all species excluding i in a diffusing system
o	wall conditions
T	turbulent
1	main-stream conditions
*	conditions in absence of mass transfer

THEORETICAL STUDIES

This investigation has used two types of theoretical analyses to predict the effect of mass transfer on the properties of the boundary

layer: The generalized, approximate method known as film theory and the more exact procedures of laminar-boundary-layer theory. The basis of the methods, the solutions obtained, and the manner of combining and editing results are discussed in the following sections.

The boundary-layer-theory solutions apply to the case of laminar flow over a plane surface; the film-theory solutions apply to a surface of unspecified shape, except that the radii of curvature of the surface must greatly exceed the film thickness. In both cases the following equations for transfer coefficients are applicable at a point on the boundary if y is taken to be the perpendicular distance from the boundary and x is measured in the downstream direction parallel to the boundary. The fluid velocity components in the x- and y-directions are u and v, respectively, the fluid temperature is T, and the mole fraction of chemical species i is X_i. The local friction coefficient, including skin friction only, is

$$c_f = \frac{2\tau_o}{\rho_1 u_1^2} \tag{1}$$

$$\frac{c_f}{2} = \frac{\mu\left(\frac{\partial u}{\partial y}\right)_o}{\rho_1 u_1^2} \tag{1a}$$

The local heat transfer coefficient, including only heat transferred to the fluid at the wall by conduction, is

$$h = \frac{(dq/dA)_o}{T_o - T_1} \tag{2}$$

$$h = -\frac{k\left(\frac{\partial T}{\partial y}\right)_o}{T_o - T_1} \tag{2a}$$

The mass transfer coefficient for a given chemical species is defined in terms of the rate of diffusion of that species at the wall:

$$K_i = \frac{N_i - X_{io}\sum_j N_j}{X_{io} - X_{il}} \tag{3}$$

$$K_i = - \frac{\frac{\rho D_{im}}{M}\left(\frac{\partial X_i}{\partial y}\right)_o}{X_{io} - X_{il}} \tag{3a}$$

where the subscripts o and 1 refer to wall conditions and mainstream conditions, respectively. It will be noted that the values of the driving forces u_1, $T_o - T_1$, and $X_{io} - X_{il}$ are the "maximum," or over-all, driving forces for the single-fluid phase under consideration, not the "bulk" driving forces commonly used for flow in closed channels; allowance for this difference is necessary when applying mass transfer corrections to coefficients based on bulk driving forces.

The diffusivity D_{im} for component i in a multicomponent mixture is defined for diffusion in the y-direction by the equation

$$N_i = - \frac{\rho D_{im}}{M} \frac{\partial X_i}{\partial y} + X_i \sum_j N_j \tag{4}$$

Equations for calculating D_{im} for gas mixtures are given by Wilke (ref. 26) and by one of the present authors; the equations

$$D_{im} = D_{12} \qquad \text{(exact for binary mixtures)} \tag{4a}$$

$$D_{im} = \frac{1 - X_i}{\sum_{j \neq i} \frac{X_j}{D_{ij}}} \qquad \text{(exact when all components except i move in unison)} \tag{4b}$$

and

$$D_{im} = \frac{D_{13}D_{12}(1 - X_1) - X_1 D_{12} D_{23} \frac{dX_2}{dX_1} - X_1 D_{13} D_{23} \frac{dX_3}{dX_1}}{X_1 D_{23} + X_2 D_{13} + X_3 D_{12}} \tag{4c}$$

which is exact for ternary mixtures[1] are recommended. Equations for D_{2m} and D_{3m} follow from equation (4c) by rotation of subscripts. These equations give the value of D_{im} at a point; satisfactory mean values for one-dimensional diffusion are obtained by using average

---

[1]Unpublished analysis by W. E. Stewart.

mole fractions, and using the ratios of mole-fraction driving forces $X_o - X_l$ in place of the ratios of the corresponding mole-fraction gradients. The term "exact" here refers to results obtained directly from the Stefan-Maxwell diffusion equations, which are very nearly exact for ideal gases, as shown by the recent work of Curtiss and Hirschfelder (ref. 27). The Stefan-Maxwell treatment assumes a preponderance of bimolecular collisions; in dense gases and liquids collisions of more than two molecules become important and the validity of equations (4b) and (4c) is in doubt.

Pending further investigation, it will be assumed that the effect of diffusion on the viscosity μ and thermal conductivity k is negligible. Momentum and energy transport are indeed affected by diffusion, but it is believed that this effect is adequately treated by adding the convective transport rates based on the mean velocity of each species present, as is done approximately in the present treatment. Equations for estimation of mixture viscosities in the absence of diffusion are given by Bromley and Wilke (ref. 28); equations for mixture thermal conductivities are given by Lindsay and Bromley (ref. 29).

For brevity, it is useful to represent the profiles of velocity, temperature, and mole fraction in dimensionless form. The dimensionless quantities

$$\left.\begin{aligned} \beta_F &= u/u_l \\ \beta_H &= \frac{T_o - T}{T_o - T_l} \\ \beta_D &= \frac{X_{io} - X_i}{X_{io} - X_{il}} \end{aligned}\right\} \tag{5}$$

reduce equations (1a), (2a), and (3a) to the analogous forms

$$\left.\begin{aligned} \frac{u_l \rho_l c_f}{2\mu} &= \left(\frac{\partial \beta_F}{\partial y}\right)_o \\ \frac{h}{k} &= \left(\frac{\partial \beta_H}{\partial y}\right)_o \\ \frac{K_i M}{D_{im}\rho} &= \left(\frac{\partial \beta_D}{\partial y}\right)_o \end{aligned}\right\} \tag{6}$$

The purpose of the following theoretical developments is to evaluate the derivatives appearing in equations (6) and, hence, to determine the transfer coefficients.

Film Theory

Film theory greatly simplifies the analytical treatment of a flow transport problem by means of an idealization which states that the transition between main-stream and wall conditions occurs entirely within a thin laminar film of thickness Δ lying immediately adjacent to the wall. The "effective film thickness" Δ is not predicted by the theory; rather, it is defined as the thickness of a laminar film of fluid which would offer the experimentally observed resistance to the transfer process. The film does not correspond to the boundary-layer concept of Prandtl; it is a much less realistic idealization.

The results of film theory, based on a crude physical picture, can be accepted only qualitatively. However, certain useful parameters have been suggested by the theory, and the analysis can be applied to cases too complex for a more refined treatment.

Consider a fluid in steady laminar motion, or statistically steady turbulent motion over a surface of moderate curvature along which the fluid does not slip and the temperature and fluid composition are reasonably constant. In conformity with the convention previously given, take the y-axis perpendicular to the wall at the given point and the x-axis parallel to the surface and pointing downstream. At a differential distance from the boundary, the state of the stagnant fluid film is governed by the following equations:

$$\frac{\partial}{\partial y}(v_i \rho_i) = 0 \tag{7}$$

$$\frac{\partial u}{\partial y} \sum_j \rho_j v_j + \frac{\partial P}{\partial x} + \rho g \frac{\partial H}{\partial x} = \frac{\partial}{\partial y}\left(\mu \frac{\partial u}{\partial y}\right) \tag{8}$$

$$\frac{\partial T}{\partial y} \sum_j \rho_j v_j c_{p_j} = \frac{\partial}{\partial y}\left(k \frac{\partial T}{\partial y}\right) + \mu \left[\frac{4}{3}\left(\frac{\partial v}{\partial y}\right)^2 + \left(\frac{\partial u}{\partial y}\right)^2\right] \tag{9}$$

$$\frac{\partial X_i}{\partial y} \sum_j \frac{\rho_j v_j}{M_j} = \frac{\partial}{\partial y}\left(\frac{\rho D_{im}}{M} \frac{\partial X_i}{\partial y}\right) \tag{10}$$

Equation (7) is a material balance for any species in the fluid, assuming steady state and no chemical reaction and noting that the tangential velocity of the fluid is negligible near the wall; the same assumptions are also involved in the other three equations. Equation (8) is a balance of forces acting on the fluid in the x-direction and includes inertial force, pressure gradient, gravitational force, and viscous forces, respectively. The force balances for the y- and z-directions indicate only that hydrostatic equilibrium is closely approached in those directions. Equation (9) is an energy balance, including energy transport by the average motion of each molecular species and by molecular motion, and the heating of the fluid by internal dissipation, but neglecting thermal diffusion effects and absorption or emission of radiant energy by the fluid. Equation (10) is a material balance combined with Fick's law as stated in equation (4).

Assuming the density ρ independent of x, neglecting internal friction, assuming μ, k, and $\rho D_{im}/M$ independent of y, and noting that the molal mass transfer rates are given by

$$N_i = \left(\frac{v_i \rho_i}{M_i}\right)_o \tag{11}$$

the above equations become

$$\frac{\partial N_i}{\partial y} = 0 \tag{12}$$

$$\frac{\partial u}{\partial y} \sum_j N_j M_j + \frac{\partial}{\partial x}(P + \rho g H) = \mu \frac{\partial^2 u}{\partial y^2} \tag{13}$$

$$\frac{\partial T}{\partial y} \sum_j N_j M_j c_{p_j} = k \frac{\partial^2 T}{\partial y^2} \tag{14}$$

$$\frac{\partial X_i}{\partial y} \sum_j N_j = \frac{\rho D_{im}}{M} \frac{\partial^2 X_i}{\partial y^2} \tag{15}$$

These are the basic differential equations of film theory, as used in the present work.

Applying equation (12) from $y = 0$ to $y = \Delta$ for each transfer process and for every species, the sums in equations (13), (14), and (15) are found to be independent of y along a given perpendicular to the wall. Also, $P + \rho gH$ is essentially constant (hydrostatic equilibrium prevails) in a plane of constant x. Equations (13), (14), and (15) therefore contain only u, T, X_i, x, and y as variables in a given physical situation and are readily integrated when x is held constant.

The solution to the system of equations (12) to (15) has been obtained for two cases: Flow without a pressure gradient and flow with a pressure gradient. Only the analysis for the zero-pressure-gradient case will be presented here. The finite-pressure-gradient case will be reported when experimental work involving finite Euler numbers is completed and available for comparison with theory.

If the variation of $P + \rho gH$ with the distance x downstream along the wall is neglected and if x and z are held constant, the substitutions

$$\left.\begin{aligned} \Gamma_F &= \frac{\Delta_F \sum_j N_j M_j}{\mu} \\ \Gamma_H &= \frac{\Delta_H \sum_j N_j M_j c_{p_j}}{k} \\ \Gamma_{Di} &= \frac{\Delta_{Di} \sum_j N_j}{\rho D_{im}/M} \end{aligned}\right\} \tag{16}$$

$$\left.\begin{aligned} m_F &= y/\Delta_F \\ m_H &= y/\Delta_H \\ m_{Di} &= y/\Delta_{Di} \end{aligned}\right\} \tag{17}$$

reduce equations (13), (14), and (15) to the single dimensionless equation

$$\Gamma\left(\frac{d\beta}{dm}\right) = \frac{d^2\beta}{dm^2} \tag{18}$$

with boundary conditions

$$\beta = 0 \quad \text{when} \quad m = 0 \tag{19}$$

and

$$\beta = 1 \quad \text{when} \quad m = 1 \tag{20}$$

Equation (20) is obtained from the assumption, already implied, that main-stream conditions prevail at the outer boundary of the film.

The Γ quantities are dimensionless measures of mass transfer rate; the m quantities are dimensionless y-coordinates.

Integrating equation (18) with the boundary conditions just given, the dimensionless velocity, temperature, and mole-fraction profiles are obtained in the form

$$\beta = \frac{e^{\Gamma m} - 1}{e^{\Gamma} - 1} \tag{21}$$

and the dimensionless gradients of these profiles at the boundary:

$$\left(\frac{d\beta}{dm}\right)_o = \frac{\Gamma}{e^{\Gamma} - 1} \tag{22}$$

These expressions reduce, in the limiting case of no mass transfer, to

$$\lim_{\Gamma \to 0} \quad \beta = m \tag{21a}$$

and

$$\lim_{\Gamma \to 0} \left(\frac{d\beta}{dm}\right)_o = \Delta_*\left(\frac{d\beta}{dy}\right)_{*_o} = 1 \tag{22a}$$

Equation (22a) provides a means for determining film thickness from transfer coefficients at zero mass transfer rate. Substituting this result in equations (6), there result

$$\left.\begin{aligned} \Delta_{*F} &= \frac{2\mu}{u_1 \rho_1 c_{f_*}} \\ \Delta_{*H} &= \frac{k}{h_*} \\ \Delta_{*Di} &= \frac{\rho D_{im}}{K_{*_i} M} \end{aligned}\right\} \tag{23a}$$

and, correspondingly, equations (16) become

$$\left.\begin{aligned} \left(\frac{\Delta_*}{\Delta}\,\Gamma\right)_F &= \frac{2\sum_j N_j M_j}{u_1 \rho_1 c_{f_*}} \equiv \phi_F \\ \left(\frac{\Delta_*}{\Delta}\,\Gamma\right)_H &= \frac{\sum_j N_j M_j c_{p_j}}{h_*} \equiv \phi_H \\ \left(\frac{\Delta_*}{\Delta}\,\Gamma\right)_{Di} &= \frac{\sum_j N_j}{K_{*_i}} \equiv \phi_{Di} \end{aligned}\right\} \tag{23b}$$

where the asterisks * indicate that these quantities are the limiting values for zero weighted mean mass transfer rate ($\Gamma = 0$) for the given transfer process. The quantity ϕ, defined by equations (23b), is more convenient to use in actual calculations and is introduced here to replace Γ.

The transfer coefficients for finite mass transfer rates are conveniently expressed in terms of correction factors θ by which the

coefficients c_{f_*}, h_*, and K_{*_i} must be multiplied to obtain the true coefficients:

$$\left.\begin{aligned} \theta_F &= c_f/c_{f_*} \\ \theta_H &= h/h_* \\ \theta_{Di} &= K_i/K_{*_i} \end{aligned}\right\} \tag{24}$$

Combining these definitions with equations (6), (22), and (22a),

$$\theta = \frac{(d\beta/dy)_o}{(d\beta/dy)_{*_o}} \tag{25}$$

or

$$\theta = \frac{\Gamma \frac{\Delta_*}{\Delta}}{e^{\Gamma} - 1} = \frac{\phi}{\left(\exp \frac{\phi\Delta}{\Delta_*}\right) - 1} \tag{26}$$

Film theory provides no information concerning the ratio of the effective film thicknesses, Δ/Δ_*. Presumably, Δ/Δ_* is a function of the mass transfer rate and distribution. Simple film theory is forced to ignore this possibility, however, and assumes that the ratio is unity. With this simplification, equation (26) becomes

$$\left.\begin{aligned} \theta &= \frac{\phi}{e^{\phi} - 1} \\ \Delta/\Delta_* &= 1 \end{aligned}\right\} \tag{27}$$

for

The variation of the transfer coefficients with the rate of mass transfer as predicted by simple film theory is given by equations (27)

and shown in figure 1. The predicted transfer coefficients show a wide variation with ϕ, increasing as ϕ becomes negative (i.e., when mass transfer occurs effectively toward the wall) and decreasing as ϕ becomes positive (i.e., when mass transfer occurs effectively away from the wall). The curve has no finite asymptotes,[2] and corrections of any magnitude may be encountered; in practice, these predicted corrections usually range from 0.5 to 2.0. Equations closely resembling equations (27) were given by Ackermann (ref. 5), Colburn and Drew (ref. 4), and Friedman (ref. 6).

If the rate of mass transfer is specified, the corrected rate coefficient may be obtained directly from figure 1. In other cases, however, the calculation of pertinent stream or boundary properties involves trial and error if only figure 1 is available. A typical trial-and-error situation is found in "transpiration cooling" where it is desired to maintain a specified wall temperature through the use of a coolant gas blown through the porous confining wall and into the main stream. Ordinarily, the main-stream conditions, the available coolant gas temperature, and the desired wall temperature are specified. The required flow of coolant through the wall is to be determined. The problem may be solved by the combination of appropriate energy balances and the relation supplied by figure 1 but involves iteration. In such circumstances, trial and error is eliminated if a new parameter, the dimensionless resistance factor R,

$$R = \phi/\theta \tag{28}$$

is used. If equation (28) is combined with equations (23b), (24), and (27), there result

$$\left.\begin{aligned} R_F &= \frac{2\sum_j N_j M_j}{u_1 \rho_1 c_f} \\ R_H &= \frac{\sum_j N_j M_j c_{p_j}}{h} = \frac{T_o - T_1}{T_s - T_o} \\ R_{Di} &= \frac{\sum_j N_j}{K_i} = \frac{X_{io} - X_{il}}{\frac{N_i}{\sum_j N_j} - X_{io}} \end{aligned}\right\} \tag{29}[3]$$

[2]However, as $\phi \to \infty$, $\theta \to 0$; as $\phi \to -\infty$, $\theta \to -\phi$. Any theory should satisfy these criteria and the film theory satisfactorily approaches the correct limiting conditions.

[3]This serves to define T_s. For injection cooling, T_s is the coolant temperature. The two expressions for R_H and R_{Di} are identities.

and

$$\phi = \log_e(R + 1) \tag{30}$$

Equation (30) is plotted in figure 2. The variation of θ with R is qualitatively similar to its variation with ϕ, since ϕ and R are of like sign and differ only by the factor θ. Equation (30) and figure 2 show that ϕ and R become equal in the limit as either of these quantities approaches zero.

Boundary-Layer Theory

When laminar flow occurs in systems of relatively simple geometry, boundary-layer theory may be used to calculate the velocity, temperature, and concentration profiles and the corresponding transfer coefficients. Although the concepts of boundary-layer theory invoke certain idealizations of the flow process, the theory represents a very close approximation to the actual physical situation. Consequently, theory and experiment may be expected to show excellent agreement when comparable situations exist.

In the application of boundary-layer theory presented here, the physical model used was the flow of a fluid over a flat plate. The calculations were further restricted to the case of uniform fluid properties, uniform velocity profile in the stream approaching the plate, zero axial pressure gradient, uniform wall temperature, and a blowing or suction velocity which varies as $1/\sqrt{x}$. The effects due to changes in the value of the main-stream Reynolds number, the blowing or suction velocity, and the Prandtl or Schmidt number of the fluid were investigated.

Although the analytical calculations could be extended to cover cases of nonuniform fluid properties, finite axial pressure gradient,[4] nonuniform wall temperature, alternate mass transfer distributions, and alternate flow geometries, this was not attempted in this work. The experimental equipment could be run under conditions which simulated closely the case studied analytically, and it was decided to determine the agreement between experiment and the theoretical results presented here and available in the literature before carrying out additional theoretical calculations.

The equations of Prandtl for the laminar boundary layer on a flat plate without pressure gradient or variation in fluid properties take the forms:

---

[4]The constant-property, constant Euler number calculations of Brown and Donoughe (ref. 21) can be expanded readily to include a range of Prandtl or Schmidt numbers if the quantity Z in the analytical solution used here is replaced by $Z(Eu + 1)$.

Total mass balance:

$$\frac{\partial u}{\partial x} + \frac{\partial v}{\partial y} = 0 \tag{31}$$

Momentum balance in x-direction:

$$u \frac{\partial u}{\partial x} + v \frac{\partial u}{\partial y} = \frac{\mu}{\rho} \frac{\partial^2 u}{\partial y^2} \tag{32}$$

Energy balance:[5]

$$u \frac{\partial T}{\partial x} + v \frac{\partial T}{\partial y} = \frac{k}{c_p \rho} \frac{\partial^2 T}{\partial y^2} \tag{33}$$

Mass balance for component i in a binary mixture:

$$u \frac{\partial X_i}{\partial x} + v \frac{\partial X_i}{\partial y} = D_{im} \frac{\partial^2 X_i}{\partial y^2} \tag{34}$$

with the boundary conditions:

$$\left.\begin{aligned} &y \to 0: \quad u \to 0, \quad v \to v_o(x), \quad T \to T_o, \quad X_i \to X_{io} \qquad \text{(wall conditions)} \\ &y \to \infty: \quad u \to u_1, \quad \frac{\partial u}{\partial y} \to 0, \quad T \to T_1, \quad \frac{\partial T}{\partial y} \to 0, \\ &\qquad X_i \to X_{i1}, \quad \frac{\partial X_i}{\partial y} \to 0 \qquad\qquad \text{(stream conditions)} \end{aligned}\right\} \tag{35}$$

Using the boundary-layer substitutions of Blasius,

---

[5]Internal dissipation of energy is neglected.

$$\left.\begin{aligned} \eta &= \frac{y}{2x}\sqrt{\frac{u_1 x\rho}{\mu}} \\ f &= f(\eta) = \frac{\psi}{\sqrt{\frac{u_1 x\mu}{\rho}}} \end{aligned}\right\} \tag{36}$$

(where ψ is the stream function, defined by $\frac{\partial\psi}{\partial y} = u$, $\frac{\partial\psi}{\partial x} = -v$) the momentum balance equation becomes:

$$f''' + ff'' = 0 \tag{37}$$

with the boundary conditions

$$\left.\begin{aligned} &\eta \to 0: \quad f'(0) \to 0; \quad f(0) \to \frac{-2v_o}{u_1}\sqrt{\frac{u_1 x\rho}{\mu}} \\ &\eta \to \infty: \quad f'(\infty) \to 2; \quad f''(\infty) \to 0 \end{aligned}\right\} \tag{38}$$

The above approach yields valid solutions only for $f(0) = \text{Constant} = C$. Consequently, all results obtained by this method apply only to the case where the mass transfer distribution is of the form

$$v_o = \frac{-Cu_1}{2\sqrt{\frac{u_1 x\rho}{\mu}}} \tag{39}$$

In addition, the results obtained here are limited to zero pressure gradient and hence constant u_1.

In spite of the severe limitation imposed on the permissible mass transfer distributions by the Blasius substitutions, the solutions are of considerable interest since this mass transfer distribution corresponds to that produced in the practical case of diffusion under a constant driving force (uniform wall and stream concentration of diffusing

component). Furthermore, this distribution leads to a uniform wall temperature in the case of injection cooling with uniform coolant and main-stream temperatures.

Blasius (ref. 24) solved equations (37) and (38) for the case $f(0) = 0$ (no mass transfer) and Schlichting and Bussmann (ref. 10) have extended the calculations and published tables of f, f', f'', and f''' as a function of η for values of $C = 5, 3, 1.5, 1.0, 0.5, 0, -0.5, -0.75$, and -1.0 (five values of suction and three of blowing). These quantities determine the velocity distribution in the boundary layer and the wall friction coefficient c_f since

$$\frac{u}{u_1} = \frac{1}{2} f'(\eta) \tag{40}$$

$$\frac{v}{v_o} = \frac{f(\eta)}{f(0)} - \frac{1}{2}\frac{y}{x}\left(\sqrt{\frac{u_1 \rho x}{\mu}}\right)\frac{f'(\eta)}{f(0)} \tag{41}$$

$$\frac{c_f}{2} = \frac{f''(0)}{4\sqrt{\frac{u_1 \rho x}{\mu}}} \tag{42}$$

The temperature and concentration profiles and the corresponding transfer coefficients are determined by generalizing equations (32), (33), and (34) and solving the resulting equation. The generalization is accomplished by the introduction of the dimensionless profile moduli (eqs. (5))

$$\beta_F = \frac{u}{u_1} = \frac{1}{2} f'(\eta)$$

$$\beta_H = \frac{T_o - T}{T_o - T_1}$$

$$\beta_D = \frac{X_{io} - X_i}{X_{io} - X_{il}}$$

and the dimensionless fluid physical property groups

$$\left.\begin{aligned} Z_F &= 1 \\ Z_H &= \frac{c_p \mu}{k} \\ Z_D &= \frac{\mu}{\rho D_{im}} \end{aligned}\right\} \tag{43}$$

into equations (32), (33), and (34). The result is the general equation

$$u \frac{\partial \beta}{\partial x} + v \frac{\partial \beta}{\partial y} = \frac{\mu}{\rho Z} \frac{\partial^2 \beta}{\partial y^2} \tag{44}$$

This equation is solvable by the methods used to resolve equation (32) provided the boundary conditions are identical. This is accomplished if the wall temperature T_o and composition X_{io} and the main-stream temperature T_1 and composition X_{i1} are independent of x. Then equation (44) becomes

$$\beta'' + Zf\beta' = 0 \tag{45}$$[6]

with the boundary conditions for β of

$$\left.\begin{aligned} &\eta \to 0, \quad \beta \to 0 \\ &\eta \to \infty, \quad \beta \to 1; \quad \beta' \to 0 \end{aligned}\right\} \tag{46}$$

As before, f denotes the solution to equations (37) and (38).

If values of $f(\eta)$ are available, $\beta(\eta)$ may be found by direct integration:

$$\beta'(\eta) = \beta'(0) \left[\exp\left(-Z \int_0^{\eta} f \, d\eta \right) \right] \tag{47}$$

---

[6]Primes denote differentiation with respect to η.

$$\beta(\eta) = \beta'(0) \int_0^{\eta} \left[\exp\left(-Z \int_0^{\eta} f \, d\eta \right) \right] d\eta \tag{48}$$

In view of the boundary condition $\beta(\infty) \longrightarrow 1$.

$$\beta'(0) = \frac{1}{\int_0^{\infty} \left[\exp\left(-Z \int_0^{\eta} f \, d\eta \right) \right] d\eta} \tag{49}$$

The $f(\eta)$ values reported by Schlichting were used to solve equations (47), (48), and (49) numerically, giving temperature and concentration profiles and gradients at the wall for a number of values of Z (Prandtl or Schmidt number). These wall gradients, proportional to the transfer coefficients, are presented in table I and were used in calculating the theoretical results plotted in figures 1 and 2. Representative β profiles are shown in figure 3, and values of β as a function of C, Z, and η are tabulated in table II.

Asymptotic analytical solutions of some interest have been obtained from equations (48) and (49) by expanding f in a Taylor's series from $\eta = 0$, $f(\eta) = f(0) + \eta f'(0) + \eta^2 f''(0)/2 + \ldots$, and observing that, in the limit, certain terms become dominant. For large values of Z, the thermal or diffusion boundary layer will become thin compared with the flow boundary layer and only the first few terms of f need be considered.

For the impenetrable plate $f(0) = 0 = f'(0)$ and $f''(0) = 1.328$. Neglecting all other terms, equation (49) gives

$$\beta'(0) \approx 0.677 Z^{1/3} \tag{50}$$

remarkably similar to Pohlhausen's (ref. 25) empirical relationship:

$$\beta'(0) = 0.664 Z^{1/3}$$

and more nearly exact for $Z > 2$. The curves for $Z \longrightarrow \infty$ shown in figures 1 and 2 were calculated by extending this method to the case of mass transfer. In a similar manner, for small values of Z, the thermal boundary layer becomes large and the small region of velocity variation near the wall can be neglected, giving

$$\beta'(0) = 1.129 Z^{1/2} \tag{51}$$

However, this equation approaches the exact solution only at very small values of Z and becomes more accurate than equation (50) only at

$$Z < 0.047$$

The values of the transfer coefficients defined by equations (1), (2), and (3) may be calculated by means of the relations

$$\frac{c_f}{2} = \frac{\beta'(0)}{2\sqrt{\frac{u_1 \rho x}{\mu}}} \tag{52}$$

$$\frac{h}{c_p u_1 \rho} = \frac{\beta'(0)}{2Z\sqrt{\frac{u_1 \rho x}{\mu}}} \tag{53}$$

$$\frac{K_i M}{u_1 \rho} = \frac{\beta'(0)}{2Z\sqrt{\frac{u_1 \rho x}{\mu}}} \tag{54}$$

The Schlichting parameter $C = \frac{-2v_o}{u_1}\sqrt{\frac{u_1 \rho x}{\mu}}$ is related to the mass transfer parameter ϕ, used in figures 1 and 2 and defined by equations (23b), by the equation

$$\phi = \frac{-ZC}{\left[\beta'(0)\right]_*} \tag{55}$$

The notation $\left[\beta'(0)\right]_*$ implies that this quantity should be evaluated at zero mass transfer $(C = \phi = 0)$. In addition, $\left[\beta'(0)\right]_*$ must be evaluated at the proper value of Z. For ϕ_F use $Z = 1$; for ϕ_H use $Z = \frac{c_p \mu}{k}$; for ϕ_{Di} use $Z = \frac{\mu}{\rho D_{im}}$.

Discussion of Theories

The effects of mass transfer on the transfer coefficients predicted by film and laminar-boundary-layer theory are compared in figure 1. Here, the correction factor θ is plotted as a function of the rate factor ϕ. It will be noted that boundary-layer theory always predicts a greater effect than does film theory. This partly results from the fact that boundary-layer theory takes into account the changes in the boundary-layer thickness due to the flow normal to the wall, whereas simple film theory ignores such changes.

The effect of Z (Prandtl or Schmidt number) predicted by boundary-layer theory is due to a similar circumstance. A large value of Z implies a thin boundary layer whose thickness is not affected by mass transfer to so great an extent as the boundary layer associated with small Z values. Again, qualitatively, the analogy between film and boundary-layer theory may be developed in more detail. Film theory appears to represent a case where the film thickness is less than that for laminar flow with $Z \rightarrow \infty$. This is the situation in turbulent flow where the eddy diffusivity largely controls the exchange processes. Consequently, it is probable that film theory will correspond more closely to experiment in the case of turbulent flow than does laminar-boundary-layer theory. On the other hand, the film thickness can be expected to show some dependence on mass transfer rate and distribution even in turbulent flow, and film theory fails to predict this effect.

EQUIPMENT USED IN EXPERIMENTAL STUDIES

The experimental apparatus used in this investigation was designed and constructed to permit a close approach to the boundary conditions used in the theoretical analysis of the boundary layer but was made sufficiently flexible to allow the experimental study of situations not amenable to theoretical calculation. Briefly, the equipment simulates the flow over a porous flat plate and provides for acceleration or deceleration of the main flow and for sucking or blowing of a gas through the flat plate out of or into the main stream. Figure 4 is a sketch of the main experimental setup. The details of the equipment are as follows; the paragraph numbers refer to the index numbers used in figure 4.

(1) Air for the main stream was provided by a Buffalo Limit-Load Conoidal Fan, rated at approximately $6\frac{1}{2}$ horsepower at 1,900 rpm, belt-driven by a $7\frac{1}{2}$-horsepower direct-current motor. The motor was energized from a motor generator whose output voltage is variable from approximately

12 to 260 volts, direct current, giving a wind-velocity range of about 4 fps to 40 fps, which could be extended to 100 fps by removal of a glass-cloth screen at the entrance to the calming chamber.

(2) The calming chamber, 72 inches long by $44\frac{3}{4}$ inches high and $22\frac{3}{8}$ inches wide, was fitted with a honeycomb of 1- by 10-inch paper tubes and seven 14- by 18-mesh screens, to reduce vortex motion and turbulence.

(3) The calming chamber discharged into a 40-inch nozzle converging from $44\frac{3}{4}$ by $22\frac{3}{8}$ inches to 9 by 13.5 inches.

(4) Immediately upstream of the test section the tunnel converged uniformly 1 inch in height in a length of 12 inches. Suction panels covered the full width of the top and bottom walls to remove, insofar as possible, the initial boundary layer and to simulate the effect of a sharp leading edge. To eliminate corner effects from build-up of boundary layer on the side walls, these walls were formed of suction screens converging uniformly so that the width of the test section decreased from 13.5 to 12 inches in its 12-foot length. Small suction panels in the bottom wall also served to prevent build-up of undesirable boundary layers.

(5) The test wall was made the top wall of the tunnel to eliminate the effect of natural convection in heat-transfer studies. This wall and the leading-edge suction panels were formed of 80-mesh Jelliff Lektromesh screen 0.004 inch thick.

(6) and (7) The bottom wall of the test section was flexible and was mounted on a ladderlike support manipulated by four screw jacks. Although this arrangement was designed for achieving uniform velocity along the length of the tunnel, the tunnel height, 8 inches at the leading edge, could be varied between approximately 5 and 13 inches at the downstream edge, providing a range of Euler numbers for study of "wedge" flow.

(8) Two window frames, designed to hold 6-inch-square optical flats, 105 inches from the leading edge of the tunnel, made possible the direct observation of boundary-layer density profiles by means of a Mach-Zehnder interferometer available in the laboratory.

(9) For control of mass transfer distribution and energy input, the space behind the test wall was divided into 15 compartments. The number of compartments was sufficiently large to provide flexibility in mass and heat transfer distribution.

(10) Mass transfer through each compartment was indicated by calibrated orifices.

(11) A separately controlled woven Nichrome heating element was mounted immediately behind the test wall in each compartment, insulated from the wall by a Fiberglas sheet to which it was sewn. A second heating element was mounted about 2 inches behind the test wall as a guard heater.

(12) A number of baffles were mounted in each compartment to distribute the flow uniformly over the heaters and through the wall. A set of thermocouples was mounted on one of these baffles approximately opposite the thermocouples on the test wall to indicate the proper adjustment of the guard heaters.

(13) Bolts were provided to adjust tension in the test-wall screen, minimizing irregularities in its surface.

(14) The temperature of the test wall was indicated by from three to seven thermocouples soldered to the back of the screen in each compartment.

(15) To minimize radiation, all interior surfaces of the tunnel were gold-plated, and gold-plated reflector plates were mounted behind the side suction screens.

(16) Suction through leading-edge screens, side-wall screens, and bottom-wall screens was provided by a steam ejector, and flow was indicated by A.S.M.E. standard orifices.

(17) Proper adjustment of the bottom wall was indicated by velocity traverses made with a hot-wire anemometer or a pitot-static tube mounted on a sled which could be moved axially along the center line of the tunnel.

Openings were provided in the bottom wall[7] at intervals for insertion of the traversing gear used to obtain boundary-layer velocity and temperature profiles. The details of the traversing measurement techniques employed in this work are described in the sections discussing the experimental measurements.

Two pressure taps were located in each top-wall compartment. One tap measured the static pressure at the top wall of the tunnel; the second tap measured the static pressure of the compartment itself. These taps provided an additional measurement of the axial pressure gradient during tunnel operation when the traversing sled was removed, and they

[7]When not in use, the openings were closed with removable covers.

served as a check on the static-pressure probe used as part of the boundary-layer velocity measuring gear.

An electric heater was installed in the manifold supplying gas to the top-wall compartments. During "constant gas temperature" runs, this heater was used to preheat the gas admitted to the compartments and subsequently blown through the porous tunnel wall and into the main stream.

EXPERIMENTAL PROCEDURE

The basic experimental procedure employed was as follows:

(1) Adjust the tunnel velocity, boundary-layer control suction, bottom-wall contour, and suction or blowing rate and distribution to correspond to the desired flow boundary conditions.

(2) Adjust the heaters (if used) so that the desired thermal boundary conditions are obtained.

(3) Allow the system to stabilize, readjusting the flow and thermal conditions if necessary. In some cases, several hours are required to obtain steady-state operation.

(4) Begin measurements.

RANGE OF MEASUREMENTS

Experimental measurements of velocity and temperature profiles and of friction and heat transfer coefficients were carried out over a range of flow conditions. Main-stream velocity was varied between 5 and 60 fps, a length Reynolds number range of 6,500 to 3,300,000 was covered, and the mass transfer velocity ranged from -0.3 to 0.26 fps and included constant axial mass transfer velocity and $1/\sqrt{x}$ and $1/x^{0.2}$ distributions. One test was made with a positive Euler number; all other results apply to zero Euler number flow.

MOMENTUM TRANSFER MEASUREMENT AND CALCULATING TECHNIQUES

The effect of mass transfer through the porous wall on boundary-layer momentum transfer was studied by measurement of boundary-layer velocity profiles. These profiles were integrated to give the boundary-layer parameters of displacement thickness δ^* and momentum thickness ϑ.

The momentum thickness, when corrected for the effect of mass transfer, is a measure of the mean friction coefficient between the leading edge of the test section and the point of the traverse. The relationship between the corrected momentum thickness and distance from the leading edge was differentiated to yield local friction coefficients. This is a more reproducible method than differentiation of the velocity profile itself, but, as discussed later, it is also subject to precision limitations.

Velocity Profiles

The velocity profile data were taken by means of pitot tubes. Two tubes were employed. For use with relatively thick boundary layers, the probe was made from 0.035-inch-outside-diameter hypodermic tubing with the tip drawn and honed to 0.019-inch outside diameter. For use in high-velocity runs with thin boundary layers, the probe was made by soldering a 0.010-inch-outside-diameter tube to a larger diameter support. A photograph of the pitot tubes and the hot-wire probe is shown as figure 5. Pressure differentials were read to the nearest 0.0005-inch of heptane (specific gravity, 0.724). Impact-tube pressures were balanced against the pressures measured by the static-pressure taps located along the porous wall. These static-pressure taps were checked by comparison with measurements made by traversing a static tube along the center line of the tunnel.

Velocity traverses normal to the test wall were made at selected stations varying from 3.6 to 96.4 inches from the leading edge of the plate.

Momentum Integrals

For each velocity profile, the momentum integral (or momentum thickness)

$$\vartheta = \int_0^\infty \frac{u}{u_1}\left(1 - \frac{u}{u_1}\right)dy \tag{56}$$

and the displacement thickness

$$\delta^* = \int_0^\infty \left(1 - \frac{u}{u_1}\right)dy \tag{57}$$

were computed by numerical integration. In making these calculations, the velocity data were not corrected for the effect of turbulence on the manometer indication.

Friction Factors

The Von Kármán momentum theorem for laminar boundary layers with mass transfer is

$$\frac{\tau_o}{\rho_1 u_1^2} - \frac{d\vartheta}{dx} + \frac{v_o}{u_1} - \left(\frac{\delta^*}{\vartheta} + 2\right)\frac{\vartheta}{u}\frac{du}{dx} = 0 \tag{58}$$

For turbulent boundary layers additional terms involving products of the fluctuating velocity components should be included. These terms are believed to be negligible except in the vicinity of the separation point (or for very high blowing rates) and have not been taken into account. For the truly flat plate the last term of equation (58) vanishes. In the present case, because of irregularities of the adjustable bottom wall of the test channel, the main-stream velocity fluctuated about ±1 percent from its mean value, and in some instances this acceleration term was significant.

Defining $\frac{c_f}{2} = \frac{\tau_o}{\rho_1 u_1^2}$, equation (58) can be rewritten

$$\frac{c_f}{2} = \frac{d}{dx}\left[\vartheta - \int_0^x \frac{v_o}{u_1}\,dx + \left(\frac{\delta^*}{\vartheta} + 2\right)_{av} \vartheta\left(\frac{u_1 - u_{1,0}}{u_{1_{av}}}\right)\right] = \frac{d}{dx}\,\vartheta' \tag{59}$$

Formula (59) was used to evaluate local coefficients from the velocity traverses. The integrated form of equation (59) was used to calculate length mean friction coefficients.

Heat Transfer Measurement and Calculating Techniques

The effect of mass transfer through the porous wall on the rate at which heat is exchanged between the wall and the main stream was studied by direct measurement of the heat transfer rate and by measurement of boundary-layer temperature profiles. These data were used to compute heat transfer coefficients.

Direct Heat Transfer Measurements

The tunnel was constructed to permit the direct measurement of the rate at which heat is exchanged between the porous test wall and the main stream. Each of the 15 independent compartments forming the porous test wall contained an electric heater placed immediately behind the porous wall. Several baffle plates were located in the compartments to distribute air flow evenly over the whole area, and above these baffles was a guard heating element. This heater served to minimize temperature gradients within the compartment and also supplied heat to the air flowing into the compartment in blowing runs. An external heater in the main air supply could also be used to heat incoming air in blowing runs. Thermocouples were fastened to the porous wall and to the baffle plate located just above the porous wall. The baffle plate was covered with aluminum foil to minimize heat transfer within the compartment by radiation.

During a run, the temperatures of the wall and baffle were measured, and the electrical energy input of the heaters was measured. A "heat balance" was written on the space from the wall to the first baffle as follows (see fig. 6):

$$q_E + Wc_pT_B = hA(T_o - T_1) + Wc_pT_o + \text{Losses} \qquad (60)$$

where

q_E electrical energy into wall heater

W air flow rate through compartments; W has a positive sign for blowing runs

T_B baffle temperature

T_o wall temperature

T_1 main-stream temperature

h heat transfer coefficient between wall and stream

The loss term includes all other methods of heat flow and was ordinarily a small correction. In making the heat balances, estimates were made of radiant heat transfer from the test wall to other walls of the tunnel, heat loss from the sides of the compartments, heat flow from one compartment to the next, and radiant and convective heat transfer between the wall and baffle. These corrections were included in the loss term. The heat-balance equation was used to find both the heat directly transferred between the wall and the main stream $hA(T_o - T_1)$ and the heat transfer coefficient between the wall and main air stream.

Temperature Profiles

Boundary-layer temperature profiles were measured by means of thermocouples mounted in a traversing device that could be positioned to 0.001 inch. Two different thermocouple systems were employed, one for low-velocity runs and the other for high-velocity measurements. A photograph of the probes appears as figure 7.

The low-velocity thermocouple consisted of a silver-soldered junction of a 36-gage Chromel wire 0.005 inch in diameter and a 40-gage Alumel wire 0.003 inch in diameter. The junction itself was 0.005 inch across in the direction normal to the wall and was located at the center of 1 inch of wire, supported parallel to the wall and perpendicular to the direction of flow. The thermocouple was moved toward the wall until electrical contact was made and then backed off from the wall, the temperature being read at selected intervals. Because of some sag in the wire and tilt of the thermocouple support, the closest readings to the wall were at a distance of about 0.013 inch. At high velocities, the system used to support this thermocouple disturbed the flow pattern sufficiently to make the temperature profile measurements unreliable. When placed near the wall, the support deflected the main air stream upward through the porous wall ahead of the support and downward through the wall behind the support. This was borne out by abnormally low readings of the wall thermocouple at the traversing thermocouple position and abnormally high readings of the wall thermocouple at the next position downstream. The flow disturbance was most pronounced during runs made without mass transfer. As would be expected, forced blowing or suction through the porous wall minimized the disturbance caused by the support.

In order to obtain reliable temperature profiles at high tunnel velocities, a small thermocouple support was constructed. The support consisted of a piece of hypodermic tubing bent at a right angle so as to point upstream. The thermocouple, consisting of 0.010-inch-diameter copper and constantan wire, projected about 1/4 inch beyond the end of the hypodermic tubing. The two wires were soldered at the tip and the junction was filed so that with the thermocouple in contact with the wall the temperature reading would correspond to a distance of about 0.005 inch from the wall. At low tunnel velocities, conduction errors, caused by the short length and high thermal conductivity of the exposed lengths of wire, became important. Consequently, this probe was not used during low-velocity runs. At intermediate velocities, this probe and the low-velocity system were in good agreement. No significant flow disturbance was noted when the high-velocity thermocouple was used.

As a rough check on the heat transfer coefficients obtained by heat balances on the compartments, values of the heat transfer coefficient were computed from the slopes of the measured temperature profile. The

rate of heat transfer from the wall may be expressed as

$$(q/A)_o = h(T_o - T_1) = -k\left(\frac{dT}{dy}\right)_o \tag{61}$$

If the temperature gradient at the wall $\left(\frac{dT}{dy}\right)_o$ can be evaluated from the temperature profile, the heat transfer coefficient can be calculated by the above relation. In general, the wall temperature gradient could not be measured with precision, and the heat transfer coefficients calculated in this way were not considered reliable.

Enthalpy Thickness

The enthalpy thickness ξ is related to the heat transfer coefficient in the same manner as the relation between the momentum thickness and the friction factor. The enthalpy thickness is defined as

$$\xi = \int_0^\infty \frac{u}{u_1}\left[1 - \left(\frac{T_o - T}{T_o - T_1}\right)\right]dy = \int_0^\infty \frac{u}{u_1}(1 - \beta_H)dy \tag{62}$$

An energy balance applied to the boundary layer yields

$$\frac{d\xi}{dx} = \frac{h}{c_p \rho u_1} + \frac{v_o}{u_1} \tag{63}$$

The enthalpy thickness ξ can be calculated from measured velocity and temperature profiles and plotted as a function of x, the distance from the leading edge of the plate. The values of $d\xi/dx$ obtained from such a plot may be used in equation (63) to calculate the local heat transfer coefficient. The integrated form of equation (63) may be used to evaluate length mean heat transfer coefficients. This method is more reliable than calculations based upon the slopes of the temperature profiles but requires measurements of both the velocity and temperature profiles. Where such data were measured, the heat transfer coefficients were calculated from the enthalpy thickness and the resulting values compared with the values obtained by alternate techniques.

In some runs only temperature profiles were measured. However, if the boundary layer were laminar and the wall velocity proportional to $1/\sqrt{x}$, the velocity profile could be estimated if it was assumed that the velocity and temperature profiles differed only as a result of the Prandtl number. Thus, according to laminar-boundary-layer theory,

$$\beta_H = \frac{T_o - T}{T_o - T_1} = \frac{\int_0^{\eta} \left\{ \exp\left[-Pr \int_0^{\eta} f(\eta) d\eta \right] \right\} d\eta}{\int_0^{\infty} \left\{ \exp\left[-Pr \int_0^{\eta} f(\eta) d\eta \right] \right\} d\eta} \tag{64}$$

and

$$\frac{u}{u_1} = \frac{\int_0^{\eta} \left\{ \exp\left[-\int_0^{\eta} f(\eta) d\eta \right] \right\} d\eta}{\int_0^{\infty} \left\{ \exp\left[-\int_0^{\eta} f(\eta) d\eta \right] \right\} d\eta} \tag{65}$$

Numerical integration of the $(1/Pr)$ power of the slope of the measured temperature profile was used to estimate the velocity profile. In the laminar-boundary-layer regime, this method was used to determine approximate values for the velocity profile, the momentum thickness, and the enthalpy thickness from the measured temperature profiles.

EXPERIMENTAL RESULTS

Velocity Profiles

Experimental data.- Velocity profiles were measured under the experimental conditions shown in table III. The measurements were made using air in both main and injected streams, except for runs V-1 and V-2 for which no fluid was injected, and at zero Euler number. Main-stream velocities ranging from 20 to 60 fps were used. Traverses were made at selected stations varying from 3.6 to 96.4 inches from the leading edge, covering a length Reynolds number range of 46,000 to 1,230,000. Mass transfer, obtained by blowing or sucking air through the wall, was controlled separately through each of the 15 test-wall sections, so that a stepwise approximation to the desired longitudinal mass transfer distribution resulted. Data were obtained under conditions of blowing with both constant velocity and constant ϕ ($v_o \propto 1/\sqrt{x}$ in the laminar regime and $v_o \propto 1/x^{0.2}$ in the turbulent regime) and of suction with constant suction velocity and constant ϕ.

The measured velocity profile data are tabulated in table IV. Representative velocity profiles are given in figures 8 and 9. Figure 8(a) shows velocity profiles for a run with no mass transfer; figure 8(b), for constant blowing velocity; figure 8(c), for constant suction velocity; and figure 8(d), for suction with an inverse square-root

distribution (constant ϕ in the laminar regime). Figures 9(a) to 9(c) show velocity profiles measured under conditions corresponding to the temperature profiles of figures 10(a) to 10(c). Figure 9(a) presents the velocity profiles for blowing at constant ϕ_H; figure 9(b), for constant blowing velocity; and figure 9(c), for suction at constant ϕ_H.

Accuracy of measurement.- The accuracy of the velocity profile measurements was limited by several factors:

(1) Uncertainties in the measurement of the wall position. The $y = 0$ position could not be reproduced to better than ± 0.002 inch.

(2) Velocity-gradient effects. In the presence of a velocity gradient the probe reading generally does not correspond to a probe position measured at the probe center line. Although the probe position readings were corrected by means of a theoretical analysis of the velocity-gradient effect, errors in the corrected probe position of the order of ± 0.002 inch are possible.

(3) Pressure differential measurements. The manometer used to measure the pressure differential caused by the velocity head gave a correct indication of the pressure differential to the nearest 0.0005 inch of heptane. The loss in precision due to the limitations of the instrument is given by the expression $\frac{\Delta u}{u} \approx \frac{0.8}{u^2}$ and becomes serious at velocities below 3 fps. Consequently, the profile measurements were not extended into the very low velocity region of the boundary layer.

(4) Reynolds number effects. At low Reynolds numbers (based upon probe diameter) it is known that the usual "pitot tube" equation fails. A check of the probes used here indicated that the pitot-tube equation could be applied without errors greater than ± 1 percent down to a probe Reynolds number of about 30. This corresponds to a velocity of about 3 fps, the same velocity at which the measurement of the pressure itself begins to introduce serious loss of precision.

(5) Turbulence effects. The fluctuating velocity components associated with turbulent flow affect the impact reading. In these experiments, however, the measured turbulence intensity was of the order of 0.3 percent, a sufficiently low value to have a negligible effect on the velocity measurements.

(6) Flow disturbance effects. Any instrument placed in the stream disturbs the flow. The probe used here was designed to minimize this disturbance. A comparison of the velocity as measured by the impact probe and by a hot-wire anemometer showed good agreement except in the immediate vicinity of the wall. Since the hot-wire was much smaller

than the impact tube, the agreement indicates that the impact probe did not seriously disturb the flow at reasonable distances from the wall. The readings of the impact tube and the hot-wire began to show significant differences at a distance of about 0.03 inch from the wall. In every case the hot-wire gave higher velocities than the pitot tube. This was found to be due to heat flowing from the hot-wire to the cool wall. Since comparison with the hot-wire did not adequately show any wall flow disturbance, a second technique was tried. The wall was heated to a temperature above that of the main stream and the wall temperature measured both with and without the probe immediately adjacent to the wall. No change in wall temperature with probe position could be detected, indicating that the disturbances caused by the probe were small.

The accuracy of the velocity profile measurements can be summarized as follows: The velocity itself could be determined with an accuracy largely fixed by the manometer employed, the error in the velocity being given by the expression $\Delta u \approx \frac{0.8}{u}$. The distance from the wall corresponding to a given velocity measurement was subject to errors of ±0.004 inch, resulting from uncertainty concerning the zero position and the effect of velocity gradient on the pitot-tube reading.

In terms of flow conditions, the velocity profile measurements are least reliable when measured in a thin-boundary-layer region. Thin boundary layers were found near the leading edge and at all positions during runs made with a high suction velocity.

Momentum and Displacement Thickness

The measured velocity profiles were used in conjunction with equations (56) and (57) to calculate the value of the momentum thickness ϑ and displacement thickness δ^* by numerical integration. The resulting values of ϑ and δ^* are tabulated in table III.

The precision with which the momentum or displacement thickness could be determined was a minimum in suction runs and a maximum in blowing runs. This follows directly from the precision of the velocity profiles from which the integrals were evaluated.

Friction Coefficients

Local friction coefficients were calculated using the values of the momentum thickness and equation (59). The technique employed was to plot the quantity ϑ', the momentum thickness corrected for mass transfer

and main-stream acceleration, as a function of the distance from the leading edge x. The slopes $d\vartheta'/dx$ of the resulting curves are equal to the local value of $c_f/2$. In a given run, the maximum number of stations at which values of ϑ' were determined was eight. Frequently, these values covered laminar and turbulent flow. These circumstances, coupled with the "scatter" of the data, made the determination of the detailed relation between ϑ' and x difficult. It was found that when the data were plotted as ϑ' versus x on logarithmic coordinates, a straight line, or two straight lines for runs in which both laminar and turbulent regimes were significant, fitted the data quite well. This is illustrated by figure 11 which shows values of ϑ' versus x for all runs made at a main-stream velocity of 26 fps. All of the data were treated in this way; a curve of the form

$$\vartheta' = ax^b$$

was fitted to the data by the method of least squares. This relationship was then differentiated to give the local friction coefficient:

$$\frac{c_f}{2} = \frac{d\vartheta'}{dx} \approx abx^{b-1}$$

The empirical equations for the local friction coefficients found in this way, generalized to include the effect of Reynolds number, are tabulated for each run in table V. Figures 12(a) to 12(k) show the local friction coefficients for each run plotted as a function of the distance from the leading edge.

It is realized that the method used to determine the local friction coefficient forces the derived relation to follow the form

$$\frac{c_f}{2} = \frac{l}{(R_x)^n}$$

and consequently masks effects which may be significant from a theoretical point of view. Although this is undesirable, it is believed that the precision of the data obtained here do not justify a more sophisticated treatment.

The accuracy of the friction coefficients obtained from momentum thickness values is a function of both the accuracy of the momentum thickness data and of the type of mass transfer. Examination of equation (59) shows that in blowing runs ϑ' represents the difference between the momentum thickness ϑ and the dimensionless blowing velocity v_o/u_1. At high blowing rates v_o/u_1 is of the same order as ϑ

and the precision of ϑ' is less than that of ϑ or v_o/u_1. In addition, the process of differentiation greatly reduces the precision of the result, and the accuracy with which the local value of the friction coefficient $\left(\frac{c_f}{2} = \frac{d\vartheta'}{dx}\right)$ is known is less than the accuarcy of ϑ' itself.

The reverse is true in the case of suction runs; ϑ' is the sum of ϑ and v_o/u_1. On the other hand, the momentum thickness itself is not known with precision in suction runs and this, when added to the effects caused by differentiation, limits the precision of the local friction coefficients with suction.

An analysis of these effects leads to the following estimates of the precision of the friction factors reported here:

Mass transfer condition	Estimated precision of friction factor, percent
High suction rate	±5
Zero mass transfer	±10
High blowing rate	±30

Direct Heat Transfer Measurements

Experimental data.- Heat transfer coefficients were measured under the experimental conditions shown in table VI. The measurements were made using air in both main and injected streams except for runs H-1 through H-4 for which no fluid was injected. With the exception of one run (H-27a), all experiments were made at zero Euler number. Main-stream velocities of approximately 5, 20, and 60 fps were used. The flow in the tunnel was largely laminar at the lowest velocity and turbulent at the highest velocity. At the intermediate velocity the flow was generally laminar in suction runs and turbulent in blowing runs. Measurements were made at points ranging from 2.8 to 111.9 inches from the leading edge, covering a length Reynolds number range of 6,500 to 3,300,000. Data were obtained with mass transfer through the test-wall sections adjusted to give both constant velocity and constant ϕ ($v_o \propto 1/\sqrt{x}$ in laminar regime and $v_o \propto 1/x^{0.2}$ in turbulent regime) with both blowing and suction. Constant-velocity runs were made with v_o varying from 0.12 to -0.12 fps and constant ϕ runs were made with ϕ_H varying from 1.2 to -3.6.

The directly measured heat transfer coefficients are tabulated in table VII. The data are shown in graphical form in figure 13. Figure 13(a) shows coefficients for no mass transfer compared with predicted values. The predicted values are obtained from boundary-layer

theory for the laminar regime. For the turbulent regime the predicted values are obtained from the Chilton-Colburn empirical relation

$$\frac{h_*}{u_1 \rho_1 c_p}\left(\frac{c_p \mu}{k}\right)^{2/3} = \frac{0.0288}{(R_x)^{0.2}}$$

This relation is based on earlier experimental work by other workers and is seen to agree quite well with the experimental data of runs H-2, H-3, and H-4.

Figures 13(b) through 13(f) show comparisons of experimentally measured coefficients with predicted values for various cases of mass transfer. Predicted values for the laminar regime are obtained from boundary-layer theory and for the turbulent regime from film theory based on the Chilton-Colburn relation. Figure 13(b) shows results for blowing at constant ϕ_H; figure 13(c), for constant blowing velocity; figure 13(e), for suction at constant ϕ_H;[8] and figure 13(f), for constant suction velocity. Figure 13(d) compares three runs for turbulent flow and blowing. Run H-20 was made with a uniform blowing velocity of 0.12 fps. Run H-21a was made with the same mean blowing velocity but with the mass transfer rate adjusted to give a uniform wall temperature as well as a uniform gas temperature. This resulted in a mass transfer distribution with a constant value of ϕ_H. Run H-27a was made with a uniform blowing velocity of 0.12 fps and was therefore identical with run H-20a except that the main stream was accelerated. In this run the experimental values are compared with results of run H-20a adjusted for differences in velocity.

Accuracy of measurement.- The accuracy of measurement of heat transfer coefficients was limited by several factors:

(1) Accuracy of temperature measurements. Temperatures were measured by thermocouples attached to the porous screen and to perforated baffle plates behind the screen. The thermal electromotive force of the thermocouples was measured by a Rubicon Type B potentiometer with an external galvanometer which was capable of readings reproducible to within 1 microvolt (0.04° F). The thermocouples were calibrated so that the uncertainty of the calibration was 0.08° F. The accuracy of individual thermocouple readings was therefore not an important source of error.

---

[8] In runs H-12 and H-24 the suction through compartment G was inadvertently turned off. As a result, all data for these runs downstream of $x = 22$ inches were affected by the irregular suction distribution.

The largest source of error in the temperature measurements arises from deviation of the thermocouple temperature from the true temperature to be measured. The wall temperatures were determined by averaging the readings of three to seven thermocouples located in each compartment. Individual thermocouple readings generally deviated about 20 to 40 microvolts from the mean value but differed as much as 100 microvolts in some cases. This effect was caused by nonuniformity of heating by the electrical heater in contact with the screen. The effect was most noticeable in high-suction runs where it appeared that in some places the suction of air through the compartment lifted the heater away from the screen. There was very little scatter of the thermocouple readings in runs with uniform blowing gas temperature in which the screen heaters were not used. Mean compartment temperatures were therefore subject to an error of about 1° F for blowing runs and 1° to 3° F for suction runs. The over-all temperature differences were generally about 20° F but in some cases were as low as 9° F or as high as 30° F. The runs with the lowest over-all temperature differences were therefore subject to the greatest percentage error in temperature measurement.

(2) Measurement of electrical energy input. Input of electrical energy was determined by measuring the voltage applied to the heaters whose electrical resistance was known. The voltage was measured by an alternating-current meter calibrated against a standard meter with a precision of ± 1 percent. There was a small uncertainty in the voltage measurements because of the current drawn by the meter itself. The resistance of the heating elements was measured very precisely and was not a significant source of error. The over-all uncertainty in the measurement of electrical energy input was about 5 percent.

(3) Measurement of compartment flow rates. In runs where there was a temperature difference between the screens and the baffle behind it, the flow rate through the compartment was needed to calculate the heat transfer coefficient (see fig. 6). This flow rate was measured by calibrated orifice meters with an uncertainty of ± 2 percent. This causes very little error in the calculation of the heat transfer coefficient if there is a low temperature difference between the screen and baffle but is more significant in runs with uniform gas temperature and with high suction rates.

(4) Estimation of heat losses. The calculation of heat transfer coefficients required the estimation of heat losses from the compartments by radiation from the test wall to other walls of the tunnel, by convection from the sides of the compartments, by conduction between compartments, and by radiation and convection within the compartments. The over-all uncertainty in these corrections is about 0.1 Btu/(hr)(sq ft)($^{\circ}$F) for runs with little difference between screen and baffle temperatures and about twice this for cases with substantial temperature differences. For runs with low coefficients such as low-velocity runs,

especially laminar blowing runs, this is a serious source of error because the coefficients may be as low as 0.4 Btu/(hr)(sq ft)($^{\circ}$F). For runs with high coefficients, this is not an important source of error.

The accuracy of the measurement of heat transfer coefficients can be summarized as follows: The principal source of error is uncertainty in the measurements of temperature differences between the test wall and the main stream and between the test wall and the baffle behind it. The temperature differences can be measured to $\pm 1^{\circ}$ F for blowing runs and $\pm 1^{\circ}$ to $\pm 3^{\circ}$ F for suction runs, depending on the suction rate. This error is most serious for runs with low over-all temperature differences between wall and main stream or high over-all temperature differences between wall and baffle. The uncertainty of estimation of heat losses can be serious if the measured coefficient is low but is unimportant for high coefficients because it is a fixed absolute error on the heat transfer coefficient. The measurement of electrical energy input is subject to an error of about ± 5 percent. Other sources of error are not important.

Temperature Profiles

Experimental data.- Temperature profiles were measured under the experimental conditions shown in table VI. These are the same conditions as those under which direct measurements were made, except that temperature profiles were not measured for every run. The experimental temperature profile measurements are tabulated in table VIII. Representative profiles are shown in figures 10 and 14. Figure 14(a) shows profiles for laminar flow with no mass transfer; figure 14(b), for laminar flow and blowing with constant ϕ_H; and figure 14(c), for laminar flow and suction with constant ϕ_H. Figure 14(d) presents profiles for turbulent flow with no mass transfer. Figures 9 and 10 show temperature and velocity profiles for turbulent flow with blowing or suction, the velocity profiles of figures 9(a) to 9(c) corresponding to the temperature profiles of figures 10(a) to 10(c). Figures 9(a) and 10(a) show profiles for blowing at constant ϕ_H; figures 9(b) and 10(b), for a constant blowing velocity; and figures 9(c) and 10(c), for suction at constant ϕ_H.

A few values of heat transfer coefficients calculated from the slopes of temperature profiles according to equation (61) are plotted as crosses in figure 13(a). This method of determining coefficients was found to be generally unreliable and was abandoned.

Accuracy of measurement.- The accuracy of measurement of temperature profiles was limited by several factors:

(1) Uncertainty in the measurement of the thermocouple position. The position of the traversing mechanism for which the thermocouple made

contact with the wall was reproducible to a precision of about ±0.002 inch. The effective thermocouple position when the probe was in contact with the wall could be determined to a precision of about ±0.001 inch, giving an over-all precision of the position of the thermocouple junction of ±0.003 inch.

(2) Accuracy of measurement of thermocouple temperature. The thermal electromotive force of the thermocouple probes was measured by a Rubicon Type B potentiometer with an external galvanometer. The potential of the copper-constantan high-velocity probe could be measured with a precision of ±1 microvolt (0.04° F). The Chromel-Alumel probe used at low velocities had a higher wire resistance and therefore a lower sensitivity. Readings could be reproduced to about $\pm 1\frac{1}{2}$ microvolts (0.06° F).

(3) Nonlinearity of thermocouple calibration. To simplify the calculations, temperature profiles reduced to a dimensionless temperature (β) were calculated directly from the thermocouple reading in microvolts rather than first converting microvolts to degrees. This was allowable because the calibrations of the thermocouples were linear over the temperature range of the profiles within the precision of the temperature measurements themselves. The rate of change of thermal electromotive force with temperature changes by not over 2 percent for the temperature range of any profile. Therefore this is not a serious source of error.

(4) Determination of wall temperature. In order to obtain dimensionless temperature profiles, it was necessary to know the value of the temperature of the wall at the point where the profile was measured. For runs with laminar flow where the probe could measure temperatures very near the wall, the wall temperature itself could be obtained by extrapolation of the measured points to $y = 0$. This could generally be done to a precision of about 5 to 10 microvolts. However, in cases of turbulent flow where it was difficult to make measurements within the laminar sublayer, or with very thin laminar boundary layers such as those obtained at high suction rates, the probe could not measure temperatures sufficiently near the wall and extrapolation was very unreliable. In these cases the wall temperature could be better estimated from the thermocouples in the wall itself, even though these were not always located directly above the probe. The uncertainty of the estimation of wall temperature in these cases was about ±30 microvolts. This can therefore be a serious source of error in some cases.

(5) Conduction error in thermocouples. A thermocouple junction in a fluid stream can lose heat by conduction along its leads unless precaution is taken to eliminate this error. The probe designed for use at low main-stream velocities had about 1/2 inch of bare wire on each side of the junction exposed to air at the same temperature as the

junction. Calculations show that the temperature of the junction will be within 0.1° F of the true air temperature down to an air velocity of 0.5 fps. This allows measurements well within the laminar boundary layer for the low-velocity runs. The probe used for high velocities had about 1/4 inch of heavier wire projecting upstream. This probe could measure temperatures within 0.1° F above an air velocity of 10 fps, but at lower velocities it was subject to serious error and was not used except in runs with a main-stream velocity of about 60 fps.

(6) Flow disturbance effects. The flow disturbance caused by insertion of the temperature-measuring probes into the tunnel was checked by observing whether or not the wall temperature changed any when the probe was brought near it. No significant effect was noticed at main-stream velocities of 5 and 20 fps when the large Chromel-Alumel probe was used, but a marked disturbance was noticed at a velocity of 60 fps. The wall temperature dropped as much as 100 microvolts (4° F) when the probe was placed in contact with the wall. The next thermocouple downstream of the probe read a higher temperature when the probe was in place. This indicated that air was being deflected up through the screen ahead of the probe and was coming back out into the main stream just downstream of the probe. This probe could not be used to make reliable temperature profile measurements at high velocities because of this disturbance. A similar test of the smaller high-velocity copper-constantan probe showed no significant flow disturbance at a main-stream velocity of 60 fps.

The accuracy of the temperature profile measurements can be summarized as follows: The possible error in position of the thermocouple junction was about ±0.003 inch. Errors in measurement of thermal electromotive force or in calculation of dimensionless temperatures from measured voltages were insignificant. Determination of wall temperature was fairly good (2 to 3 percent) in laminar profiles which could be extrapolated to the wall position but was serious (up to 10 percent) for thin boundary layers or turbulent profiles with thin laminar regions. The low-velocity probe was not subject to error by conduction along the thermocouple leads at velocities above 0.5 fps, but this probe disturbed the flow pattern markedly at a velocity of 60 fps. The high-velocity probe caused no significant flow disturbance but was in error because of conduction along the leads at velocities below 10 fps and could therefore be used only for the runs at 60 fps.

Enthalpy Thickness

Simultaneous velocity and temperature profiles are necessary in order to evaluate enthalpy thicknesses. In all cases where simultaneous profile measurements were made, the enthalpy thickness ξ was calculated by numerical integration according to equation (62). The resulting values of ξ are tabulated in table VI. In some cases in the laminar flow regime only a temperature profile was measured, but a velocity

profile could be derived from it if it was assumed that the profiles were similar except for a Prandtl number effect. These derived velocity profiles were calculated from temperature profiles according to equations (64) and (65) and are tabulated in table IX. The values of ξ calculated from these temperature and derived velocity profiles are also tabulated in table VI.

As in the case of the calculation of momentum thicknesses and displacement thicknesses, the precision with which the enthalpy thickness could be determined was a minimum in suction runs and a maximum in blowing runs.

Heat Transfer Coefficients From Enthalpy Thicknesses

Local heat transfer coefficients were calculated using the values of the enthalpy thickness and equation (63). The technique employed was to plot the quantity ξ', the enthalpy thickness corrected for mass transfer, as a function of the distance from the leading edge x. The slopes $d\xi'/dx$ of the resulting curves were equal to the local value of the Stanton group $h/\rho u_1 c_p$. As in the case of corrected momentum thicknesses, the experimental points were fitted with a straight line on logarithmic coordinates, resulting in a relation of the form $\xi' = ax^b$. The relationship was then differentiated to give the local Stanton group:

$$\frac{h}{\rho u_1 c_p} = \frac{d\xi'}{dx} \approx abx^{b-1}$$

The empirical equations for local heat transfer coefficients found in this way, generalized to include the effect of Reynolds number, are tabulated in table V.

The heat transfer coefficients derived from enthalpy integrals are in substantial agreement with the corresponding directly measured coefficients. For clarity, these relations have not been plotted in figures 13(a) to 13(f) except in the case of run H-1, shown in figure 13(a).

The values of heat transfer coefficients calculated from enthalpy thicknesses are subject to the same type of errors as the values of the local friction factors calculated from momentum thicknesses. The precision of the two results is roughly the same.

DISCUSSION OF EXPERIMENTAL RESULTS AND COMPARISON WITH THEORY

Velocity Profiles

Laminar regime.- Laminar-boundary-layer velocity profile data obtained in suction runs are compared with the predictions of laminar-

boundary-layer theory in figures 15 and 16. In figure 15 profiles are plotted for two runs with the same main-stream conditions but with two different rates of uniform suction. According to Schlichting and Bussmann (ref. 10), the laminar boundary layer on a flat plate with uniform suction should asymptotically approach the relationship

$$\frac{u}{u_1} = 1 - \exp\left(\frac{v_o \rho y}{\mu}\right)$$

at a great distance from the leading edge. Examination of figure 15 shows that the asymptotic profile is approached, the profile at $x = 22.1$ inches agreeing well with the theoretical profile in each case. The scatter in the data may be ascribed to several factors: (1) The asymptotic profile is attained only at a considerable distance from the leading edge. Near the leading edge the profiles should be steeper and the boundary layer thinner, in line with the general trend of figure 15. However, the calculations of Iglisch (ref. 20) indicate that this effect should be less than that shown in figure 15. (2) It was impossible completely to eliminate acceleration of the free stream, with the result that there was in each case acceleration between the leading edge and station C, deceleration between stations C and D, and acceleration between stations D and E. These velocity fluctuations were of the order of ±1 percent of the mean velocity. (3) The test wall possesses irregularities which could cause the effective position of the probe when in contact with the wall to vary by a few thousandths of an inch from station to station. In most cases it can be seen that the experimental data are displaced from the asymptotic profile by a very few thousandths of an inch.

A third run was made at a still lower suction velocity, but transition to turbulent boundary layer occurred before the asymptotic profile was approached. It is believed that the data of figure 15 are in agreement with laminar-boundary-layer theory within the limits of experimental precision.

In figure 16 laminar-boundary-layer profiles for the case of suction with an inverse square-root distribution are compared with the calculated profiles of Schlichting and Bussmann (ref. 10). These profiles are in qualitative agreement with the theoretical curves. The discrepancies probably result from the acceleration and deceleration of the main stream and from irregularities in the test surface which introduce errors in the measured value of y.

In blowing runs transition to turbulent flow occurred at such a low Reynolds number that the laminar velocity profiles were not measured with adequate precision. Work now in progress with more sensitive velocity measuring equipment has shown that this difficulty can be overcome and the incomplete data show good agreement with theory.

Turbulent regime.- In figures 17 and 18 the dimensionless velocity ratio u/u_1 is plotted as a function of the dimensionless distance ratio y/ϑ for cases when the boundary layer was turbulent. Each curve represents data obtained at several different traversing stations and consequently represents a wide variation in downstream distance. Figure 17 presents data obtained under zero mass transfer conditions at $u_1 = 25.8$ fps, figure 18(a) presents data obtained with blowing at constant $\phi_H = 1.23$ and $u_1 = 19.6$ fps, and figure 18(b) presents data obtained with a constant blowing velocity $v_o = 0.04$ fps and $u_1 = 20$ fps. When plotted in this way, the velocity profiles for a given run are found to be similar with the exception of the region very near the wall. The profiles obtained with a constant blowing velocity exhibit somewhat greater deviation from the mean curve than the data obtained at $\phi = 0$ and $\phi_H = 1.23$. The precision of the constant v_o data does not warrant any definite conclusions concerning departure from similarity when a constant blowing rate is imposed on the flow, but close examination of the original data indicates that at a given value of y/ϑ the values of u/u_1 decrease as the distance from the leading edge is increased. This question and other topics related to the turbulent velocity profiles are discussed more fully when the turbulent velocity and temperature profiles are compared.

Friction Factors

Laminar regime.- A comparison of measured laminar region friction coefficients with those predicted by theory is shown in figure 12.

In all suction runs, the measured friction coefficients are in good agreement with values predicted by laminar-boundary-layer calculations of Schlichting and Bussmann (ref. 10) for inverse square-root suction and Iglisch (ref. 20) for uniform suction.

In the data reported here, only indications of the agreement between theory and experiment were obtained in the case of laminar, no-mass-transfer flow. The x points of figures 12(a) to 12(f) are coefficients estimated from wall velocity gradients of the first two profiles of run V-1. The circled point is estimated from the value of ϑ' obtained at $x = 3.6$ inches, $R_x = 46{,}000$, run V-1, by means of the relationship

$$(c_f/2)_{\text{local, laminar}} = \frac{1}{2}(c_f/2)_{\text{mean, laminar}} = \frac{1}{2}\left(\frac{\vartheta'}{x}\right)$$

which is valid for the Blasius solution. These coefficients are in reasonable agreement with theory, considering transition to occur between $x = 3.6$ and $x = 6.9$ inches. In figures 12(g) to 12(k) the

"experimental" no-mass-transfer laminar friction-coefficient values shown were calculated from velocity profiles derived from the measured laminar-region temperature profiles of run H-1. Reasonable agreement is found between the "data" and theory.

In view of the poor precision of the laminar velocity profiles obtained under blowing conditions, no friction-factor calculations were attempted.

Turbulent regime.- Figures 12(a) to 12(k) compare measured friction-factor values with those predicted by film theory or, in the case of no-mass-transfer runs, with the values predicted by the customary engineering relation

$$\frac{c_{f_*}}{2} = \frac{0.0296}{(R_x)^{0.2}}$$

In those cases in which film theory was applied, the value of c_{f_*}, the friction coefficient in the absence of mass transfer used to calculate θ and ϕ, was the experimentally measured coefficient at the same mainstream conditions.

Zero-mass-transfer friction coefficients were measured at mainstream velocities of 20, 26, and 59 fps. A comparison of the empirical friction-factor and Reynolds number relations derived from the experimental data with the expected smooth-plate, turbulent-flow equation

$$\frac{c_{f_*}}{2} = \frac{0.0296}{(R_x)^{0.2}}$$

discloses some significant differences. At 20 fps measured friction factors agree well with the expected relation. At 26 fps the relation derived from the experimental results is $\frac{c_{f_*}}{2} = \frac{0.012}{(R_x)^{0.123}}$. Measured and expected values are equal at $R_x = 128{,}000$, but the experimental value is 15 percent higher at $R_x = 1{,}280{,}000$. At 59 fps the relation derived from the experimental results is $\frac{c_{f_*}}{2} = \frac{0.044}{(R_x)^{0.216}}$. The measured values are 24 percent higher than expected at $R_x = 10^5$ and 17.5 percent higher at $R_x = 10^6$. It is believed that these differences result from the behavior of the porous wall; the basis for this opinion is discussed more fully later.

The comparison with film theory shown in figures 12(a) to 12(k) is presented in the form of the measured correction factor $\theta_F = c_f/c_{f_*}$ plotted as a function of the rate factor $\phi_F = 2v_o/u_1 c_{f_*}$ in figure 19. The comparisons are subject to greater error than are the measured values of c_f or c_{f_*} alone. Consequently, the scatter of the data points shown in figure 19 is to be expected. The data points appear to indicate that film theory somewhat overpredicts the effect of mass transfer. This actually may be the case, but, in light of the precision of the data, such a conclusion cannot be justified. The true state of affairs is in doubt. Within the precision of the experimental results, film theory predicts the measured effect of mass transfer on the friction coefficients.

Temperature Profiles

Laminar regime.- Laminar-boundary-layer temperature profile data are compared with the predictions of laminar-boundary-layer theory in figures 20(a) to 20(c). Profiles for a run with no mass transfer are shown in figure 20(a) in comparison with the theoretical profile calculated by Pohlhausen (ref. 25). The profiles show good similarity and are in close agreement with each other, but all of the experimental profiles are slightly steeper than the theoretical profile, indicating that the heat transfer coefficient is higher than the theoretical value.

Figure 20(b) shows laminar temperature profiles for a run with an inverse square-root blowing distribution. Theoretical profiles are plotted for no mass transfer and for the blowing rate used in this run. The measured profiles indicate that the thermal boundary layer is thicker than it would be in the absence of blowing but is not thickened by the amount predicted by boundary-layer theory, indicating that the heat transfer coefficient is substantially higher than the theoretical coefficient.

Figure 20(c) shows laminar temperature profiles for a run with an inverse square-root suction distribution. These are compared with the theoretical profiles for no mass transfer and for the suction rate used in this run. The two upper profiles are in fair agreement with each other and are slightly steeper than the theoretical profile. The third profile was measured at a point further downstream and probably applies to the start of the transition to turbulent flow. These profiles indicate that the heat transfer coefficient is slightly higher than the theoretical value.

The temperature profile measurements give profiles that are generally steeper than the theoretical profiles, with the greatest deviation from theory occurring in blowing runs and the least deviation occurring in

suction runs. These results will be discussed more fully following the section covering direct heat transfer measurements.

Turbulent regime.- In figures 18 and 21 the dimensionless temperature $\beta_H = \frac{T_o - T}{T_o - T_1}$ is plotted as a function of the dimensionless distance ratio y/ξ for cases where the boundary layer was turbulent. Each curve represents data obtained at several different traversing stations and consequently represents a wide variation in downstream distance. Figure 21 shows data obtained in a run with no mass transfer at $u_1 = 16.2$ fps. Figure 18(a) shows data obtained with blowing at constant $\phi_H = 1.23$ and $u_1 = 19.6$ fps, and figure 18(b) presents data obtained with a constant blowing velocity $v_o = 0.04$ fps and $u_1 = 20$ fps. In the latter two figures, the data are compared directly with corresponding velocity profiles. When plotted in this way, the profiles for a given run are all found to be similar except in the region very near the wall.

The degree of similarity of the profiles is best in the runs with no mass transfer or with blowing at constant ϕ_H. Although the precision of the experimental data does not permit a definite conclusion, it appears that, in the run with constant blowing velocity, there is a slight change in the shapes of the temperature and velocity profiles with distance from the leading edge, possibly because of the change in the value of ϕ_H.

The turbulent profiles were examined on logarithmic coordinates to investigate their tendency to follow a power-law distribution. The resulting plots could be fitted by a straight line, although the scatter of the data was such that there is no assurance that the profiles actually should give a straight line. Inspection of the data shows that the points might be better fitted by a line with some upward curvature, but the precision of the data was not good enough to justify trying to fit such a curve to the results. The velocity profile with no mass transfer (fig. 17, $u_1 = 25.8$ fps) had a slope of 0.214 and the temperature profile with no mass transfer (fig. 21, $u_1 = 16.2$ fps) had a slope of 0.19 when plotted on logarithmic coordinates. The profiles made with blowing at constant ϕ_H (fig. 18(a)) had a slope of 0.265 and the profiles made with a constant blowing velocity of 0.04 fps ($\phi_H = 0.55$ to 0.85) had a mean slope of 0.25. These slopes are valid for values of y/ϑ or y/ξ greater than about 0.1. The results indicate that an increase in the blowing rate increased the slope of the turbulent profiles when plotted on logarithmic coordinates.

The comparison of profiles for similarity was made by making the distance from the wall dimensionless by dividing the distance by the momentum or enthalpy thickness. However, if the profiles are similar

when based on this measure of boundary-layer thickness, it can be shown that they will be similar when compared on the basis of the 99-percent-point thickness and will have the same power-law exponent if a power law is applicable.

Heat Transfer Coefficients

Laminar regime.- The results of direct measurements of heat transfer coefficients are presented in figures 13(a) to 13(f). Figure 13(a) shows results for all runs with no mass transfer. The data for the laminar regime for these runs show that the measured coefficients are generally in fair agreement with boundary-layer theory but tend to be high. This is in agreement with the finding that the temperature profiles are steeper than the theoretical profiles. This deviation from theory is believed to be due to the nature of the test wall used for these experiments and will be discussed more fully later.

Figure 13(b) shows results for runs with blowing at a constant value of ϕ_H (inverse square-root distribution for the laminar regime). Because the stability of the boundary layer is decreased by blowing and transition occurs at a lower length Reynolds number, all of the laminar data for blowing had to be measured in the front compartments of the tunnel. These compartments had fewer thermocouples and the wall temperature measurements were less precise. In addition, errors due to heat losses were important because of the low absolute values of the coefficients. Consequently, the precision of these measurements was poor. The data indicate that, generally, the measured coefficients are substantially higher than the values predicted by boundary-layer theory, although this is not true in all cases. Some of the measurements are in fair agreement with theory. The fact that the measurements are generally high is in agreement with the previous observation that the thermal boundary layer as indicated by the temperature profile is not thickened to the extent predicted by theory.

Figure 13(c) shows the results for runs with a constant blowing velocity. No theoretical calculations were available for the case of heat transfer with uniform blowing in laminar flow, so an approximate curve, indicating predicted values, was determined by calculating the value of ϕ_H at the point in question and then using the correction factor θ_H corresponding to that value of ϕ_H as predicted by laminar-boundary-layer theory for a $1/\sqrt{x}$ blowing distribution. The agreement between the measured coefficients and the "predicted" values is fair, although the precision of the measured values is poor.

The results of runs with suction with an inverse square-root distribution are presented in figure 13(e). The data are in fair agreement with boundary-layer theory but tend to be high, again in agreement with

the measured temperature profiles. Figure 13(f) shows runs with uniform suction velocity. These data are also seen to be somewhat high at low suction rates; but at high suction rates the agreement with theory is good, although individual points scatter widely. This was due to the fact that in runs with high suction rates nonuniformity of heating of the screen caused the readings of the wall thermocouples to scatter, resulting in poor precision of the heat transfer measurements.

Turbulent regime.- Figure 13(a) presents results of runs with no mass transfer. The experimental points in the turbulent region are compared with the predictions of the Chilton-Colburn empirical relation

$$\frac{h_*}{u_1 \rho_1 c_p}\left(\frac{c_p \mu}{k}\right)^{2/3} = \frac{0.0288}{(R_x)^{0.2}}$$

This relation is seen to be in good agreement with the experimental data.

Experimental data for runs with blowing or suction are presented in figures 13(b) to 13(f). In all cases except run H-27a of figure 13(d), the experimental points are compared with the predictions of film theory, using the Chilton-Colburn relation to predict h_*.

In addition, figure 22 compares film theory and experiment on the basis of the correction factor $\theta_H = h/h_*$ plotted as a function of the rate factor $\phi_H = v_o \rho c_p / h_*$. In every case, when the flow has become fully turbulent the experimental data, despite the scatter, appear to be in agreement with film theory provided that the mass transfer distribution upstream of the points where the measurements were taken was reasonably constant. This is the case in all runs with constant suction velocity and all runs with a constant value of ϕ_H in the turbulent region ($v_o \propto 1/x^{0.2}$). In runs where there was some other mass transfer distribution, the experimental results differ from film theory. This can be seen in figure 13(b), run H-10, and figure 13(e), runs H-13 and H-15. In these runs an inverse square-root distribution was used throughout the entire tunnel, including the turbulent region. In these cases the mass transfer rate upstream of a given point was higher than it would have been if there had been a constant velocity equal to the local velocity at the given point. As a result, the boundary layer in the blowing run was thicker than it would have been with uniform blowing, and the measured coefficient was lower than the prediction of film theory. Similarly, in the suction runs the boundary layer was thinner than it would have been with uniform suction, resulting in coefficients higher than the values predicted by film theory. In run H-12, in which suction through compartment G was inadvertently omitted, the coefficients downstream of this point were all lower than the predicted values based

on local suction rates. This indicates that the boundary-layer thickness downstream of compartment G was greater than it would have been if that compartment had had normal suction.

It was pointed out earlier that simple film theory makes no allowance for the effect of variations of film thickness. Apparently this is not a serious defect if the mass transfer distribution is reasonably constant, but some allowance should be made for film thickness if there is an unusual mass transfer distribution upstream of the point at which the calculation is to be made. The data for the $1/\sqrt{x}$ distribution in the turbulent regime are in better agreement with film theory if equation (26)

$$\theta = \frac{\phi}{\left(\exp \frac{\phi\Delta}{\Delta_*}\right) - 1}$$

is used and Δ/Δ_* is taken to be equal to $\bar{v}_o/v_o$ where $\bar{v}_o$ is the length mean mass transfer velocity. It is possible that some correction of this type will be found suitable, but the preferred form cannot be defined at this time. The limited data presented here are sufficient to show the desirability of an allowance of this sort but are not considered adequate to show how much this correction should be.

The blowing runs were made under two different conditions of heating. Runs denoted by the letter "a" were made with air at a uniform temperature blown into each compartment. There was no additional heat supplied to the test wall; the wall was allowed to reach an equilibrium temperature. In runs denoted by the letter "b" additional heat was supplied to the test wall so that it reached a uniform temperature equal to that of the gas being blown through the compartment. There was no noticeable difference between the heat transfer coefficients determined in the two cases when conditions otherwise were the same. In constant-gas-temperature runs, a wall velocity proportional to $1/x^{0.2}$ resulted in a constant wall temperature.

Figure 13(d) presents the results of run H-27a. This run was made with a constant blowing velocity of 0.12 fps and with a uniform blowing gas temperature. The main-stream velocity was about 60 fps at the leading edge and accelerated uniformly to about 70 fps at the end of the tunnel. This run was therefore identical with run H-20a except for the addition of acceleration of the main stream. The experimental points are compared with values obtained at the same compartments in run H-20a after adjusting these values for the Reynolds number effect due to small differences in main-stream velocity. The experimental results are also

tabulated in table VII. The measurement of Euler number in this run was quite rough. This was an exploratory test and the results should not be considered conclusive. There is a qualitative indication that at Euler numbers significantly different from zero acceleration of the main stream increases the heat transfer coefficient by an amount substantially greater than the increase predicted solely on the basis of the increased Reynolds number. This is a crude method of predicting the transfer coefficient and more refined techniques might result in better agreement.

Transition Reynolds Number

The Reynolds number at which transition to turbulent flow occurred is plotted as a function of the dimensionless mass transfer velocity at the transition point v_o/u_1 in figure 23. These transition points were not measured directly but were estimated from plots of friction factor and/or heat transfer coefficients as a function of length Reynolds number. The plot can be used only to exhibit trends. Qualitatively, it is evident that mass transfer has a significant effect on the transition to turbulence. In agreement with theory it was found that suction delays the onset of turbulence while blowing hastens its occurrence.

Behavior of Porous Wall

The experimental results deviate in a number of respects from what might be expected on the basis of previous experimental and theoretical work. With no mass flow, transition to turbulence in the tunnel occurred at a Reynolds number of approximately 1.5×10^5, an unusually low value. Measured turbulent friction factors were generally higher than the values that would be predicted by the usual equation

$$\frac{c_{f_*}}{2} = \frac{0.0296}{(R_x)^{0.2}}$$

and the experimentally measured effect of Reynolds number was a function of the main-stream velocity. Turbulent velocity profiles, although similar, did not vary as $\left(\frac{y}{\vartheta}\right)^{1/7}$ but generally exhibited a larger exponent. Laminar temperature profiles were usually steeper than theoretical profiles.

These and similar effects might result from one or more of the following factors: Error in measurement, high over-all turbulence level in the tunnel, roughness of the porous surface, and vibration of the porous test wall.

Although measurement error can explain moderate deviations in the data, it does not account for a number of significant effects.

The turbulence level of the tunnel was measured by means of a hot-wire technique. The turbulence intensity of the main stream was approximately 0.3 percent. A level of this magnitude cannot explain the effects noted.

It appears probable that the porous surface, although superficially smooth, is aerodynamically rough. A rough surface could account for many of the over-all effects noted but does not seem to be the complete explanation. For example, in the absence of other effects, a rough surface would not be expected to result in a friction coefficient which varied with velocity in a manner which was not directly related to the variation in Reynolds number.

Study of the test wall under operating conditions disclosed the presence of an oscillation of the wall that appeared to be directly related to vibrations in the blower which supplied the main-stream air. These oscillations were of very small amplitude in the vertical plane and exhibited maximum amplitude at a main-stream velocity of about 26 fps. Unfortunately, the vibration was not isolated until late in the program when it became apparent that an anomalous effect was influencing the results. Subsequent work has shown that the screen oscillation can be eliminated, but this was not done in the work reported here. It is believed that the screen oscillation significantly affected the data obtained at 26 fps but was of secondary importance at other velocities.

SUMMARY OF RESULTS

The effect on the boundary layer of blowing or sucking air through a porous flat plate into or out of a main air stream flowing parallel to the plate was studied theoretically and experimentally. Theory and experiment showed qualitative agreement in all cases. Suction decreased the boundary-layer thickness, increased the magnitude of the friction and heat transfer coefficients, and delayed the transition from laminar to turbulent flow. Blowing increased the boundary-layer thickness, decreased the magnitude of the friction and heat transfer coefficients, and hastened the transition from laminar to turbulent flow.

In the laminar regime the predictions of boundary-layer theory were not always in quantitative agreement with experiment. The largest deviations were observed when blowing occurred. The discrepancies appeared to be due to test-wall roughness and vibration.

An adequate theoretical treatment of the turbulent boundary layer is not available. A simplified approximate method of analysis termed "film theory" was used in this work. Within the accuracy of the experimental data, film theory predicted the experimentally observed effect of mass transfer on the turbulent friction and heat transfer coefficients when the mass transfer rate was independent of x (the axial distance from the leading edge of the plate) or varied as $1/x^{0.2}$. When the mass transfer rate varied more rapidly with x, simple film theory showed greater departures from experiment. The accuracy of the experimentally measured coefficients, particularly of the friction coefficients, did not provide a conclusive confirmation of the predictions of film theory. Film theory appears to be the best prediction technique now available, but further work may lead to a more realistic method.

Measured turbulent velocity and temperature boundary-layer profiles were found to be similar when the mass transfer rate was independent of distance from the leading edge of the plate or varied as $1/x^{0.2}$. The similarity was observed when the dimensionless velocity u/u_1 was plotted versus the dimensionless distance y/ϑ and the dimensionless temperature $\frac{T_o - T}{T_o - T_1}$ was plotted versus the dimensionless distance y/ξ, where u denotes the x component of the local velocity; u_1, the main-stream velocity; y, the normal distance from the plate; ϑ, the momentum thickness; T, the local temperature; T_o, the wall temperature at $y = 0$; T_1, the main-stream temperature; and ξ, the enthalpy thickness. The relationship between the dimensionless profile parameter and the dimensionless distance parameter could be fitted reasonably well by a straight line on logarithmic coordinates. The slope of this line was a function of the mass transfer rate, increasing with an increase in blowing rate.

Massachusetts Institute of Technology,
Cambridge, Mass., February 4, 1953.

REFERENCES

1. Stefan, J.: Sitzungsber. Kaiser Akad. Wiss. Wien, Math. naturwiss. Klasse, Bd. 68, 1874, p. 385. (See Jakob, Max: Heat Transfer. Vol. I. John Wiley & Sons, Inc., c. 1949, pp. 598, 601.)

2. Lewis, W. K., and Chang, K. C.: The Mechanism of Rectification, III. Trans. Am. Inst. Chem. Eng., vol. 21, 1928, pp. 127-138.

3. Sherwood, T. K.: Absorption and Extraction. First ed., McGraw-Hill Book Co., Inc., 1937, p. 11.

4. Colburn, A. P., and Drew, T. B.: The Condensation of Mixed Vapors. Trans. Am. Inst. Chem. Eng., vol. 33, 1937, pp. 197-212.

5. Ackermann, G.: Warmeübergang und molekulare Stoffübertragung im gleichen Feld bei grossen Temperatur- und Partialdruckdifferenzen. Forschungsheft 382, Forsch. Geb. Ing.-Wes., 1937.

6. Friedman, J.: Studies of the Gas Phase Transpiration Cooling Process Using Air as a Coolant. Symposium on Heat Transfer Problems in Jet Propulsion (Los Angeles and Pasadena), 1948. (Paper not generally available.)

7. Prandtl, L.: Über Flüssigkeitsbewegung bei sehr kleiner Reibung. Verh. dritten Internationalen Mathematikerkongresses (Heidelberg, 1904), Teubner (Leipzig), 1905, pp. 484-491. (Available in English translation as NACA TM 452.)

8. Fluid Motion Panel of the Aeronautical Research Committee and Others (S. Goldstein, ed.): Modern Developments in Fluid Dynamics. Vol. II. The Clarendon Press (Oxford), 1938, p. 534.

9. Damköhler, Gerhard: Die laminare Grenzschicht beim Stofftransport von und zur Längsangeströmten ebenen Platte. Zs. Elektrochemie, vol. 48, no. 4, 1942, pp. 178-181.

10. Schlichting, H., and Bussmann, K.: Exakte Lösungen für die laminare Grenzschicht mit Absaugung und Ausblasen. Schriften, Deutsche Akad. Luftfahrtforschung, Sonderdruck aus Bd. 7B, Heft 2, 1943, pp. 25-69.

11. Schlichting, H.: The Boundary Layer of the Flat Plate Under Conditions of Suction and Air Injection. Luftfahrtforschung, Bd. 19, Lfg. 9, Oct. 20, 1942, pp. 293-301. (Available in English translation as RTP Translation 1753, British Ministry of Aircraft Production.)

12. Schlichting, H.: An Approximate Method for Calculation of the Laminar Boundary Layer With Suction for Bodies of Arbitrary Shape. NACA TM 1216, 1949.

13. Schuh, H.: The Solution of the Laminar-Boundary-Layer Equation for the Flat Plate for Velocity and Temperature Fields for Variable Physical Properties and for the Diffusion Field at High Concentration. NACA TM 1275, 1950.

14. Thwaites, B.: An Exact Solution of the Boundary-Layer Equations Under Particular Conditions of Porous Surface Suction. R. & M. No. 2241, British A.R.C., 1946.

15. Yuan, Shao Wen: Heat Transfer in Laminar Compressible Boundary Layer on a Porous Flat Plate With Fluid Injection. Jour. Aero. Sci., vol. 16, no. 12, Dec. 1949, pp. 741-748.

16. Eckert, E., and Lieblein, V.: Berechnung des Stoffüberganges an einer ebenen Längsangeströmten Oberfläche bei grossen Teildruckgefälle. Forsch. Geb. Ing.-Wes., Bd. 16, Nr. 2, Sept.-Oct. 1949, pp. 33-42. (See also Eckert, E.R.G.: Introduction to the Transfer of Heat and Mass. First ed., McGraw-Hill Book Co., Inc., 1950, p. 67.)

17. Ulrich, A.: Theoretical Investigation of Drag Reduction in Maintaining the Laminar Boundary Layer by Suction. NACA TM 1121, 1947.

18. Lew, H. G.: On the Compressible Boundary Layer Over a Flat Plate With Uniform Suction. Reissner Anniversary Volume, J. W. Edwards Co. (Ann Arbor), 1949, pp. 43-60.

19. Ringleb, Friedrich O.: Computation of the Laminar Boundary Layer With Suction. Jour. Aero. Sci., vol. 19, no. 1, Jan. 1952, pp. 48-54.

20. Iglisch, R.: Exakte Berechnung der laminaren Grenzschicht an der Längsangeströmten ebenen Platte mit homogener Absaugung. Schriften, Deutsche Akad. Luftfahrtforschung, Bd. 8B, Heft 1, 1944. (Available in English translation as NACA TM 1205.)

21. Brown, W. Byron, and Donoughe, Patrick L.: Tables of Exact Laminar-Boundary-Layer Solutions When the Wall Is Porous and Fluid Properties Are Variable. NACA TN 2479, 1951.

22. Libby, Paul A., Kaufman, Lawrence, and Harrington, R. Paul: An Experimental Investigation of the Isothermal Laminar Boundary Layer on a Porous Flat Plate. Jour. Aero. Sci., vol. 19, no. 2, Feb. 1952, pp. 127-134.

23. Duwez, Pol, and Wheeler, H. L., Jr.: Experimental Study of Cooling by Injection of a Fluid Through a Porous Material. Jour. Aero. Sci., vol. 15, no. 9, Sept. 1948, pp. 509-521.

24. Blasius, H.: Grenzschichten in Flüssigkeiten mit kleiner Reibung. Zs. Math. und Phys., Bd. 56, Heft 1, 1908, pp. 1-37. (Available in English translation as NACA TM 1256.)

25. Pohlhausen, E.: Der Wärmeaustausch zwischen festen Körpern und Flüssigkeiten mit kleiner Reibung und kleiner Wärmeleitung. Z.a.M.M., Bd. 1, Heft 2, Apr. 1921, pp. 115-121.

26. Wilke, C. R.: Diffusional Properties of Multicomponent Gases. Chem. Eng. Prog., vol. 46, no. 2, Feb. 1950, pp. 95-104.

27. Curtiss, C. F., and Hirschfelder, J. O.: Transport Properties of Multicomponent Gas Mixtures. Jour. Chem. Phys., vol. 17, no. 6, June 1949, pp. 550-555.

28. Bromley, L. A., and Wilke, C. R.: Viscosity Behavior of Gases. Ind. and Eng. Chem., vol. 43, July 1951, pp. 1641-1648.

29. Lindsay, A. L., and Bromley, L. A.: Thermal Conductivity of Gas Mixtures. Ind. and Eng. Chem., vol. 42, Aug. 1950, pp. 1508-1511.

TABLE I.- THEORETICAL VALUES OF $2\beta'(0)$ CALCULATED FROM LAMINAR-BOUNDARY-LAYER THEORY

C	$2\beta'(0)$								
	Z = 0.6	Z = 0.7	Z = 0.8	Z = 0.9	Z = 1.0	Z = 1.1	Z = 1.4	Z = 2.0	Z = 5.0
-1.0	0.2321	0.2067	0.1831	0.1615	0.1419	0.1242	0.08219	0.03423	0.0002818
-.75	.4448	.4290	.4116	.3933	.3747	.3560	.3019	.2098	.02531
-.5	.6600	.6644	.6649	.6626	.6580	.6516	.6527	.5587	.2533
-.25					.9787				
0	1.108	1.170	1.228	1.280	1.328	1.374		1.689	
.5	1.579	1.716	1.845	1.970	2.092	2.213		3.193	
1.0	2.069	2.288	2.501	2.709	2.916	3.121		4.892	
1.5	2.576	2.885	3.189	3.487	3.784	4.080		6.699	
3.0	4.174	4.765	5.354	5.943	6.529	7.115		12.41	
5.0	6.417	7.402	8.388	9.374	10.36	11.35		20.26	

TABLE II.- THEORETICAL VALUES OF $\beta(\eta)$ CALCULATED FROM LAMINAR-BOUNDARY-LAYER THEORY

$$\left[C = -\frac{2v_o}{u_1}\sqrt{\frac{u_1\rho x}{\mu}};\ \eta = \frac{y}{2x}\sqrt{\frac{u_1\rho x}{\mu}};\ \beta_F = u/u_1;\ \beta_H = \frac{T_o - T}{T_o - T_1};\ \beta_D = \frac{X_{io} - X_i}{X_{io} - X_{il}};\ Z_F = 1;\ Z_H = \frac{c_p\mu}{k};\ Z_D = \frac{\mu}{\rho D_{im}} \right]$$

η	$\beta(\eta)$				
	Z = 0.60	Z = 0.72	Z = 1.00	Z = 2.00	Z = 5.00
Suction; C = 0.5					
0		0	0		
.2		.1680	.1990		
.4		.3233	.3774		
.6		.4645	.5337		
.8		.5895	.6658		
1.0		.6965	.7722		
1.2		.7844	.8532		
1.4		.8533	.9110		
1.6		.9046	.9494		
1.8		.9409	.9731		
2.0		.9651	.9867		
2.2		.9804	.9939		
2.4		.9896	.9974		
2.6		.9947	.9990		
2.8		.9975	.9997		
3.0		.9989	.9999		
3.2		.9995	1.0000		
3.4		.9998			
3.6		.9999			
3.8		1.0000			
Suction; C = 1.0					
0	0	0	0	0	0
.2	.1949	.2170	.2641	.4024	.6728
.4	.3665	.4032	.4776	.6659	.9073
.6	.5149	.5596	.6453	.8287	.9785
.8	.6398	.6869	.7714	.9209	.9961
1.0	.7416	.7864	.8609	.9675	.9996
1.2	.8213	.8606	.9205	.9883	1.0000
1.4	.8811	.9132	.9575	.9961	
1.6	.9240	.9485	.9788	.9989	
1.8	.9534	.9710	.9901	.9998	
2.0	.9736	.9844	.9957	.9999	
2.2	.9845	.9921	.9983	1.0000	
2.4	.9917	.9962	.9994		
2.6	.9957	.9983	.9998		
2.8	.9979	.9993	.9999		
3.0	.9990	.9997	1.0000		
3.2	.9996	.9999	1.0000		
3.4	.9998	1.0000			
3.6	.9999	1.0000			
3.8	1.0000				

TABLE II.- THEORETICAL VALUES OF $\beta(\eta)$ CALCULATED FROM LAMINAR-BOUNDARY-LAYER THEORY - Continued

η	$\beta(\eta)$				
	Z = 0.60	Z = 0.72	Z = 1.00	Z = 2.00	Z = 5.00
			Suction; C = 1.5		
0		0	0		
.2		.2646	.3263		
.4		.4754	.5644		
.6		.6393	.7324		
.8		.7620	.8449		
1.0		.8499	.9156		
1.2		.9097	.9571		
1.4		.9484	.9796		
1.6		.9719	.9910		
1.8		.9855	.9963		
2.0		.9929	.9986		
2.2		.9967	.9996		
2.4		.9986	.9999		
2.6		.9994	1.0000		
2.8		.9998			
3.0		1.0000			
			Suction; C = 3.0		
0		0	0		
.1		.2471	.2820		
.2		.4174	.4902		
.3		.5535	.6428		
.4		.6615	.7534		
.5		.7462	.8325		
.6		.8120	.8880		
.7		.8624	.9265		
.8		.9006	.9526		
.9		.9291	.9700		
1.0		.9501	.9813		
1.1		.9653	.9886		
1.2		.9762	.9932		
1.3		.9839	.9960		
1.4		.9892	.9977		
1.5		.9929	.9987		
1.6		.9954	.9993		
1.7		.9970	.9996		
1.8		.9981	.9998		
1.9		.9988	.9999		
2.0		.9993	1.0000		
2.2		.9998			
2.4		.9999			
2.6		.9999			
2.8		1.0000			
			Suction; C = 5.0		
0	0	0	0	0	
.04	.1209	.1416	.1882	.3339	
.08	.2282	.2641	.3421	.5577	
.12	.3232	.3701	.4681	.7072	
.16	.4073	.4618	.5709	.8070	
.20	.4818	.5409	.6548	.8733	
.28	.6057	.6678	.7766	.9463	
.36	.7019	.7615	.8577	.9777	
.44	.7761	.8302	.9104	.9910	
.52	.8330	.8801	.9443	.9965	
.60	.8763	.9160	.9657	.9987	
.68	.9091	.9417	.9792	.9995	
.76	.9336	.9599	.9875	.9999	
.84	.9519	.9726	.9926	.9999	
.92	.9654	.9815	.9957	1.0000	
1.00	.9753	.9876	.9975		
1.08	.9825	.9918	.9986		
1.16	.9877	.9946	.9992		
1.24	.9914	.9965	.9996		
1.32	.9940	.9978	.9998		
1.40	.9959	.9986	.9999		
1.48	.9972	.9991	1.0000		
1.56	.9981	.9995			
1.64	.9987	.9997			
1.72	.9992	.9998			
1.80	.9994	.9999			
1.88	.9996	1.0000			
1.96	.9998	1.0000			
2.04	.9999				
2.12	.9999				
2.20	.9999				
2.28	1.0000				
2.36	1.0000				

TABLE II.- THEORETICAL VALUES OF $\beta(\eta)$ CALCULATED FROM LAMINAR-BOUNDARY-LAYER THEORY - Continued

η	$\beta(\eta)$				
	Z = 0.60	Z = 0.72	Z = 1.00	Z = 2.00	Z = 5.00
No mass transfer; C = 0					
0	0	0	0	0	
.2	.1108	.1182	.1328	.1688	
.4	.2211	.2359	.2647	.3355	
.6	.3300	.3517	.3938	.4950	
.8	.4358	.4636	.5168	.6399	
1.0	.5363	.5689	.6298	.7623	
1.2	.6293	.6647	.7290	.8567	
1.4	.7125	.7486	.8115	.9221	
1.6	.7843	.8189	.8761	.9624	
1.8	.8438	.8750	.9233	.9839	
2.0	.8911	.9176	.9555	.9940	
2.2	.9269	.9482	.9759	.9981	
2.4	.9529	.9690	.9878	.9994	
2.6	.9709	.9823	.9942	.9999	
2.8	.9828	.9904	.9975	1.0000	
3.0	.9902	.9951	.9990		
3.2	.9947	.9976	.9996		
3.4	.9972	.9989	.9999		
3.6	.9986	.9995	1.0000		
3.8	.9994	.9998	1.0000		
4.0	.9997	.9999			
4.2	.9999	.9999			
4.4	1.0000	1.0000			
Blowing; C = -0.25					
0	0	0	0	0	0
.2	.0894	.0934	.1003	.1117	.1114
.4	.1813	.1900	.2053	.2340	.2510
.6	.2750	.2888	.3138	.3646	.4160
.8	.3694	.3886	.4237	.4985	.5913
1.0	.4629	.4871	.5317	.6279	.7524
1.2	.5533	.5818	.6339	.7439	.8751
1.4	.6383	.6698	.7262	.8385	.9496
1.6	.7158	.7484	.8052	.9080	.9844
1.8	.7838	.8157	.8688	.9533	.9964
2.0	.8411	.8706	.9168	.9790	.9994
2.2	.8875	.9131	.9505	.9917	.9999
2.4	.9234	.9443	.9724	.9968	1.0000
2.6	.9498	.9660	.9856	.9992	
2.8	.9685	.9802	.9930	.9998	
3.0	.9810	.9891	.9969	1.0000	
3.2	.9890	.9943	.9987		
3.4	.9939	.9972	.9995		
3.6	.9968	.9987	.9998		
3.8	.9984	.9994	.9999		
4.0	.9992	.9997	1.0000		
4.2	.9996	.9999			
4.4	.9998	1.0000			
4.6	.9999				
4.8	1.0000				
Blowing; C = -0.5					
0	0	0	0	0	0
.2	.0680	.0688	.06918	.0618	.0328
.4	.1401	.1424	.1454	.1368	.0860
.6	.2161	.2208	.2286	.2263	.1685
.8	.2955	.3032	.3182	.3298	.2872
1.0	.3774	.3887	.4124	.4444	.4402
1.2	.4604	.4754	.5088	.5643	.6109
1.4	.5426	.5613	.6038	.6807	.7697
1.6	.6220	.6438	.6933	.7842	.8885
1.8	.6963	.7200	.7734	.8672	.9576
2.0	.7634	.7878	.8411	.9266	.9877
2.2	.8218	.8454	.8948	.9639	.9974
2.4	.8704	.8919	.9344	.9844	.9996
2.6	.9093	.9277	.9617	.9941	1.0000
2.8	.9389	.9538	.9791	.9981	1.0000
3.0	.9605	.9719	.9893	.9995	
3.2	.9755	.9837	.9949	.9999	
3.4	.9854	.9910	.9978	1.0000	
3.6	.9917	.9953	.9991	1.0000	
3.8	.9954	.9976	.9997		
4.0	.9976	.9989	.9999		
4.2	.9988	.9995	1.0000		
4.4	.9994	.9998	1.0000		
4.6	.9997	.9999	1.0000		
4.8	.9999	1.0000	1.0000		
5.0	1.0000	1.0000	1.0000		
5.2	1.0000	1.0000			
5.4	1.0000	1.0000			
5.6	1.0000				

TABLE II.- THEORETICAL VALUES OF $\beta(\eta)$ CALCULATED FROM LAMINAR-BOUNDARY-LAYER THEORY - Concluded

η	$\beta(\eta)$				
	Z = 0.60	Z = 0.72	Z = 1.00	Z = 2.00	Z = 5.00
Blowing; C = -0.75					
0	0	0	0	0	0
.2	.0465	.0452	.0404	.0245	.0038
.4	.0974	.0954	.0873	.0574	.0116
.6	.1528	.1508	.1414	.1011	.0278
.8	.2129	.2118	.2032	.1583	.0591
1.0	.2774	.2780	.2728	.2309	.1160
1.2	.3460	.3491	.3499	.3198	.2100
1.4	.4178	.4241	.4331	.4232	.3468
1.6	.4915	.5014	.5201	.5362	.5175
1.8	.5655	.5792	.6076	.6507	.6938
2.0	.6379	.6548	.6919	.7569	.8398
2.2	.7064	.7258	.7689	.8456	.9336
2.4	.7691	.7899	.8352	.9116	.9790
2.6	.8242	.8450	.8890	.9549	.9951
2.8	.8708	.8903	.9295	.9797	.9992
3.0	.9085	.9257	.9580	.9920	.9999
3.2	.9377	.9520	.9766	.9973	1.0000
3.4	.9592	.9704	.9878	.9992	
3.6	.9743	.9826	.9941	.9998	
3.8	.9845	.9903	.9974	1.0000	
4.0	.9910	.9948	.9989		
4.2	.9950	.9974	.9996		
4.4	.9974	.9988	.9999		
4.6	.9987	.9995	1.0000		
4.8	.9994	.9998			
5.0	.9997	.9999			
5.2	.9999	1.0000			
5.4	1.0000				
Blowing; C = -1.0					
0	0	0	0	0	0
.2	.0247	.0222	.0157	.0042	.000047
.4	.0525	.0477	.0349	.0105	.000179
.6	.0837	.0770	.0582	.0198	.000530
.8	.1189	.1105	.0865	.0335	.00145
1.0	.1582	.1488	.1207	.0534	.0038
1.2	.2020	.1922	.1616	.0819	.0096
1.4	.2505	.2409	.2100	.1218	.0228
1.6	.3036	.2952	.2664	.1760	.0512
1.8	.3611	.3549	.3308	.2467	.1005
2.0	.4226	.4193	.4028	.3349	.2019
2.2	.4872	.4875	.4808	.4385	.3442
2.4	.5535	.5579	.5625	.5519	.5224
2.6	.6200	.6285	.6445	.6663	.7042
2.8	.6848	.6969	.7229	.7710	.8505
3.0	.7459	.7608	.7940	.8571	.9407
3.2	.8013	.8180	.8547	.9199	.9822
3.4	.8498	.8668	.9032	.9601	.9961
3.6	.8904	.9065	.9393	.9825	.9994
3.8	.9230	.9372	.9643	.9933	.9999
4.0	.9480	.9598	.9804	.9978	1.0000
4.2	.9662	.9754	.9899	.9994	1.0000
4.4	.9790	.9857	.9952	.9998	
4.6	.9874	.9921	.9979	1.0000	
4.8	.9928	.9953	.9991	1.0000	
5.0	.9961	.9979	.9997		
5.2	.9974	.9990	.9999		
5.4	.9990	.9996	1.0000		
5.6	.9995	.9998	1.0000		
5.8	.9998	.9999	1.0000		
6.0	.9999	1.0000	1.0000		
6.2	1.0000	1.0000			
6.4	1.0000				
6.6	1.0000				

TABLE III.- SUMMARY OF VELOCITY PROFILE MEASUREMENTS

Run	u_1, fps	Axial Euler number	Main-stream fluid	Injected fluid	Axial mass transfer distribution	x, in.	R_x	v_o (local), fps	δ^*, in.	ϑ, in.
V-1	25.8	0	Air	None	No transfer	3.6	46,000	0	0.026	0.011
						6.9	88,000		.044	.023
						16.2	206,000		.075	.052
						22.1	280,000		.092	.064
						30.1	382,000		.123	.085
						38.8	492,000		.150	.105
						46.9	595,000		.170	.122
						70.8	898,000		.260	.185
						96.4	1,220,000		.322	.234
V-2	58.7	0	Air	None	No transfer	6.9	200,000	0	.044	.028
						22.1	640,000		.101	.070
						46.9	1,350,000		.173	.125
						70.8	2,040,000		.254	.182
						96.4	2,780,000		.286	.215
V-3	26.0	0	Air	Air	Uniform blowing	3.6	46,000	.0542	.040	.018
						6.9	88,000	.0535	.063	.041
						16.2	207,000	.0534	.119	.078
						22.1	283,000	.0535	.156	.103
						30.1	385,000	.0534	.204	.133
						38.8	496,000	.0535	.254	.168
						46.9	600,000	.0538	.295	.198
						83.5	1,070,000	.0540	.525	.340
						96.4	1,230,000	.0544	.582	.388
V-4	25.9	0	Air	Air	Uniform blowing	3.6	46,000	.128	.050	.029
						6.9	88,000	.128	.096	.062
						16.2	206,000	.128	.205	.123
						30.1	383,000	.131	.348	.201
						46.9	598,000	.131	.522	.304
						83.5	1,064,000	.130	.914	.516
V-5 (H-8)	19.6	0	Air	Air	Blowing at constant ϕ_H; $\phi_H = 1.2$	6.6	63,100	.0923	.088	.059
						22.1	217,200	.0736	.211	.134
						46.5	462,000	.0639	.373	.237
						83.1	803,000	.0577	.604	.384
V-6	26.3	0	Air	Air	Uniform blowing	3.6	47,000	.260	.072	.043
						6.9	89,000	.265	.156	.089
						11.2	145,000	.260	.240	.131
						16.2	210,000	.258	.409	.186
						22.1	286,000	.260	.496	.249
						30.1	389,000	.260	.721	.323
						46.9	607,000	.258	1.080	.482
V-7	25.8	0	Air	Air	Uniform suction	3.6	46,000	-.260	.006	.003
						6.9	88,000	-.266	.009	.004
						11.2	142,000	-.260	.006	.003
						16.2	206,000	-.260	.006	.003
						22.1	280,000	-.261	.008	.004
						30.1	382,000	-.261	.007	.004

TABLE III.- SUMMARY OF VELOCITY PROFILE MEASUREMENTS - Concluded

Run	u_1, fps	Axial Euler number	Main-stream fluid	Injected fluid	Axial mass transfer distribution	x, in.	R_x	v_o (local), fps	δ^*, in.	ϑ, in.
V-8	25.7	0	Air	Air	Uniform suction	3.6	46,000	-0.130	0.009	0.004
						6.9	87,000	-.131	.016	.008
						11.2	142,000	-.130	.013	.006
						16.2	205,000	-.129	.011	.006
						22.1	279,000	-.130	.016	.008
						30.1	380,000	-.130	.015	.009
						38.8	490,000	-.130	.019	.012
						46.9	593,000	-.129	.022	.014
						70.8	895,000	-.130	.016	.009
V-9	26.7	0	Air	Air	Suction; $v_o \propto 1/\sqrt{x}$; $C = 5.0$	3.6	47,000	-.311	.004	.002
						6.9	91,000	-.224	.010	.005
						11.2	147,000	-.174	.008	.005
						16.2	213,000	-.143	.009	.005
						22.1	290,000	-.121	.015	.007
						30.1	395,000	-.105	.022	.013
						38.8	510,000	-.0922	.026	.017
						46.9	616,000	-.0832	.032	.023
						70.8	930,000	-.0687	.056	.041
						83.5	1,100,000	-.0630	.068	.050
						96.4	1,270,000	-.0585	.086	.066
V-10	25.9	0	Air	Air	Suction; $v_o \propto 1/\sqrt{x}$; $C = 3.0$	3.6	46,000	-.188	.006	.003
						6.9	88,000	-.134	.015	.007
						11.2	142,000	-.104	.013	.007
						16.2	206,000	-.0856	.014	.008
						22.1	280,000	-.0726	.022	.013
						30.1	383,000	-.0627	.034	.023
						46.9	598,000	-.0496	.058	.041
						83.5	1,064,000	-.0377	.118	.087
V-11	25.9	0	Air	Air	Uniform suction	3.6	46,000	-.0520	.015	.007
						6.9	88,000	-.0524	.024	.011
						11.2	142,000	-.0521	.023	.012
						16.2	206,000	-.0519	.028	.017
						22.1	280,000	-.0521	.038	.026
						30.1	383,000	-.0521	.052	.036
						46.9	598,000	-.0507	.076	.056
						83.5	1,064,000	-.0518	.129	.097
H-12	19.8	0	Air	Air	Suction; constant $\phi_H = -1.2$	6.1	58,800	-.040	.027	.011
						10.7	100,000	-.031	.037	.016
						21.5	214,600	-.000	.062	.026
						38.1	371,800	-.059	.060	.040
						58.4	570,100	-.059	.060	.043
						83.3	810,000	-.055	.075	.053
H-14	20.2	0	Air	Air	Suction; constant $\phi_H = -3.5$	10.7	102,300	-.091	.018	.008
						58.4	581,300	-.039	.038	.020
H-17a	20.0	0	Air	Air	Constant blowing velocity; $v_o = 0.04$ fps	6.1	59,100	.041	.066	.030
						10.7	100,800	.037	.079	.050
						21.5	216,200	.039	.147	.097
						38.1	373,600	.040	.246	.160
						58.4	572,300	.039	.337	.220
						83.3	813,200	.039	.411	.273
H-25	19.6	0	Air	Air	Constant suction velocity; $v_o = -0.12$ fps	46.2	461,800	-.120	.016	.007

TABLE IV.- VELOCITY PROFILE MEASUREMENTS

Station C		Station D		Station E		Station F		Station G		Station H		Station I		Station J		Station K		Station L		Station M		Station N	
y, in.	$\frac{u}{u_1}$	y, in.	$\frac{u}{u_1}$	y, in.	$\frac{u}{u_1}$	y, in.	$\frac{u}{u_1}$	y, in.	$\frac{u}{u_1}$	y, in.	$\frac{u}{u_1}$	y, in.	$\frac{u}{u_1}$	y, in.	$\frac{u}{u_1}$	y, in.	$\frac{u}{u_1}$	y, in.	$\frac{u}{u_1}$	y, in.	$\frac{u}{u_1}$	y, in.	$\frac{u}{u_1}$
Run V-1; no transfer; u_1 = 25.8 fps																							
x = 3.6 in. R_x = 46,000		x = 6.9 in. R_x = 88,000				x = 16.2 in. R_x = 206,000		x = 22.1 in. R_x = 280,000		x = 30.1 in. R_x = 382,000		x = 38.8 in. R_x = 492,000		x = 46.9 in. R_x = 595,000				x = 70.8 in. R_x = 898,000				x = 96.4 in. R_x = 1,220,000	
0.013	0.355	0.013	0.365			0.013	0.440	0.013	0.440	0.013	0.372	0.013	0.398	0.013	0.407			0.013	0.314			0.013	0.357
.016	.407	.016	.418			.016	.472	.016	.479	.016	.417	.016	.416	.016	.436			.016	.344			.019	.412
.019	.452	.019	.473			.019	.504	.019	.504	.019	.452	.019	.445	.019	.463			.021	.396			.024	.444
.022	.502	.022	.516			.023	.542	.024	.546	.024	.494	.022	.474	.024	.499			.029	.460			.034	.489
.025	.544	.025	.558			.029	.581	.031	.584	.031	.543	.027	.512	.031	.537			.039	.508			.054	.544
.030	.627	.030	.615			.038	.624	.039	.615	.039	.579	.034	.549	.041	.576			.054	.548			.079	.584
.035	.692	.035	.661			.053	.664	.049	.645	.049	.608	.042	.579	.056	.609			.074	.582			.104	.609
.040	.761	.042	.711			.073	.704	.064	.673	.074	.647	.052	.604	.081	.644			.104	.612			.154	.636
.045	.815	.050	.757			.103	.746	.089	.708	.094	.672	.067	.629	.116	.677			.154	.648			.254	.684
.050	.854	.060	.793			.133	.780	.139	.761	.134	.710	.092	.659	.166	.709			.224	.683			.354	.716
.055	.893	.075	.833			.163	.817	.189	.809	.194	.758	.142	.702	.241	.753			.324	.725			.504	.760
.060	.922	.095	.878			.203	.856	.239	.846	.264	.808	.192	.735	.341	.799			.424	.765			.654	.798
.065	.955	.125	.926			.253	.906	.289	.883	.344	.855	.292	.798	.441	.838			.524	.798			.854	.837
.075	.982	.165	.965			.303	.943	.339	.916	.444	.910	.392	.846	.541	.878			.624	.840			1.054	.878
.090	.998	.215	.990			.353	.967	.389	.945	.544	.954	.492	.890	.641	.914			.874	.890			1.254	.913
.125	1.000	.290	.996			.453	.989	.439	.966	.644	.980	.592	.926	.741	.940			1.074	.934			1.454	.948
		.390	.998			.553	.998	.539	.988	.744	.992	.692	.958	.891	.976			1.274	.968			1.654	.972
		.590	1.000			.753	1.000	.639	.997	.944	.998	.842	.984	1.041	.990			1.474	.982			1.854	.990
								.739	1.000	1.244	1.000	1.042	.999	1.241	1.000			1.674	.993			2.054	.998
												1.392	1.000					1.874	.998			2.254	1.000
																		2.074	1.000				
Run V-2; no transfer; u_1 = 58.7 fps																							
		x = 6.9 in. R_x = 200,000						x = 22.1 in. R_x = 640,000						x = 46.9 in. R_x = 1,350,000				x = 70.8 in. R_x = 2,040,000				x = 96.4 in. R_x = 2,780,000	
		0.013	0.461					0.013	0.493					0.013	0.524			0.013	0.363			0.013	0.493
		.016	.501					.017	.505					.017	.537			.018	.429			.018	.523
		.019	.540					.020	.518					.022	.551			.023	.472			.023	.547
		.022	.572					.023	.531					.032	.568			.028	.502			.028	.563
		.025	.599					.028	.546					.042	.582			.038	.536			.038	.582
		.028	.625					.033	.563					.057	.598			.048	.554			.053	.602
		.033	.656					.043	.588					.082	.628			.068	.581			.078	.623
		.038	.680					.053	.608					.122	.652			.098	.604			.118	.645
		.045	.704					.070	.636					.182	.694			.138	.629			.173	.673
		.055	.730					.095	.672					.282	.753			.198	.661			.243	.697
		.065	.753					.130	.712					.382	.803			.298	.708			.343	.733
		.080	.781					.180	.764					.482	.850			.398	.748			.443	.762
		.100	.826					.230	.810					.582	.887			.558	.802			.593	.800
		.125	.876					.280	.856					.682	.922			.758	.861			.743	.833
		.155	.927					.330	.889					.782	.955			.958	.916			.943	.873
		.185	.963					.380	.923					.882	.976			1.158	.957			1.143	.912
		.215	.984					.430	.951					1.042	.995			1.358	.987			1.343	.944
		.245	.995					.480	.976					1.242	1.000			1.558	.998			1.543	.971
		.275	.999					.530	.989									1.758	1.000			1.743	.987
		.325	1.000					.630	1.000													1.943	.997
																						2.143	1.000

TABLE IV.- VELOCITY PROFILE MEASUREMENTS - Continued

Station C		Station D		Station E		Station F		Station G		Station H		Station I		Station J		Station K		Station L		Station M		Station N	
y, in.	$\frac{u}{u_1}$	y, in.	$\frac{u}{u_1}$	y, in.	$\frac{u}{u_1}$	y, in.	$\frac{u}{u_1}$	y, in.	$\frac{u}{u_1}$	y, in.	$\frac{u}{u_1}$	y, in.	$\frac{u}{u_1}$	y, in.	$\frac{u}{u_1}$	y, in.	$\frac{u}{u_1}$	y, in.	$\frac{u}{u_1}$	y, in.	$\frac{u}{u_1}$	y, in.	$\frac{u}{u_1}$
Run V-3; blowing with constant $v_o = 0.054$; $u_1 = 26.0$ fps																							
x = 3.6 in. R_x = 46,000		x = 6.9 in. R_x = 88,000				x = 16.2 in. R_x = 207,000		x = 22.1 in. R_x = 283,000		x = 30.1 in. R_x = 385,000		x = 38.8 in. R_x = 496,000		x = 46.9 in. R_x = 600,000						x = 83.5 in. R_x = 1,070,000		x = 96.4 in. R_x = 1,230,000	
0.013	0.284	0.013	0.369			0.013	0.340	0.013	0.339	0.013	0.258	0.013	0.279	0.013	0.335					0.013	0.210	0.013	0.234
.016	.317	.016	.407			.017	.384	.017	.374	.017	.313	.017	.330	.017	.355					.021	.271	.021	.297
.020	.367	.021	.477			.022	.423	.022	.423	.021	.340	.021	.359	.022	.381					.031	.321	.031	.355
.025	.408	.026	.527			.032	.476	.027	.459	.027	.393	.027	.400	.032	.420					.046	.377	.046	.399
.030	.462	.036	.617			.042	.534	.037	.500	.034	.429	.034	.430	.047	.461					.071	.426	.071	.445
.035	.514	.046	.671			.062	.587	.047	.535	.044	.468	.044	.462	.072	.510					.111	.470	.111	.486
.040	.562	.056	.704			.082	.627	.067	.577	.059	.508	.059	.493	.107	.550					.181	.514	.186	.537
.050	.651	.076	.746			.112	.665	.107	.624	.084	.559	.084	.530	.157	.587					.301	.573	.286	.579
.060	.726	.096	.785			.162	.722	.167	.680	.119	.597	.124	.570	.217	.626					.501	.642	.411	.616
.070	.799	.116	.810			.212	.774	.227	.725	.159	.625	.194	.623	.297	.661					.701	.697	.561	.652
.080	.867	.156	.861			.262	.815	.317	.788	.219	.674	.294	.686	.397	.716					.901	.748	.761	.702
.090	.921	.196	.903			.312	.856	.417	.854	.309	.734	.394	.732	.497	.751					1.101	.796	.961	.738
.100	.957	.236	.933			.362	.891	.517	.912	.409	.787	.494	.778	.647	.800					1.301	.834	1.211	.786
.110	.977	.276	.953			.412	.924	.617	.954	.509	.838	.594	.823	.797	.853					1.501	.876	1.461	.837
.120	.990	.336	.979			.462	.944	.717	.979	.609	.887	.694	.862	.947	.902					1.701	.910	1.711	.878
.140	.997	.416	.993			.562	.982	.817	.996	.709	.930	.794	.898	1.097	.940					1.901	.944	1.961	.918
.180	1.000	.516	1.000			.662	.994	.917	.998	.809	.956	.894	.932	1.247	.966					2.101	.972	2.211	.952
						.762	.998	1.117	1.000	.909	.982	.994	.956	1.397	.986					2.301	.987	2.461	.978
						.962	1.000			1.009	.994	1.094	.973	1.597	.994					2.501	.996	2.711	.991
										1.109	.999	1.194	.985	1.797	.999					2.701	1.000	2.961	.997
										1.309	1.000	1.394	.995	2.097	1.000							3.211	1.000
												1.594	.999										
												1.794	1.000										
Run V-4; blowing with constant $v_o = 0.13$; $u_1 = 25.9$ fps																							
x = 3.6 in. R_x = 46,000		x = 6.9 in. R_x = 88,000				x = 16.2 in. R_x = 206,000				x = 30.1 in. R_x = 383,000				x = 46.9 in. R_x = 598,000						x = 83.5 in. R_x = 1,064,000			
0.013	0.421	0.013	0.298			0.013	0.233			0.013	0.150			0.013	0.122					0.013	0.100		
.018	.468	.019	.368			.019	.281			.020	.199			.022	.172					.019	.133		
.023	.501	.026	.441			.027	.330			.030	.249			.032	.213					.029	.174		
.028	.528	.034	.502			.037	.372			.045	.315			.047	.258					.044	.213		
.038	.587	.044	.562			.052	.422			.070	.373			.072	.306					.069	.270		
.048	.625	.054	.600			.072	.461			.110	.435			.112	.351					.109	.305		
.063	.672	.069	.649			.102	.507			.170	.478			.172	.403					.169	.351		
.083	.741	.094	.697			.147	.567			.270	.560			.272	.471					.269	.404		
.103	.801	.119	.731			.197	.618			.370	.631			.382	.539					.429	.462		
.123	.860	.159	.779			.267	.682			.470	.684			.532	.603					.629	.523		
.143	.907	.199	.817			.347	.752			.590	.743			.732	.676					.879	.587		
.163	.945	.264	.874			.447	.821			.740	.809			.932	.745					1.179	.648		
.183	.969	.344	.928			.547	.887			.890	.874			1.132	.811					1.479	.714		
.203	.986	.424	.965			.647	.934			1.040	.935			1.332	.875					1.779	.782		
.223	.994	.504	.988			.747	.968			1.190	.974			1.532	.931					2.079	.843		
.253	1.000	.584	.995			.847	.988			1.340	.992			1.732	.968					2.379	.895		
		.684	1.000			.947	1.000			1.540	.997			1.932	.989					2.679	.941		
										1.740	1.000			2.132	.998					2.979	.976		
														2.382	1.000					3.279	.996		
																				3.579	1.000		

TABLE IV.- VELOCITY PROFILE MEASUREMENTS - Continued

Station C		Station D		Station E		Station F		Station G		Station H		Station I		Station J		Station K		Station L		Station M		Station N	
y, in.	$\frac{u}{u_1}$	y, in.	$\frac{u}{u_1}$	y, in.	$\frac{u}{u_1}$	y, in.	$\frac{u}{u_1}$	y, in.	$\frac{u}{u_1}$	y, in.	$\frac{u}{u_1}$	y, in.	$\frac{u}{u_1}$	y, in.	$\frac{u}{u_1}$	y, in.	$\frac{u}{u_1}$	y, in.	$\frac{u}{u_1}$	y, in.	$\frac{u}{u_1}$	y, in.	$\frac{u}{u_1}$
Run V-5 (H-8); blowing with constant $\phi_H = 1.2$; $u_1 = 19.6$ fps																							
		x = 6.6 in. R_x = 63,100						x = 22.1 in. R_x = 217,200						x = 46.5 in. R_x = 462,000						x = 83.1 in. R_x = 803,000			
		0.013	0.263					0.013	0.254					0.013	0.2285					0.013	0.145		
		.016	.301					.016	.286					.016	.244					.018	.194		
		.023	.399					.024	.347					.023	.287					.028	.2425		
		.033	.505					.034	.404					.033	.3385					.048	.330		
		.043	.576					.059	.472					.045	.406					.088	.415		
		.058	.633					.109	.548					.088	.454					.148	.472		
		.083	.723					.209	.635					.138	.511					.208	.5145		
		.133	.766					.309	.703					.188	.546					.288	.550		
		.208	.833					.409	.770					.288	.594					.388	.580		
		.308	.912					.509	.834					.388	.646					.538	.6215		
		.408	.963					.609	.888					.488	.681					.688	.655		
		.608	1.000					.709	.940					.638	.733					.888	.698		
		.808	1.000					.809	.970					.788	.7955					1.188	.767		
								1.009	.994					.938	.843					1.488	.835		
								1.209	1.000					1.088	.888					1.788	.896		
														1.238	.9285					2.088	.946		
														1.388	.963					2.388	.977		
														1.538	.991					2.688	.996		
														1.638	1.000					2.988	1.000		
														1.888	1.000					3.288	1.000		
Run V-6; blowing with constant v_o = 0.26; u_1 = 26.3 fps																							
x = 3.6 in. R_x = 47,000		x = 6.9 in. R_x = 89,000		x = 11.2 in. R_x = 145,000		x = 16.2 in. R_x = 210,000		x = 22.1 in. R_x = 286,000		x = 30.1 in. R_x = 389,000				x = 46.9 in. R_x = 607,000									
0.013	0.383	0.013	0.208	0.013	0.211	0.013	(a)	0.013	0.146	0.013	(a)			0.013	(a)								
.018	.419	.018	.240	.017	.216	.019	(a)	.019	.175	.020	(a)			.018	(a)								
.024	.467	.026	.295	.022	.237	.029	0.085	.029	.194	.030	0.069			.028	(a)								
.031	.506	.036	.340	.032	.274	.044	.148	.044	.217	.045	.097			.043	0.083								
.039	.547	.051	.405	.047	.317	.069	.191	.069	.266	.070	.046			.068	.107								
.049	.577	.071	.476	.072	.378	.109	.274	.109	.307	.110	.195			.103	.159								
.064	.612	.096	.533	.112	.446	.149	.315	.164	.357	.170	.243			.153	.179								
.084	.658	.126	.589	.162	.519	.209	.378	.264	.412	.255	.312			.228	.244								
.109	.712	.166	.643	.222	.579	.299	.459	.414	.499	.355	.361			.328	.287								
.134	.773	.211	.701	.292	.645	.399	.550	.564	.595	.505	.438			.453	.325								
.159	.821	.261	.760	.362	.716	.499	.628	.714	.676	.705	.532			.603	.383								
.184	.867	.311	.810	.442	.779	.599	.702	.864	.762	.905	.619			.803	.444								
.209	.908	.361	.850	.517	.842	.699	.773	1.014	.840	1.105	.715			1.053	.529								
.234	.942	.411	.887	.592	.889	.799	.839	1.164	.906	1.305	.817			1.303	.602								
.259	.967	.486	.936	.667	.926	.899	.895	1.314	.953	1.507	.887			1.553	.674								
.284	.983	.561	.975	.742	.962	.999	.943	1.464	.986	1.705	.948			1.803	.763								
.309	.993	.636	.992	.817	.981	1.099	.977	1.614	.998	1.905	.983			2.053	.838								
.334	.999	.711	.998	.892	.996	1.199	.992	1.764	1.000	2.105	.996			2.303	.904								
.359	1.000	.786	1.000	.967	1.000	1.299	.998			2.305	1.000			2.553	.953								
						1.399	1.000							2.803	.984								
														3.053	.996								
														3.303	.998								
														3.553	1.000								

[a]Approximately zero.

TABLE IV.- VELOCITY PROFILE MEASUREMENTS - Continued

Station C		Station D		Station E		Station F		Station G		Station H		Station I		Station J		Station K		Station L		Station M		Station N	
y, in.	$\frac{u}{u_1}$	y, in.	$\frac{u}{u_1}$	y, in.	$\frac{u}{u_1}$	y, in.	$\frac{u}{u_1}$	y, in.	$\frac{u}{u_1}$	y, in.	$\frac{u}{u_1}$	y, in.	$\frac{u}{u_1}$	y, in.	$\frac{u}{u_1}$	y, in.	$\frac{u}{u_1}$	y, in.	$\frac{u}{u_1}$	y, in.	$\frac{u}{u_1}$	y, in.	$\frac{u}{u_1}$
Run V-7; suction with constant $v_o = -0.26$; $u_1 = 25.8$ fps																							
$x = 3.6$ in. $R_x = 46{,}000$		$x = 6.9$ in. $R_x = 88{,}000$		$x = 11.2$ in. $R_x = 142{,}000$		$x = 16.2$ in. $R_x = 206{,}000$		$x = 22.1$ in. $R_x = 280{,}000$		$x = 30.1$ in. $R_x = 382{,}000$													
0.013	0.905	0.013	0.753	0.013	0.893	0.013	0.910	0.013	0.829	0.013	0.859												
.016	.943	.016	.830	.016	.924	.016	.942	.016	.878	.016	.904												
.019	.967	.019	.883	.021	.955	.019	.960	.019	.911	.019	.936												
.024	.986	.022	.923	.030	.987	.024	.980	.024	.947	.024	.962												
.029	.995	.027	.964	.040	.996	.030	.992	.029	.970	.030	.982												
.034	.999	.034	.987	.050	1.000	.036	.999	.039	.990	.040	.996												
.039	1.000	.044	.995			.042	1.000	.050	.998	.055	1.000												
		.059	.998					.065	1.000														
		.074	1.000																				
Run V-8; suction with constant $v_o = -0.13$; $u_1 = 25.7$ fps																							
$x = 3.6$ in. $R_x = 46{,}000$		$x = 6.9$ in. $R_x = 87{,}000$		$x = 11.2$ in. $R_x = 142{,}000$		$x = 16.2$ in. $R_x = 205{,}000$		$x = 22.1$ in. $R_x = 279{,}000$		$x = 30.1$ in. $R_x = 380{,}000$		$x = 38.8$ in. $R_x = 490{,}000$		$x = 46.9$ in. $R_x = 593{,}000$				$x = 70.8$ in. $R_x = 895{,}000$					
0.013	0.782	0.013	0.544	0.013	0.691	0.013	0.728	0.013	0.617	0.013	0.664	0.013	0.636	0.013	0.573			0.013	0.666				
.016	.832	.016	.606	.016	.736	.016	.765	.016	.661	.016	.718	.016	.671	.016	.634			.016	.698				
.019	.877	.019	.662	.019	.784	.019	.817	.019	.690	.019	.765	.019	.711	.019	.693			.019	.749				
.022	.911	.022	.721	.022	.824	.022	.856	.022	.735	.022	.800	.022	.735	.022	.735			.022	.784				
.025	.933	.025	.773	.025	.862	.022	.899	.025	.779	.027	.845	.027	.775	.025	.770			.027	.844				
.030	.959	.028	.821	.028	.890	.032	.932	.028	.818	.032	.883	.032	.813	.030	.810			.030	.872				
.035	.975	.031	.857	.033	.922	.042	.966	.033	.865	.042	.922	.037	.842	.035	.843			.035	.908				
.045	.992	.036	.901	.038	.944	.052	.983	.038	.898	.052	.946	.044	.880	.045	.886			.040	.929				
.055	.998	.041	.931	.048	.972	.062	.993	.043	.929	.067	.970	.054	.912	.060	.913			.050	.955				
.065	1.000	.051	.966	.061	.989	.077	.997	.048	.952	.092	.982	.069	.947	.085	.945			.060	.968				
		.066	.987	.091	.997	.092	1.000	.058	.975	.117	.993	.094	.973	.125	.967			.076	.980				
		.092	.999	.131	1.000			.073	.989	.157	1.000	.119	.982	.185	.991			.101	.986				
		.117	1.000					.103	.999			.159	.992	.245	.997			.141	.994				
								.153	1.000			.199	.996	.305	1.000			.181	.998				
												.239	.999					.221	1.000				
												.279	1.000										
Run V-9; suction; $v_o \propto 1/\sqrt{x}$; $C = 5.0$; $u_1 = 26.7$ fps																							
$x = 3.6$ in. $R_x = 47{,}000$		$x = 6.9$ in. $R_x = 91{,}000$		$x = 11.2$ in. $R_x = 147{,}000$		$x = 16.2$ in. $R_x = 213{,}000$		$x = 22.1$ in. $R_x = 290{,}000$		$x = 30.1$ in. $R_x = 395{,}000$		$x = 38.8$ in. $R_x = 510{,}000$		$x = 46.9$ in. $R_x = 616{,}000$				$x = 70.8$ in. $R_x = 930{,}000$		$x = 83.5$ in. $R_x = 1{,}100{,}000$		$x = 96.4$ in. $R_x = 1{,}270{,}000$	
0.013	0.944	0.013	0.718	0.013	0.788	0.013	0.764	0.013	0.630	0.013	0.558	0.013	0.597	0.013	0.610			0.015	0.527	0.013	0.477	0.013	0.514
.016	.970	.016	.790	.016	.833	.016	.814	.016	.684	.016	.578	.016	.638	.016	.647			.018	.576	.016	.522	.016	.564
.019	.988	.019	.850	.019	.872	.019	.861	.019	.729	.019	.586	.019	.673	.019	.675			.021	.619	.019	.562	.019	.591
.022	.994	.022	.896	.022	.901	.022	.892	.022	.775	.022	.625	.024	.714	.024	.718			.024	.644	.022	.598	.024	.636
.025	.998	.025	.926	.027	.940	.025	.918	.025	.816	.025	.672	.030	.755	.030	.756			.029	.691	.027	.645	.030	.664
.028	1.000	.030	.964	.032	.965	.030	.948	.028	.848	.030	.738	.040	.809	.040	.802			.036	.727	.035	.694	.040	.700
		.037	.981	.037	.980	.037	.976	.033	.892	.035	.785	.050	.842	.050	.834			.046	.766	.045	.728	.055	.732
		.045	.994	.044	.989	.045	.984	.040	.930	.040	.821	.065	.882	.065	.858			.061	.795	.060	.768	.080	.765
		.055	1.000	.056	.994	.055	.995	.050	.970	.050	.867	.080	.910	.090	.890			.082	.820	.085	.798	.120	.800
				.062	.998	.065	.998	.060	.984	.060	.900	.100	.938	.130	.926			.122	.852	.125	.834	.180	.833
				.072	.999	.080	1.000	.070	.994	.075	.930	.125	.960	.190	.964			.182	.894	.185	.873	.280	.882
				.092	1.000			.080	.996	.100	.962	.160	.977	.250	.986			.252	.928	.280	.916	.380	.918
								.100	1.000	.125	.982	.200	.990	.320	.995			.352	.967	.380	.955	.480	.950
										.150	.990	.240	.998	.400	.999			.452	.988	.480	.981	.580	.974
										.190	.997	.280	1.000	.500	1.000			.552	.998	.580	.992	.680	.988
										.230	.999							.652	1.000	.680	.999	.780	.998
										.330	1.000									.780	1.000	.880	1.000

TABLE IV.- VELOCITY PROFILE MEASUREMENTS - Continued

Station C		Station D		Station E		Station F		Station G		Station H		Station I		Station J		Station K		Station L		Station M		Station N	
y, in.	$\frac{u}{u_1}$	y, in.	$\frac{u}{u_1}$	y, in.	$\frac{u}{u_1}$	y, in.	$\frac{u}{u_1}$	y, in.	$\frac{u}{u_1}$	y, in.	$\frac{u}{u_1}$	y, in.	$\frac{u}{u_1}$	y, in.	$\frac{u}{u_1}$	y, in.	$\frac{u}{u_1}$	y, in.	$\frac{u}{u_1}$	y, in.	$\frac{u}{u_1}$	y, in.	$\frac{u}{u_1}$
Run V-10; suction; $v_o \propto 1/\sqrt{x}$; C = 3.0; u_1 = 25.9 fps																							
x = 3.6 in. R_x = 46,000		x = 6.9 in. R_x = 88,000		x = 11.2 in. R_x = 142,000		x = 16.2 in. R_x = 206,000		x = 22.1 in. R_x = 280,000		x = 30.1 in. R_x = 383,000				x = 46.9 in. R_x = 598,000						x = 83.5 in. R_x = 1,064,000			
0.013	0.867	0.013	0.559	0.013	0.662	0.013	0.628	0.013	0.579	0.013	0.518			0.013	0.484					0.013	0.407		
.016	.909	.016	.636	.016	.712	.016	.688	.016	.623	.016	.581			.016	.536					.016	.453		
.019	.939	.019	.699	.019	.752	.019	.731	.019	.657	.019	.621			.019	.579					.019	.493		
.024	.971	.022	.748	.024	.805	.022	.770	.024	.701	.024	.681			.024	.630					.024	.541		
.030	.990	.025	.794	.030	.870	.027	.833	.032	.758	.030	.727			.030	.674					.034	.609		
.040	1.000	.030	.858	.040	.938	.032	.877	.040	.818	.040	.778			.040	.719					.050	.662		
		.035	.910	.050	.972	.037	.910	.050	.861	.050	.812			.055	.757					.070	.702		
		.040	.942	.060	.985	.045	.946	.060	.902	.065	.842			.080	.794					.100	.728		
		.045	.955	.070	.992	.055	.971	.070	.930	.085	.875			.120	.834					.140	.762		
		.055	.980	.080	.998	.070	.993	.085	.959	.110	.908			.180	.884					.200	.799		
		.065	.993	.090	1.000	.090	.999	.100	.974	.140	.935			.240	.921					.300	.845		
		.075	.998			.110	1.000	.120	.987	.180	.964			.300	.954					.400	.889		
		.085	1.000					.140	.993	.220	.983			.400	.987					.500	.921		
								.160	.996	.260	.994			.500	.998					.600	.949		
								.180	.998	.300	.999			.600	1.000					.700	.975		
								.230	1.000	.340	1.000									.800	.986		
																				.900	.993		
																				1.000	.998		
																				1.100	1.000		
Run V-11; suction with constant v_o = -0.052; u_1 = 25.9 fps																							
x = 3.6 in. R_x = 46,000		x = 6.9 in. R_x = 88,000		x = 11.2 in. R_x = 142,000		x = 16.2 in. R_x = 206,000		x = 22.1 in. R_x = 280,000		x = 30.1 in. R_x = 383,000				x = 46.9 in. R_x = 598,000						x = 83.5 in. R_x = 1,064,000			
0.013	0.583	0.013	0.434	0.013	0.455	0.013	0.520	0.013	0.561	0.013	0.476			0.013	0.562					0.013	0.435		
.016	.646	.016	.445	.016	.501	.016	.555	.016	.599	.016	.529			.018	.575					.018	.502		
.019	.705	.019	.493	.021	.582	.019	.587	.021	.652	.019	.575			.023	.623					.028	.582		
.022	.753	.024	.583	.026	.649	.024	.636	.027	.692	.024	.616			.033	.682					.048	.664		
.025	.792	.029	.664	.031	.702	.029	.659	.035	.728	.030	.659			.048	.722					.088	.723		
.030	.856	.034	.729	.036	.757	.036	.713	.045	.765	.040	.719			.073	.759					.148	.766		
.035	.902	.039	.791	.041	.800	.046	.776	.060	.806	.050	.750			.113	.799					.248	.818		
.040	.942	.044	.841	.050	.870	.056	.831	.085	.844	.065	.779			.173	.838					.398	.872		
.050	.976	.049	.879	.060	.923	.071	.892	.120	.896	.090	.816			.273	.897					.598	.929		
.065	.997	.057	.928	.070	.954	.086	.931	.160	.933	.130	.855			.373	.939					.798	.972		
.090	1.000	.065	.957	.080	.974	.101	.957	.210	.969	.190	.910			.473	.972					.998	.992		
		.075	.978	.090	.986	.126	.978	.260	.987	.250	.946			.573	.991					1.198	.999		
		.085	.987	.100	.993	.151	.989	.310	.996	.350	.986			.673	.997					1.398	1.000		
		.099	.996	.110	.998	.186	.991	.360	1.000	.450	1.000			.773	1.000								
		.119	1.000	.130	1.000	.236	.998																
						.286	1.000																

TABLE IV.- VELOCITY PROFILE MEASUREMENTS - Continued

Station C		Station D		Station E		Station F		Station G		Station H		Station I		Station J		Station K		Station L		Station M		Station N	
y, in.	$\frac{u}{u_1}$	y, in.	$\frac{u}{u_1}$	y, in.	$\frac{u}{u_1}$	y, in.	$\frac{u}{u_1}$	y, in.	$\frac{u}{u_1}$	y, in.	$\frac{u}{u_1}$	y, in.	$\frac{u}{u_1}$	y, in.	$\frac{u}{u_1}$	y, in.	$\frac{u}{u_1}$	y, in.	$\frac{u}{u_1}$	y, in.	$\frac{u}{u_1}$	y, in.	$\frac{u}{u_1}$
Run H-12; suction with constant $\phi_H = -1.2$; $u_1 = 19.8$ fps																							
		x = 6.1 in. R_x = 58,800		x = 10.8 in. R_x = 100,000				x = 21.4 in. R_x = 214,600				x = 38.1 in. R_x = 371,800				x = 58.3 in. R_x = 570,100				x = 83.3 in. R_x = 810,000			
		0.016	0.363	0.016	0.287			0.016	0.189			0.016	0.433			0.016	0.473			0.016	0.393		
		.020	.453	.019	.337			.020	.219			.020	.498			.020	.547			.020	.437		
		.024	.550	.023	.411			.025	.260			.025	.562			.025	.613			.025	.518		
		.028	.629	.027	.481			.030	.303			.030	.613			.030	.669			.030	.598		
		.032	.688	.031	.535			.035	.351			.040	.679			.035	.709			.035	.644		
		.036	.737	.035	.591			.040	.394			.050	.716			.045	.749			.045	.716		
		.040	.775	.040	.651			.050	.485			.070	.762			.060	.798			.060	.770		
		.045	.828	.045	.697			.060	.578			.090	.801			.080	.829			.080	.817		
		.050	.869	.052	.762			.070	.650			.130	.857			.110	.869			.110	.848		
		.055	.901	.060	.816			.080	.708			.170	.892			.150	.888			.160	.874		
		.060	.919	.070	.872			.090	.763			.230	.924			.200	.912			.230	.906		
		.070	.956	.080	.912			.100	.813			.300	.956			.300	.944			.300	.931		
		.080	.976	.090	.943			.110	.854			.400	.983			.400	.966			.400	.950		
		.100	.996	.100	.958			.120	.883			.500	.996			.500	.979			.500	.967		
		.120	1.000	.120	.976			.140	.925			.600	1.000			.700	.996			.700	.986		
				.140	.988			.160	.955							.900	1.000			.900	.996		
				.160	1.000			.180	.971											1.100	1.000		
								.220	.992														
								.260	.996														
								.300	1.000														
Run H-14; suction with constant $\phi_H = -3.5$; $u_1 = 20.2$ fps																							
				x = 10.7 in. R_x = 102,300												x = 58.4 in. R_x = 581,300							
				0.016	0.577											0.016	0.387						
				.019	.645											.020	.443						
				.022	.700											.025	.510						
				.025	.748											.030	.574						
				.030	.814											.035	.623						
				.035	.861											.040	.660						
				.040	.891											.050	.728						
				.045	.925											.060	.787						
				.050	.945											.070	.827						
				.060	.973											.080	.867						
				.070	.987											.100	.920						
				.080	.996											.120	.947						
				.100	1.000											.160	.978						
				.120												.200	.996						
																.250	1.000						

TABLE IV.- VELOCITY PROFILE MEASUREMENTS - Concluded

Station C		Station D		Station E		Station F		Station G		Station H		Station I		Station J		Station K		Station L		Station M		Station N	
y, in.	$\frac{u}{u_1}$	y, in.	$\frac{u}{u_1}$	y, in.	$\frac{u}{u_1}$	y, in.	$\frac{u}{u_1}$	y, in.	$\frac{u}{u_1}$	y, in.	$\frac{u}{u_1}$	y, in.	$\frac{u}{u_1}$	y, in.	$\frac{u}{u_1}$	y, in.	$\frac{u}{u_1}$	y, in.	$\frac{u}{u_1}$	y, in.	$\frac{u}{u_1}$	y, in.	$\frac{u}{u_1}$
Run H-17a; blowing with constant $v_o = 0.04$; $u_1 = 20.0$ fps																							
		$x = 6.1$ in. $R_x = 59,100$		$x = 10.7$ in. $R_x = 100,800$				$x = 21.5$ in. $R_x = 216,200$				$x = 38.1$ in. $R_x = 373,600$				$x = 58.4$ in. $R_x = 572,300$				$x = 83.3$ in. $R_x = 813,200$			
		0.016	0.203	0.016	0.385			0.016	0.316			0.016	0.235			0.016	0.200			0.016	0.156		
		.019	.240	.019	.434			.019	.348			.019	.268			.019	.240			.019	.180		
		.022	.279	.022	.477			.023	.387			.023	.298			.022	.282			.023	.220		
		.025	.314	.027	.518			.028	.428			.028	.344			.026	.319			.028	.270		
		.029	.345	.034	.555			.035	.474			.035	.396			.031	.358			.035	.336		
		.034	.384	.044	.616			.045	.525			.045	.446			.038	.388			.045	.392		
		.041	.439	.060	.684			.060	.566			.060	.491			.048	.426			.060	.440		
		.050	.483	.080	.724			.080	.606			.080	.529			.063	.570			.080	.487		
		.065	.554	.110	.772			.110	.645			.110	.564			.085	.507			.110	.523		
		.080	.624	.150	.817			.150	.686			.150	.600			.118	.540			.150	.568		
		.100	.727	.200	.869			.200	.727			.200	.631			.166	.572			.200	.592		
		.120	.817	.250	.901			.270	.777			.270	.673			.236	.613			.270	.622		
		.140	.896	.320	.944			.370	.842			.370	.725			.336	.659			.370	.656		
		.160	.945	.400	.982			.470	.901			.500	.789			.486	.713			.500	.698		
		.180	.973	.500	.998			.570	.938			.650	.851			.686	.787			.700	.751		
		.200	.990	.600	1.000			.670	.973			.800	.909			.886	.852			.900	.808		
		.225	.998					.770	.994			.950	.955			1.086	.905			1.150	.856		
		.250	1.000					.870	1.000			1.100	.983			1.286	.950			1.400	.907		
												1.250	.996			1.486	.982			1.650	.954		
												1.400	1.000			1.686	.996			1.900	.986		
																1.886	1.000			2.150	1.000		
Run H-25; suction with constant $v_o = -0.12$; $u_1 = 19.6$ fps																							
														$x = 46.2$ in. $R_x = 461,800$									
														0.016	0.648								
														.019	.710								
														.022	.767								
														.025	.810								
														.030	.865								
														.035	.903								
														.045	.943								
														.055	.976								
														.065	.988								
														.085	.996								
														.105	1.000								

TABLE V.- TABULATION OF EMPIRICAL FRICTION-FACTOR EQUATIONS DERIVED FROM MOMENTUM INTEGRALS AND HEAT-TRANSFER-COEFFICIENT EQUATIONS DERIVED FROM ENTHALPY INTEGRALS

Mass transfer condition	Main flow condition	Run	u_1, fps	v_o, fps	Friction-factor equation $f/2 = l/(R_x)^n$		Heat-transfer equation $h/u_1\rho_1 c_p = l/(R_x)^n$	
					l	n	l	n
None	Laminar	H-1	4.4	0			0.49	0.51
None	Turbulent	V-1	25.8	0	0.012	0.12		
None	Turbulent	V-2	58.7	0	.044	.22		
Blowing	Turbulent	H-17a	20.0	0.04	0.072	0.31	0.017	0.16
Blowing	Turbulent	V-3	26.0	.054	.024	.20		
Blowing	Turbulent	V-4	25.9	.13	.57	.50		
Blowing	Turbulent	V-6	26.3	.26	5.2	.79		
Blowing		V-5 (H-8)	19.6	$\phi_H = 1.2$	0.012	0.20	0.013	0.20
Suction	Laminar	H-23	4.8	-0.04			0.056	0.18
Suction	Laminar	V-11	25.9	-.052	0.035	0.23		
Suction	Turbulent	V-11	25.9	-.052	.0032	0		
Suction	Laminar	V-8	25.7	-.13	.013	.08		
Suction	Turbulent	V-8	25.7	-.13	.0052	0		
Suction	Laminar	V-7	25.8	-.26	.020	.07		
Suction	Laminar	H-11	4.8	$\phi_H = -1.2$			0.26	0.37
Suction	Laminar	H-12	19.8	$\phi_H = -1.2$	0.48	0.46	.29	.42
Suction	Turbulent	H-12	19.8	$\phi_H = -1.2$[a]	.00075	-.11	.00054	-.13
Suction	Laminar	H-14	20.2	$\phi_H = -3.5$	.13	.49	1.73	.51
Suction	Laminar	V-10	25.9	$\phi_F = -4.5$	1.1	.47		
Suction	Turbulent	V-10	25.9	$v_o \propto 1/\sqrt{x}$	.31	.35		
Suction	Laminar	V-9	26.7	$\phi_F = -7.6$	2.1	.49		
Suction	Turbulent	V-9	26.7	$v_o \propto 1/\sqrt{x}$	1.3	.44		

[a]In run H-12 suction distribution in turbulent region was adjusted to give $v_o \propto 1/x^{0.2}$. However, the flow through compartment G was inadvertently left off, so results downstream of this compartment are affected by the interrupted suction distribution.

TABLE VI.- SUMMARY OF MEASUREMENTS OF HEAT TRANSFER COEFFICIENTS AND TEMPERATURE PROFILES

Run	u_1, fps	Axial Euler number	Injected fluid	Axial mass transfer distribution	x, in.	R_x	v_o (local), fps	ξ, in.
H-1	4.4	0	None	No transfer				
				Range of direct measurements	3.4	7,270	0	
					97.0	210,000		
				Measurements of profiles	6.5	14,220		0.048
					21.8	48,930		.094
					38.4	83,600		.120
					46.5	104,100		.127
					70.4	152,800		.155
					96.0	210,000		.209
H-2	16.2	0	None	No transfer				
				Range of direct measurements	3.4	26,400	0	
					111.9	868,000		
				Measurements of profiles	6.5	51,700		
					21.8	177,700		
					38.4	303,500		
					46.5	378,200		
					70.4	555,100		
					96.0	758,400		
H-3	27.0	0	None	No transfer				
				Range of direct measurements	10.8	145,100	0	
					97.0	1,300,500		
H-4	58.8	0	None	No transfer				
				Range of direct measurements	3.4	97,100	0	
					97.0	2,802,000		
H-5	4.6	0	Air	Blowing with constant $\phi_H = 0.63$				
				Range of direct measurements	1.2	2,700	.0230	
					111.9	251,000	.0089	
				Measurements of profiles	6.5	14,720	.0097	.045
					21.8	50,650	.0070	
					46.5	107,800	.0104	
					70.4	158,200	.0097	
					96.0	217,400	.0091	
H-6	17.6	0	Air	Blowing with constant $\phi_H = 0.63$				
				Range of direct measurements	3.4	29,300	.0267	
					111.9	974,000	.0252	
				Measurement of profile	46.5	419,000	.0298	
H-7	60.7	0	Air	Blowing with constant $\phi_H = 0.60$				
				Range of direct measurements	6.6	199,000	.1142	
					97.1	2,924,000	.0666	
H-8	19.6	0	Air	Blowing with constant $\phi_H = 1.2$				
				Range of direct measurements	6.6	63,100	.0923	
					111.9	1,076,000	.0550	
				Measurements of profiles	46.5	462,000	.0639	.241
					83.1	803,000	.0577	.404

TABLE VI.- SUMMARY OF MEASUREMENTS OF HEAT TRANSFER COEFFICIENTS AND TEMPERATURE PROFILES - Continued

Run	u_1, fps	Axial Euler number	Injected fluid	Axial mass transfer distribution	x, in.	R_x	v_o (local), fps	ξ, in.
H-9	60.9	0	Air	Blowing with constant $\phi_H = 1.2$				
				Range of direct measurements	10.9	324,000	0.2040	
					70.6	2,109,000	.1393	
[a]H-10	5.30	0	Air	Blowing with $v_o \propto 1/\sqrt{x}$; $\phi_H = 1.2$; in laminar region				
				Range of direct measurements	2.8	7,200	.0302	
					111.6	289,000	.0047	
				Measurements of profiles	6.0	15,600	.0207	0.046
					10.7	26,500	.0159	.063
H-11	4.8	0	Air	Suction with constant $\phi_H = -1.2$				
				Range of direct measurements	2.8	6,600	-.272	
					111.7	263,400	-.0047	
				Measurements of profiles	6.0	14,200	-.205	.025
					21.4	51,800	-.107	.057
					46.1	112,600	-.0073	.126
					83.2	195,200	-.0055	
H-12	19.8	0	Air	Suction with constant $\phi_H = -1.2$				
				Range of direct measurements	2.8	27,200	-.0587	
					82.8	810,000	-.0550	
				Measurements of profiles	6.1	58,800	-.0401	.0060
					10.7	100,000	-.0307	.0114
					21.5	214,600	0	.019
					38.1	371,800	-.0591	.028
					58.4	570,100	-.0591	.027
					83.3	810.000	-.0550	.028
H-13	60.5	0	Air	Suction with $v_o \propto 1/\sqrt{x}$; $\phi_H = -1.2$; in laminar region				
				Range of direct measurements	2.8	82,600	-.1047	
					111.6	3,315,000	-.0168	
H-14	20.2	0	Air	Suction with constant $\phi_H = -3.5$				
				Range of direct measurements	2.8	27,800	-.1717	
					111.6	1,115,000	-.0285	
				Measurements of profiles	10.7	102,300	-.0914	.011
					58.4	581,300	-.0393	.015
H-15	59.7	0	Air	Suction with $v_o \propto 1/\sqrt{x}$; $\phi_H = -3.6$; in laminar region				
				Range of direct measurements	2.8	81,800	-.3092	
					111.6	3,284,000	-.0487	

[a]Uniform wall temperature.

TABLE VI.- SUMMARY OF MEASUREMENTS OF HEAT TRANSFER COEFFICIENTS

AND TEMPERATURE PROFILES - Continued

Run	u_1, fps	Axial Euler number	Injected fluid	Axial mass transfer distribution	x, in.	R_x	v_o (local), fps	ξ, in.
[b]H-16a	5.0	0	Air	Blowing with constant $v_o = 0.01$				
				Range of direct measurements	2.8	6,730	0.0104	
					82.9	200,700	.0099	
[b]H-17a	20.0	0	Air	Blowing with constant $v_o = 0.04$				
				Range of direct measurements	2.8	27,300	.0395	
					111.6	1,095,000	.0402	
				Measurements of profiles	6.1	59,100	.0406	0.013
					10.7	100,800	.0369	.050
					21.5	216,200	.0393	.102
					38.1	373,600	.0395	.170
					58.4	572,300	.0388	.254
					83.3	813,200	.0394	.349
[a]H-17b	18.8	0	Air	Blowing with constant $v_o = 0.04$				
				Range of direct measurements	2.8	25,600	.0392	
					111.6	1,029,000	.0399	
[b]H-18a	59.8	0	Air	Blowing with constant $v_o = 0.04$				
				Range of direct measurements	6.1	179,300	.0397	
					111.6	3,291,000	.0398	
[b]H-19a	19.9	0	Air	Blowing with constant $v_o = 0.12$				
				Range of direct measurements	10.3	100,500	.1198	
					111.6	1,090,500	.1190	
[a]H-19b	19.8	0	Air	Blowing with constant $v_o = 0.12$				
				Range of direct measurements	10.3	100,200	.1190	
					111.6	1,087,000	.1193	
				Measurements of profiles	2.8	27,600	.1257	
					10.7	100,210	.1190	
					29.4	286,600	.1189	
					83.3	807,600	.1188	
[b]H-20a	60.7	0	Air	Blowing with constant $v_o = 0.12$				
				Range of direct measurements	2.8	84,400	.1200	
					111.6	3,319,000	.1199	
[a]H-20b	60.0	0	Air	Blowing with constant $v_o = 0.12$				
				Range of direct measurements	2.8	83,600	.1207	
					111.6	3,285,000	.1202	
				Measurements of profiles	29.4	865,900	.1207	
					83.3	2,441,000	.1201	
[c]H-21a	59.8	0	Air	Blowing with constant $\phi_H = 0.91$; v_o (mean) = 0.12				
				Range of direct measurements	2.8	83,900	.2034	
					96.8	2,857,000	.1002	
				Measurements of profiles	6.1	179,700	.1746	
					29.4	869,300	.1269	
					46.2	1,408,600	.1153	
					83.3	2,450,000	.1033	

[a]Uniform wall temperature.

[b]Uniform blowing gas temperature.

[c]Uniform blowing gas temperature with mass transfer distribution set to give uniform wall temperature.

TABLE VI.- SUMMARY OF MEASUREMENTS OF HEAT TRANSFER COEFFICIENTS AND TEMPERATURE PROFILES - Concluded

Run	u_1, fps	Axial Euler number	Injected fluid	Axial mass transfer distribution	x, in.	R_x	v_o (local), fps	ξ, in.
H-22	4.9	0	Air	Suction with constant $v_o = -0.01$				
				Range of direct measurements	2.8	6,700	-0.0104	
					111.7	269,600	-.0100	
				Measurements of profiles	6.0	14,500	-.0097	0.029
					21.4	53,000	-.0100	.062
					46.1	115,200	-.0099	.118
H-23	4.8	0	Air	Suction with constant $v_o = -0.04$				
				Range of direct measurements	2.8	6,500	-.0394	
					111.7	261,700	-.0367	
				Measurements of profiles	6.0	14,100	-.0396	.024
					21.4	51,500	-.0354	.033
					83.2	193,900	-.0390	.066
H-24	19.3	0	Air	Suction with constant $v_o = -0.04$				
				Range of direct measurements	2.8	26,400	-.0381	
					111.6	1,062,000	-.0391	
H-25	19.6	0	Air	Suction with constant $v_o = -0.12$				
				Range of direct measurements	6.0	58,300	-.1197	
					70.0	677,400	-.1207	
				Measurement of profile	46.2	461,800	-.1205	.015
H-26	60.0	0	Air	Suction with constant $v_o = -0.12$				
				Range of direct measurements	2.8	82,400	-.1208	
					70.1	2,076,000	-.1197	
				Measurements of profiles	21.5	653,200	-.1205	
					46.2	1,412,000	-.1195	
[b]H-27a	60 to 70	0.02 to 0.3	Air	Blowing with constant $v_o = 0.12$				
				Range of direct measurements	2.8	83,900	.1200	
					96.8	3,265,000	.1206	
				Measurements of profiles	29.4	897,000	.1196	.157
					83.4	2,736,000	.1204	.394

[b]Uniform blowing gas temperature.

TABLE VII.- THEORETICAL AND DIRECTLY MEASURED HEAT TRANSFER COEFFICIENTS

(a) Euler number, 0

Compartment	Theoretical values (a)								Experimental
	R_x	$T_o - T_1$	h_{*_L}	ϕ_{H_L}	h_L	h_{*_T}	ϕ_{H_T}	h_T	h^b
Run H-1: Main air stream: Velocity, 4.4 fps; temperature, 81° F; pressure, 29.9 in. Hg; distribution of air flowing through porous wall, zero mass transfer; porous-wall temperature distribution, constant wall									
A	303	25.5	6.79	0	6.79				8.71
B	2,640	27.2	2.28	0	2.28				1.30
C	7,270	23.8	1.38	0	1.38				1.47
D	14,220	23.8	.98	0	.98				1.08
E	23,430	23.8	.77	0	.77				.87
F	35,030	24.4	.63	0	.63				.70
G	48,930	25.0	.53	0	.53				.50
H	65,040	23.8	.46	0	.46				.49
I	83,600	24.1	.41	0	.41				.45
J	104,100	24.5	.36	0	.36				.49
K	127,500	27.3	.33	0	.33				.41
L	152,800	27.7	.30	0	.30				.39
M	180,800	26.6	.28	0	.28				.40
N	210,000	27.8	.26	0	.26				.32
O	242,300	24.5	.24	0	.24				.35
Run H-2: Main air stream: Velocity, 16.2 fps; temperature, 84.5° F; pressure, 30.2 in. Hg; distribution of air flowing through porous wall, zero mass transfer; porous-wall temperature distribution, constant wall									
A	1,100	23.0	13.03	0	13.03	8.71	0	8.71	20.12
B	9,590	22.9	4.38	0	4.38	5.92	0	5.92	5.59
C	26,400	23.7	2.64	0	2.64	4.84	0	4.84	2.10
D	51,700	23.4	1.89	0	1.89	4.24	0	4.24	2.25
E	85,100	23.1	1.47	0	1.47	3.84	0	3.84	1.78
F	127,200	24.8	1.20	0	1.20	3.54	0	3.54	2.40
G	177,700	22.9	1.02	0	1.02	3.32	0	3.32	3.22
H	236,200	23.9	.88	0	.88	3.13	0	3.13	3.07
I	303,500	24.2	.78	0	.78	2.98	0	2.98	3.19
J	378,200	24.6	.70	0	.70	2.85	0	2.85	2.98
K	463,100	24.4	.63	0	.63	2.74	0	2.74	2.62
L	555,100	24.5	.58	0	.58	2.64	0	2.64	2.43
M	655,900	24.7	.52	0	.52	2.52	0	2.52	2.37
N	758,400	24.1	.47	0	.47	2.34	0	2.34	2.46
O	868,000	22.7	.43	0	.43	2.24	0	2.24	2.46
Run H-3: Main air stream: Velocity, 27.0 fps; temperature, 71° F; pressure, 30.3 in. Hg; distribution of air flowing through porous wall, zero mass transfer; porous-wall temperature distribution, constant wall									
A	1,880	25.6	16.66	0	16.66	13.06	0	13.06	72.10
B	16,360	(16.18)	5.59	0	5.59	8.87	0	8.87	7.55
C	45,050	24.0	3.37	0	3.37	7.26	0	7.26	4.49
D	88,100	24.4	2.41	0	2.41	6.36	0	6.36	9.80
E	145,100	20.6	1.88	0	1.88	5.76	0	5.76	5.55
F	216,900	23.0	1.54	0	1.54	5.31	0	5.31	5.91
G	303,000	23.3		0		4.98	0	4.98	4.93
H	402,800	23.1		0		4.69	0	4.69	4.50
I	517,500	23.6		0		4.47	0	4.47	4.51
J	645,000	23.1		0		4.27	0	4.27	4.59
K	790,000	22.8		0		4.10	0	4.10	4.24
L	947,000	22.5		0		3.96	0	3.96	3.59
M	1,119,500	21.7		0		3.83	0	3.83	3.73
N	1,300,500	23.2		0		3.71	0	3.71	3.83
O	1,500,000	20.1		0		3.61	0	3.61	4.47
Run H-4: Main air stream: Velocity, 58.8 fps; temperature, 77° F; pressure, 30.1 in. Hg; distribution of air flowing through porous wall, no mass transfer; porous-wall temperature distribution, constant wall									
A	4,040	21.7	24.66	0	24.66	24.35	0	24.35	104.80
B	35,200	(20)	8.28	0	8.28	16.54	0	16.54	25.98
C	97,100	22.3	4.99	0	4.99	13.54	0	13.54	14.69
D	189,800	24.0	3.57	0	3.57	11.85	0	11.85	17.77
E	312,500	19.9	2.78	0	2.78	10.73	0	10.73	11.17
F	467,400	21.2		0		9.90	0	9.90	10.28
G	652,800	21.7		0		9.28	0	9.28	8.37
H	867,700	20.3		0		8.75	0	8.75	8.40
I	1,115,000	21.8		0		8.33	0	8.33	8.53
J	1,389,000	20.8		0		7.96	0	7.96	10.99
K	1,701,000	20.6		0		7.65	0	7.65	7.87
L	2,039,000	20.5		0		7.38	0	7.38	6.99
M	2,412,000	21.4		0		7.14	0	7.14	7.99
N	2,802,000	20.4		0		6.92	0	6.92	10.44
O	3,232,000	16.1		0		6.73	0	6.73	13.50

[a] Explanation of symbols: R_x, Reynolds number of main stream; T_o and T_1, wall and main-stream temperature, respectively, °F; h_{*_L} and h_{*_T}, heat transfer coefficients for laminar and turbulent flow, respectively, with main-stream conditions of experiment, no flow through wall, Btu/(hr)(sq ft)(°F); h_L and h_T, heat transfer coefficients predicted by laminar-boundary-layer theory and film theory, respectively, Btu/(hr)(sq ft)(°F); ϕ_{H_L}, laminar rate factor, $\frac{\sum_j N_j M_j c_{p_j}}{h_{*_L}} = \frac{3{,}600 v_o \rho c_p}{h_{*_L}}$; ϕ_{H_T}, turbulent rate factor, $\frac{\sum_j N_j M_j c_{p_j}}{h_{*_T}} = \frac{3{,}600 v_o \rho c_p}{h_{*_T}}$.

[b] h, experimentally measured heat transfer coefficient, Btu/(hr)(sq ft)(°F).

TABLE VII.- THEORETICAL AND DIRECTLY MEASURED HEAT TRANSFER COEFFICIENTS - Continued

(a) Euler number, 0 - Continued

Compartment	Theoretical values (a)								Experimental h^b
	R_x	$T_o - T_1$	h_{*_L}	ϕ_{H_L}	h_L	h_{*_T}	ϕ_{H_T}	h_T	
Run H-5: Main air stream: Velocity, 4.6 fps; temperature, 80° F; pressure, 30.3 in. Hg; distribution of air flowing through porous wall, blowing with $\phi_H = 0.63$ ($v_o \propto 1/\sqrt{x}$, laminar; $v_o \propto 1/x^{0.2}$, turbulent); porous-wall temperature distribution, constant wall									
A	314	24.4	6.95	0.62	4.00	3.19	1.34	1.51	8.13
B	2,734	26.4	2.33	.63	1.33	2.16	.68	1.52	1.22
C	7,530	26.2	1.41	.62	.81	1.77	.49	1.37	.85
D	14,720	25.6	1.01	.61	.58	1.55	.40	1.26	.68
E	24,250	26.0	.78	.61	.45	1.40	.34	1.18	.52
F	36,260	27.4	.64	.63	.36	1.30	.31	1.10	.31
G	50,650	27.8	.54	.82	.23	1.21	.37	1.01	.30
H	67,320	28.5	.47	1.11	.11	1.15	.46	.90	.35
I	86,500	27.8	.41	1.56	.02	1.09	.59	.80	.59
J	107,800	26.7	.37	1.78	.01	1.04	.63	.75	.76
K	132,000	27.0				1.00	.64	.72	.65
L	158,200	27.1				.97	.64	.69	.62
M	187,100	27.1				.93	.64	.67	.64
N	217,400	28.3				.91	.64	.65	.48
O	250,800	27.6				.88	.64	.63	.56
Run H-6: Main air stream: Velocity, 17.6 fps; temperature 71° F; pressure, 30.3 in. Hg; distribution of air flowing through porous wall, blowing with $\phi_H = 0.63$ ($v_o \propto 1/\sqrt{x}$, laminar; $v_o \propto 1/x^{0.2}$, turbulent); porous-wall temperature distribution: constant wall									
A	1,220	15.08	13.42	0.62	7.7	9.25	0.90	5.71	31.33
B	10,620	19.72	4.51	.63	2.56	6.28	.45	4.93	5.58
C	29,250	22.78	2.72	.63	1.54	5.14	.33	4.34	2.06
D	57,190	20.03	1.94	.89	.73	4.50	.39	3.69	5.37
E	94,200	20.95	1.51	1.69	.02	4.07	.63	2.93	3.20
F	140,900	20.42				3.76	.62	2.71	3.01
G	196,700	20.51				3.52	.63	2.54	2.50
H	261,500	21.51				3.32	.62	2.40	2.31
I	336,000	21.99				3.16	.63	2.28	2.33
J	419,000	20.90				3.02	.63	2.17	2.12
K	513,000	21.07				2.90	.62	2.09	1.98
L	615,000	20.90				2.80	.63	2.01	1.86
M	727,000	20.68				2.71	.63	1.95	2.00
N	844,000	21.33				2.63	.63	1.89	1.86
O	974,000	20.11				2.55	.63	1.84	1.96
Run H-7: Main air stream: Velocity, 60.7 fps; temperature, 71° F; pressure, 30.5 in. Hg; distribution of air flowing through porous wall, blowing with $\phi_H = 0.60$ ($v_o \propto 1/\sqrt{x}$, laminar; $v_o \propto 1/x^{0.2}$, turbulent); porous-wall temperature distribution, constant wall									
A	4,200	5.5	24.96	0.60	14.57	24.95	0.60	18.20	125.20
B	36,700	(10)	8.38	.61	4.85	16.95	.30	14.54	12.34
C	102,400	16.6				13.87	.60	10.15	19.30
D	199,000	19.8				12.14	.60	8.87	11.27
E	326,700	19.8				11.00	.60	8.04	10.79
F	488,700	21.3				10.15	.60	7.42	8.91
G	677,600	21.4				9.51	.60	6.95	7.31
H	907,300	20.6				8.97	.57	6.64	7.13
I	1,159,000	22.1				8.54	.60	6.25	7.12
J	1,454,000	20.0				8.16	.60	5.96	7.60
K	1,777,000	22.0				7.84	.60	5.73	6.09
L	2,126,000	20.8				7.56	.60	5.53	5.67
M	2,514,000	22.4				7.31	.60	5.35	6.11
N	2,924,000	22.8				7.10	.60	5.19	6.13
O	3,376,000	18.0				6.89	.60	5.04	10.45
Run H-8: Main air stream: Velocity, 19.6 fps; temperature, 78° F; pressure, 30.2 in. Hg; distribution of air flowing through porous wall, blowing with $\phi_H = 1.2$ ($v_o \propto 1/\sqrt{x}$, laminar; $v_o \propto 1/x^{0.2}$, turbulent); porous-wall temperature distribution, constant wall									
A	1,350	9.2	14.26	1.22	2.51	10.12	1.72	3.79	53.90
B	11,700	(20)	4.79	1.23	.84	6.87	.85	4.36	3.18
C	32,300	21.2	3.05	1.27	.45	5.63	.65	3.99	3.45
D	63,100	25.2	2.06	2.84	.00	4.92	1.19	2.56	3.22
E	104,000	24.5	1.61	3.39	.00	4.46	1.22	2.28	3.24
F	155,500	25.9				4.11	1.22	2.11	2.68
G	217,200	25.3				3.85	1.22	1.97	1.90
H	288,700	25.1				3.64	1.22	1.86	1.86
I	371,000	26.4				3.46	1.23	1.76	1.81
J	462,000	25.8				3.31	1.23	1.68	1.44
K	566,000	28.3				3.18	1.23	1.62	1.52
L	679,000	25.6				3.07	1.23	1.56	1.49
M	803,000	26.2				2.97	1.24	1.50	1.97
N	932,000	27.3				2.88	1.24	1.45	1.58
O	107,600	24.6				2.80	1.25	1.40	1.46

[a] Explanation of symbols: R_x, Reynolds number of main stream; T_o and T_1, wall and main-stream temperature, respectively, °F; h_{*_L} and h_{*_T}, heat transfer coefficients for laminar and turbulent flow, respectively, with main-stream conditions of experiment, no flow through wall, Btu/(hr)(sq ft)(°F); h_L and h_T, heat transfer coefficients predicted by laminar-boundary-layer theory and film theory, respectively, Btu/(hr)(sq ft)(°F); ϕ_{H_L}, laminar rate factor, $\frac{\sum_j N_j M_j c_{p_j}}{h_{*_L}} = \frac{3{,}600 v_o \rho c_p}{h_{*_L}}$; ϕ_{H_T}, turbulent rate factor, $\frac{\sum_j N_j M_j c_{p_j}}{h_{*_T}} = \frac{3{,}600 v_o \rho c_p}{h_{*_T}}$.

[b] h, experimentally measured heat transfer coefficient, Btu/(hr)(sq ft)(°F).

TABLE VII.- THEORETICAL AND DIRECTLY MEASURED HEAT TRANSFER COEFFICIENTS - Continued

(a) Euler number, 0 - Continued

Compartment	Theoretical values (a)								Experimental h^b
	R_x	$T_o - T_l$	h_{*_L}	ϕ_{H_L}	h_L	h_{*_T}	ϕ_{H_T}	h_T	
Run H-9: Main air stream: Velocity, 60.9 fps; temperature, 78.5° F; pressure, 29.9 in. Hg; distribution of air flowing through porous wall, blowing with $\phi_H = 1.2$ ($v_o \propto 1/\sqrt{x}$, laminar; $v_o \propto 1/x^{0.2}$, turbulent); porous-wall temperature distribution, constant wall									
C	101,600	21.9				13.94	1.17	7.33	11.89
D	197,500	20.0				12.20	1.18	6.41	12.32
E	324,100	21.7				11.05	1.17	5.80	7.08
F	484,800	22.6				10.19	1.17	5.38	6.00
G	672,100	21.7				9.55	1.17	5.03	4.33
H	900,000	21.3				9.01	1.17	4.74	4.67
I	1,150,000	22.1				8.58	1.17	4.51	5.15
J	1,443,000	20.1				8.19	1.17	4.31	4.62
K	1,762,000	20.3				7.88	1.18	4.13	4.52
L	2,109,000	17.8				7.60	1.17	4.01	4.04
M	2,494,000	17.7				7.35	1.16	3.90	6.06
N	2,901,000	12.7				7.13	.58	5.25	4.17
O	3,349,000	10.2				6.93	.00		9.79
Run H-10: Main air stream: Velocity, 5.3 fps; temperature, 85° F; pressure, 29.7 in. Hg; distribution of air flowing through porous wall, blowing with $\phi_H = 1.2$ ($v_o \propto 1/\sqrt{x}$, laminar); porous-wall temperature distribution, constant wall									
B	1,036	(22)	4.38	1.17	0.96				
C	7,200	21.9	1.66	1.16	.38				1.17
D	15,600	22.8	1.13	1.17	.25				.84
E	26,500	25.3	.86	1.17	.19	1.59	0.64	1.14	.45
F	40,500	24.1	.70	1.18	.16	1.46	.56	1.09	.66
G	57,000	21.5	.59	1.19	.12	1.37	.51	1.05	1.07
H	76,200	21.7	.51	1.17	.11	1.29	.46	1.01	1.16
I	98,600	22.4				1.22	.43	.98	1.00
J	123,400	22.9				1.17	.40	.95	.94
K	151,100	23.2				1.12	.38	.93	.84
L	181,500	22.6				1.08	.36	.90	.79
M	214,700	22.2				1.05	.33	.88	.83
N	250,400	22.7				1.02	.31	.87	.77
O	289,000	22.6				.99	.31	.84	.58
Run H-11: Main air stream: Velocity, 4.8 fps; temperature, 84.4° F; pressure, 29.7 in. Hg; distribution of air flowing through porous wall, suction with $\phi_H = -1.2$ ($v_o \propto 1/\sqrt{x}$, laminar); porous-wall temperature distribution, constant wall									
B	940	18	4.18	-1.22	8.27				(9.11)
C	6,600	17.5	1.58	-1.10	2.97				4.65
D	14,200	18.2	1.08	-1.21	2.13				2.84
E	24,100	19.3	.83	-1.21	1.63				1.97
F	36,900	19.4	.67	-1.21	1.32				1.68
G	51,800	20.4	.56	-1.21	1.12				1.31
H	69,500	20.4	.49	-1.21	.96				1.24
I	89,600	19.8	.43	-1.20	.84				1.11
J	112,600	20.0	.38	-1.22	.76				1.08
K	137,300	20.9	.35	-1.20	.68				.93
L	165,100	20.6	.32	-1.21	.63				.85
M	195,200	19.2	.29	-1.21	.57				1.02
N	228,200	19.9	.27	-1.20	.53				.79
O	263,400	16.8	.25	-1.20	.49				1.13
Run H-12: Main air stream: Velocity, 19.8 fps; temperature, 76.5° F; pressure, 30 in. Hg; distribution of air flowing through porous wall, suction with $\phi_H = -1.2$ ($v_o \propto 1/\sqrt{x}$, laminar; $v_o \propto 1/x^{0.2}$, turbulent); porous-wall temperature distribution, constant wall									
C	27,200	25.0	3.18	-1.18	6.21				9.25
D	58,800	31.4	2.17	-1.18	4.24				4.90
E	100,000	27.4	1.66	-1.18	3.24				3.81
F	152,800	25.9	1.34	-1.18	2.63				3.18
[c]G	214,600	27.9	1.13	0	1.13				1.93
H	287,700	26.1	.98	-1.84	2.49	3.69	-0.49	4.66	2.50
I	371,800	23.1	.86	-4.38	4.14	3.50	-1.08	5.72	5.04
J	465,700	27.0				3.35	-1.17	5.67	4.82
K	570,100	24.2				3.22	-1.17	5.46	5.20
L	684,600	23.8				3.10	-1.19	5.31	4.63
M	810,000	26.0				3.00	-1.17	5.08	4.22
N	944,650	19.3				2.91	-.69	4.02	(3.08)
O	1,090,400					2.82			

[a] Explanation of symbols: R_x, Reynolds number of main stream; T_o and T_l, wall and main-stream temperature, respectively, °F; h_{*_L} and h_{*_T}, heat transfer coefficients for laminar and turbulent flow, respectively, with main-stream conditions of experiment, no flow through wall, Btu/(hr)(sq ft)(°F); h_L and h_T, heat transfer coefficients predicted by laminar-boundary-layer theory and film theory, respectively, Btu/(hr)(sq ft)(°F); ϕ_{H_L}, laminar rate factor, $\frac{\sum_j N_j M_j c_{p_j}}{h_{*_L}} = \frac{3{,}600 v_o \rho c_p}{h_{*_L}}$; ϕ_{H_T}, turbulent rate factor, $\frac{\sum_j N_j M_j c_{p_j}}{h_{*_T}} = \frac{3{,}600 v_o \rho c_p}{h_{*_T}}$.

[b] h, experimentally measured heat transfer coefficient, Btu/(hr)(sq ft)(°F).

[c] Orifice misalined; negligible flow through compartment G.

TABLE VII.- THEORETICAL AND DIRECTLY MEASURED HEAT TRANSFER COEFFICIENTS - Continued

(a) Euler number, 0 - Continued

Compartment	Theoretical values (a)								Experimental h^b
	R_x	$T_o - T_1$	h_{*_L}	ϕ_{H_L}	h_L	h_{*_T}	ϕ_{H_T}	h_T	
Run H-13: Main air stream: Velocity, 60.5 fps; temperature, 80° F; pressure, 29.7 in. Hg; distribution of air flowing through porous wall, suction with $\phi_H = -1.2$ ($v_o \propto 1/\sqrt{x}$, laminar); porous-wall temperature distribution, constant wall									
B	11,900	9.9	4.74	-1.19	28.90	19.55	-0.90	29.63	38.45
C	82,600	8.7	5.58	-1.20	11.00	14.39	-.46	17.99	12.85
D	178,900	9.0	3.80	-1.29	7.69	12.37	-.40	14.97	26.60
E	305,600	9.3	2.91	-1.20	5.73	11.13	-.31	12.95	11.35
F	464,800	8.4	2.36	-1.20	4.64	10.24	-.28	11.72	12.31
G	654,800	8.6				9.56	-.25	10.81	10.47
H	873,700	8.5				9.02	-.23	10.10	10.86
I	1,131,200	7.9				8.57	-.21	9.52	12.22
J	1,415,600	8.2				8.19	-.20	9.04	11.36
K	1,733,000	8.4				7.87	-.18	8.61	10.96
L	2,081,000	8.5				7.59	-.18	8.28	9.08
M	2,462,000	8.5				7.33	-.17	7.98	8.98
N	2,872,000	8.3				7.11	-.16	7.69	9.18
O	3,315,000	9.1				6.91	-.16	7.46	7.64
Run H-14: Main air stream: Velocity, 20.2 fps; temperature, 74.4° F; pressure, 30.5 in. Hg; distribution of air flowing through porous wall, suction with $\phi_H = -3.5$ ($v_o \propto 1/\sqrt{x}$, laminar); porous-wall temperature distribution, constant wall									
C	27,800	20.1	3.21	-3.41	12.6				18.82
D	60,100	14.6	2.18	-3.49	8.71				10.80
E	102,300	20.7	1.68	-3.48	6.67				7.60
F	156,200	20.2	1.36	-3.47	5.38				7.13
G	219,400	19.0	1.14	-3.55	4.62				4.39
H	294,200	20.3	.99	-3.58	4.02				4.55
I	379,500	19.8	.87	-3.55	3.51				5.22
J	476,600	20.4	.78	-3.56	3.14				3.49
K	581,300	21.9	.70	-3.57	2.85				3.73
L	699,100	22.0	.64	-3.56	2.59				3.28
M	826,400	21.6	.59	-3.57	2.39				3.58
N	966,100	21.3	.54	-3.56	2.21				3.87
O	1,115,200	20.7	.51	-3.58	2.07				3.61
Run H-15: Main air stream: Velocity, 59.7 fps; temperature, 77.7° F; pressure, 29.8 in. Hg; distribution of air flowing through porous wall, suction with $\phi_H = -3.6$ ($v_o \propto 1/\sqrt{x}$, laminar); porous-wall temperature distribution, constant wall									
C	81,800	8.0	5.53	-3.56	22.4	14.23	-1.39	26.30	32.02
D	178,000	4.5	3.76	-3.55	15.2	12.23	-1.09	20.09	43.48
E	302,600	9.2	2.89	-3.61	11.8	11.01	-.95	17.03	16.74
F	460,400	9.1				10.13	-.83	14.90	18.06
G	648,700	9.2				9.46	-.75	13.46	13.46
H	865,500	8.9				8.92	-.69	12.35	13.52
I	1,120,600	8.8				8.47	-.64	11.46	18.50
J	1,402,400	9.2				8.10	-.60	10.76	12.44
K	1,717,000	8.6				7.78	-.56	10.17	14.74
L	2,062,000	8.8				7.50	-.53	9.67	12.08
M	2,439,000	8.7				7.25	-.51	9.24	9.81
N	2,845,000	8.4				7.03	-.48	8.87	11.95
O	3,284,000	8.8				6.83	-.45	8.50	8.33
Run H-16a: Main air stream: Velocity, 5.0 fps; temperature, 93.9° F; pressure, 30.2 in. Hg; distribution of air flowing through porous wall, constant blowing velocity with $v_o = 0.01$ fps and $v_o/u_1 = 0.002$; porous-wall temperature distribution, constant blowing gas temperature									
C	6,730	12.4	1.62	0.41	1.14				1.15
D	14,570	17.0	1.10	.56	.67				.59
E	24,790	18.7	.85	.74	.41				.42
F	37,860	19.4	.69	.93	.24				.35
G	53,300	19.2	.58	1.09	.14	1.31	0.48	1.02	.35
H	71,200	16.5	.50	1.27	.08	1.24	.51	.95	.48
I	92,200	15.4				1.18	.54	.89	.66
J	115,400	15.9				1.12	.56	.84	.63
K	141,300	15.5				1.08	.59	.79	.72
L	169,700	16.2				1.04	.61	.76	.68
M	200,700	16.1				1.01	.63	.72	.66
N	234,100					.98	.66	.69	
O	270,200					.95	.67	.67	

[a] Explanation of symbols: R_x, Reynolds number of main stream; T_o and T_1, wall and main-stream temperature, respectively, °F; h_{*_L} and h_{*_T}, heat transfer coefficients for laminar and turbulent flow, respectively, with main-stream conditions of experiment, no flow through wall, Btu/(hr)(sq ft)(°F); h_L and h_T, heat transfer coefficients predicted by laminar-boundary-layer theory and film theory, respectively, Btu/(hr)(sq ft)(°F); ϕ_{H_L}, laminar rate factor, $\frac{\sum_j N_j M_j c_{p_j}}{h_{*_L}} = \frac{3{,}600 v_o \rho c_p}{h_{*_L}}$; ϕ_{H_T}, turbulent rate factor, $\frac{\sum_j N_j M_j c_{p_j}}{h_{*_T}} = \frac{3{,}600 v_o \rho c_p}{h_{*_T}}$.

[b] h, experimentally measured heat transfer coefficient, Btu/(hr)(sq ft)(°F).

TABLE VII.- THEORETICAL AND DIRECTLY MEASURED HEAT TRANSFER COEFFICIENTS - Continued

(a) Euler number, 0 - Continued

Compartment	Theoretical values (a)								Experimental h^b
	R_x	$T_o - T_1$	h_{*_L}	ϕ_{H_L}	h_L	h_{*_T}	ϕ_{H_T}	h_T	
Run H-17a: Main air stream: Velocity, 20.0 fps; temperature, 77° F; pressure, 30.1 in. Hg; distribution of air flowing through porous wall, constant blowing velocity with v_o = 0.04 fps and v_o/u_1 = 0.002; porous-wall temperature distribution, constant blowing gas temperature									
C	27,300	7.9	3.20	0.79	1.21	5.91	0.43	4.74	1.92
D	59,100	10.7	2.17	1.19	.41	5.08	.51	3.89	.43
E	100,800	6.1	1.67	1.41	.17	4.57	.51	3.50	2.90
F	153,500	6.4				4.20	.56	3.14	2.73
G	216,200	6.9				3.93	.64	2.81	2.63
H	288,500	7.0				3.70	.62	2.68	2.29
I	373,600	8.0				3.52	.72	2.41	2.23
J	467,500	8.1				3.36	.73	2.29	2.18
K	572,300	8.9				3.23	.77	2.15	2.00
L	687,300	9.4				3.12	.79	2.05	1.85
M	813,200	9.1				3.01	.84	1.93	1.97
N	948,400	9.4				2.92	.84	1.86	1.78
O	1,094,700	9.7				2.84	.90	1.75	1.67
Run H-17b: Main air stream: Velocity, 18.8 fps; temperature, 77° F; pressure, 30.1 in. Hg; distribution of air flowing through porous wall, constant blowing velocity with v_o = 0.04 fps and v_o/u_1 = 0.002; porous-wall temperature distribution, constant wall									
C	25,600	15.9	3.10	0.81	1.36	5.62	0.44	4.47	1.59
D	55,800	18.0	2.11	1.22	.39	4.83	.53	3.66	3.11
E	94,900	16.4				4.35	.54	3.28	3.62
F	144,300	15.2				4.00	.59	2.94	3.05
G	203,300	15.8				3.74	.67	2.63	2.42
H	271,200	15.9				3.53	.64	2.51	2.29
I	351,200	16.7				3.35	.75	2.25	2.16
J	439,500	16.4				3.20	.76	2.14	2.20
K	538,100	17.5				3.08	.80	2.00	1.80
L	646,100	18.1				2.97	.83	1.91	1.80
M	764,500	17.6				2.87	.87	1.80	1.76
N	891,600	17.7				2.78	.88	1.74	1.72
O	1,029,000	17.7				2.70	.94	1.63	1.66
Run H-18a: Main air stream: Velocity, 59.8 fps; temperature, 78° F; pressure, 29.8 in. Hg; distribution of air flowing through porous wall, constant blowing velocity with v_o = 0.04 fps and v_o/u_1 = 0.00067; porous-wall temperature distribution, constant blowing gas temperature									
C	83,740	2.8				14.27	0.22	12.76	14.07
D	179,280	5.6				12.26	.21	11.04	5.91
E	303,410	3.6				11.03	.23	9.82	7.38
F	461,500	3.9				10.15	.25	8.93	6.47
G	650,200	4.1				9.48	.25	8.35	6.61
H	867,500	4.4				8.94	.32	7.60	8.08
I	1,123,100	4.3				8.49	.30	7.29	6.90
J	1,405,600	3.8				8.12	.31	6.92	8.69
K	1,720,800	4.7				7.80	.33	6.60	6.56
L	2,066,400	5.1				7.52	.34	6.32	6.15
M	2,445,000	4.2				7.27	.35	6.07	7.85
N	2,851,000	4.6				7.05	.36	5.85	6.96
O	3,291,000	6.1				6.85	.37	5.66	4.10
Run H-19a: Main air stream: Velocity, 19.9 fps; temperature, 80° F; pressure, 30.0 in. Hg; distribution of air flowing through porous wall, constant blowing velocity with v_o = 0.12 fps and v_o/u_1 = 0.006; porous-wall temperature distribution, constant blowing gas temperature									
C	27,500	16.3				5.91	1.36	2.77	2.85
D	59,400	13.6				5.08	1.50	2.19	4.54
E	100,500	15.4				4.57	1.67	1.77	2.14
F	152,900	16.8				4.21	1.81	1.49	1.95
G	215,400	16.5				3.93	1.94	1.28	1.42
H	287,400	17.1				3.71	2.05	1.12	1.27
I	372,100	17.6				3.52	2.16	.99	.93
J	465,700	17.6				3.37	2.26	.89	.92
K	570,100	18.2				3.23	2.35	.80	.72
L	684,600	18.3				3.12	2.44	.73	.63
M	810,100	18.2				3.01	2.52	.66	.83
N	944,700	18.7				2.92	2.61	.61	.56
O	1,090,500	18.3				2.84	2.67	.56	.62
Run H-19b: Main air stream: Velocity, 19.8 fps; temperature, 79.4° F; pressure, 30.0 in. Hg; distribution of air flowing through porous wall, constant blowing velocity with v_o = 0.12 fps and v_o/u_1 = 0.006; porous-wall temperature distribution, constant wall									
C	27,600	20.2				5.89	1.36	2.77	2.09
D	59,200	18.2				5.06	1.50	2.19	4.62
E	100,210	20.2				4.56	1.66	1.77	2.13
F	152,400	21.3				4.19	1.80	1.49	1.83
G	214,800	21.0				3.91	1.93	1.28	1.34
H	286,600	21.6				3.69	2.05	1.12	1.21
I	371,000	21.7				3.51	2.14	1.00	.94
J	464,300	21.7				3.35	2.26	.88	.93
K	568,400	22.5				3.22	2.36	.80	.70
L	682,500	22.4				3.11	2.44	.72	.68
M	807,600	22.3				3.00	2.52	.66	.80
N	941,800	22.8				2.91	2.64	.59	.61
O	1,087,100	22.3				2.83	2.69	.55	.64

[a] Explanation of symbols: R_x, Reynolds number of main stream; T_o and T_1, wall and main-stream temperature, respectively, °F; h_{*_L} and h_{*_T}, heat transfer coefficients for laminar and turbulent flow, respectively, with main-stream conditions of experiment, no flow through wall, Btu/(hr)(sq ft)(°F); h_L and h_T, heat transfer coefficients predicted by laminar-boundary-layer theory and film theory, respectively, Btu/(hr)(sq ft)(°F); ϕ_{H_L}, laminar rate factor, $\frac{\sum_j N_j M_j c_{p_j}}{h_{*_L}} = \frac{3{,}600 v_o \rho c_p}{h_{*_L}}$; ϕ_{H_T}, turbulent rate factor, $\frac{\sum_j N_j M_j c_{p_j}}{h_{*_T}} = \frac{3{,}600 v_o \rho c_p}{h_{*_T}}$.

[b] h, experimentally measured heat transfer coefficient, Btu/(hr)(sq ft)(°F).

TABLE VII.- THEORETICAL AND DIRECTLY MEASURED HEAT TRANSFER COEFFICIENTS - Continued

(a) Euler number, 0 - Continued

Compartment	Theoretical values (a)								Experimental h^b
	R_x	$T_o - T_1$	h_{*_L}	ϕ_{H_L}	h_L	h_{*_T}	ϕ_{H_T}	h_T	
Run H-20a: Main air stream: Velocity, 60.7 fps; temperature, 82.8° F; pressure, 30.3 in. Hg; distribution of air flowing through porous wall, constant blowing velocity with v_o = 0.12 fps and v_o/u_1 = 0.002; porous-wall temperature distribution, constant blowing gas temperature									
C	84,440	8.3				14.46	0.53	10.97	12.24
D	180,760	7.7				12.42	.62	8.98	13.89
E	305,930	10.1				11.18	.69	7.78	8.21
F	465,300	10.8				10.29	.75	6.92	6.58
G	655,600	11.1				9.60	.80	6.27	6.34
H	874,700	11.2				9.06	.85	5.76	6.24
I	1,132,400	12.2				8.61	.89	5.33	5.15
J	1,417,300	11.3				8.23	.93	4.99	6.15
K	1,735,000	12.7				7.91	.97	4.68	4.64
L	2,083,500	13.1				7.62	1.01	4.42	4.20
M	2,465,000	12.0				7.37	1.04	4.19	5.05
N	2,875,000	12.7				7.15	1.08	3.98	4.43
O	3,318,500	13.9				6.94	1.10	3.81	3.24
Run H-20b: Main air stream: Velocity, 60.0 fps; temperature, 80.8° F; pressure, 30.3 in. Hg; distribution of air flowing through porous wall, constant blowing velocity with v_o = 0.12 fps and v_o/u_1 = 0.002; porous-wall temperature distribution, constant wall									
C	83,590	20.7				14.30	0.54	10.80	12.66
D	178,960	20.6				12.29	.63	8.84	11.72
E	302,900	20.3				11.06	.70	7.66	8.40
F	460,600	20.4				10.18	.76	6.81	7.49
G	649,000	20.8				9.50	.81	6.17	6.41
H	865,900	20.5				8.97	.86	5.66	6.32
I	1,121,100	21.4				8.52	.90	5.24	5.28
J	1,403,100	19.7				8.14	.94	4.89	6.65
K	1,717,700	20.7				7.82	.98	4.59	5.15
L	2,063,000	21.5				7.54	1.02	4.34	4.66
M	2,441,000	20.2				7.29	1.05	4.12	5.00
N	2,846,000	20.6				7.07	1.09	3.91	4.68
O	3,285,000	20.8				6.87	1.12	3.73	4.02
Run H-21a: Main air stream: Velocity, 59.8 fps; temperature, 76.5° F; pressure, 29.8 in. Hg; distribution of air flowing through porous wall, blowing with $\phi_H = 0.91$ ($v_o \propto 1/x^{0.2}$; mean v_o = 0.12 fps); porous-wall temperature distribution, constant blowing gas temperature with mass transfer distribution to give constant wall temperature									
C	83,920	10.7				14.26	0.91	8.74	9.86
D	179,700	9.6				12.25	.91	7.51	10.70
E	304,100	10.5				11.03	.91	6.78	6.64
F	462,400	11.0				10.14	.91	6.23	5.79
G	651,500	10.7				9.47	.91	5.82	5.73
H	869,300	10.4				8.94	.91	5.49	5.74
I	1,125,500	11.0				8.49	.91	5.22	4.62
J	1,408,600	10.0				8.12	.91	4.99	5.61
K	1,724,500	11.1				7.80	.91	4.79	4.08
L	2,071,000	11.2				7.52	.91	4.62	3.92
M	2,450,000	10.1				7.26	.91	4.46	4.85
N	2,857,000	10.6				7.05	.91	4.33	4.10
O	3,298,000	10.7				6.85	.83	4.38	2.64
Run H-22: Main air stream: Velocity, 4.9 fps; temperature, 84.4° F; pressure, 29.7 in. Hg; distribution of air flowing through porous wall, constant suction velocity with v_o = -0.01 fps and v_o/u_1 = -0.002; porous-wall temperature distribution, constant wall									
C	6,710	18.9	1.60	-0.41	2.27				3.28
D	14,500	19.7	1.09	-.57	1.67				2.28
E	24,700	20.3	.83	-.76	1.34				1.72
F	36,700	20.4	.68	-.94	1.19				1.52
G	53,000	21.3	.57	-1.12	1.08				1.29
H	71,100	20.6	.49	-1.31	1.01				1.23
I	91,800	19.6	.43	-1.48	.96				1.26
J	115,200	20.1	.39	-1.64	.91				1.15
K	140,500	20.7	.35	-1.85	.88				1.08
L	169,000	20.7	.32	-2.00	.85				1.06
M	199,800	20.3	.29	-2.21	.83				1.22
N	233,600	20.9	.27	-2.36	.81				1.02
O	269,600	19.1	.25	-2.53	.79				1.27

[a] Explanation of symbols: R_x, Reynolds number of main stream; T_o and T_1, wall and main-stream temperature, respectively, °F; h_{*_L} and h_{*_T}, heat transfer coefficients for laminar and turbulent flow, respectively, with main-stream conditions of experiment, no flow through wall, Btu/(hr)(sq ft)(°F); h_L and h_T, heat transfer coefficients predicted by laminar-boundary-layer theory and film theory, respectively, Btu/(hr)(sq ft)(°F); ϕ_{H_L}, laminar rate factor, $\frac{\sum_j N_j M_j c_{p_j}}{h_{*_L}} = \frac{3{,}600 v_o \rho c_p}{h_{*_L}}$; ϕ_{H_T}, turbulent rate factor, $\frac{\sum_j N_j M_j c_{p_j}}{h_{*_T}} = \frac{3{,}600 v_o \rho c_p}{h_{*_T}}$.

[b] h, experimentally measured heat transfer coefficient, Btu/(hr)(sq ft)(°F).

TABLE VII.- THEORETICAL AND DIRECTLY MEASURED HEAT TRANSFER COEFFICIENTS - Continued

(a) Euler number, 0 - Concluded

Compartment	Theoretical values (a)								Experimental h^b
	R_x	$T_o - T_1$	h_{*_L}	ϕ_{H_L}	h_L	h_{*_T}	ϕ_{H_T}	h_T	
Run H-23: Main air stream: Velocity, 4.8 fps; temperature, 78.4° F; pressure, 29.9 in. Hg; distribution of air flowing through porous wall, constant suction velocity with v_o = -0.04 fps and v_o/u_1 = -0.008; porous-wall temperature distribution, constant wall									
C	6,510	17.7	1.56	-1.61	3.38				4.78
D	14,100	16.4	1.06	-2.38	3.17				4.20
E	24,000	18.2	.82	-3.10	2.97				3.27
F	36,600	17.7	.66	-3.80	2.82				3.18
G	51,500	18.9	.56	-4.06	2.51				2.47
H	69,000	18.4	.48	-4.90	2.56				2.59
I	89,100	16.8	.42	-5.64	2.54				3.00
J	111,800	18.3	.38	-6.66	2.63				2.35
K	136,400	17.5	.34	-7.14	2.54				3.72
L	164,000	17.9	.31	-8.06	2.60				2.57
M	193,900	17.9	.29	-8.66	2.56				2.34
N	226,700	17.7	.25	-9.12	2.48				2.38
O	261,700	17.9	.25	-9.49	2.40				2.60
Run H-24: Main air stream: Velocity, 19.3 fps; temperature, 77.5° F; pressure, 29.9 in. Hg; distribution of air flowing through porous wall, constant suction velocity with v_o = -0.04 fps and v_o/u_1 = -0.002; porous-wall temperature distribution, constant wall									
B	3,800	(25)	8.31	-0.29	10.4				12.87
C	26,400	24.8	3.15	-.77	5.10				7.31
D	57,300	33.3	2.14	-1.14	4.10				4.29
E	97,400	26.5	1.64	-1.50	3.64				4.21
F	148,800	24.1	1.33	-1.85	3.35				3.63
[c]G	209,000	27.9	1.12	0	1.12				2.14
H	280,200	23.7	.97	-2.57	3.03	3.61	-0.6875	5.00	2.31
I	362,100	21.7	.85	-2.90	2.93	3.43	-.7192	4.81	3.55
J	453,500	23.8				3.28	-.7552	4.68	3.44
K	555,200	22.1				3.15	-.7847	4.55	4.03
L	666,700	21.5				3.04	-.8176	4.45	3.95
M	788,800	22.4				2.94	-.8483	4.36	4.15
N	919,900	20.5				2.85	-.8735	4.27	4.39
O	1,061,800	24.0				2.77	-.8997	4.20	4.12
Run H-25: Main air stream: Velocity, 19.6 fps; temperature, 78.5° F; pressure, 30.3 in. Hg; distribution of air flowing through porous wall, constant suction velocity with v_o = -0.12 fps and v_o/u_1 = -0.006; porous-wall temperature distribution, constant wall									
C	26,900	9.5	3.18	-2.42	9.57				1.64
D	58,250	8.9	2.16	-3.53	8.69				12.35
E	99,100	10.1	1.66	-4.63	8.37				8.32
F	151,300	8.3	1.34	-5.68	8.10				8.41
G	212,600	8.1	1.13	-6.84	8.07				6.67
H	285,100	9.1	.98	-7.90	7.98				7.66
I	367,800	8.9	.86	-8.80	7.78				12.76
J	461,800	10.3	.77	-10.01	7.68				5.64
K	563,200	8.2	.70	-11.04	7.68				10.64
L	677,400	8.4	.63	-12.14	7.70				7.88
M	800,800	9.0	.58	-7.28	4.41				(4.34)
Run H-26: Main air stream: Velocity, 60.0 fps; temperature, 77.2° F; pressure, 29.9 in. Hg; distribution of air flowing through porous wall, constant suction velocity with v_o = -0.12 fps and v_o/u_1 = -0.002; porous-wall temperature distribution, constant wall									
C	82,350	11.2	5.55	-1.39	11.80	14.30	-0.54	18.50	12.83
D	178,300	12.8	3.77	-1.96	9.89	12.29	-.60	16.36	20.25
E	303,300	10.3	2.89	-2.65	9.35	11.06	-.69	15.34	14.10
F	463,600	9.8				10.18	-.75	14.44	25.76
G	653,200	9.4				9.50	-.81	13.85	16.51
H	871,500	9.9				8.96	-.85	13.29	15.05
I	1,128,000	9.5				8.51	-.88	12.78	22.33
J	1,412,000	9.5				8.14	-.94	12.54	5.26
K	1,729,000	8.9				7.82	-.97	12.23	10.05
L	2,076,000	9.0				7.54	-1.01	11.99	9.97

[a]Explanation of symbols: R_x, Reynolds number of main stream; T_o and T_1, wall and main-stream temperature, respectively, °F; h_{*_L} and h_{*_T}, heat transfer coefficients for laminar and turbulent flow, respectively, with main-stream conditions of experiment, no flow through wall, Btu/(hr)(sq ft)(°F); h_L and h_T, heat transfer coefficients predicted by laminar-boundary-layer theory and film theory, respectively, Btu/(hr)(sq ft)(°F); ϕ_{H_L}, laminar rate factor, $\frac{\sum_j N_j M_j c_{p_j}}{h_{*_L}} = \frac{3{,}600 v_o \rho c_p}{h_{*_L}}$; ϕ_{H_T}, turbulent rate factor, $\frac{\sum_j N_j M_j c_{p_j}}{h_{*_T}} = \frac{3{,}600 v_o \rho c_p}{h_{*_T}}$.

[b] h, experimentally measured heat transfer coefficient, Btu/(hr)(sq ft)(°F).

[c]Orifice misalined; negligible flow through compartment G.

TABLE VII.- THEORETICAL AND DIRECTLY MEASURED HEAT TRANSFER COEFFICIENTS - Concluded

(b) Euler number, 0.02 to 0.3

Compartment	Mainstream velocity, fps	Distance from leading edge, x, in.	Euler number	Turbulent rate factor, ϕ_{H_T} [a]	"Expected" heat transfer coefficient based on run H-20a	Measured heat transfer coefficient	Ratio of measured to "expected" coefficients
Run H-27a: Main air stream: Velocity, 60 to 70 fps; temperature, 87.4° F; pressure, 30.3 in. Hg; distribution of air flowing through porous wall, constant blowing velocity with v_o = 0.12 fps; porous-wall temperature distribution, constant blowing gas temperature							
C	60.7	2.8	------	0.53	12.26	11.90	0.97
D	61.0	6.1	0.017	.62	13.98	12.26	.88
E	61.4	10.3	.022	.68	8.33	7.85	.94
F	61.7	15.7	.031	.74	6.71	7.54	1.12
G	62.1	22.1	.056	.78	6.50	6.15	.95
H	62.7	29.5	.057	.82	6.52	6.49	1.00
I	63.0	38.1	.112	.87	5.39	6.27	1.16
J	64.4	47.7	.167	.89	6.62	7.22	1.09
K	65.3	58.4	.122	.92	5.07	5.05	1.00
L	65.9	70.1	.193	.95	4.64	5.00	1.08
M	67.5	82.9	.319	.96	5.78	8.51	1.47
N	69.4	96.7	.290	.97	5.26	6.91	1.32

[a] $$\phi_{H_T} = \frac{\sum_j -N_j M_j c_{p_j}}{h_{*_T}} = \frac{3{,}600 v_o \rho c_p}{h_{*_T}}.$$

TABLE VIII.- TEMPERATURE PROFILE MEASUREMENTS

Station C		Station D		Station E		Station G		Station H		Station I		Station J		Station K		Station L		Station M		Station N	
y, in.	β	y, in.	β	y, in.	β	y, in.	β	y, in.	β	y, in.	β	y, in.	β	y, in.	β	y, in.	β	y, in.	β	y, in.	β
Run H-1; no transfer; u_1 = 4.4 fps																					
		x = 6.5 in. R_x = 14,200				x = 21.8 in. R_x = 48,930				x = 38.4 in. R_x = 83,600		x = 46.5 in. R_x = 104,100				x = 70.4 in. R_x = 152,800				x = 96.0 in. R_x = 210,000	
		0.018	0.149			0.022	0.087			0.007	0.032	0.017	0.055			0.023	0.041			0.027	0.039
		.023	.153			.026	.093			.010	.038	.022	.059			.029	.047			.032	.046
		.028	.162			.031	.101			.015	.045	.027	.069			.034	.058			.042	.070
		.038	.208			.041	.141			.025	.070	.037	.093			.044	.081			.052	.081
		.048	.268			.051	.175			.035	.100	.047	.121			.054	.110			.062	.096
		.058	.335			.061	.209			.045	.130	.057	.149			.064	.135			.082	.135
		.068	.384			.071	.241			.055	.163	.067	.180			.084	.180			.102	.175
		.078	.441			.081	.274			.065	.193	.077	.210			.104	.223			.122	.207
		.088	.477			.091	.306			.075	.221	.087	.236			.124	.266			.142	.242
		.098	.519			.101	.336			.085	.248	.097	.263			.144	.308			.162	.273
		.108	.583			.111	.366			.095	.276	.107	.285			.164	.336			.182	.306
		.118	.603			.121	.392			.105	.299	.117	.305			.184	.372			.202	.338
		.128	.645			.131	.416			.125	.342	.127	.325			.204	.408			.222	.359
		.138	.678			.141	.443			.145	.382	.147	.364			.224	.444			.242	.385
		.148	.703			.151	.471			.165	.425	.167	.402			.244	.480			.292	.447
		.158	.738			.161	.497			.185	.459	.187	.440			.264	.514			.342	.508
		.168	.778			.171	.527			.205	.501	.207	.469			.284	.547			.392	.562
		.178	.809			.181	.553			.225	.544	.227	.499			.304	.572			.442	.609
		.188	.840			.191	.577			.245	.575	.267	.572			.324	.601			.492	.653
		.198	.871			.201	.600			.265	.611	.307	.636			.344	.622			.542	.695
		.208	.891			.211	.618			.285	.645	.347	.701			.364	.649			.592	.730
		.218	.907			.221	.642			.305	.673	.387	.749			.414	.696			.642	.765
		.228	.925			.231	.664			.325	.705	.427	.790			.464	.748			.692	.800
		.238	.938			.241	.680			.345	.741	.477	.838			.514	.793			.742	.830
		.248	.949			.251	.698			.365	.766	.527	.881			.564	.833			.792	.853
		.268	.962			.261	.716			.385	.790	.577	.913			.614	.865			.842	.877
		.288	.971			.271	.732			.405	.811	.627	.941			.664	.896			.892	.898
		.308	.987			.281	.751			.425	.832	.677	.962			.714	.921			.942	.916
		.328	.987			.301	.779			.445	.849	.727	.972			.764	.939			.992	.933
		.348	.993			.321	.811			.465	.866	.777	.984			.864	.964			1.042	.947
		.398	.996			.341	.837			.485	.883	.827	.994			.964	.982			1.142	.963
		.448	.996			.391	.893			.505	.898	.927	.998			1.064	.989			1.242	.979
		.548	.998			.441	.932			.555	.924	1.127	1.000			1.164	.995			1.342	.989
		.748	1.000			.541	.966			.605	.953	1.427	1.000			1.364	.996			1.442	.991
		.948	1.000			.741	.994			.705	.975	1.927	1.000			1.564	.998			1.742	1.000
						.941	.998			.805	.985					1.964	1.000			2.042	1.000
						1.141	1.000			.905	.994					2.164	1.000			2.542	1.000
						1.441	1.000			1.405	.998										
										1.905	1.000										

TABLE VIII.- TEMPERATURE PROFILE MEASUREMENTS - Continued

Station C		Station D		Station E		Station G		Station H		Station I		Station J		Station K		Station L		Station M		Station N	
y, in.	β	y, in.	β	y, in.	β	y, in.	β	y, in.	β	y, in.	β	y, in.	β	y, in.	β	y, in.	β	y, in.	β	y, in.	β
Run H-2; no transfer; u_1 = 16.2 fps																					
		x = 6.5 in. R_x = 51,700				x = 21.8 in. R_x = 177,700				x = 38.4 in. R_x = 303,500		x = 46.5 in. R_x = 378,200				x = 70.4 in. R_x = 555,100				x = 96.0 in. R_x = 758,400	
		0.020	0.205			0.0195	0.205			0.020	0.275	0.020	0.316			0.020	0.301			0.020	0.347
		.021	.236			.020	.214			.021	.301	.021	.326			.021	.299			.021	.357
		.022	.236			.021	.250			.022	.308	.022	.355			.022	.299			.022	.365
		.023	.270			.022	.292			.023	.327	.023	.376			.023	.314			.023	.377
		.024	.283			.023	.282			.024	.358	.024	.385			.025	.353			.024	.382
		.025	.283			.024	.302			.025	.363	.025	.402			.026	.369			.025	.391
		.027	.298			.025	.315			.026	.379	.026	.418			.027	.389			.027	.415
		.029	.317			.027	.328			.028	.398	.027	.431			.028	.404			.029	.428
		.031	.338			.029	.347			.030	.417	.028	.438			.029	.431			.031	.441
		.033	.357			.031	.370			.032	.443	.030	.457			.030	.431			.033	.459
		.038	.413			.033	.393			.034	.448	.032	.477			.031	.438			.035	.464
		.043	.444			.035	.406			.037	.479	.034	.493			.032	.458			.037	.479
		.048	.497			.037	.422			.040	.491	.036	.514			.033	.459			.039	.487
		.053	.528			.042	.455			.045	.519	.038	.520			.034	.462			.041	.503
		.058	.590			.047	.503			.050	.519	.040	.534			.035	.471			.043	.501
		.063	.637			.052	.529			.055	.540	.042	.543			.037	.489			.048	.527
		.068	.665			.057	.542			.060	.550	.045	.555			.039	.510			.053	.550
		.073	.708			.067	.578			.070	.569	.048	.567			.041	.518			.058	.550
		.078	.736			.077	.610			.080	.600	.053	.587			.043	.528			.063	.566
		.083	.786			.087	.633			.090	.623	.058	.601			.045	.542			.073	.586
		.088	.811			.097	.649			.100	.637	.063	.617			.050	.560			.083	.594
		.093	.835			.117	.708			.110	.635	.068	.629			.055	.578			.093	.609
		.103	.888			.137	.740			.120	.652	.078	.645			.060	.593			.113	.634
		.113	.922			.157	.782			.140	.673	.088	.661			.065	.609			.133	.646
		.123	.941			.177	.828			.160	.690	.098	.672			.075	.629			.183	.669
		.133	.963			.197	.776			.180	.687	.108	.688			.085	.642			.233	.683
		.153	.991			.217	.799			.200	.725	.128	.699			.105	.662			.283	.704
		.173	1.000			.237	.831			.220	.720	.148	.718			.125	.681			.333	.714
		.193	1.000			.257	.838			.270	.746	.168	.729			.145	.691			.433	.741
		.213	1.000			.297	.886			.320	.784	.198	.750			.165	.704			.533	.774
		.233	1.000			.337	.912			.370	.825	.228	.770			.215	.730			.633	.795
						.387	.948			.420	.841	.278	.794			.265	.752			.733	.811
						.437	.961			.520	.882	.328	.816			.365	.788			.933	.853
						.537	.987			.620	.934	.428	.851			.465	.817			1.133	.893
						.637	.990			.720	.960	.528	.883			.565	.848			1.333	.937
						.737	.994			.820	.981	.628	.910			.665	.869			1.533	.970
						.937	1.000			.920	.979	.728	.940			.765	.891			1.733	.984
										1.120	1.000	.928	.959			.965	.930			1.933	.995
										1.420	1.000	1.428	1.000			1.165	.961			2.533	1.000
												1.928	1.000			1.465	.990				
																1.965	1.000				

TABLE VIII.- TEMPERATURE PROFILE MEASUREMENTS - Continued

Station C		Station D		Station E		Station G		Station H		Station I		Station J		Station K		Station L		Station M		Station N	
y, in.	β	y, in.	β	y, in.	β	y, in.	β	y, in.	β	y, in.	β	y, in.	β	y, in.	β	y, in.	β	y, in.	β	y, in.	β
Run H-5; blowing with constant $\phi_H = 0.63$; $u_1 = 4.6$ fps																					
		x = 6.5 in. R_x = 14,720				x = 21.8 in. R_x = 50,650						x = 46.5 in. R_x = 107,800				x = 70.4 in. R_x = 158,200				x = 96.0 in. R_x = 217,400	
		0.008	0.066			0.008	0.019					0.010	0.018			0.010	0.044			0.011	0.046
		.009	.066			.011	.019					.012	.024			.012	.044			.013	.046
		.010	.066			.016	.021					.014	.028			.015	.046			.018	.052
		.012	.066			.021	.023					.019	.042			.018	.048			.023	.070
		.017	.075			.026	.029					.024	.053			.023	.056			.028	.083
		.022	.094			.031	.038					.029	.055			.028	.062			.033	.096
		.027	.111			.036	.044					.034	.064			.033	.067			.038	.120
		.032	.139			.041	.048					.039	.083			.038	.071			.043	.129
		.037	.158			.046	.058					.044	.090			.043	.091			.048	.155
		.042	.179			.051	.071					.049	.116			.048	.106			.053	.179
		.047	.200			.056	.083					.054	.138			.053	.137			.058	.192
		.052	.222			.061	.085					.059	.154			.058	.152			.063	.201
		.057	.245			.071	.106					.064	.178			.063	.177			.068	.238
		.062	.260			.081	.131					.069	.189			.068	.200			.073	.251
		.067	.281			.091	.158					.074	.189			.073	.222			.078	.259
		.072	.309			.101	.175					.084	.240			.078	.241			.083	.277
		.077	.333			.111	.181					.094	.286			.083	.256			.088	.296
		.082	.348			.121	.212					.104	.299			.088	.266			.093	.294
		.087	.365			.131	.219					.114	.306			.098	.304			.103	.325
		.092	.394			.141	.227					.134	.312			.108	.331			.113	.351
		.097	.412			.161	.277					.154	.328			.118	.356			.123	.368
		.102	.435			.181	.317					.174	.328			.128	.368			.133	.386
		.112	.473			.201	.335					.194	.350			.138	.403			.143	.399
		.122	.514			.221	.369					.214	.358			.148	.407			.153	.410
		.132	.552			.241	.415					.264	.420			.168	.451			.173	.433
		.142	.591			.261	.419					.314	.453			.188	.476			.193	.466
		.162	.661			.281	.450					.364	.484			.208	.505			.213	.488
		.182	.719			.301	.473					.414	.499			.228	.524			.233	.494
		.202	.793			.321	.521					.514	.565			.248	.549			.263	.505
		.222	.846			.341	.544					.614	.637			.268	.568			.313	.523
		.242	.876			.361	.577					.714	.690			.298	.590			.363	.577
		.262	.900			.381	.623					.814	.765			.348	.624			.413	.593
		.302	.955			.401	.644					.914	.829			.398	.649			.463	.604
		.352	.981			.421	.685					1.014	.892			.448	.659			.513	.643
		.402	.994			.471	.748					1.114	.930			.548	.696			.613	.654
		.502	.998			.521	.802					1.214	.945			.748	.757			.713	.697
		.702	1.000			.571	.858					1.414	.983			.948	.815			.913	.736
		.902	1.000			.621	.888					1.914	.998			1.148	.852			1.113	.776
						.721	.950					2.214	1.000			1.348	.875			1.513	.845
						.821	.971									1.648	.919			2.013	.900
						.921	.981									1.948	.967			2.513	.961
						1.421	.992									2.318	.988			2.763	.983
						1.921	.998														

TABLE VIII.- TEMPERATURE PROFILE MEASUREMENTS - Continued

Station C		Station D		Station E		Station G		Station H		Station I		Station J		Station K		Station L		Station M		Station N	
y, in.	β	y, in.	β	y, in.	β	y, in.	β	y, in.	β	y, in.	β	y, in.	β	y, in.	β	y, in.	β	y, in.	β	y, in.	β
Run H-6; blowing with constant $\phi_H = 0.63$; $u_1 = 17.6$ fps																					
												x = 46.5 in. R_x = 419,000									
												0.010	0.103								
												.011	.105								
												.013	.114								
												.015	.131								
												.017	.128								
												.019	.140								
												.021	.151								
												.023	.182								
												.025	.211								
												.027	.231								
												.029	.239								
												.031	.256								
												.033	.271								
												.035	.282								
												.037	.293								
												.039	.311								
												.041	.322								
												.043	.333								
												.048	.348								
												.053	.365								
												.058	.379								
												.063	.379								
												.068	.393								
												.073	.407								
												.083	.416								
												.093	.433								
												.103	.456								
												.113	.462								
												.123	.467								
												.143	.499								
												.163	.504								
												.183	.521								
												.203	.530								
												.223	.544								
												.243	.564								
												.263	.578								
												.283	.590								
												.303	.595								
												.323	.607								
												.343	.618								
												.363	.627								
												.383	.632								
												.403	.650								
												.443	.689								
												.483	.695								
												.523	.712								
												.563	.724								
												.603	.752								
												.653	.764								
												.703	.783								
												.753	.801								
												.803	.821								
												.853	.843								
												.903	.866								
												.953	.877								
												1.003	.895								
												1.053	.923								
												1.103	.932								
												1.153	.937								
												1.203	.960								
												1.253	.977								
												1.303	.980								
												1.403	.986								
												1.503	.991								
												1.603	.994								
												1.703	1.000								
												1.903	1.000								
												2.103	1.000								

TABLE VIII.- TEMPERATURE PROFILE MEASUREMENTS - Continued

Station C		Station D		Station E		Station G		Station H		Station I		Station J		Station K		Station L		Station M		Station N	
y, in.	β	y, in.	β	y, in.	β	y, in.	β	y, in.	β	y, in.	β	y, in.	β	y, in.	β	y, in.	β	y, in.	β	y, in.	β
Run H-8; blowing with constant ϕ_H = 1.2; u_1 = 19.6 fps																					
												x = 46.5 in. R_x = 462,000						x = 83.1 in. R_x = 803,000			
												0.013	0.205					0.013	0.171		
												.014	.225					.014	.175		
												.015	.239					.016	.201		
												.016	.249					.018	.225		
												.018	.268					.020	.235		
												.020	.276					.023	.263		
												.022	.286					.026	.277		
												.024	.300					.031	.305		
												.029	.335					.036	.325		
												.034	.349					.041	.343		
												.044	.385					.046	.365		
												.054	.414					.056	.376		
												.064	.436					.066	.402		
												.074	.452					.076	.418		
												.094	.477					.096	.440		
												.124	.511					.126	.472		
												.154	.536					.156	.492		
												.194	.562					.196	.508		
												.244	.584					.246	.522		
												.294	.611					.296	.546		
												.344	.635					.396	.582		
												.394	.657					.496	.618		
												.494	.692					.596	.637		
												.594	.726					.796	.685		
												.694	.767					.996	.729		
												.794	.795					1.196	.765		
												.894	.828					1.396	.809		
												1.094	.886					1.596	.851		
												1.294	.929					1.796	.886		
												1.494	.972					1.996	.916		
												1.694	.990					2.196	.940		
												1.894	.996								
												2.094	1.000								

TABLE VIII.- TEMPERATURE PROFILE MEASUREMENTS - Continued

Station C		Station D		Station E		Station G		Station H		Station I		Station J		Station K		Station L		Station M		Station N	
y, in.	β	y, in.	β	y, in.	β	y, in.	β	y, in.	β	y, in.	β	y, in.	β	y, in.	β	y, in.	β	y, in.	β	y, in.	β
Run H-10; blowing; $v_o \propto 1/\sqrt{x}$; $\phi_H = 1.2$; $u_1 = 5.3$ fps; laminar region																					
		x = 6.0 in. R_x = 15,600		x = 10.7 in. R_x = 26,500																	
		0.0097	0.064	0.0091	0.017																
		.011	.061	.010	.024																
		.012	.061	.012	.034																
		.014	.068	.017	.053																
		.016	.071	.022	.072																
		.019	.073	.032	.115																
		.022	.079	.042	.156																
		.027	.093	.052	.204																
		.032	.113	.062	.250																
		.037	.133	.072	.286																
		.042	.159	.082	.329																
		.047	.179	.092	.353																
		.052	.208	.102	.397																
		.057	.232	.112	.428																
		.062	.257	.122	.466																
		.067	.278	.132	.493																
		.072	.301	.142	.529																
		.077	.325	.152	.565																
		.082	.351	.162	.606																
		.087	.371	.172	.637																
		.092	.401	.182	.666																
		.097	.425	.192	.697																
		.102	.440	.202	.733																
		.107	.465	.212	.752																
		.112	.495	.222	.767																
		.117	.515	.242	.813																
		.122	.542	.262	.863																
		.127	.560	.282	.901																
		.132	.580	.302	.916																
		.137	.601	.322	.942																
		.142	.631	.342	.954																
		.147	.655	.392	.974																
		.152	.677	.442	.990																
		.157	.699	.542	1.000																
		.162	.715	.642	1.000																
		.172	.755																		
		.182	.785																		
		.192	.818																		
		.202	.849																		
		.212	.867																		
		.222	.892																		
		.232	.909																		
		.252	.940																		
		.272	.960																		
		.292	.969																		
		.312	.987																		
		.362	.998																		
		.412	1.000																		
		.512	1.000																		

TABLE VIII.- TEMPERATURE PROFILE MEASUREMENTS - Continued

Station C		Station D		Station E		Station G		Station H		Station I		Station J		Station K		Station L		Station M		Station N	
y, in.	β	y, in.	β	y, in.	β	y, in.	β	y, in.	β	y, in.	β	y, in.	β	y, in.	β	y, in.	β	y, in.	β	y, in.	β
Run H-11; suction with constant $\phi_H = -1.2$; $u_1 = 4.8$ fps																					
		x = 6.0 in. R_x = 14,200				x = 21.4 in. R_x = 51,800						x = 46.1 in. R_x = 112,600						x = 83.2 in. R_x = 195,200			
		0.0097	0.195			0.010	0.081					0.010	0.053					0.0095	0.021		
		.010	.201			.011	.089					.011	.053					.010	.021		
		.011	.198			.012	.091					.012	.064					.012	.021		
		.012	.208			.014	.102					.014	.072					.015	.027		
		.013	.208			.017	.110					.016	.072					.018	.033		
		.015	.223			.020	.125					.018	.096					.0234	.027		
		.019	.247			.024	.154					.023	.107					.028	.051		
		.023	.277			.029	.991					.028	.131					.033	.048		
		.025	.302			.034	.222					.033	.149					.038	.063		
		.027	.329			.039	.248					.038	.163					.048	.099		
		.029	.361			.044	.277					.048	.195					.058	.132		
		.031	.386			.049	.313					.058	.259					.168	.177		
		.033	.414			.054	.350					.068	.264					.078	.228		
		.035	.438			.059	.371					.078	.317					.088	.273		
		.037	.457			.064	.384					.088	.339					.098	.339		
		.039	.481			.069	.410					.098	.379					.108	.321		
		.041	.503			.074	.426					.108	.392					.118	.354		
		.044	.536			.084	.483					.118	.456					.128	.363		
		.047	.561			.089	.509					.128	.456					.138	.390		
		.050	.596			.094	.543					.138	.459					.158	.417		
		.053	.615			.099	.559					.148	.504					.178	.480		
		.057	.637			.104	.567					.158	.517					.198	.529		
		.061	.672			.114	.598					.168	.533					.218	.535		
		.065	.700			.124	.634					.178	.576					.238	.562		
		.069	.719			.134	.687					.188	.595					.258	.589		
		.073	.743			.144	.708					.198	.581					.278	.604		
		.078	.768			.154	.728					.218	.624					.298	.559		
		.083	.793			.164	.739					.238	.648					.318	.643		
		.088	.825			.174	.770					.258	.680					.338	.661		
		.093	.844			.184	.815					.278	.707					.358	.574		
		.098	.866			.194	.836					.298	.741					.378	.655		
		.103	.885			.204	.838					.318	.779					.418	.622		
		.108	.899			.224	.851					.338	.787					.468	.709		
		.113	.910			.244	.880					.358	.808					.518	.646		
		.123	.937			.264	.930					.378	.803					.568	.667		
		.133	.956			.284	.953					.398	.821					.618	.685		
		.143	.965			.304	.961					.448	.896					.718	.736		
		.153	.978			.324	.971					.498	.925					.818	.781		
		.173	.991			.374	.987					.598	.933					.918	.799		
		.193	.994			.424	.995					.698	.947					1.018	.790		
		.213	.997			.524	1.000					.898	1.000					1.218	.835		
		.263	1.000			.624	1.000											1.418	.916		
		.313	1.000															1.618	.949		
																		1.818	1.012		
																		2.018	.937		
																		2.218	1.000		

TABLE VIII.- TEMPERATURE PROFILE MEASUREMENTS - Continued

Station C		Station D		Station E		Station G		Station H		Station I		Station J		Station K		Station L		Station M		Station N	
y, in.	β	y, in.	β	y, in.	β	y, in.	β	y, in.	β	y, in.	β	y, in.	β	y, in.	β	y, in.	β	y, in.	β	y, in.	β
Run H-12; suction with constant $\phi_H = -1.2$; $u_1 = 19.8$ fps																					
		x = 6.1 in. R_x = 58,800		x = 10.7 in. R_x = 100,000		x = 21.5 in. R_x = 214,600				x = 38.1 in. R_x = 371,800				x = 58.4 in. R_x = 570,100				x = 83.3 in. R_x = 810,000			
		0.0055	0.404	0.0048	0.272	0.0055	0.182			0.005	0.280			0.005	0.237			0.005	0.109		
		.006	.433	.006	.358	.006	.219			.006	.352			.006	.241			.006	.129		
		.007	.477	.007	.385	.007	.243			.007	.367			.007	.266			.007	.143		
		.008	.503	.008	.408	.008	.267			.008	.398			.008	.313			.008	.165		
		.009	.525	.009	.423	.009	.275			.009	.417			.009	.345			.009	.241		
		.010	.547	.010	.444	.010	.294			.011	.430			.010	.383			.010	.288		
		.011	.567	.011	.457	.011	.310			.013	.463			.011	.408			.011	.320		
		.012	.587	.012	.474	.013	.318			.015	.498			.012	.429			.012	.334		
		.013	.602	.013	.486	.015	.340			.017	.517			.014	.465			.013	.356		
		.014	.618	.014	.493	.017	.368			.019	.535			.016	.503			.015	.388		
		.016	.657	.016	.526	.019	.383			.021	.530			.018	.529			.017	.427		
		.018	.688	.018	.549	.022	.421			.024	.557			.020	.554			.019	.447		
		.020	.716	.020	.568	.025	.441			.027	.574			.022	.573			.021	.471		
		.022	.745	.022	.589	.029	.468			.032	.609			.027	.634			.023	.501		
		.024	.765	.024	.608	.033	.496			.037	.633			.032	.672			.025	.521		
		.026	.791	.026	.625	.037	.530			.042	.661			.037	.715			.027	.547		
		.028	.811	.028	.651	.041	.563			.047	.683			.042	.744			.030	.584		
		.030	.829	.030	.665	.045	.587			.057	.735			.047	.770			.033	.608		
		.032	.846	.032	.684	.050	.623			.067	.772			.052	.793			.036	.638		
		.034	.855	.034	.703	.055	.662			.0773	.802			.057	.797			.039	.658		
		.036	.875	.036	.714	.060	.694			.087	.820			.062	.816			.043	.694		
		.040	.895	.041	.754	.065	.719			.107	.863			.072	.841			.048	.726		
		.044	.916	.046	.781	.070	.747			.127	.896			.082	.858			.053	.736		
		.049	.934	.051	.815	.075	.763			.147	.920			.092	.879			.058	.771		
		.054	.945	.056	.842	.085	.808			.167	.948			.112	.899			.063	.795		
		.059	.958	.061	.867	.095	.842			.197	.967			.132	.932			.068	.815		
		.064	.967	.066	.888	.105	.883			.247	.978			.152	.947			.073	.821		
		.074	.982	.076	.922	.115	.897			.297	.993			.182	.956			.083	.847		
		.084	.989	.086	.947	.125	.923			.347	.996			.212	.964			.093	.869		
		.094	.991	.096	.964	.135	.939			.447	.998			.252	.973			.103	.885		
		.114	.996	.116	.981	.145	.953			.547	1.000			.302	.983			.123	.920		
		.144	1.000	.136	.989	.165	.972							.352	.985			.143	.932		
		.194	1.000	.186	.998	.185	.982							.452	.992			.193	.966		
		.244	1.000	.236	1.000	.215	.992							.552	.996			.243	.970		
				.336	1.000	.265	1.000							.652	1.000			.343	.982		
						.315	1.000							.752	1.000			.443	.992		
						.365	1.000							.852	1.000			.543	.998		
																		.643	1.000		
																		.743	1.000		

TABLE VIII.- TEMPERATURE PROFILE MEASUREMENTS - Continued

Station C		Station D		Station E		Station G		Station H		Station I		Station J		Station K		Station L		Station M		Station N	
y, in.	β	y, in.	β	y, in.	β	y, in.	β	y, in.	β	y, in.	β	y, in.	β	y, in.	β	y, in.	β	y, in.	β	y, in.	β
Run H-14; suction with constant $\phi_H = -3.5$; $u_1 = 20.2$ fps																					
				x = 10.7 in. R_x = 102,300										x = 58.4 in. R_x = 581,300							
				0.0054	0.250									0.0055	[a]0.163						
				.006	.338										.090						
				.007	.373									.006	.283						
				.008	.390										.083						
				.0091	.430									.007	.390						
				.011	.504										.313						
				.013	.558									.008	.413						
				.015	.693										.390						
				.017	.662									.009	.540						
				.019	.640										.423						
				.019	.750									.011	.530						
				.021	.732										.400						
				.023	.772									.013	.580						
				.025	.816										.440						
				.027	.811									.015	.567						
				.029	.803										.500						
				.031	.785									.017	.510						
				.036	.785										.500						
				.041	.803									.022	.557						
				.041	.864										.537						
				.051	.908									.027	.583						
				.061	.912										.557						
				.081	.982									.032	.750						
				.101	.956										.580						
				.131	1.035									.037	.847						
				.181	1.009										.747						
				.231	1.000									.047	.863						
				.331	1.000										.827						
														.057	.883						
															.823						
														.067	.843						
															.823						
														.087	.960						
															.857						
														.107	1.000						
															.940						
														.137	.960						
															.937						

[a]Temperature fluctuated widely. Two readings were made at each position of the probe.

TABLE VIII.- TEMPERATURE PROFILE MEASUREMENTS - Continued

Station C		Station D		Station E		Station G		Station H		Station I		Station J		Station K		Station L		Station M		Station N	
y, in.	β	y, in.	β	y, in.	β	y, in.	β	y, in.	β	y, in.	β	y, in.	β	y, in.	β	y, in.	β	y, in.	β	y, in.	β
Run H-17a; blowing with constant v_o = 0.04; u_1 = 20.0 fps																					
		x = 6.1 in. R_x = 59,100		x = 10.7 in. R_x = 100,800		x = 21.5 in. R_x = 216,200				x = 38.1 in. R_x = 373,600				x = 58.4 in. R_x = 572,300				x = 83.3 in. R_x = 813,200			
		0.005	0.255	0.005	0.250	0.0055	0.139			0.005	0.098			0.005	0.194			0.005	0.134		
		.006	.327	.006	.315	.006	.162			.006	.133			.006	.214			.006	.146		
		.007	.355	.007	.315	.007	.221			.007	.142			.007	.222			.008	.158		
		.008	.336	.009	.381	.008	.221			.009	.177			.009	.243			.010	.170		
		.010	.373	.011	.394	.010	.280			.011	.208			.013	.279			.012	.176		
		.012	.382	.016	.434	.012	.303			.013	.234			.017	.308			.017	.189		
		.014	.400	.021	.487	.015	.326			.015	.256			.022	.344			.022	.207		
		.016	.418	.031	.539	.020	.383			.017	.283			.027	.379			.032	.286		
		.018	.427	.041	.618	.025	.419			.022	.337			.032	.408			.042	.353		
		.020	.436	.051	.645	.030	.442			.027	.372			.037	.421			.052	.411		
		.025	.491	.071	.684	.040	.499			.032	.381			.047	.436			.062	.439		
		.030	.536	.091	.737	.050	.535			.037	.398			.057	.450			.072	.460		
		.035	.573	.141	.802	.070	.593			.047	.442			.077	.486			.082	.482		
		.040	.609	.191	.868	.090	.593			.057	.460			.097	.515			.092	.499		
		.050	.636	.241	.868	.110	.628			.067	.460			.147	.544			.102	.518		
		.060	.673	.291	.921	.130	.651			.087	.504			.197	.579			.122	.542		
		.070	.727	.341	.961	.180	.709			.107	.531			.247	.615			.132	.549		
		.080	.800	.391	.987	.230	.743			.157	.575			.297	.650			.142	.561		
		.090	.845	.491	1.000	.330	.825			.207	.619			.347	.679			.162	.567		
		.100	.891			.430	.872			.257	.664			.397	.686			.192	.585		
		.110	.927			.530	.895			.307	.690			.497	.714			.222	.597		
		.130	.955			.730	.988			.407	.744			.597	.758			.322	.628		
		.150	.973			.930	1.000			.507	.796			.697	.793			.422	.659		
		.170	1.000			1.230	.988			.607	.863			.797	.815			.522	.671		
										.707	.877			.997	.850			.722	.744		
										.807	.902			1.197	.879			.922	.787		
										.907	.929			1.397	.936			1.122	.817		
										1.007	.965			1.597	.958			1.322	.854		
										1.107	.965			1.797	.993			1.522	.890		
										1.207	.973			1.997	1.000			1.722	.914		
										1.407	1.000			2.197	.971			1.922	.939		
										1.607	1.000							2.122	.957		
										1.807	.991							2.322	.957		
																		2.822	.988		
																		3.322	1.019		
																		3.822	1.000		

TABLE VIII.- TEMPERATURE PROFILE MEASUREMENTS - Continued

Station C		Station D		Station E		Station G		Station H		Station I		Station J		Station K		Station L		Station M		Station N	
y, in.	β	y, in.	β	y, in.	β	y, in.	β	y, in.	β	y, in.	β	y, in.	β	y, in.	β	y, in.	β	y, in.	β	y, in.	β
Run H-19b; blowing with constant v_o = 0.12; u_1 = 19.8 fps																					
x = 2.8 in. R_x = 27,600				x = 10.7 in. R_x = 100,210				x = 29.4 in. R_x = 286,600										x = 83.3 in. R_x = 807,600			
0.0057	0.044			0.006	0.084			0.0055	0.101									0.006	0.146		
.006	.058			.007	.121			.006	.115									.007	.176		
.007	.082			.008	.137			.007	.129									.008	.194		
.008	.090			.009	.161			.008	.144									.009	.196		
.009	.101			.010	.171			.008	.160									.010	.204		
.011	.121			.011	.182			.012	.174									.013	.215		
.013	.140			.013	.205			.014	.188									.016	.227		
.015	.156			.015	.232			.016	.205									.021	.249		
.017	.178			.017	.250			.021	.231									.026	.263		
.021	.203			.019	.274			.026	.256									.031	.273		
.025	.230			.021	.292			.031	.280									.036	.285		
.029	.263			.023	.308			.036	.294									.046	.306		
.033	.299			.025	.334			.046	.315									.056	.328		
.037	.329			.027	.347			.056	.339									.076	.350		
.041	.356			.032	.368			.066	.355									.096	.364		
.045	.395			.0371	.400			.076	.374									.126	.381		
.049	.419			.042	.426			.096	.416									.156	.395		
.053	.455			.047	.439			.116	.433									.196	.421		
.057	.488			.052	.453			.136	.461									.246	.435		
.062	.537			.057	.476			.156	.477									.296	.455		
.067	.578			.067	.500			.176	.496									.346	.482		
.072	.619			.077	.524			.196	.506									.396	.492		
.077	.660			.087	.539			.216	.529									.496	.526		
.082	.701			.107	.584			.266	.555									.596	.538		
.087	.742			.127	.618			.316	.588									.696	.557		
.092	.770			.147	.655			.366	.616									.796	.581		
.097	.811			.167	.682			.416	.645									.896	.597		
.102	.836			.187	.705			.466	.673									.996	.619		
.107	.863			.207	.726			.516	.696									1.196	.658		
.112	.882			.227	.747			.556	.718									1.396	.682		
.117	.910			.267	.784			.616	.739									1.596	.717		
.127	.945			.317	.821			.716	.781									1.796	.749		
.137	.964			.367	.858			.816	.816									1.996	.769		
.147	.975			.417	.884			.916	.852									2.196	.800		
.157	.984			.467	.913			1.016	.887									2.396	.830		
.177	.989			.517	.934			1.116	.922									2.596	.856		
.207	1.000			.567	.958			1.216	.946									2.796	.887		
.257	1.000			.617	.971			1.316	.965									2.996	.909		
.357	1.000			.667	.987			1.516	.991									3.196	.931		
				.767	.997			1.716	.998									3.396	.947		
				.867	1.000			2.016	1.000									3.596	.966		
								2.516	1.000									3.796	.984		
																		3.996	.998		
																		4.196	1.000		
																		4.596	1.000		
																		5.096	1.000		

TABLE VIII.- TEMPERATURE PROFILE MEASUREMENTS - Continued

Station C		Station D		Station E		Station G		Station H		Station I		Station J		Station K		Station L		Station M		Station N	
y, in.	β	y, in.	β	y, in.	β	y, in.	β	y, in.	β	y, in.	β	y, in.	β	y, in.	β	y, in.	β	y, in.	β	y, in.	β
Run H-20b; blowing with constant $v_o = 0.12$; $u_1 = 60.0$ fps																					
								x = 29.4 in. R_x = 865,900										x = 83.3 in. R_x = 2,441,000			
								0.006	0.081									0.006	0.104		
								.007	.089									.0085	.107		
								.009	.116									.010	.178		
								.011	.116									.012	.208		
								.013	.114									.014	.239		
								.016	.149									.016	.254		
								.019	.170									.018	.266		
								.022	.190									.020	.272		
								.025	.197									.023	.274		
								.029	.220									.028	.292		
								.034	.241									.033	.305		
								.039	.334									.038	.315		
								.044	.352									.048	.363		
								.049	.367									.058	.396		
								.054	.387									.068	.414		
								.059	.400									.078	.429		
								.069	.415									.088	.419		
								.079	.443									.108	.449		
								.089	.473									.128	.475		
								.099	.481									.168	.497		
								.109	.478									.208	.513		
								.129	.534									.258	.533		
								.149	.534									.308	.541		
								.179	.544									.358	.579		
								.209	.608									.408	.614		
								.239	.618									.458	.609		
								.269	.633									.508	.635		
								.309	.648									.608	.662		
								.359	.681									.708	.675		
								.409	.716									.808	.731		
								.459	.754									.908	.739		
								.509	.797									1.108	.805		
								.559	.835									1.308	.822		
								.609	.868									1.508	.871		
								.659	.881									1.708	.921		
								.759	.937									1.908	1.018		
								.859	.959									2.108	1.000		

TABLE VIII.- TEMPERATURE PROFILE MEASUREMENTS - Continued

Station C		Station D		Station E		Station G		Station H		Station I		Station J		Station K		Station L		Station M		Station N	
y, in.	β	y, in.	β	y, in.	β	y, in.	β	y, in.	β	y, in.	β	y, in.	β	y, in.	β	y, in.	β	y, in.	β	y, in.	β
Run H-2la; blowing with constant ϕ_H = 0.91; u_1 = 59.8 fps																					
		x = 6.1 in. R_x = 179,700						x = 29.4 in. R_x = 869,300				x = 46.2 in. R_x = 1,408,600						x = 83.3 in. R_x = 2,450,000			
		0.006	0.264					0.006	0.234			0.0055	0.303					0.006	0.245		
		.007	.329					.007	.277			.006	.309					.007	.305		
		.008	.421					.008	.272			.007	.309					.008	.320		
		.009	.350					.010	.288			.009	.314					.010	.330		
		.010	.307					.013	.342			.012	.320					.014	.345		
		.013	.357					.016	.359			.015	.326					.019	.365		
		.018	.400					.020	.370			.020	.337					.024	.380		
		.023	.429					.025	.375			.025	.343					.034	.415		
		.028	.436					.030	.397			.035	.337					.054	.440		
		.038	.429					.040	.418			.045	.343					.074	.455		
		.068	.557					.050	.446			.065	.366					.124	.470		
		.098	.657					.060	.435			.085	.383					.174	.500		
		.128	.693					.080	.467			.105	.389					.274	.530		
		.168	.814					.100	.446			.155	.503					.374	.600		
		.208	.893					.120	.522			.205	.497					.474	.595		
		.258	1.000					.140	.462			.255	.514					.574	.585		
		.308	1.000					.160	.473			.305	.531					.774	.635		
		.358	1.000					.180	.505			.405	.600					.974	.705		
		.408	1.000					.220	.527			.505	.646					1.174	.775		
		.508	1.000					.270	.533			.605	.691					1.374	.795		
								.320	.609			.705	.737					1.574	.875		
								.370	.652			.805	.777					1.774	.890		
								.420	.696			.905	.811					1.974	.940		
								.470	.728			1.105	.891					2.174	.965		
								.520	.793			1.305	.949					2.374	1.000		
								.570	.799			1.505	.966					2.574	1.020		
								.620	.853			1.705	.989					3.074	1.005		
								.720	.880			2.005	1.006					3.574	1.030		
								.820	.929			2.505	1.000					4.074	1.000		
								.920	.967			3.005	1.000					4.574	.995		
								1.120	.989												
								1.320	1.005												
								1.520	.989												
								2.020	1.000												

TABLE VIII.- TEMPERATURE PROFILE MEASUREMENTS - Continued

Station C		Station D		Station E		Station G		Station H		Station I		Station J		Station K		Station L		Station M		Station N	
y, in.	β	y, in.	β	y, in.	β	y, in.	β	y, in.	β	y, in.	β	y, in.	β	y, in.	β	y, in.	β	y, in.	β	y, in.	β
Run H-22; suction with constant v_o = -0.01; u_1 = 4.9 fps																					
		x = 6.0 in. R_x = 14,500				x = 21.4 in. R_x = 53,000						x = 46.1 in. R_x = 115,200									
		0.0095	0.218			0.009	0.090					0.0095	0.054								
		.010	.223			.010	.095					.010	.059								
		.011	.228			.012	.105					.011	.061								
		.013	.240			.014	.110					.013	.068								
		.015	.245			.017	.120					.015	.083								
		.017	.250			.020	.140					.017	.095								
		.019	.265			.023	.158					.021	.115								
		.021	.274			.026	.183					.027	.144								
		.025	.318			.030	.211					.032	.168								
		.027	.345			.034	.238					.037	.190								
		.029	.369			.038	.256					.042	.210								
		.031	.388			.042	.281					.047	.234								
		.033	.405			.046	.308					.052	.249								
		.036	.442			.050	.326					.057	.261								
		.039	.468			.055	.351					.067	.300								
		.043	.505			.060	.378					.077	.324								
		.047	.532			.070	.416					.087	.354								
		.051	.561			.075	.444					.097	.398								
		.055	.590			.080	.459					.107	.410								
		.059	.617			.090	.491					.117	.441								
		.064	.650			.100	.531					.127	.478								
		.069	.680			.110	.566					.137	.500								
		.074	.701			.120	.596					.147	.529								
		.079	.728			.130	.634					.157	.551								
		.084	.752			.140	.664					.167	.566								
		.089	.777			.150	.687					.177	.580								
		.094	.799			.160	.722					.197	.615								
		.099	.820			.170	.742					.217	.633								
		.104	.840			.180	.764					.237	.688								
		.109	.862			.190	.787					.257	.712								
		.119	.891			.200	.805					.277	.732								
		.129	.917			.210	.825					.297	.768								
		.139	.934			.220	.847					.317	.740								
		.149	.954			.240	.872					.337	.815								
		.169	.968			.260	.897					.357	.832								
		.189	.985			.280	.920					.377	.856								
		.209	.998			.300	.940					.397	.868								
		.259	1.000			.320	.952					.447	.898								
		.309	.998			.370	.980					.497	.927								
		.409	1.000			.420	.987					.597	.944								
						.520	1.000					.697	.968								
						.620	1.000					.897	.985								
												1.097	.993								
												1.297	.995								
												1.497	1.000								
												1.897	1.000								

TABLE VIII.- TEMPERATURE PROFILE MEASUREMENTS - Continued

Station C		Station D		Station E		Station G		Station H		Station I		Station J		Station K		Station L		Station M		Station N	
y, in.	β	y, in.	β	y, in.	β	y, in.	β	y, in.	β	y, in.	β	y, in.	β	y, in.	β	y, in.	β	y, in.	β	y, in.	β
Run H-23; suction with constant v_o = -0.04; u_1 = 4.8 fps																					
		x = 6.0 in. R_x = 14,100				x = 21.4 in. R_x = 51,500												x = 83.2 in. R_x = 193,900			
		0.010	0.217			0.0095	0.185											0.0098	0.180		
		.011	.223			.010	.188											.011	.195		
		.012	.231			.011	.191											.012	.200		
		.014	.244			.012	.191											.014	.200		
		.016	.252			.014	.202											.016	.210		
		.018	.278			.016	.217											.019	.246		
		.020	.299			.018	.243											.022	.282		
		.022	.316			.020	.267											.025	.319		
		.025	.365			.022	.290											.028	.328		
		.028	.417			.025	.326											.032	.352		
		.030	.450			.028	.355											.036	.382		
		.032	.474			.031	.387											.041	.427		
		.035	.512			.034	.408											.046	.470		
		.038	.554			.038	.446											.051	.500		
		.041	.581			.042	.478											.056	.542		
		.044	.605			.047	.510											.061	.564		
		.047	.642			.052	.543											.066	.579		
		.050	.666			.057	.584											.076	.624		
		.053	.694			.062	.622											.086	.661		
		.056	.710			.067	.645											.096	.694		
		.059	.732			.072	.672											.106	.731		
		.062	.748			.077	.698											.116	.731		
		.066	.776			.082	.730											.126	.746		
		.070	.791			.087	.754											.136	.761		
		.074	.805			.092	.771											.156	.794		
		.078	.833			.102	.809											.176	.809		
		.082	.846			.112	.845											.196	.825		
		.087	.863			.122	.871											.236	.851		
		.092	.883			.132	.891											.276	.879		
		.097	.896			.142	.918											.326	.925		
		.102	.915			.152	.933											.376	.948		
		.112	.931			.162	.947											.476	1.000		
		.122	.945			.182	.974											.576	1.000		
		.132	.967			.202	.985														
		.152	.978			.222	.991														
		.172	.983			.272	.994														
		.212	.989			.322	.997														
		.262	.994			.422	1.000														
		.312	.997																		
		.412	1.000																		

TABLE VIII.- TEMPERATURE PROFILE MEASUREMENTS - Continued

Station C		Station D		Station E		Station G		Station H		Station I		Station J		Station K		Station L		Station M		Station N	
y, in.	β	y, in.	β	y, in.	β	y, in.	β	y, in.	β	y, in.	β	y, in.	β	y, in.	β	y, in.	β	y, in.	β	y, in.	β
Run H-25; suction with constant v_o = -0.12; u_1 = 19.6 fps																					
												x = 46.2 in. R_x = 461,800									
												0.0056	[a]0.191								
													.128								
												.006	.447								
													.128								
												.007	.436								
													.266								
												.008	.372								
													.362								
												.009	.362								
													.585								
												.011	.351								
													.596								
												.013	.479								
													.745								
												.015	.511								
													.809								
												.020	.574								
													.787								
												.025	.585								
													.638								
												.030	.766								
													.574								
												.035	.702								
													.713								
												.040	.755								
													.766								
												.045	.989								
													.745								
												.050	.979								
													.681								
												.055	.947								
													.670								
												.060	.894								
													.702								
												.065	.872								
													.702								
												.075	.819								
													.702								
												.085	.819								
													.702								
												.105	1.053								
													.681								
												.125	1.021								
													.670								
												.145	.936								
													1.734								

[a]Temperature fluctuated widely. Two readings were made at each position of the probe.

TABLE VIII.- TEMPERATURE PROFILE MEASUREMENTS - Concluded

Station C		Station D		Station E		Station G		Station H		Station I		Station J		Station K		Station L		Station M		Station N	
y, in.	β	y, in.	β	y, in.	β	y, in.	β	y, in.	β	y, in.	β	y, in.	β	y, in.	β	y, in.	β	y, in.	β	y, in.	β
Run H-26; suction with constant v_o = -0.12; u_1 = 60.0 fps																					
						x = 21.5 in. R_x = 653,200						x = 46.2 in. R_x = 1,412,000									
						0.0055	0.338					0.0058	0.323								
						.006	.354					.006	.331								
						.007	.346					.007	.323								
						.008	.331					.009	.346								
						.010	.369					.011	.354								
						.012	.385					.015	.354								
						.014	.400					.019	.377								
						.019	.392					.029	.385								
						.024	.438					.049	.423								
						.034	.462					.069	.462								
						.044	.477					.089	.523								
						.064	.531					.109	.562								
						.084	.585					.129	.554								
						.104	.646					.169	.600								
						.124	.669					.209	.662								
						.144	.677					.259	.723								
						.184	.731					.309	.762								
						.224	.777					.359	.815								
						.274	.815					.409	.877								
						.324	.892					.459	.900								
						.374	.962					.509	.877								
						.424	.977					.609	.946								
						.474	.977					.709	.985								
						.524	.954					.809	1.000								
						.624	.977					.909	.992								
						.724	1.008					1.309	1.000								
						.924	1.000														
						1.324	.992														
Run H-27a; blowing with constant v_o = 0.12; u_1 = 60 to 70 fps																					
								x = 29.4 in. R_x = 897,000										x = 83.3 in. R_x = 2,736,000			
								0.005	0.266									0.0053	0.429		
								.006	.297									.006	.439		
								.0095	.323									.008	.450		
								.011	.333									.011	.455		
								.013	.354									.014	.466		
								.016	.359									.019	.481		
								.019	.375									.024	.487		
								.022	.370									.034	.508		
								.027	.380									.054	.508		
								.037	.401									.074	.529		
								.042	.401									.104	.566		
								.052	.411									.134	.571		
								.072	.432									.184	.603		
								.092	.432									.234	.646		
								.122	.448									.284	.688		
								.172	.479									.334	.720		
								.222	.474									.384	.746		
								.322	.521									.434	.772		
								.422	.557									.534	.847		
								.522	.604									.634	.878		
								.622	.641									.734	.937		
								.722	.677									.834	.958		
								.822	.703									.934	.979		
								1.022	.771									1.034	.984		
								1.222	.812									1.134	.989		
								1.422	.865									1.634	.995		
								1.622	.906									2.134	1.000		
								1.822	.943									2.634	1.000		
								2.022	.969												
								2.222	.979												
								2.522	.990												
								2.922	1.000												
								3.222	1.000												

TABLE IX.- VELOCITY PROFILES CALCULATED FROM MEASURED LAMINAR TEMPERATURE PROFILES

Station C		Station D		Station E		Station F		Station G		Station H		Station I		Station J		Station K		Station L		Station M		Station N	
y, in.	$\frac{u}{u_1}$	y, in.	$\frac{u}{u_1}$	y, in.	$\frac{u}{u_1}$	y, in.	$\frac{u}{u_1}$	y, in.	$\frac{u}{u_1}$	y, in.	$\frac{u}{u_1}$	y, in.	$\frac{u}{u_1}$	y, in.	$\frac{u}{u_1}$	y, in.	$\frac{u}{u_1}$	y, in.	$\frac{u}{u_1}$	y, in.	$\frac{u}{u_1}$	y, in.	$\frac{u}{u_1}$
Run H-1; no transfer; u_1 = 4.4 fps																							
		x = 6.5 in. R_x = 14,220						x = 21.8 in. R_x = 48,930				x = 38.4 in. R_x = 83,600		x = 46.5 in. R_x = 104,100				x = 70.4 in. R_x = 152,800					
		0.010	0.070					0.020	0.084			0.027	0.093	0.030	0.097			0.036	0.094				
		.021	.139					.041	.168			.053	.185	.060	.194			.072	.187				
		.031	.208					.061	.251			.080	.274	.089	.288			.108	.278				
		.042	.277					.082	.331			.107	.358	.119	.370			.144	.364				
		.052	.344					.102	.405			.134	.429	.149	.441			.181	.443				
		.062	.407					.123	.473			.160	.502	.179	.505			.217	.515				
		.073	.468					.143	.536			.187	.563	.209	.563			.253	.580				
		.083	.524					.163	.594			.214	.618	.238	.616			.289	.638				
		.094	.577					.184	.646			.240	.668	.268	.666			.325	.689				
		.104	.625					.204	.694			.267	.713	.298	.711			.361	.732				
		.115	.670					.225	.736			.294	.753	.328	.752			.397	.771				
		.125	.712					.245	.774			.320	.789	.358	.789			.433	.805				
		.135	.750					.266	.808			.347	.821	.388	.822			.470	.836				
		.146	.785					.286	.838			.374	.850	.417	.851			.506	.863				
		.156	.818					.307	.865			.401	.875	.447	.876			.542	.887				
		.167	.847					.327	.888			.427	.897	.477	.899			.578	.909				
		.177	.874					.347	.908			.454	.917	.507	.918			.614	.926				
		.187	.897					.368	.927			.481	.935	.537	.935			.650	.941				
		.198	.919					.388	.942			.507	.949	.566	.949			.686	.953				
		.208	.937					.409	.955			.534	.960	.596	.961			.722	.962				
		.219	.953					.429	.965			.561	.970	.626	.971			.758	.970				
		.229	.964					.450	.973			.588	.977	.656	.979			.795	.977				
		.240	.972					.470	.978			.614	.984	.686	.985			.831	.982				
		.250	.978					.490	.982			.641	.988	.715	.989			.867	.986				
		.260	.983					.511	.985			.668	.991	.745	.992			.903	.990				
		.271	.986					.531	.988			.694	.994	.775	.995			.939	.992				
		.281	.989					.552	.990			.721	.995	.805	.997			.975	.904				
		.292	.991					.572	.992			.748	.996	.835	.998			1.011	.996				
		.302	.993					.593	.993			.774	.997	.865	.999			1.047	.997				
		.312	.995					.613	.995			.801	.998	.894	.999			1.083	.998				
		.323	.996					.633	.996			.828	.998	.924	1.000			1.120	.999				
		.333	.997					.654	.997			.855	.999	.954	1.000			1.156	.999				
		.344	.998					.674	.997			.881	.999	.984	1.000			1.192	.999				
		.354	.998					.695	.998			.908	.999	1.014	1.000			1.228	1.000				
		.364	.999					.715	.999			.935	1.000	1.043	1.000			1.264	1.000				
		.375	.999					.736	.999			.961	1.000	1.073	1.000			1.300	1.000				
		.385	.999					.756	.999			.988	1.000					1.336	1.000				
		.396	1.000					.776	1.000			1.015	1.000					1.372	1.000				
		.406	1.000					.797	1.000			1.041	1.000					1.409	1.000				
		.417	1.000					.817	1.000			1.068	1.000										

TABLE IX.- VELOCITY PROFILES CALCULATED FROM MEASURED LAMINAR TEMPERATURE PROFILES - Continued

Station C		Station D		Station E		Station F		Station G		Station H		Station I		Station J		Station K		Station L		Station M		Station N	
y, in.	$\frac{u}{u_1}$	y, in.	$\frac{u}{u_1}$	y, in.	$\frac{u}{u_1}$	y, in.	$\frac{u}{u_1}$	y, in.	$\frac{u}{u_1}$	y, in.	$\frac{u}{u_1}$	y, in.	$\frac{u}{u_1}$	y, in.	$\frac{u}{u_1}$	y, in.	$\frac{u}{u_1}$	y, in.	$\frac{u}{u_1}$	y, in.	$\frac{u}{u_1}$	y, in.	$\frac{u}{u_1}$
Run H-5; blowing with constant $\phi_H = 0.63$; $u_1 = 4.6$ fps																							
		$x = 6.5$ in. $R_x = 14{,}720$																					
		0	0																				
		.02	.098																				
		.04	.195																				
		.06	.291																				
		.08	.384																				
		.10	.477																				
		.12	.567																				
		.14	.652																				
		.16	.727																				
		.18	.792																				
		.20	.846																				
		.22	.889																				
		.24	.922																				
		.26	.947																				
		.28	.965																				
		.30	.977																				
		.32	.986																				
		.34	.991																				
		.36	.994																				
		.38	.996																				
		.40	.998																				
		.42	.998																				
		.44	.999																				
		.46	.999																				
		.48	.999																				
		.50	.999																				
		.52	.999																				
		.54	1.000																				
		.56	1.000																				
		.58	1.000																				
		.60	1.000																				

TABLE IX.- VELOCITY PROFILES CALCULATED FROM MEASURED LAMINAR TEMPERATURE PROFILES - Continued

Station C		Station D		Station E		Station F		Station G		Station H		Station I		Station J		Station K		Station L		Station M		Station N	
y, in.	$\frac{u}{u_1}$	y, in.	$\frac{u}{u_1}$	y, in.	$\frac{u}{u_1}$	y, in.	$\frac{u}{u_1}$	y, in.	$\frac{u}{u_1}$	y, in.	$\frac{u}{u_1}$	y, in.	$\frac{u}{u_1}$	y, in.	$\frac{u}{u_1}$	y, in.	$\frac{u}{u_1}$	y, in.	$\frac{u}{u_1}$	y, in.	$\frac{u}{u_1}$	y, in.	$\frac{u}{u_1}$
Run H-10; blowing; $v_o \propto 1/\sqrt{x}$; $\phi_H = 1.2$; $u_1 = 5.3$ fps; laminar region																							
		x = 6.0 in. R_x = 15,600		x = 10.7 in. R_x = 26,500																			
		0	0	0	0																		
		.010	.027	.010	.028																		
		.020	.063	.020	.066																		
		.030	.106	.030	.112																		
		.040	.154	.040	.161																		
		.050	.205	.050	.211																		
		.060	.258	.060	.260																		
		.070	.311	.070	.307																		
		.080	.364	.080	.352																		
		.090	.417	.090	.396																		
		.100	.470	.100	.437																		
		.110	.523	.110	.478																		
		.120	.575	.120	.517																		
		.130	.628	.130	.555																		
		.140	.678	.140	.592																		
		.150	.724	.150	.628																		
		.160	.767	.160	.664																		
		.170	.805	.170	.697																		
		.180	.839	.180	.728																		
		.190	.869	.190	.758																		
		.200	.894	.200	.785																		
		.210	.916	.210	.810																		
		.220	.933	.220	.833																		
		.230	.948	.230	.855																		
		.240	.960	.240	.875																		
		.250	.969	.250	.893																		
		.260	.976	.260	.909																		
		.270	.982	.270	.923																		
		.280	.987	.280	.936																		
		.290	.990	.290	.946																		
		.300	.993	.300	.955																		
		.310	.995	.310	.963																		
		.320	.996	.320	.969																		
		.330	.997	.330	.975																		
		.340	.998	.340	.979																		
		.350	.999	.350	.983																		
		.360	.999	.360	.986																		
		.370	1.000	.370	.988																		
		.380	1.000	.380	.990																		
		.390	1.000	.390	.992																		
		.400	1.000	.400	.993																		
		.410	1.000	.410	.994																		
				.420	.995																		
				.430	.996																		
				.440	.997																		
				.450	.998																		
				.460	.999																		
				.470	.999																		
				.480	.999																		
				.490	1.000																		
				.500	1.000																		
				.510	1.000																		
				.520	1.000																		
				.530	1.000																		
				.540	1.000																		

TABLE IX.- VELOCITY PROFILES CALCULATED FROM MEASURED LAMINAR TEMPERATURE PROFILES - Continued

Station C		Station D		Station E		Station F		Station G		Station H		Station I		Station J		Station K		Station L		Station M		Station N	
y, in.	$\frac{u}{u_1}$	y, in.	$\frac{u}{u_1}$	y, in.	$\frac{u}{u_1}$	y, in.	$\frac{u}{u_1}$	y, in.	$\frac{u}{u_1}$	y, in.	$\frac{u}{u_1}$	y, in.	$\frac{u}{u_1}$	y, in.	$\frac{u}{u_1}$	y, in.	$\frac{u}{u_1}$	y, in.	$\frac{u}{u_1}$	y, in.	$\frac{u}{u_1}$	y, in.	$\frac{u}{u_1}$
Run H-11; suction with constant $\phi_H = -1.2$; $u_1 = 4.8$ fps																							
		x = 6.0 in. R_x = 14,200						x = 21.4 in. R_x = 51,800						x = 46.1 in. R_x = 112,600									
		0.006	0.089					0.010	0.084					0.020	0.131								
		.012	.179					.020	.164					.040	.248								
		.018	.270					.030	.242					.060	.351								
		.024	.361					.040	.315					.080	.437								
		.030	.451					.050	.383					.100	.507								
		.036	.536					.060	.447					.120	.562								
		.042	.607					.070	.505					.140	.609								
		.048	.665					.080	.558					.160	.649								
		.054	.713					.090	.606					.180	.686								
		.060	.755					.100	.650					.200	.720								
		.066	.791					.110	.689					.220	.751								
		.072	.823					.120	.725					.240	.779								
		.078	.851					.130	.758					.260	.805								
		.084	.876					.140	.787					.280	.827								
		.090	.898					.150	.813					.300	.848								
		.096	.917					.160	.836					.320	.866								
		.102	.933					.170	.858					.340	.881								
		.108	.947					.180	.875					.360	.895								
		.114	.959					.190	.891					.380	.907								
		.120	.968					.200	.905					.400	.917								
		.126	.975					.210	.918					.420	.926								
		.132	.981					.220	.929					.440	.934								
		.138	.986					.230	.940					.460	.940								
		.144	.989					.240	.948					.480	.946								
		.150	.992					.250	.957					.500	.952								
		.156	.994					.260	.964					.520	.957								
		.162	.996					.270	.970					.540	.961								
		.168	.997					.280	.975					.560	.965								
		.174	.998					.290	.980					.580	.969								
		.180	.998					.300	.984					.600	.972								
		.186	.999					.310	.988					.620	.975								
		.192	.999					.320	.991					.640	.978								
		.198	1.000					.330	.993					.660	.980								
		.204	1.000					.340	.995					.680	.983								
		.210	1.000					.350	.996					.700	.985								
		.216	1.000					.360	.998					.720	.987								
		.222	1.000					.370	.998					.740	.989								
		.228	1.000					.380	.999					.760	.991								
		.234	1.000					.390	.999					.780	.992								
		.240	1.000					.400	.999					.800	.994								
		.246	1.000					.410	1.000					.820	.995								
								.420	1.000					.840	.997								
								.430	1.000					.860	.998								
								.440	1.000					.880	.999								
								.450	1.000					.900	1.000								
								.460	1.000														

TABLE IX.- VELOCITY PROFILES CALCULATED FROM MEASURED LAMINAR TEMPERATURE PROFILES - Concluded

Station C		Station D		Station E		Station F		Station G		Station H		Station I		Station J		Station K		Station L		Station M		Station N	
y, in.	$\frac{u}{u_1}$	y, in.	$\frac{u}{u_1}$	y, in.	$\frac{u}{u_1}$	y, in.	$\frac{u}{u_1}$	y, in.	$\frac{u}{u_1}$	y, in.	$\frac{u}{u_1}$	y, in.	$\frac{u}{u_1}$	y, in.	$\frac{u}{u_1}$	y, in.	$\frac{u}{u_1}$	y, in.	$\frac{u}{u_1}$	y, in.	$\frac{u}{u_1}$	y, in.	$\frac{u}{u_1}$
Run H-23; suction with constant $v_o = -0.04$; $u_1 = 4.8$ fps																							
		$x = 6.0$ in. $R_x = 14{,}100$						$x = 21.4$ in. $R_x = 51{,}500$												$x = 83.2$ in. $R_x = 193{,}900$			
		0.008	0.161					0.010	0.188											0.010	0.185		
		.016	.313					.020	.347											.020	.344		
		.024	.451					.030	.469											.030	.473		
		.032	.573					.040	.566											.040	.573		
		.040	.674					.050	.645											.050	.652		
		.048	.752					.060	.712											.060	.716		
		.056	.811					.070	.767											.070	.765		
		.064	.855					.080	.813											.080	.803		
		.072	.889					.090	.851											.090	.830		
		.080	.916					.100	.882											.100	.849		
		.088	.937					.110	.907											.110	.864		
		.096	.954					.120	.928											.120	.876		
		.104	.966					.130	.946											.130	.887		
		.112	.976					.140	.959											.140	.896		
		.120	.983					.150	.971											.150	.904		
		.128	.988					.160	.979											.160	.911		
		.136	.992					.170	.986											.170	.918		
		.144	.994					.180	.991											.180	.924		
		.152	.996					.190	.994											.190	.929		
		.160	.997					.200	.996											.200	.934		
		.168	.998					.210	.997											.210	.938		
		.176	.998					.220	.998											.220	.942		
		.184	.998					.230	.998											.230	.946		
		.192	.999					.240	.999											.240	.950		
		.200	.999					.250	.999											.250	.953		
		.208	.999					.260	.999											.260	.956		
		.216	.999					.270	.999											.270	.960		
		.224	.999					.280	1.000											.280	.963		
		.232	.999					.290	1.000											.290	.966		
		.240	.999					.300	1.000											.300	.968		
		.248	.999					.310	1.000											.310	.971		
		.256	.999					.320	1.000											.320	.974		
		.264	1.000					.330	1.000											.330	.976		
		.272	1.000					.340	1.000											.340	.978		
		.280	1.000					.350	1.000											.350	.980		
		.288	1.000																	.360	.982		
		.296	1.000																	.370	.984		
		.304	1.000																	.380	.986		
		.312	1.000																	.390	.987		
		.320	1.000																	.400	.988		
		.328	1.000																	.410	.990		
		.336	1.000																	.420	.992		
		.344	1.000																	.430	.993		
																				.440	.994		
																				.450	.995		
																				.460	.996		
																				.470	.997		
																				.480	.998		
																				.490	.999		
																				.500	.999		
																				.510	1.000		
																				.520	1.000		
																				.530	1.000		

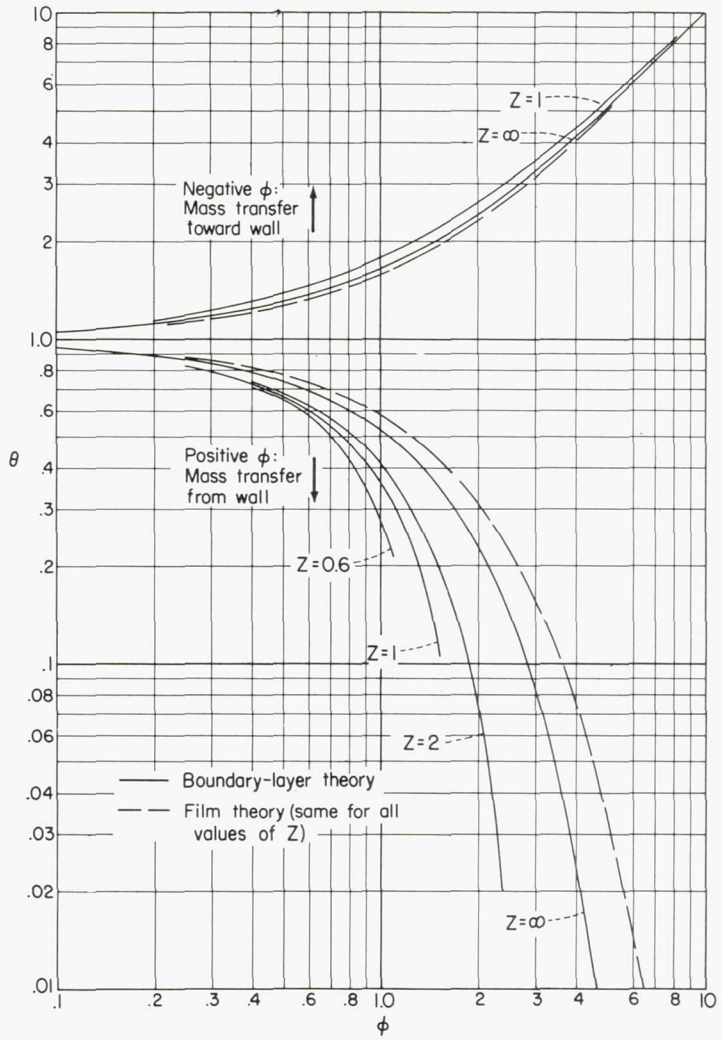

Figure 1.- Theoretical predictions of the effect of mass transfer on the transfer coefficients plotted as θ versus ϕ.

Process	Z	Correction factor, θ (a)	Rate factor, ϕ (a)
Momentum transfer	1	$\frac{c_f}{c_{f_*}}$	$\frac{2\sum_j N_j M_j}{u_1 \rho_1 c_{f_*}}$
Heat transfer	$\frac{c_p \mu}{k}$	$\frac{h}{h_*}$	$\frac{\sum_j N_j M_j c_{p_j}}{h_*}$
Diffusion of species i	$\frac{\mu}{\rho D_{im}}$	$\frac{K_i}{K_{*_i}}$	$\frac{\sum_j N_j}{K_{*_i}}$

[a]Asterisk indicates value in absence of mass transfer ($\phi = 0$).

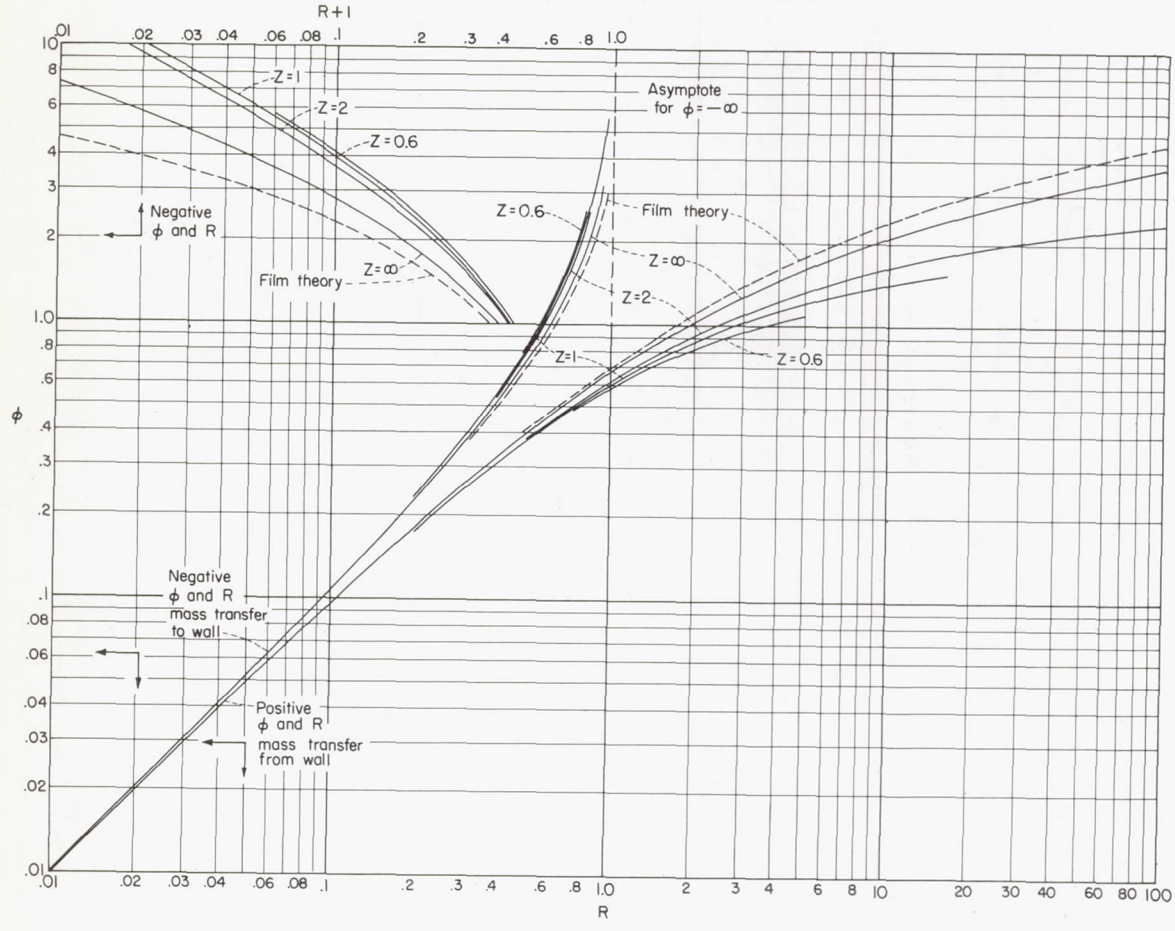

Figure 2.- Theoretical predictions of the effect of mass transfer on the transfer coefficients plotted as ϕ versus R.

Process	Z	Rate factor, ϕ (a)	Resistance factor, R
Momentum transfer	1	$\frac{2\sum_j N_j M_j}{u_1 \rho_1 c_{f_*}}$	$\frac{2\sum_j N_j M_j}{u_1 \rho_1 c_f}$
Heat transfer	$\frac{c_p \mu}{k}$	$\frac{\sum_j N_j M_j c_{p_j}}{h_*}$	$\frac{\sum_j N_j M_j c_{p_j}}{h} = \frac{T_o - T_1}{T_s - T_o}$
Diffusion of species i	$\frac{\mu}{\rho D_{im}}$	$\frac{\sum_j N_j}{K_{*_i}}$	$\frac{\sum_j N_j}{K_i} = \frac{X_{io} - X_{il}}{\frac{N_i}{\sum_j N_j} - X_{io}}$

[a]Asterisk indicates value in absence of mass transfer ($R = \phi = 0$).

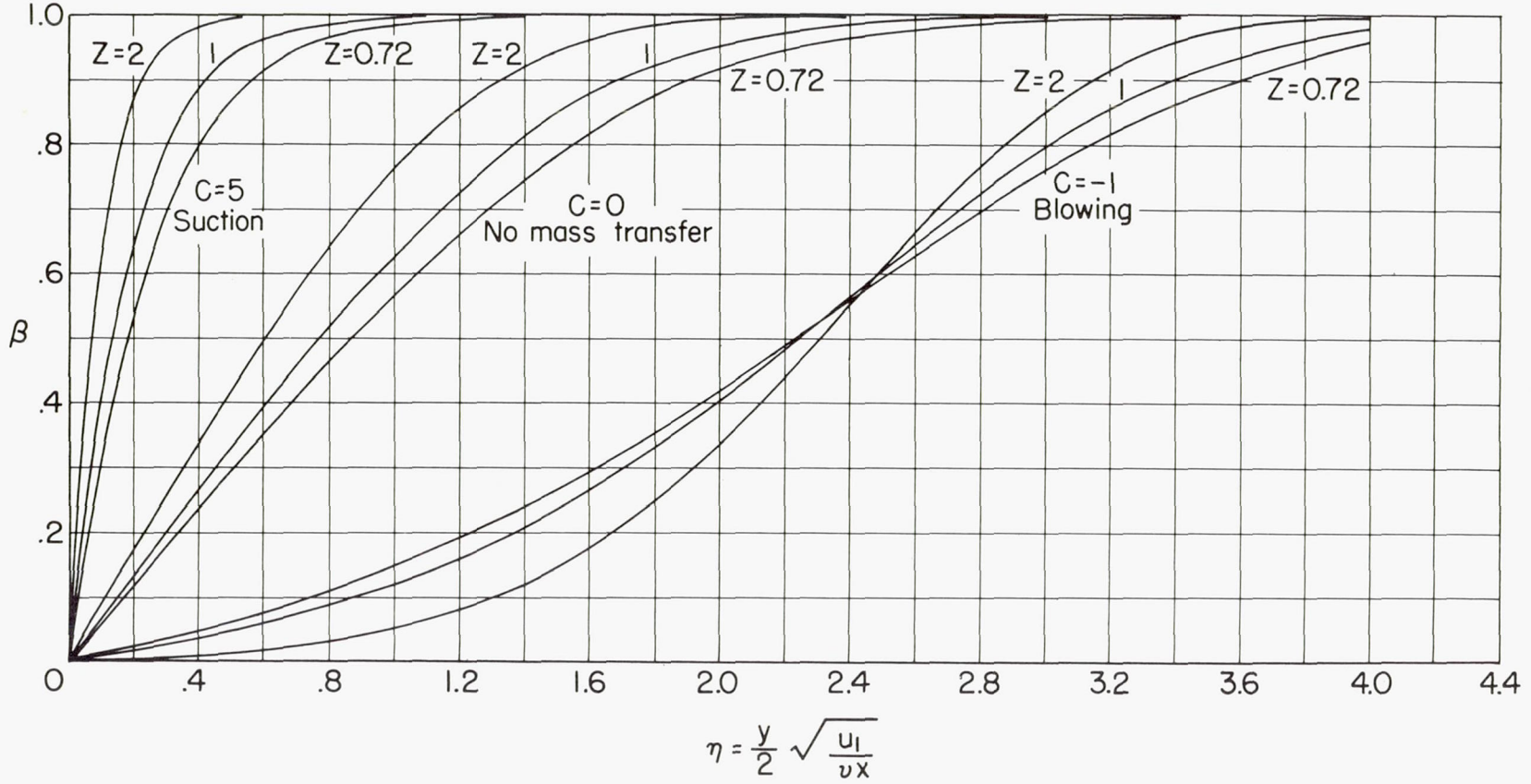

Figure 3.- Theoretical laminar-boundary-layer profiles with suction and blowing (mass transfer rate varying as $1/\sqrt{x}$). $\beta_F = \frac{u}{u_1}$; $\beta_H = \frac{T_o - T}{T_o - T_1}$; $\beta_D = \frac{X_{io} - X_i}{X_{io} - X_{il}}$; $Z_F = 1$; $Z_H = \frac{c_p \mu}{k}$; $Z_D = \frac{\mu}{\rho D_{im}}$; $C = -\frac{2v_o}{u_1}\sqrt{\frac{u_1 x \rho}{\mu}}$.

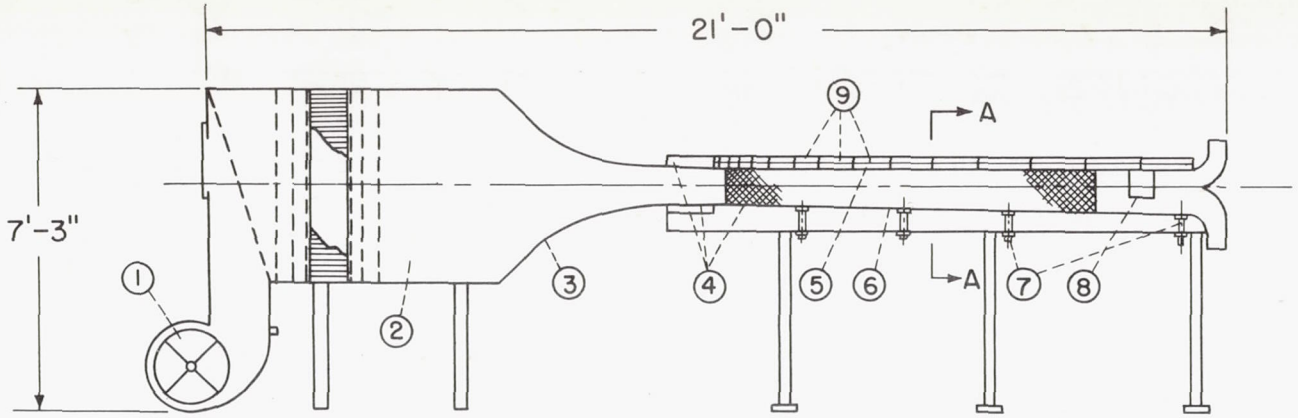

① Fan
② Calming chamber
③ Nozzle
④ Suction screens
⑤ Porous test wall 1×10 ft
⑥ Flexible bottom wall
⑦ Screw jacks
⑧ Windows
⑨ Compartments above test wall
⑩ To orifice
⑪ Heating elements
⑫ Baffles
⑬ Bolts to adjust tension of screens
⑭ Test-wall heating element; fiberglas cloth; thermocouples; 80-mesh electroformed screen
⑮ Gold-plated reflector sheets (screens are also gold-plated)
⑯ Suction pipes to orifices and ejector
⑰ Traveling hot-wire anemometer (on sled)

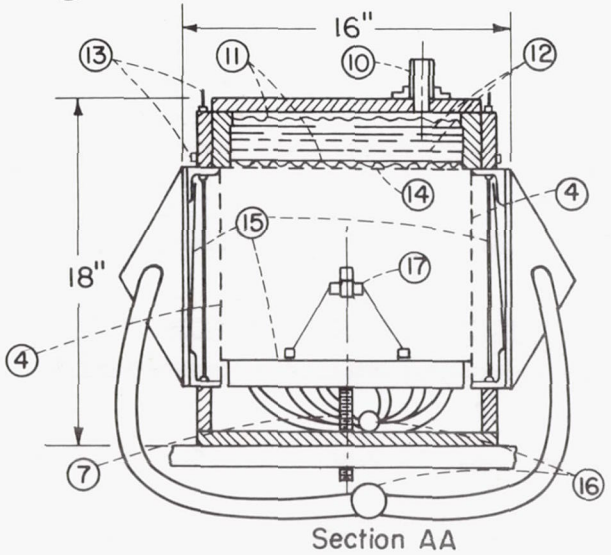

Section AA

Figure 4.- Over-all view of tunnel.

L-83668

Figure 5.- Velocity measuring probes. From left to right, hot-wire, 0.019-inch outside-diameter boundary-layer impact tube, and 0.010-inch outside-diameter boundary-layer impact tube.

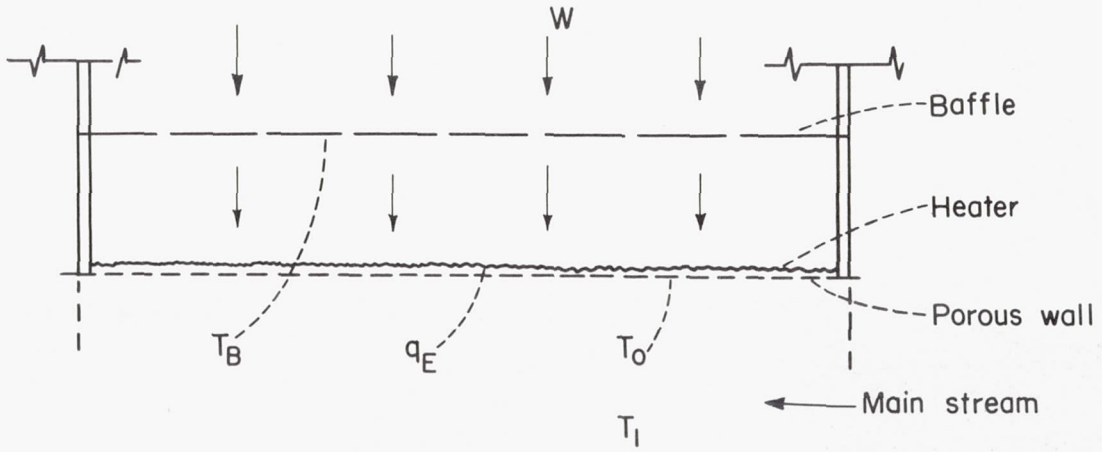

Figure 6.- Control volume used for energy balance calculations. Energy input, $q_E + Wc_pT_B$; energy output, $hA(T_o - T_1) + Wc_pT_o$ + Losses.

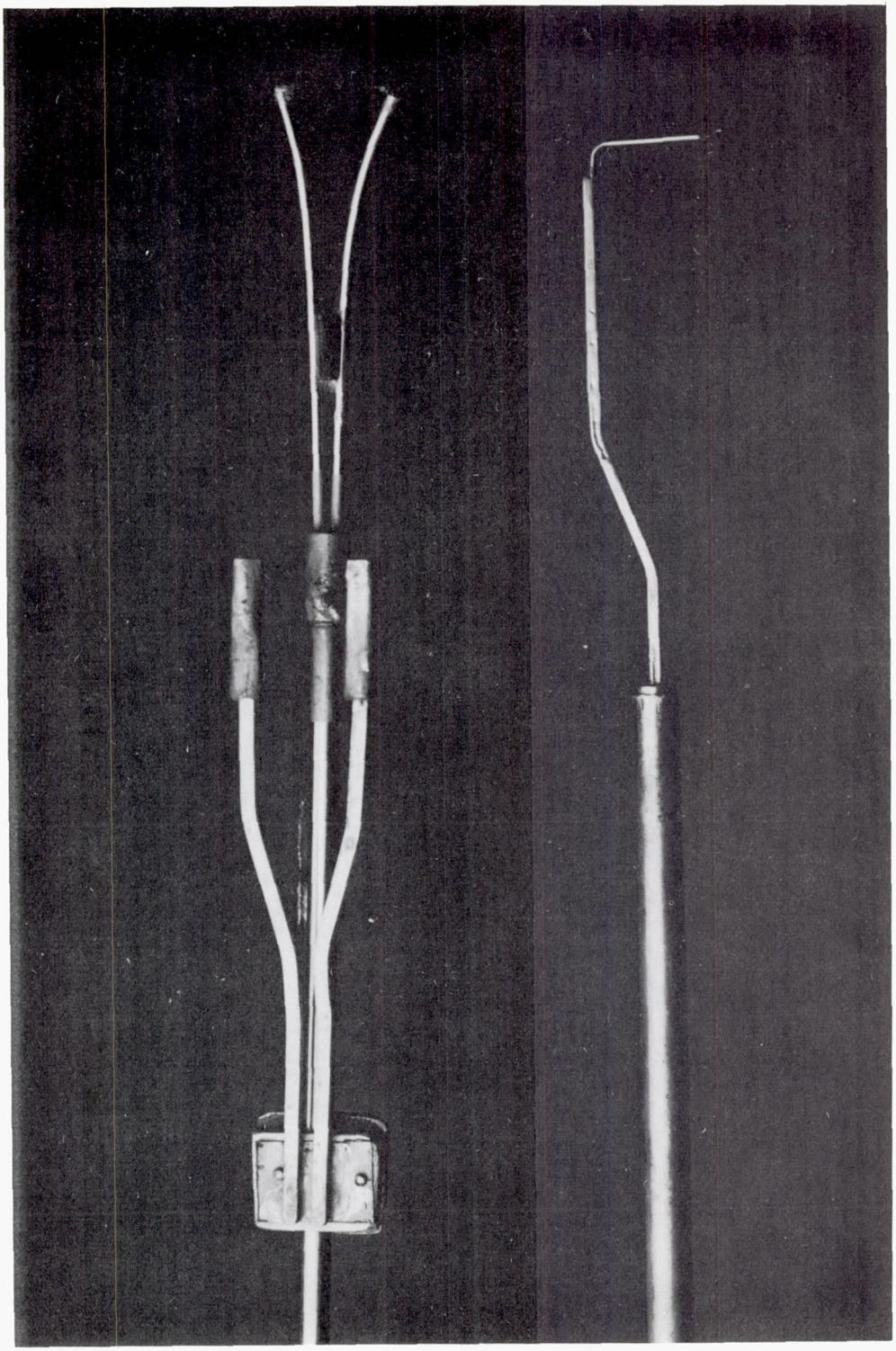

L-83669

Figure 7.- Temperature measuring probes. From left to right, low-velocity probe and high-velocity probe.

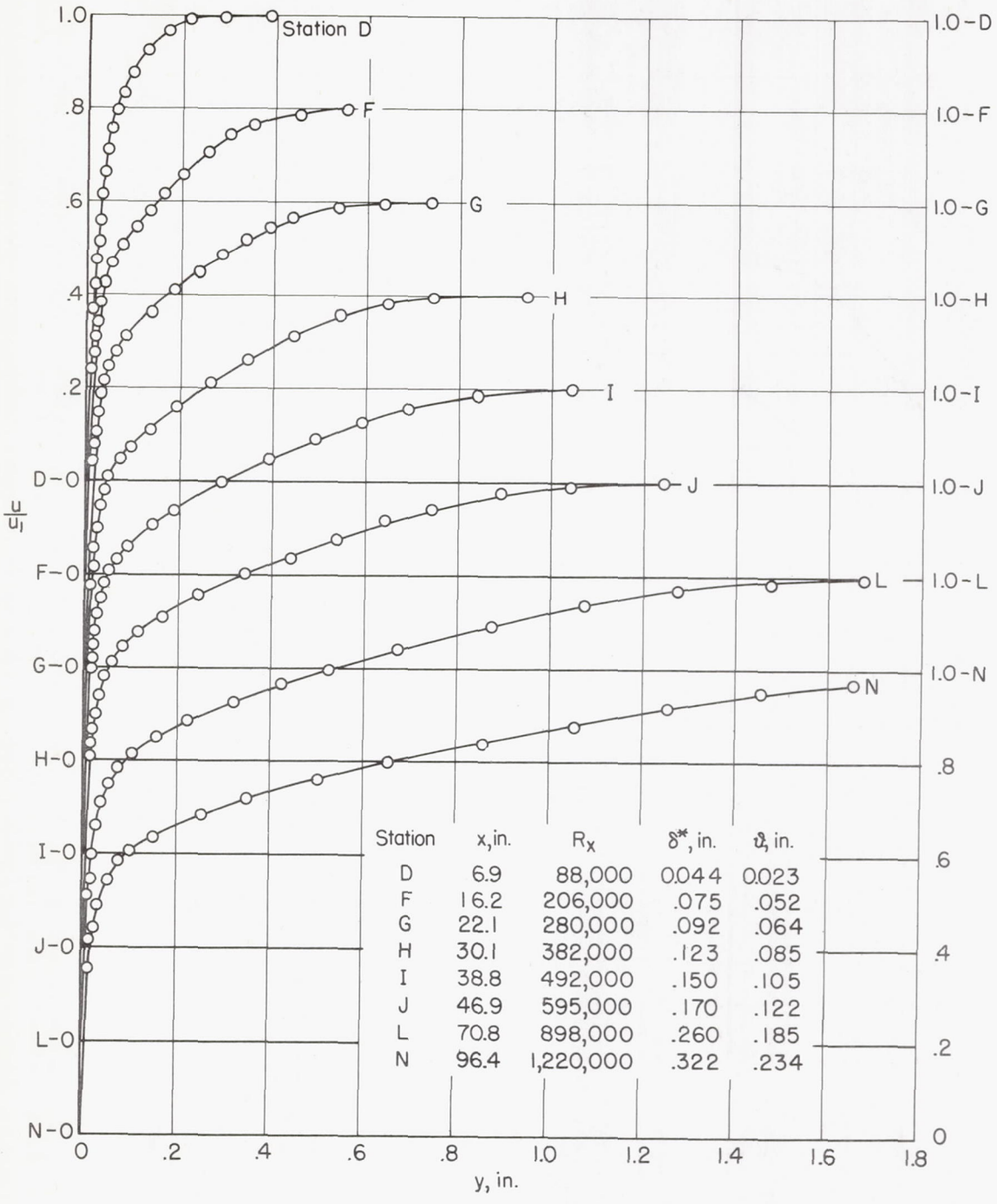

Station	x, in.	R_x	δ^*, in.	ϑ, in.
D	6.9	88,000	0.044	0.023
F	16.2	206,000	.075	.052
G	22.1	280,000	.092	.064
H	30.1	382,000	.123	.085
I	38.8	492,000	.150	.105
J	46.9	595,000	.170	.122
L	70.8	898,000	.260	.185
N	96.4	1,220,000	.322	.234

(a) Run V-1. No mass transfer; u_1 = 25.8 fps.

Figure 8.- Mean velocity profiles.

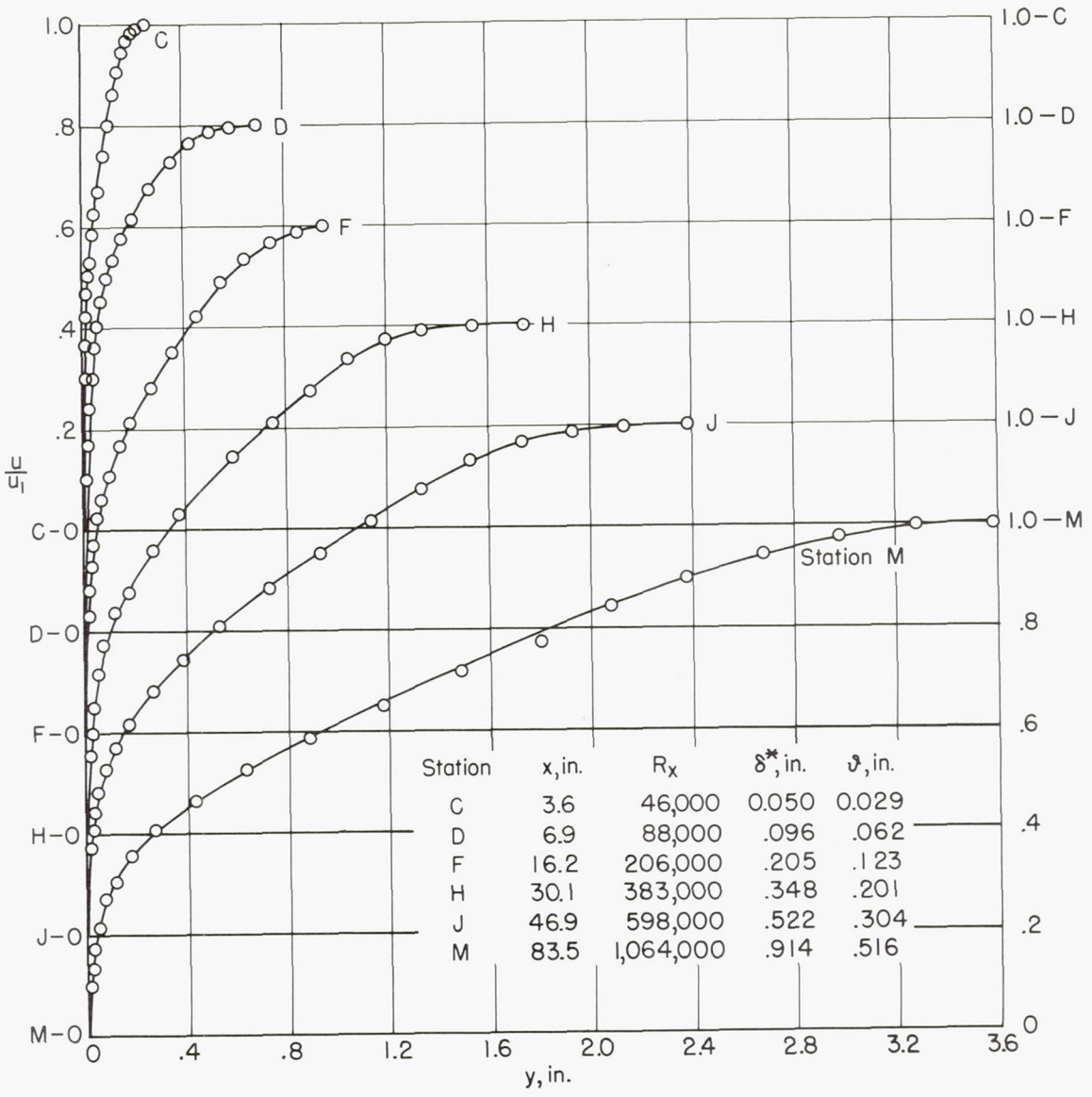

(b) Run V-4. Uniform blowing rate of 0.13 fps; u_1 = 25.9 fps.

Figure 8.- Continued.

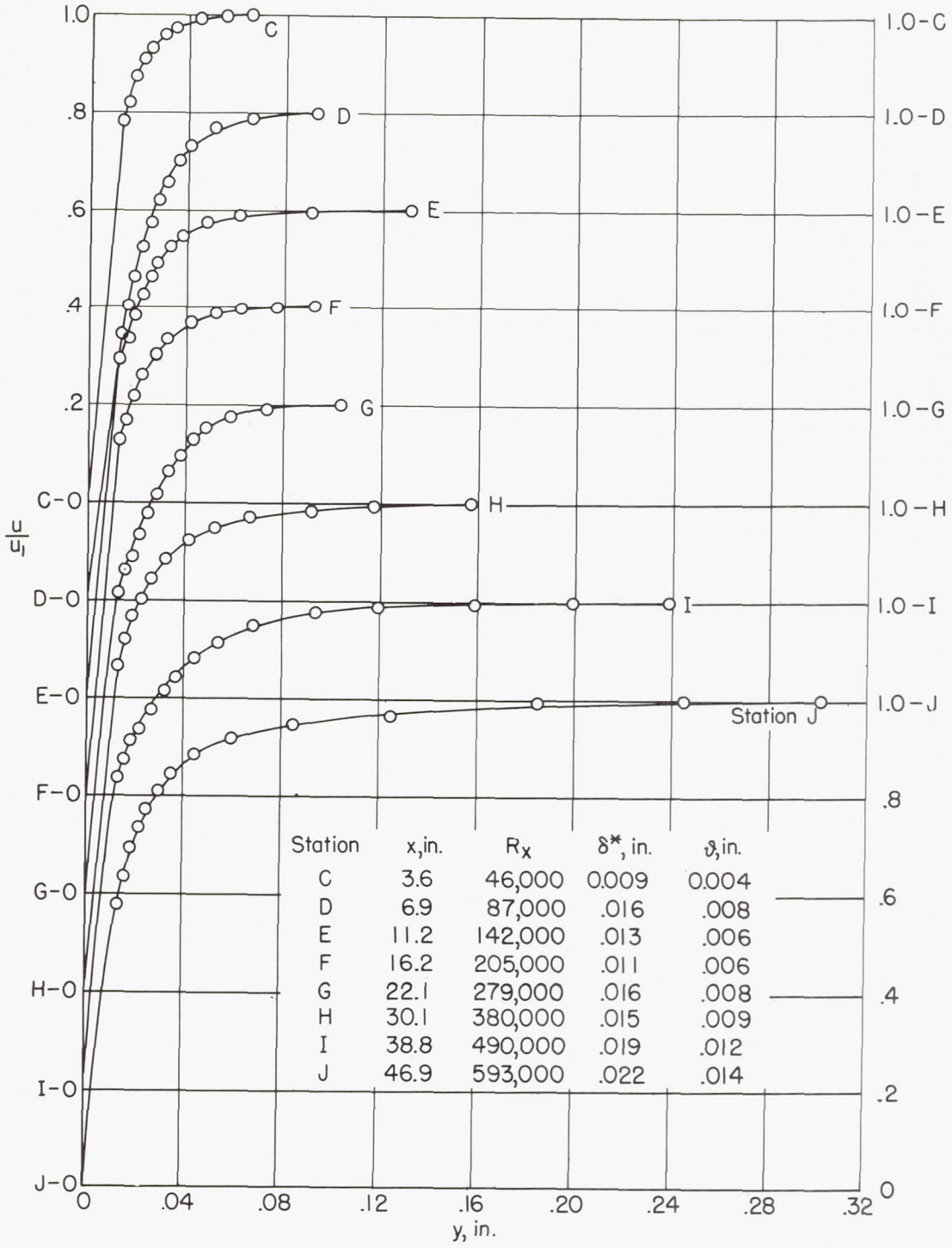

(c) Run V-8. Uniform suction rate of -0.13 fps; u_1 = 25.7 fps.

Figure 8.- Continued.

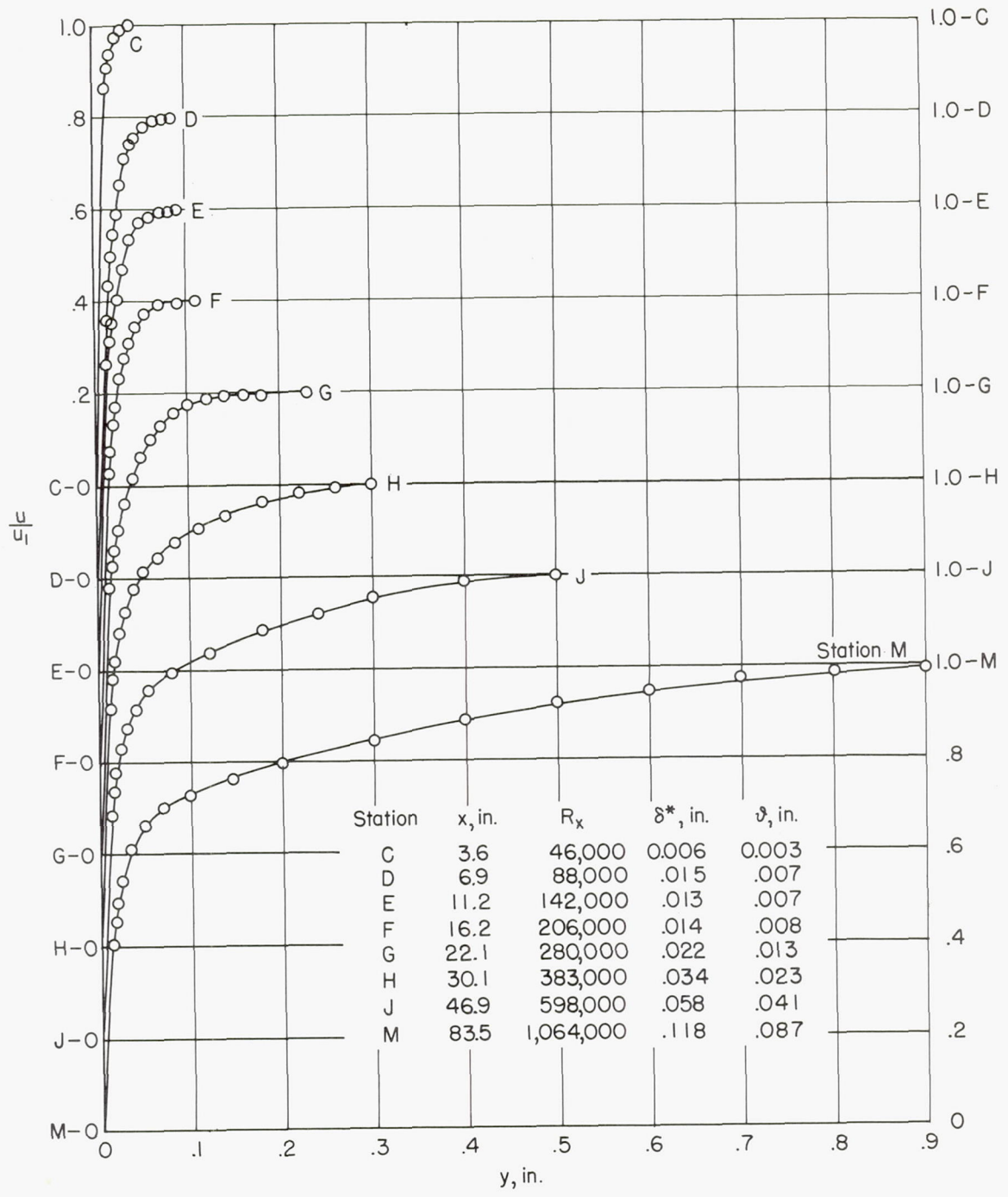

Station	x, in.	R_x	δ^*, in.	ϑ, in.
C	3.6	46,000	0.006	0.003
D	6.9	88,000	.015	.007
E	11.2	142,000	.013	.007
F	16.2	206,000	.014	.008
G	22.1	280,000	.022	.013
H	30.1	383,000	.034	.023
J	46.9	598,000	.058	.041
M	83.5	1,064,000	.118	.087

(d) Run V-10. Suction with inverse square-root distribution;
$C = -2\frac{v_o}{u_1}\sqrt{R_x} = 3.0$; $u_1 = 25.9$ fps.

Figure 8.- Concluded.

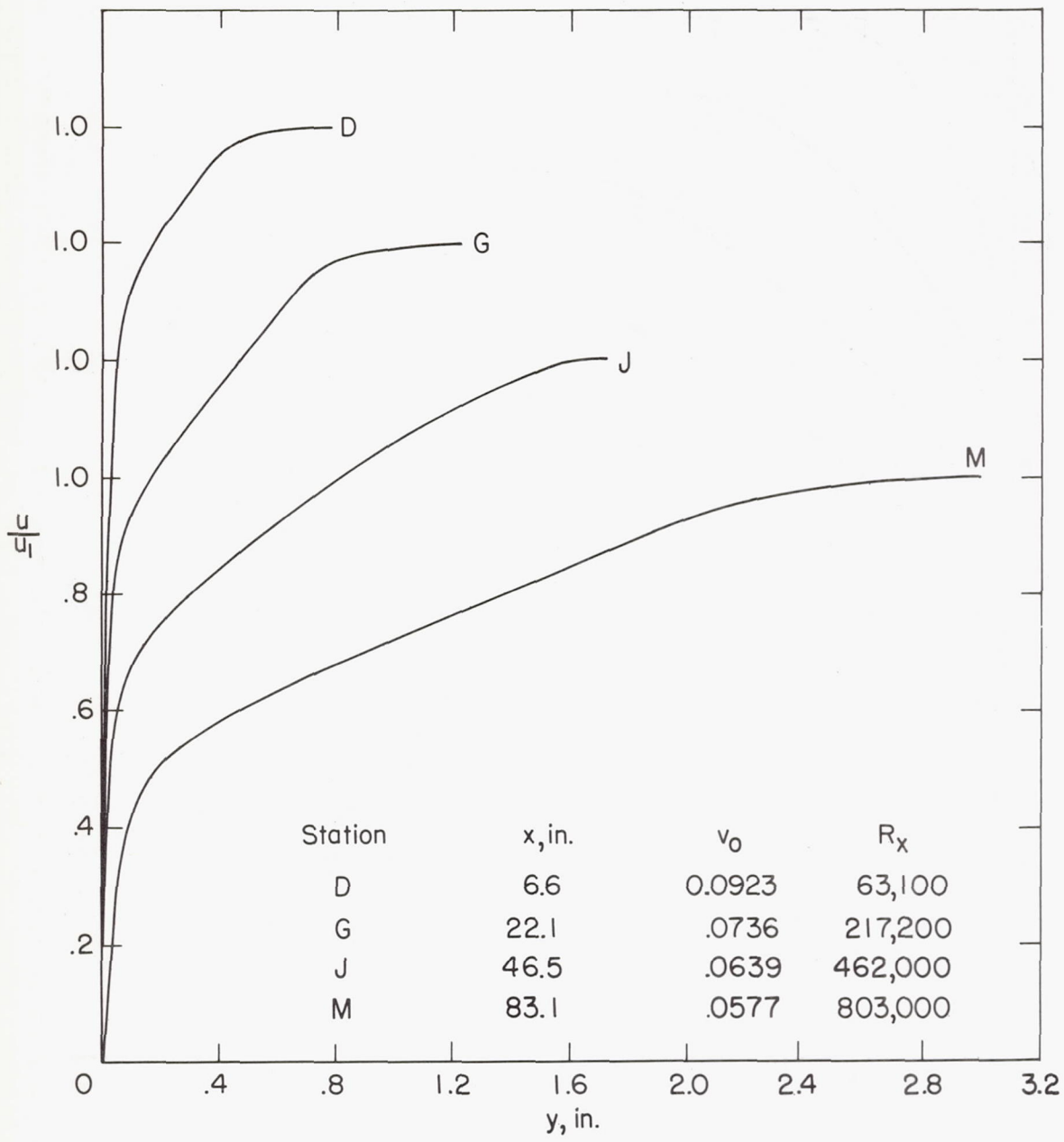

(a) Run H-8. Blowing with $\phi_H = 1.2$; $u_1 = 19.6$ fps.

Figure 9.- Mean velocity profiles.

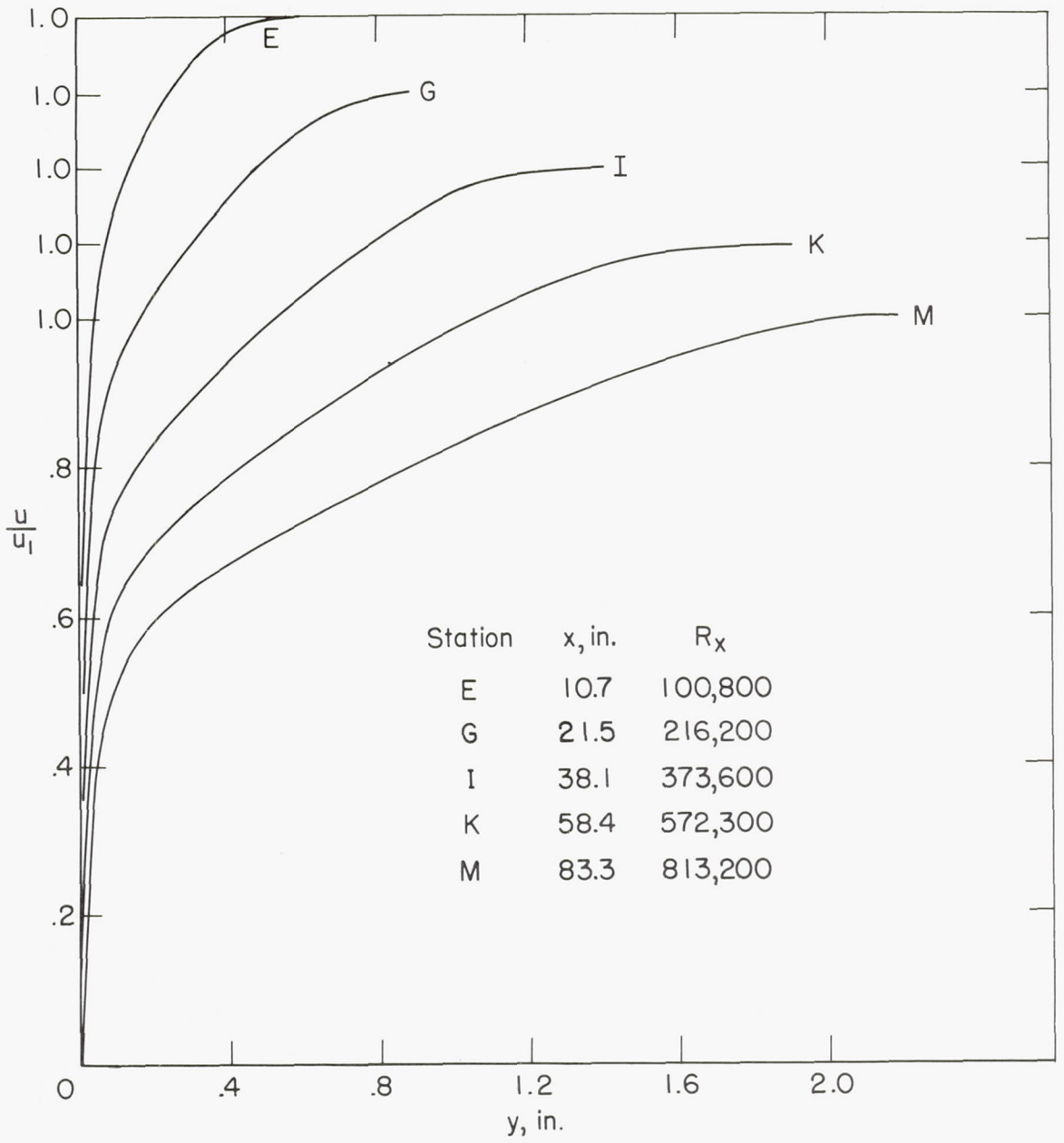

(b) Run H-17a. Uniform blowing v_o = 0.04 fps; u_1 = 20.0 fps.

Figure 9.- Continued.

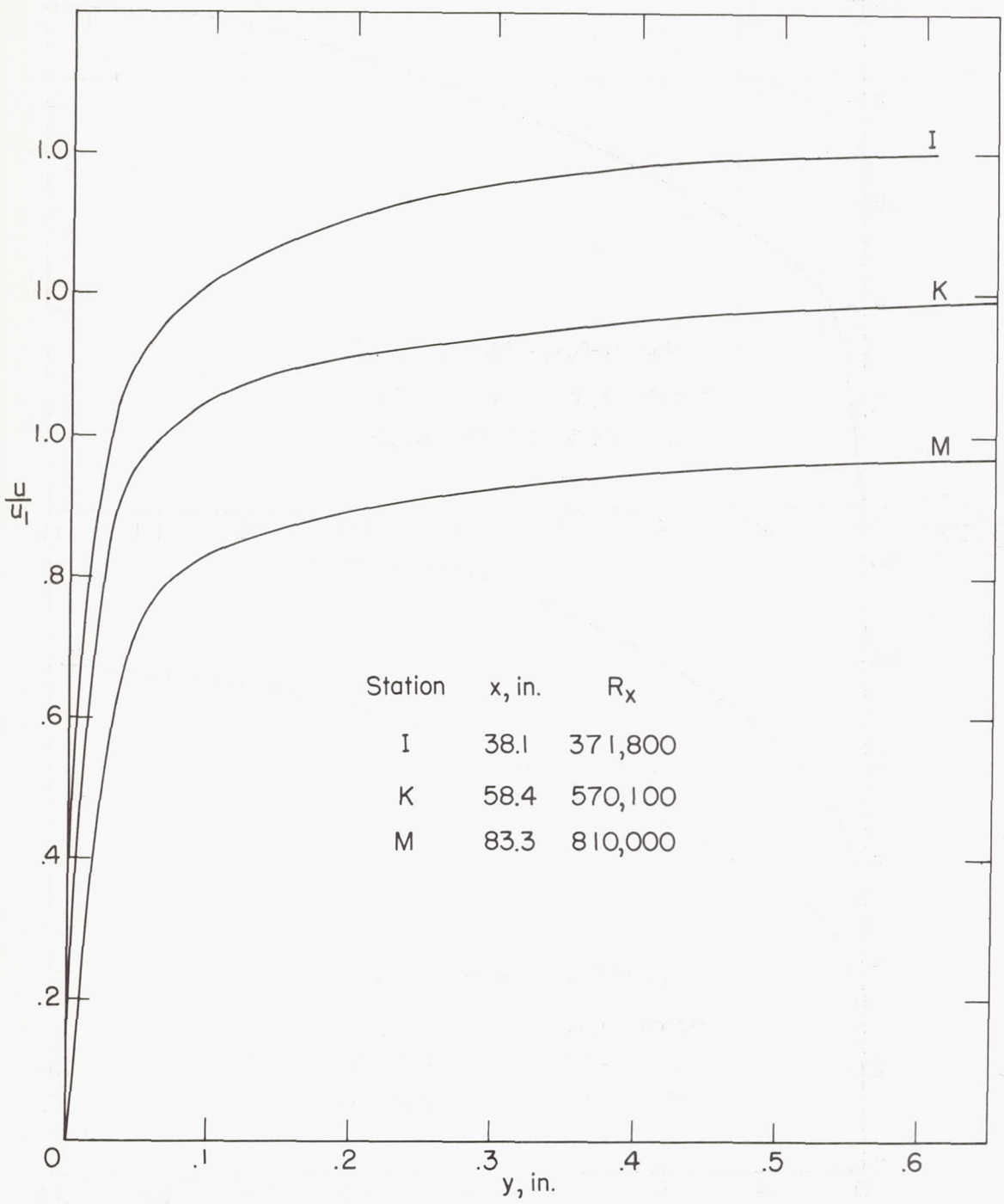

(c) Run H-12. Suction with $\emptyset_H = -1.2$; $u_1 = 19.8$ fps.

Figure 9.- Concluded.

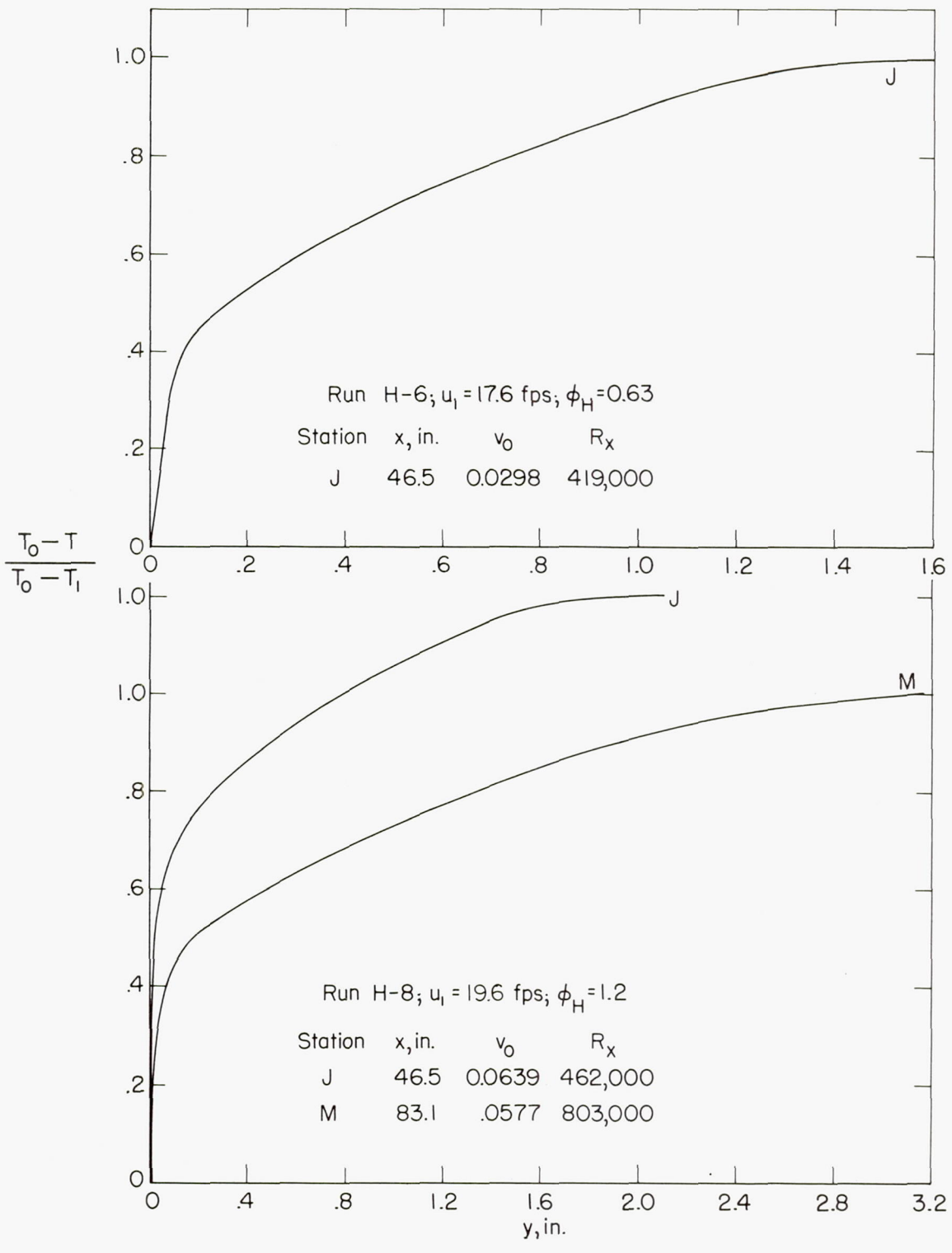

(a) Runs H-6 and H-8. Blowing with constant ϕ_H.

Figure 10.- Temperature profiles.

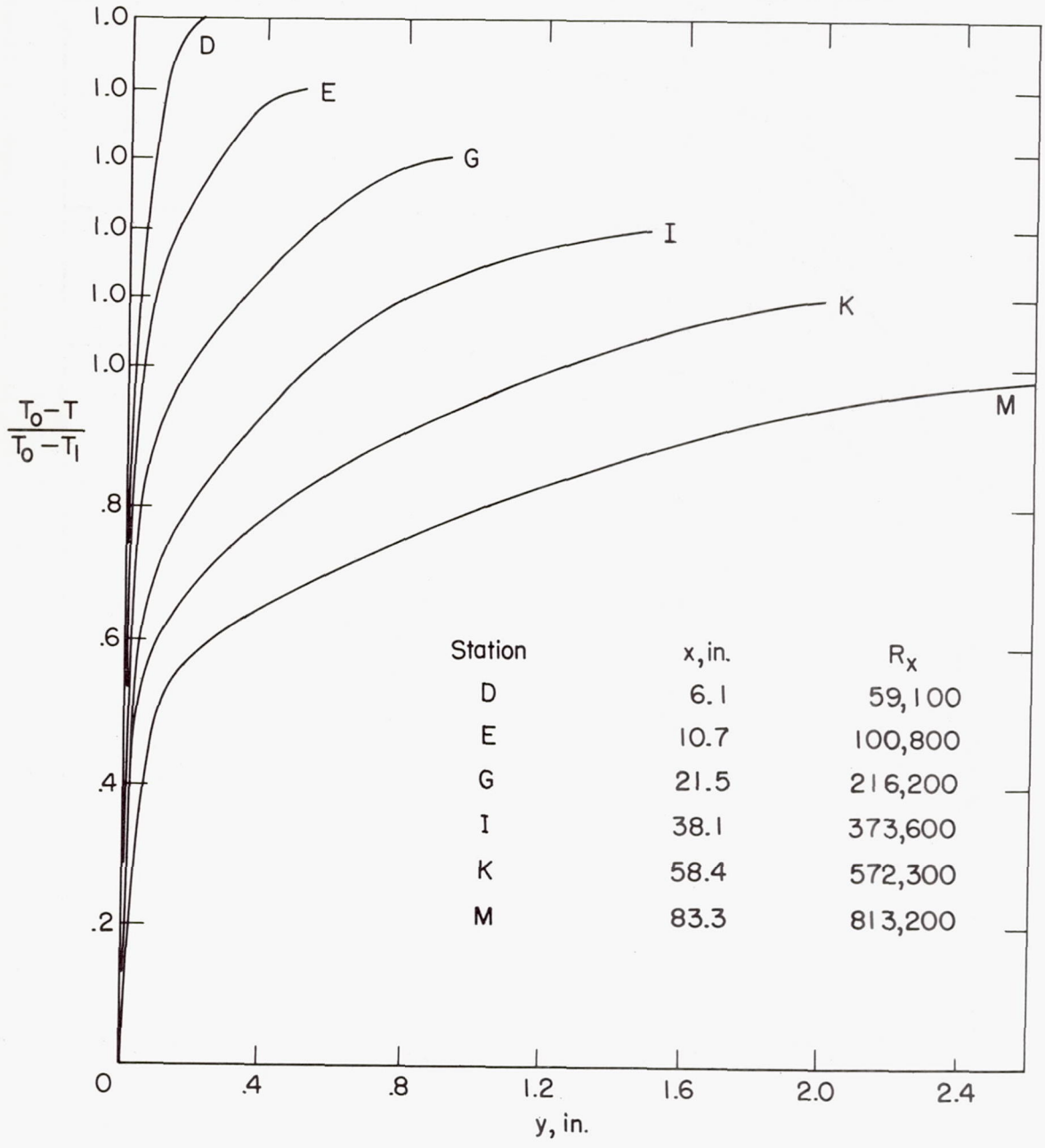

(b) Run H-17a. Uniform blowing v_o = 0.04 fps; u_1 = 20.0 fps.

Figure 10.- Continued.

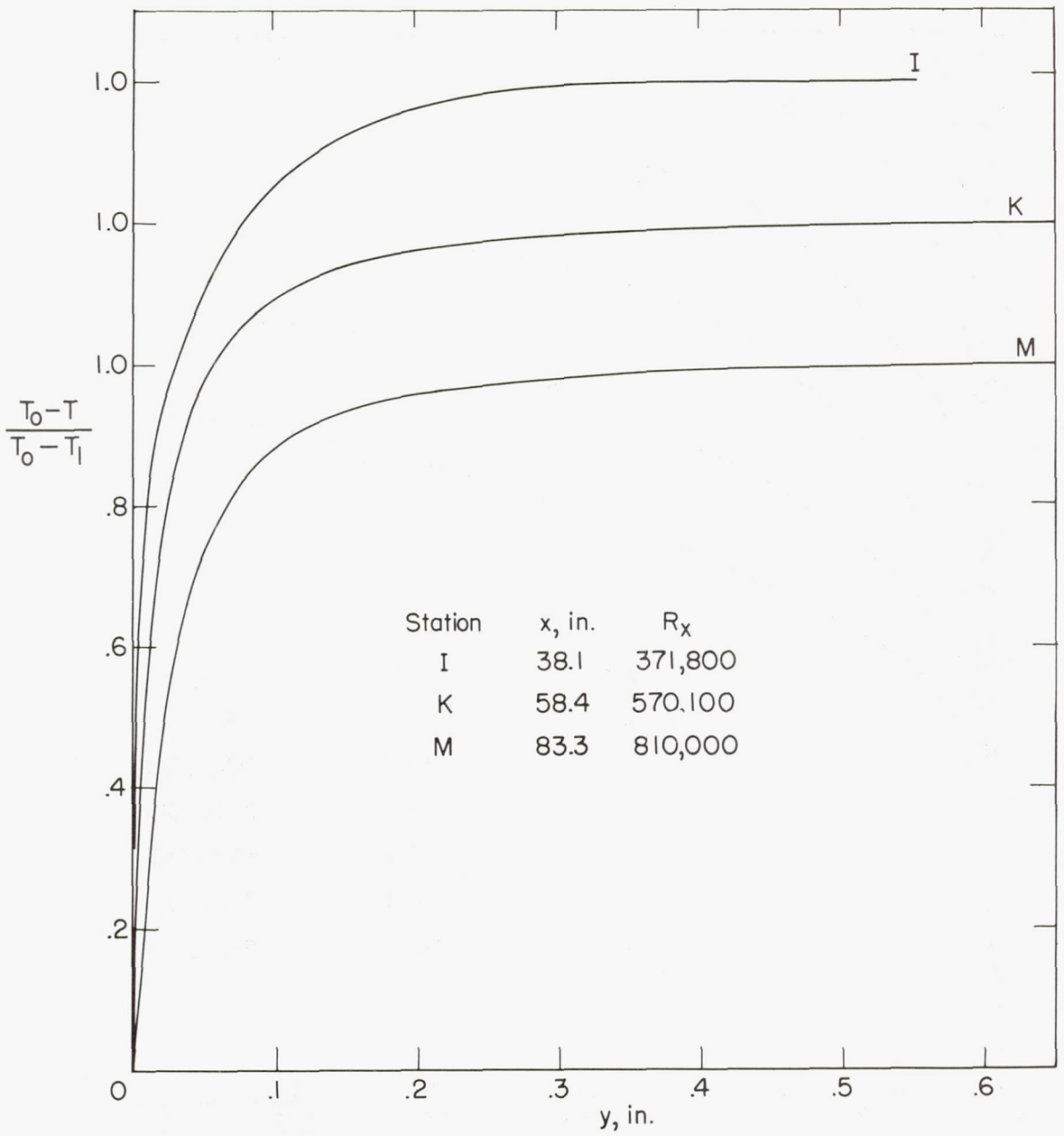

(c) Run H-12. Suction with $\phi_H = -1.2$; $u_1 = 19.8$ fps.

Figure 10.- Concluded.

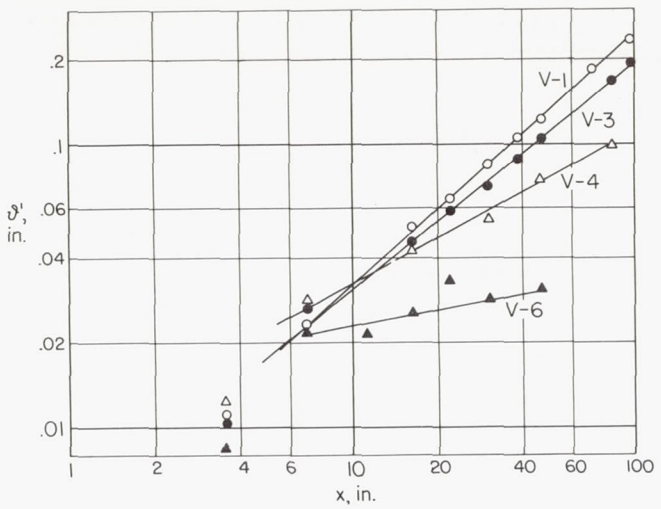

(a) Blowing.

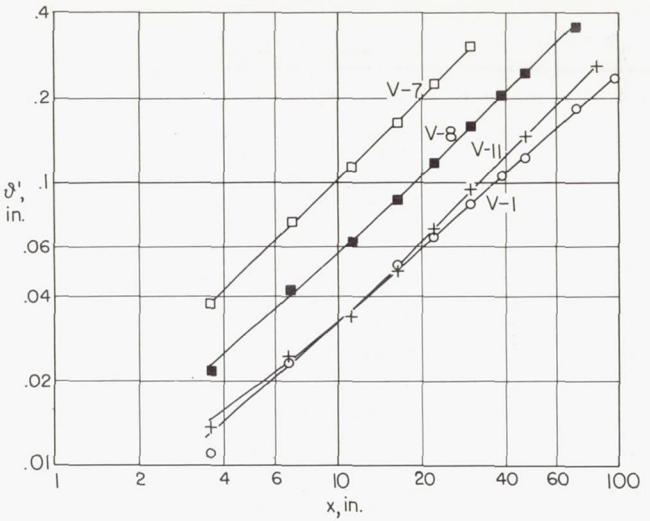

(b) Uniform suction.

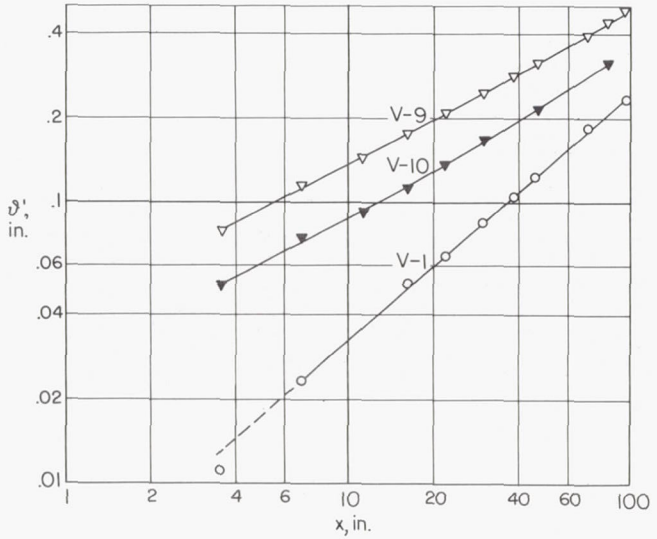

(c) Suction with inverse square-root distribution.

Mass transfer condition	Run	u_1	v_o	Eq. of curves $\vartheta' = ax^b$ a	b
No mass transfer	V-1	25.8	0	0.0043	0.88
Blowing	V-3	26.0	0.054	0.0047	0.81
	V-4	25.9	.13	.010	.50
	V-6	26.3	.26	.014	.21
Uniform suction	V-11	25.9	-0.052	0.0053	0.77
	(Turbulent)			.0032	1.00
	V-8	25.7	-.13	.0066	.92
	(Turbulent)			.0052	1.00
	V-7	25.8	-.26	.011	.93
Suction with inverse square-root distribution	V-10	25.9	[a]3.0	0.026	0.53
	(Turbulent)			.018	.65
	V-9	26.7	[a]5.0	.041	.51
	(Turbulent)			.036	.56

[a]Values of C; $v_o = \frac{-Cu_1}{2\sqrt{R_x}}$

Figure 11.- Momentum integrals corrected for mass transfer.

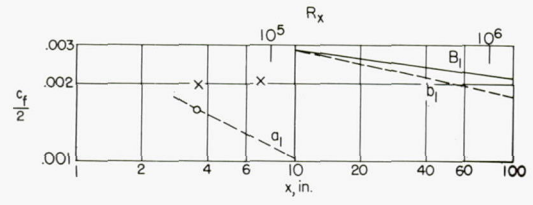

(a) No mass transfer.

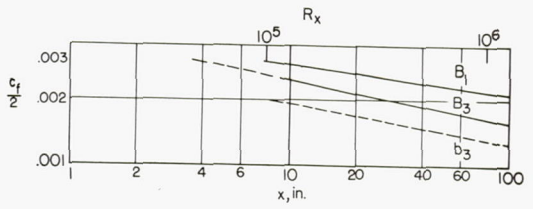

(b) Uniform blowing.

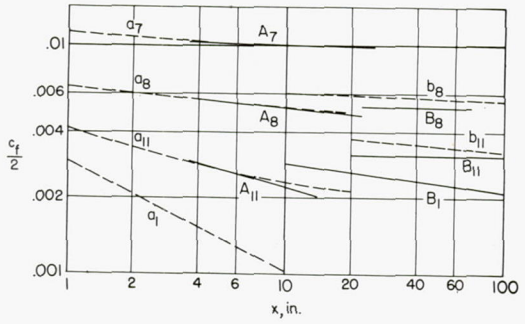

(c) Uniform suction.

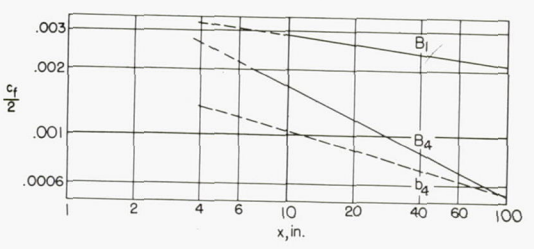

(d) Uniform blowing.

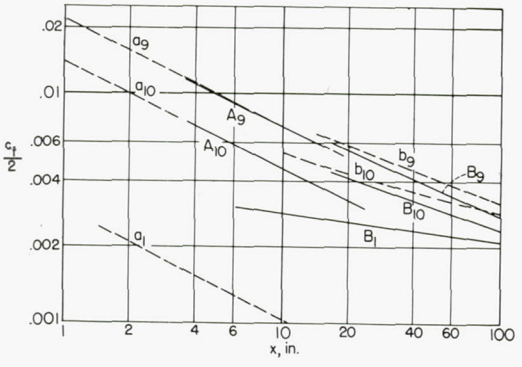

(e) Suction with inverse square-root distribution.

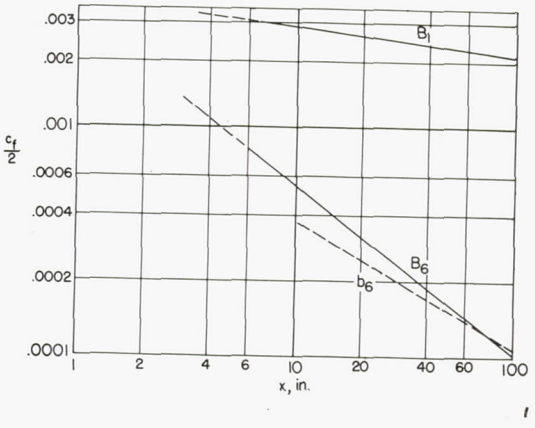

(f) Uniform blowing.

Designation of curves

Observed laminar friction factors, A
Predicted laminar friction factors, a
Observed turbulent friction factors, B
Predicted turbulent friction factors, b
Subscripts refer to run numbers

Mass transfer conditions	Run	v_o, fps
No mass transfer	V-1	0
Blowing	V-3	0.054
	V-4	.13
	V-6	.26
Suction	V-7	-0.26
	V-8	-.13
	V-9	$-2.5\sqrt{\frac{u_1 \nu}{x}}$
	V-10	$-1.5\sqrt{\frac{u_1 \nu}{x}}$
	V-11	-.052

Predicted relationships:

a_1 - Blasius' solution of boundary-layer equations

$a_{7,8,11}$ - Iglisch's solution of boundary-layer equations for homogeneous suction

$a_{9,10}$ - Schlichting's solution of boundary-layer equations for suction with square-root distribution

$b_1 - \frac{c_f}{2} = 0.0296\ R_x^{-0.2}$

$b_{3,4,6,7,8,9,10,11}$ - Predicted by film theory on basis of B_1

Figure 12.- Measured local friction coefficients compared with predicted values.

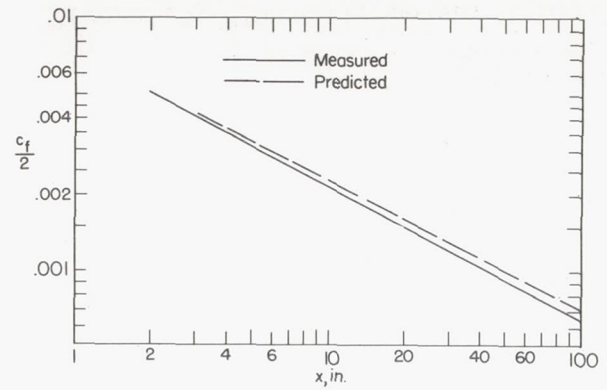

(g) Run H-1. No mass transfer.

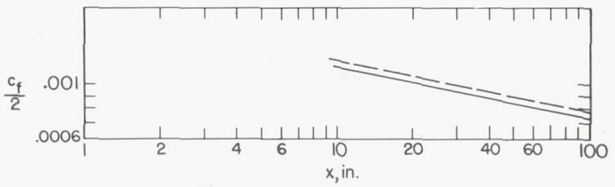

(i) Run H-8. Blowing at constant ϕ_H.

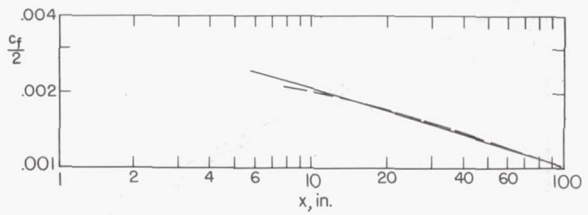

(k) Run H-17a. Uniform blowing.

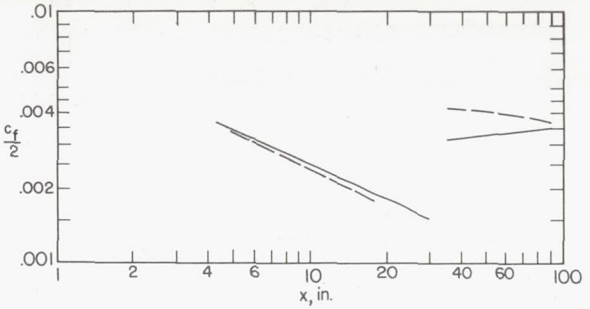

(h) Run H-12. Suction at constant ϕ_H.

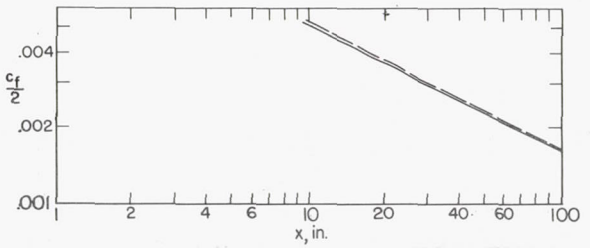

(j) Run H-14. Suction at constant ϕ_H.

Mass transfer condition	Run	u_1	v_{o_L}	v_{o_T}	ϕ_H
No mass transfer	H-1	4.4	0		0
Blowing with constant ϕ_H	H-8	19.6	$.51\sqrt{\frac{u_1\nu}{x}}$	$0.044u_1\left(\frac{\nu}{u_1 x}\right)^{0.2}$	1.2
Suction with constant ϕ_H	H-12	19.8	$-.49\sqrt{\frac{u_1\nu}{x}}$	$-.042u_1\left(\frac{\nu}{u_1 x}\right)^{0.2}$	-1.2
Suction with constant ϕ_H	H-14	20.2	$-1.46\sqrt{\frac{u_1\nu}{x}}$		-3.5
Uniform blowing	H-17a	20.0		.039	

Figure 12.- Concluded.

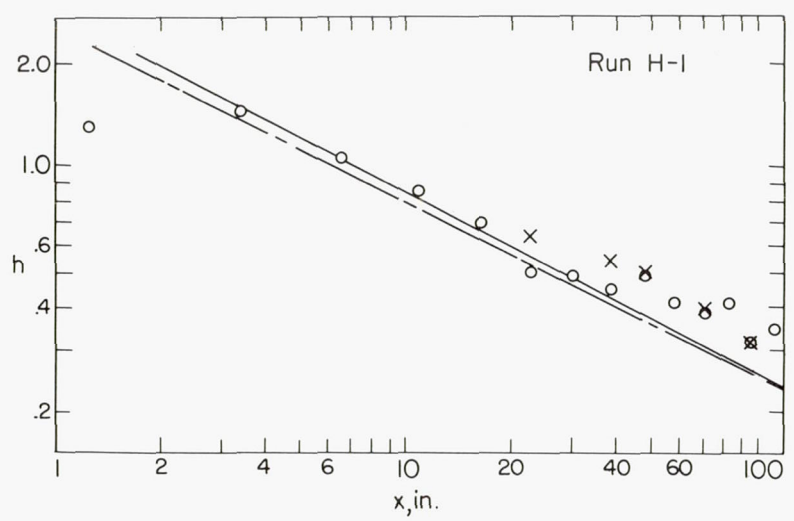

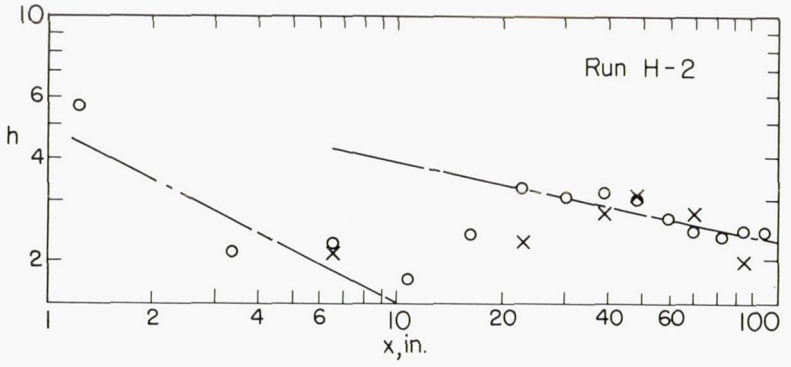

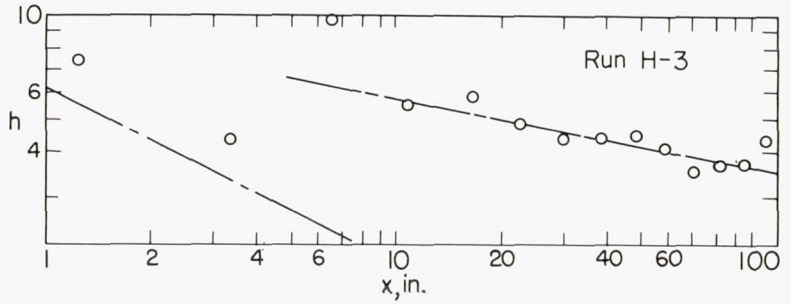

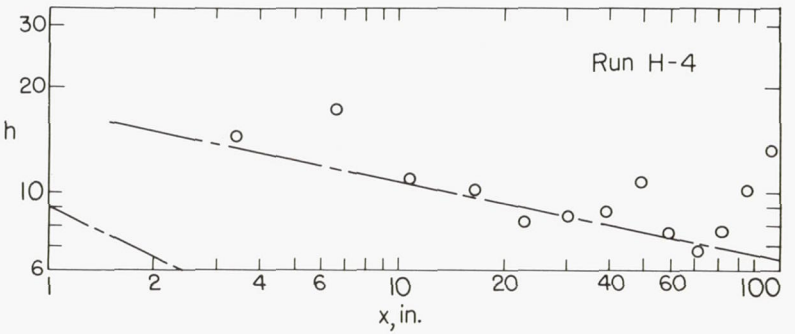

Mass transfer condition	Run	u_1	v_o
No mass transfer	H-1	4.4	0
	H-2	16.2	0
	H-3	27.0	0
	H-4	58.8	0

(a) No mass transfer.

Figure 13.- Directly measured local heat transfer coefficients compared with predicted values. h in Btu/(hr)(sq ft)(°F).

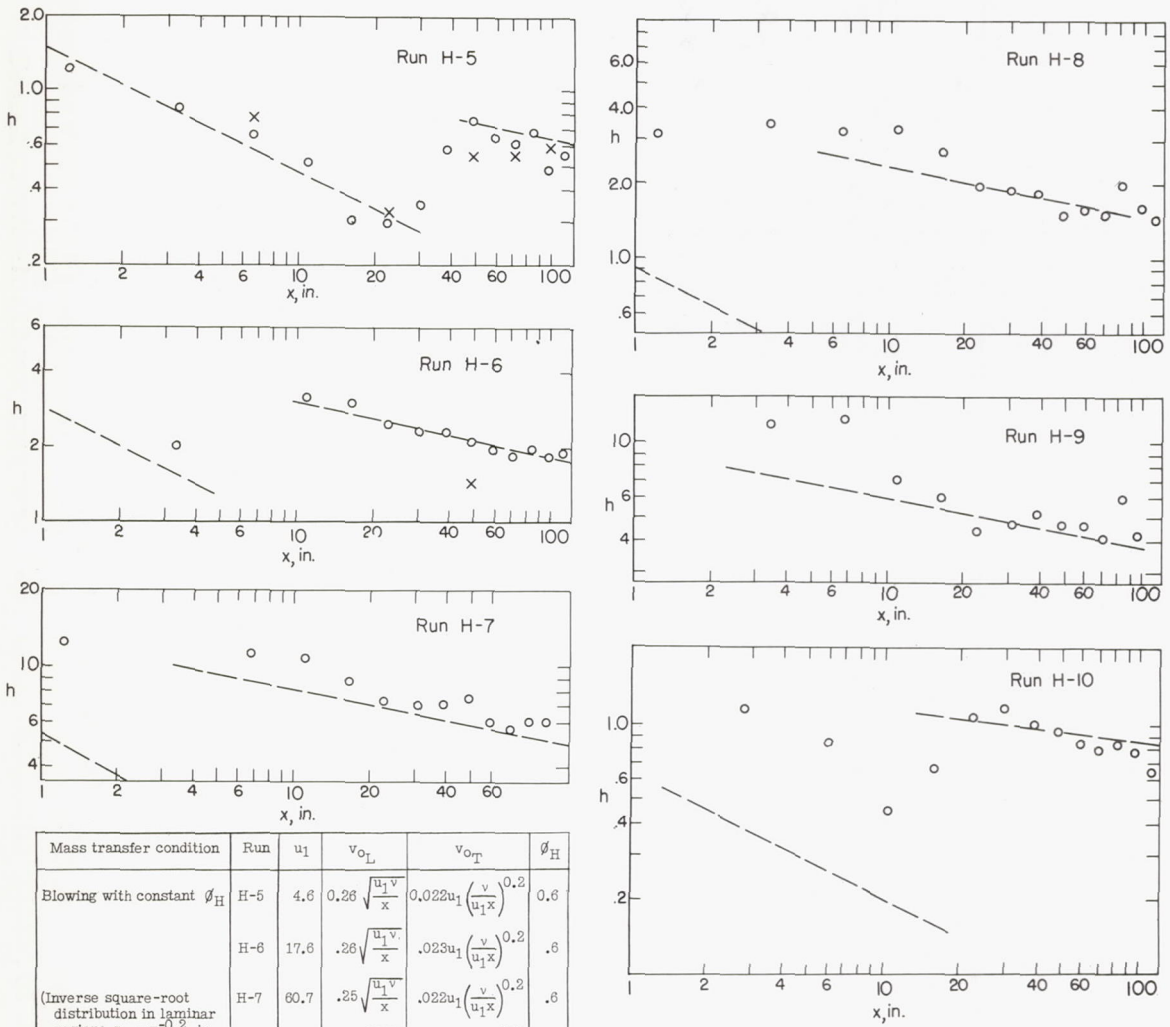

Mass transfer condition	Run	u_1	v_{o_L}	v_{o_T}	ϕ_H
Blowing with constant ϕ_H	H-5	4.6	$0.26\sqrt{\frac{u_1\nu}{x}}$	$0.022u_1\left(\frac{\nu}{u_1 x}\right)^{0.2}$	0.6
	H-6	17.6	$.26\sqrt{\frac{u_1\nu}{x}}$	$.023u_1\left(\frac{\nu}{u_1 x}\right)^{0.2}$	.6
(Inverse square-root distribution in laminar region; $v_o \propto x^{-0.2}$ in turbulent region)	H-7	60.7	$.25\sqrt{\frac{u_1\nu}{x}}$	$.022u_1\left(\frac{\nu}{u_1 x}\right)^{0.2}$	.6
	H-8	19.6	$.51\sqrt{\frac{u_1\nu}{x}}$	$.044u_1\left(\frac{\nu}{u_1 x}\right)^{0.2}$	1.2
	H-9	60.9	$.49\sqrt{\frac{u_1\nu}{x}}$	$.042u_1\left(\frac{\nu}{u_1 x}\right)^{0.2}$	1.2
	H-10	5.3	$.49\sqrt{\frac{u_1\nu}{x}}$	$.49\sqrt{\frac{u_1\nu}{x}}$	1.2

(b) Blowing at constant ϕ_H.

Figure 13.- Continued.

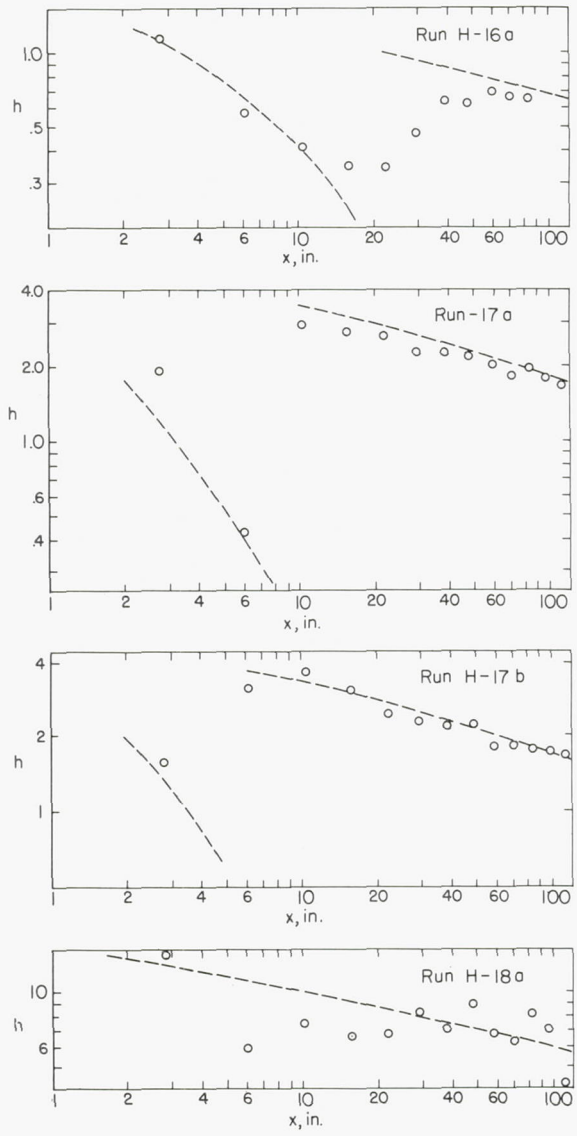

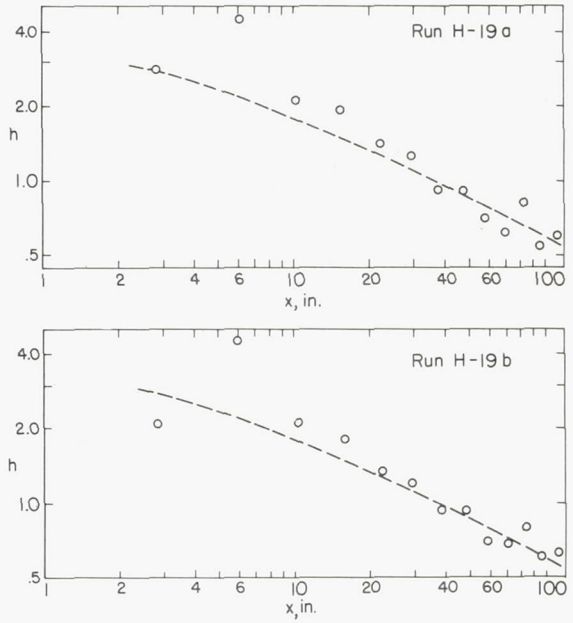

Mass transfer condition	Run	u_1	v_o
Uniform blowing	H-16a	5.0	0.01
	H-17a	20.0	.04
a-Uniform blowing gas temperature	H-17b	18.8	.04
	H-18a	59.8	.04
b-Uniform wall temperature	H-19a	19.9	.12
	H-19b	19.8	.12

(c) Uniform blowing.

Figure 13.- Continued.

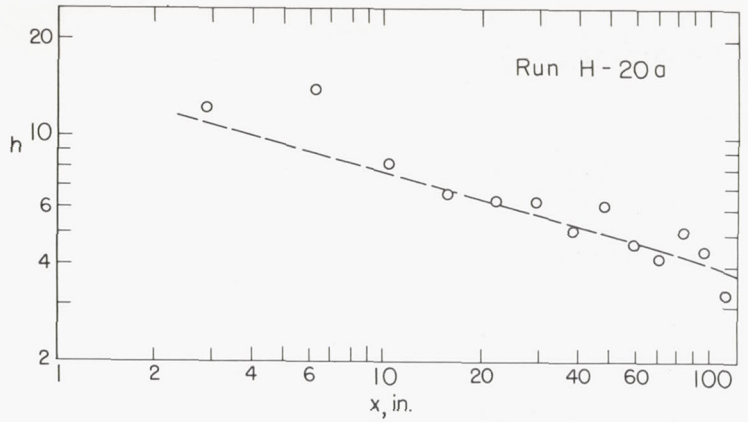

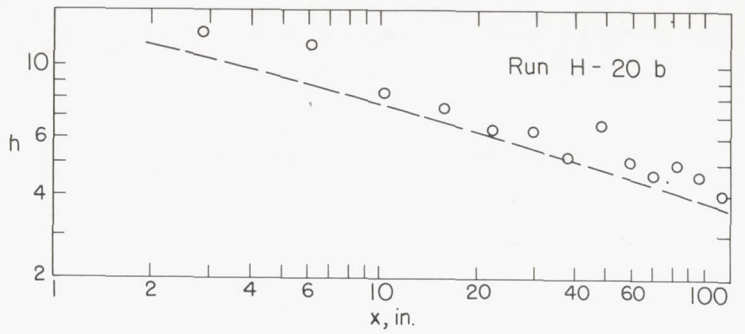

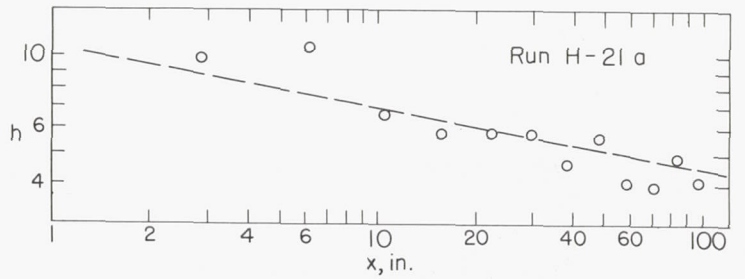

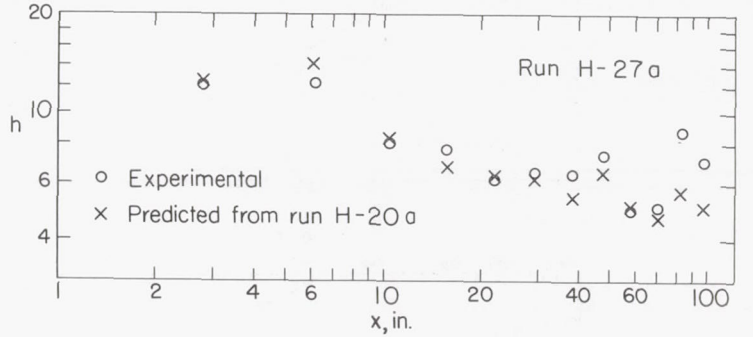

Mass transfer condition	Run	u_1	v_o
Uniform blowing Uniform blowing gas temperature Uniform wall temperature	H-20a H-20b	60.7 60.0	0.12 .12
Blowing with constant ϕ_H Mean $v_o = 0.12$ Uniform blowing gas temperature	H-21a	59.8	$0.033u_1\left(\frac{\nu}{u_1 x}\right)^{0.2}$
Uniform blowing with acceleration of main stream Uniform blowing gas temperature Experimental points compared with adjusted results of run H-20a	H-27a	60 to 70	0.12

(d) Blowing with uniform blowing gas temperature.

Figure 13.- Continued.

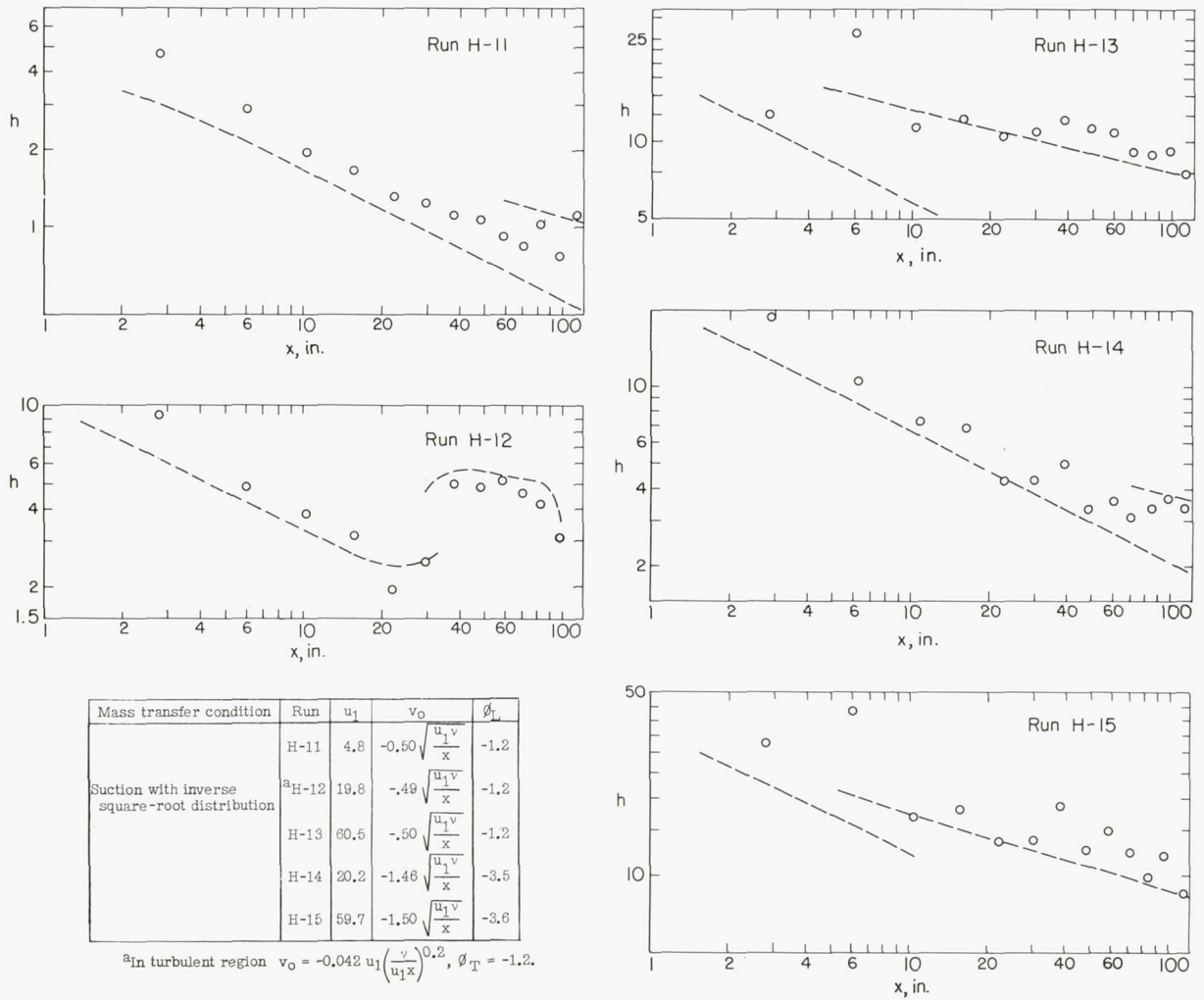

Mass transfer condition	Run	u_1	v_o	ϕ_L
Suction with inverse square-root distribution	H-11	4.8	$-0.50\sqrt{\frac{u_1 \nu}{x}}$	-1.2
	[a]H-12	19.8	$-.49\sqrt{\frac{u_1 \nu}{x}}$	-1.2
	H-13	60.5	$-.50\sqrt{\frac{u_1 \nu}{x}}$	-1.2
	H-14	20.2	$-1.46\sqrt{\frac{u_1 \nu}{x}}$	-3.5
	H-15	59.7	$-1.50\sqrt{\frac{u_1 \nu}{x}}$	-3.6

[a]In turbulent region $v_o = -0.042\, u_1 \left(\frac{\nu}{u_1 x}\right)^{0.2}$, $\phi_T = -1.2$.

(e) Suction at constant ϕ_H.

Figure 13.- Continued.

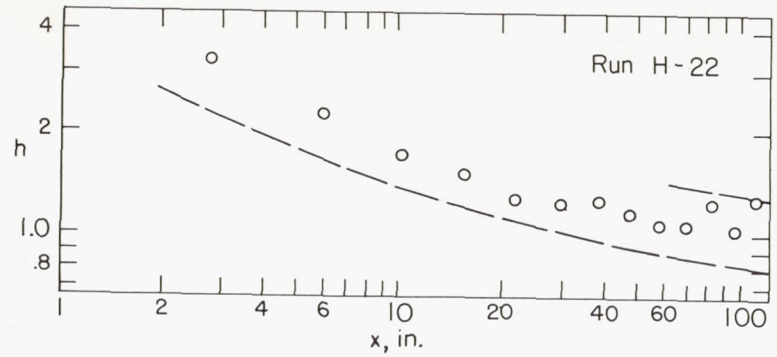

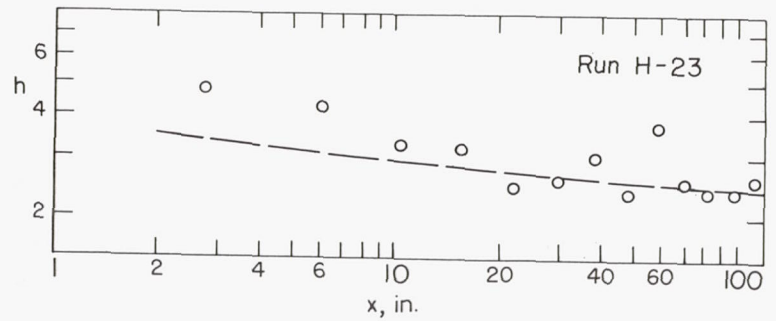

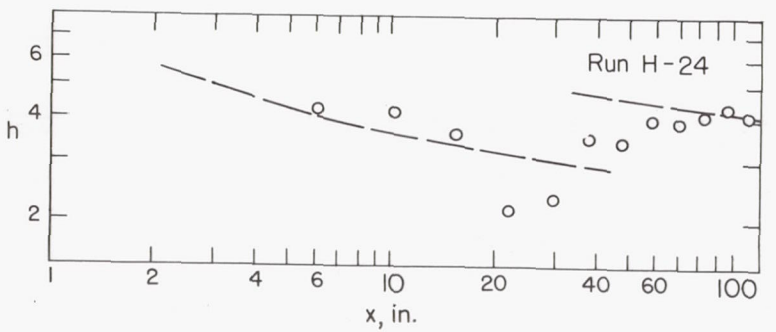

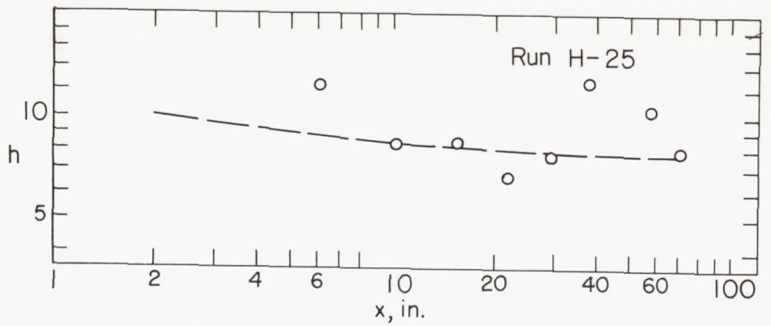

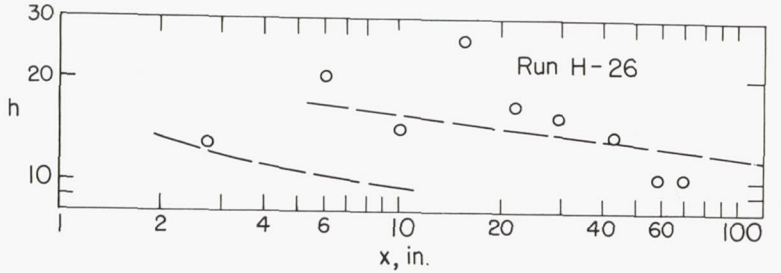

Mass transfer condition	Run	u_1	v_o
Uniform suction	H-22	4.9	-0.01
	H-23	4.8	-.04
	H-24	19.3	-.04
	H-25	19.6	-.12
	H-26	60.0	-.12

(f) Uniform suction.

Figure 13.- Concluded.

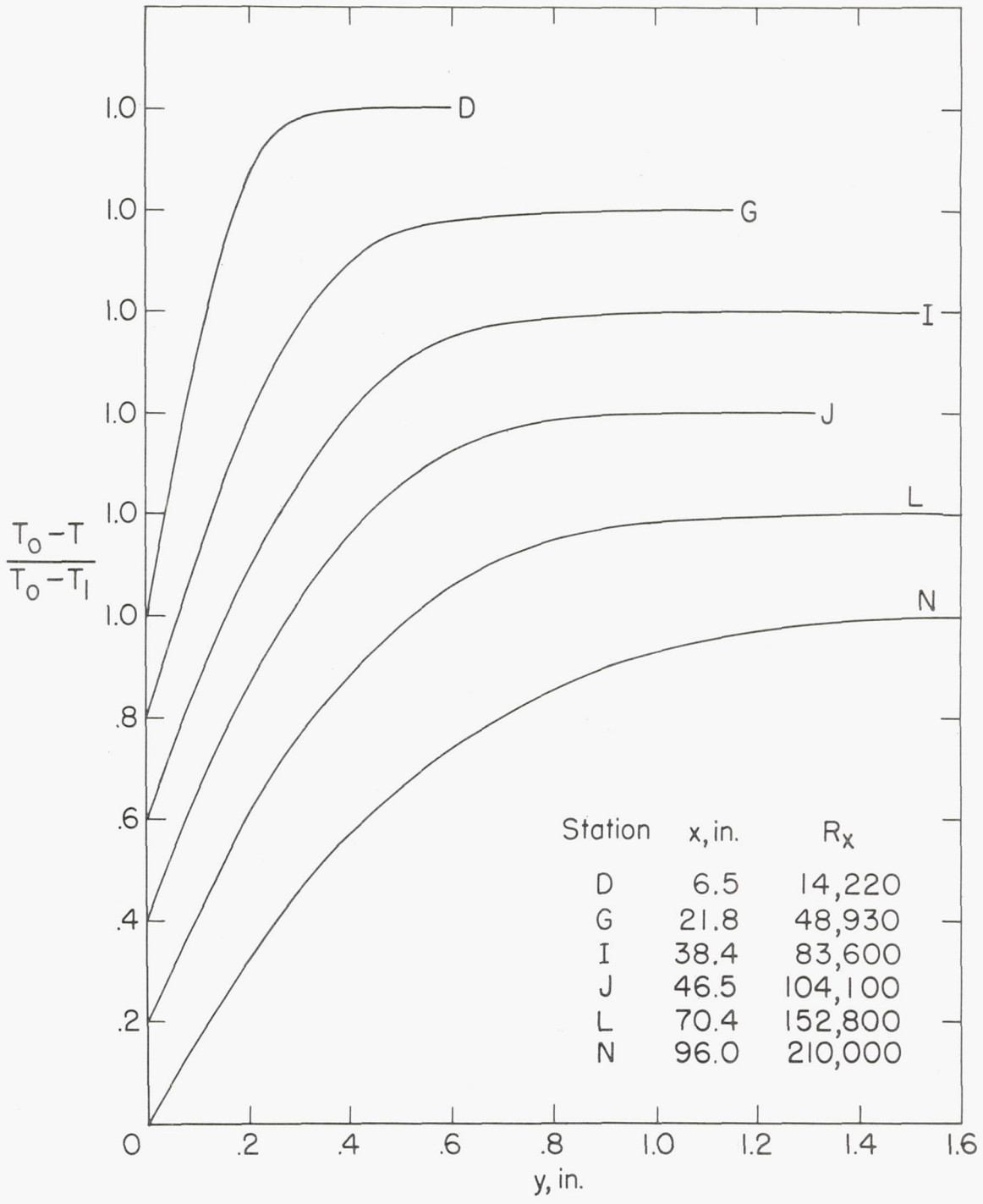

(a) Run H-1. No mass transfer $(\phi_H = 0)$; $u_1 = 4.4$ fps.

Figure 14.- Temperature profiles.

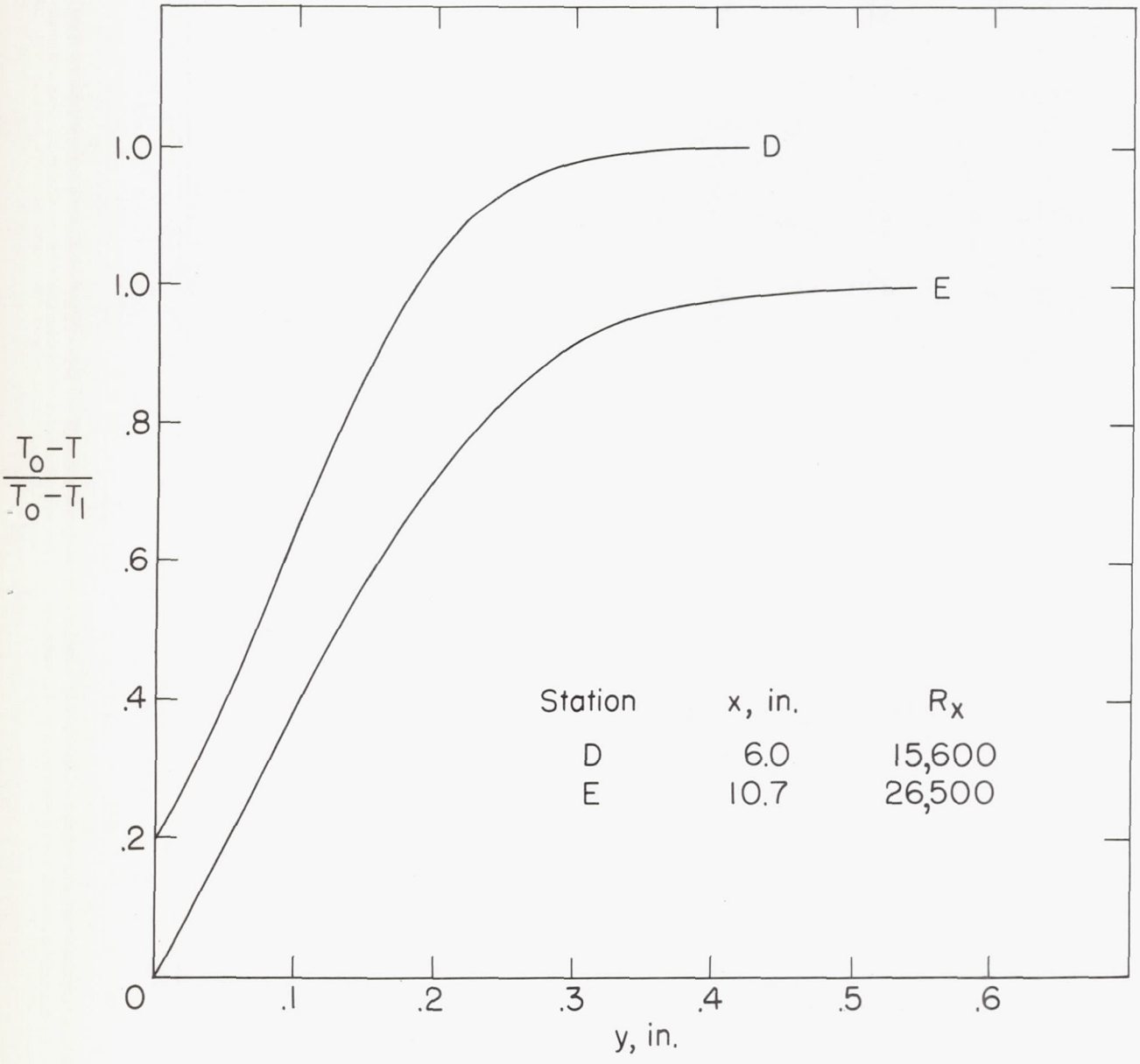

(b) Run H-10. Blowing with $\emptyset_H = 1.2$; $u_1 = 5.3$ fps.

Figure 14.- Continued.

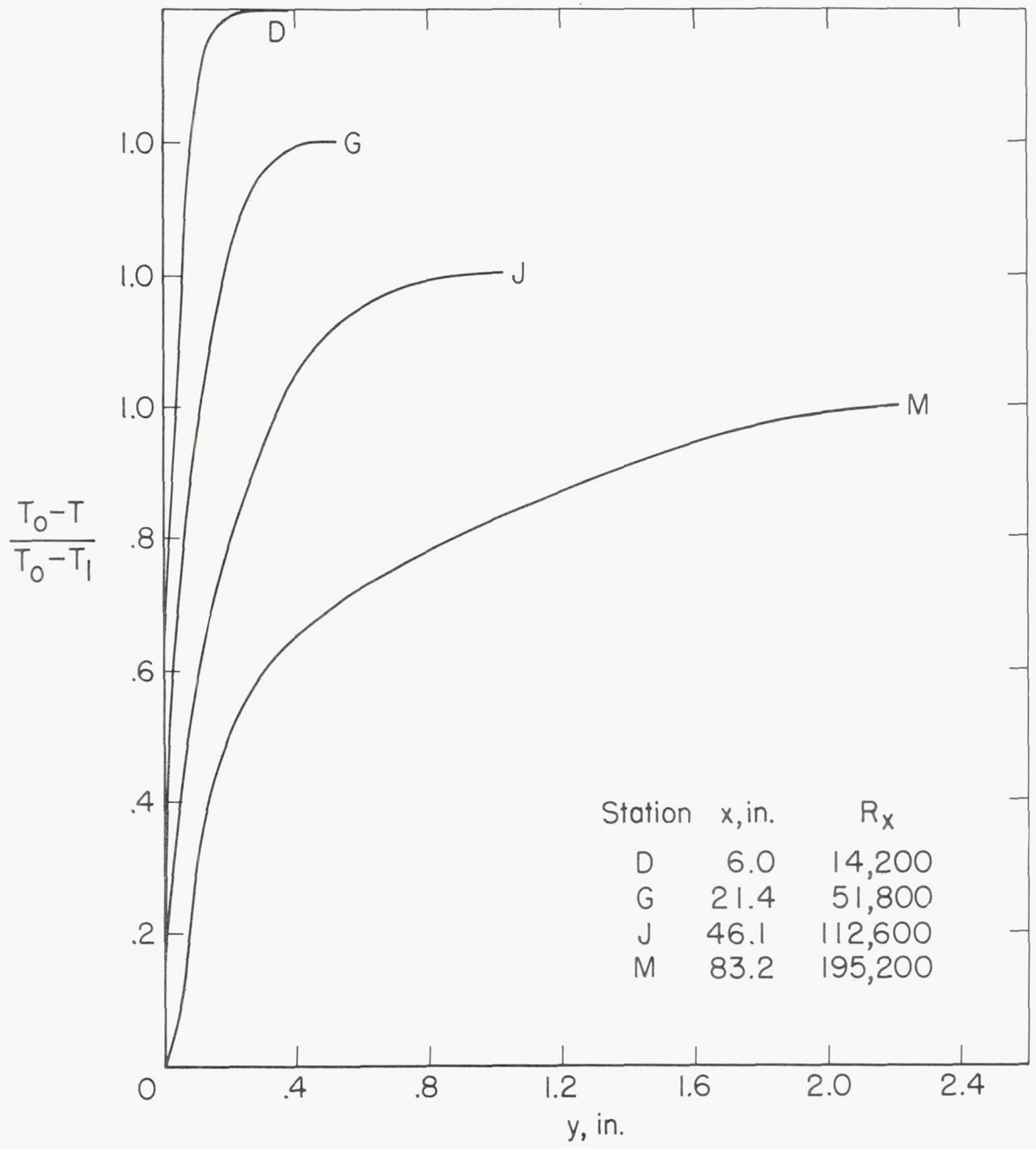

(c) Run H-11. Suction with $\phi_H = -1.2$; $u_l = 4.8$ fps.

Figure 14.- Continued.

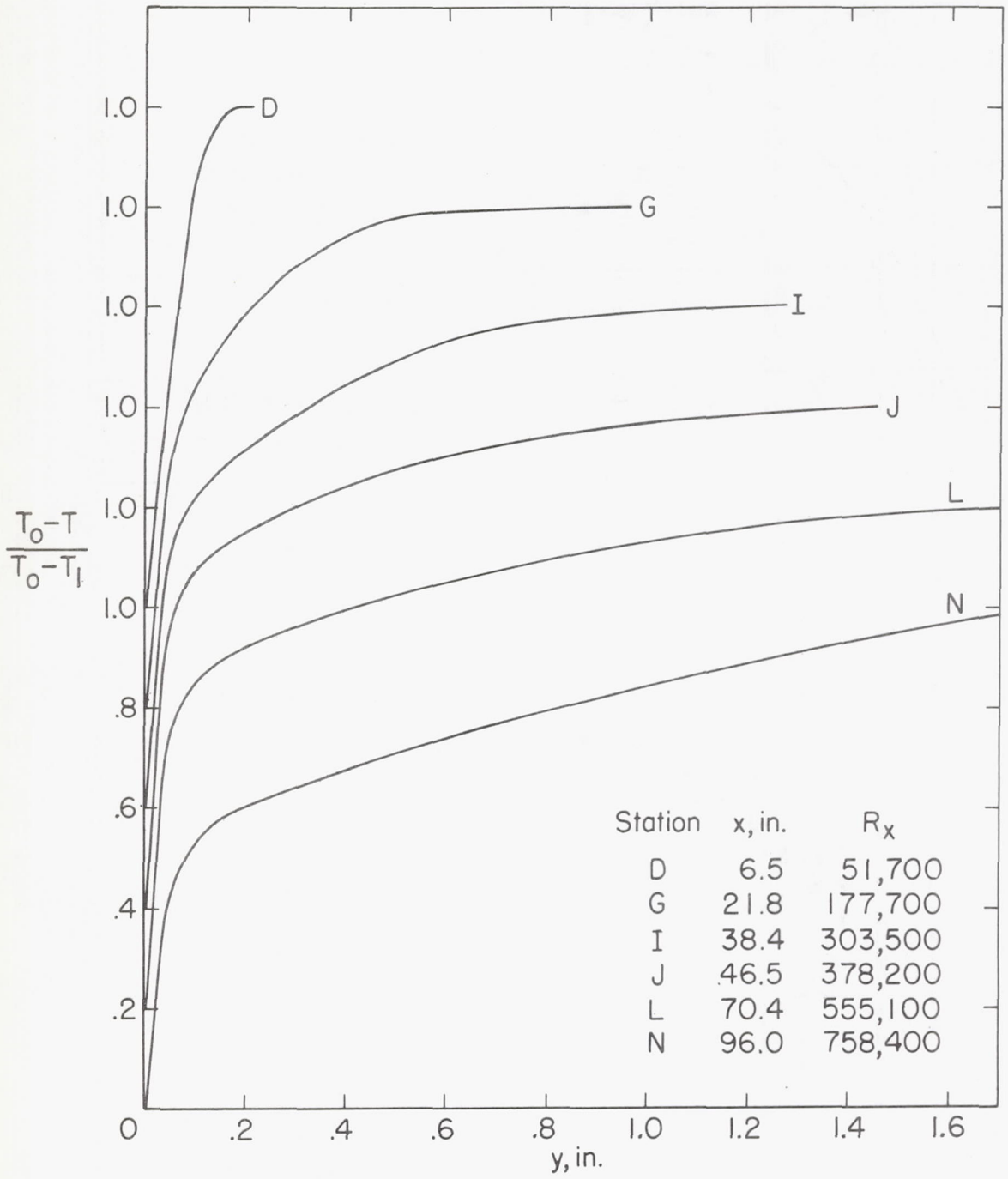

(d) Run H-2. No mass transfer $(\phi_H = 0)$; u_1 = 16.2 fps.

Figure 14.- Concluded.

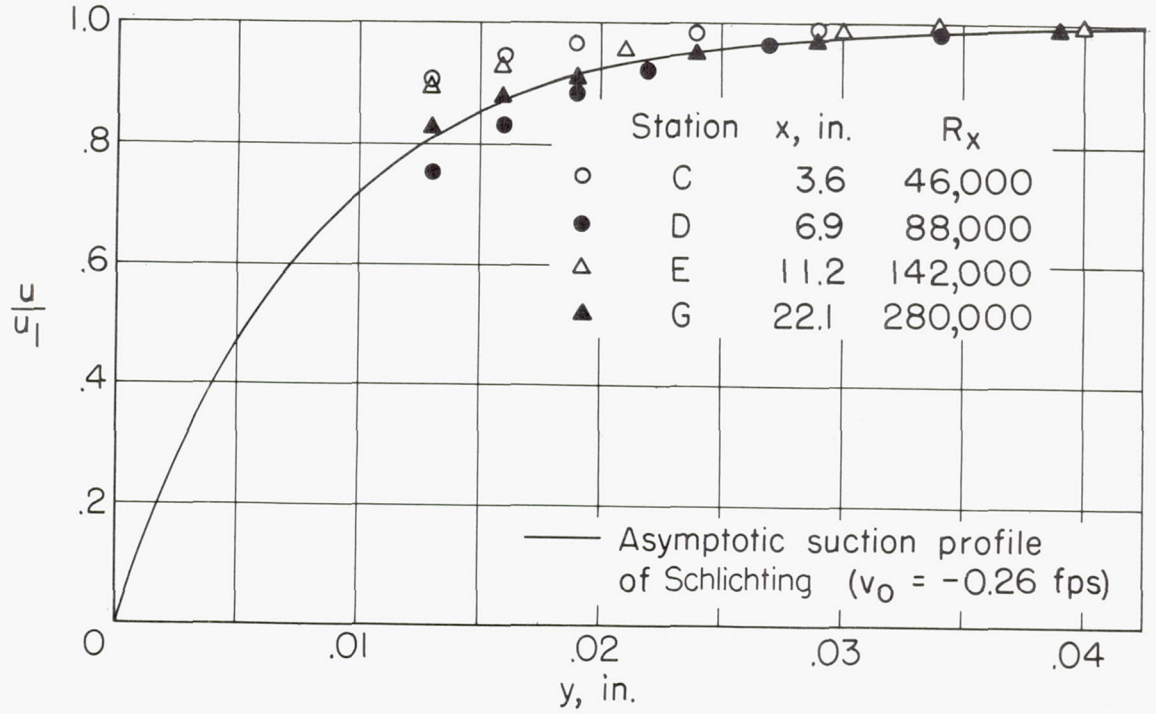

(a) Run V-7. u_1 = 25.8 fps; v_o = -0.26 fps.

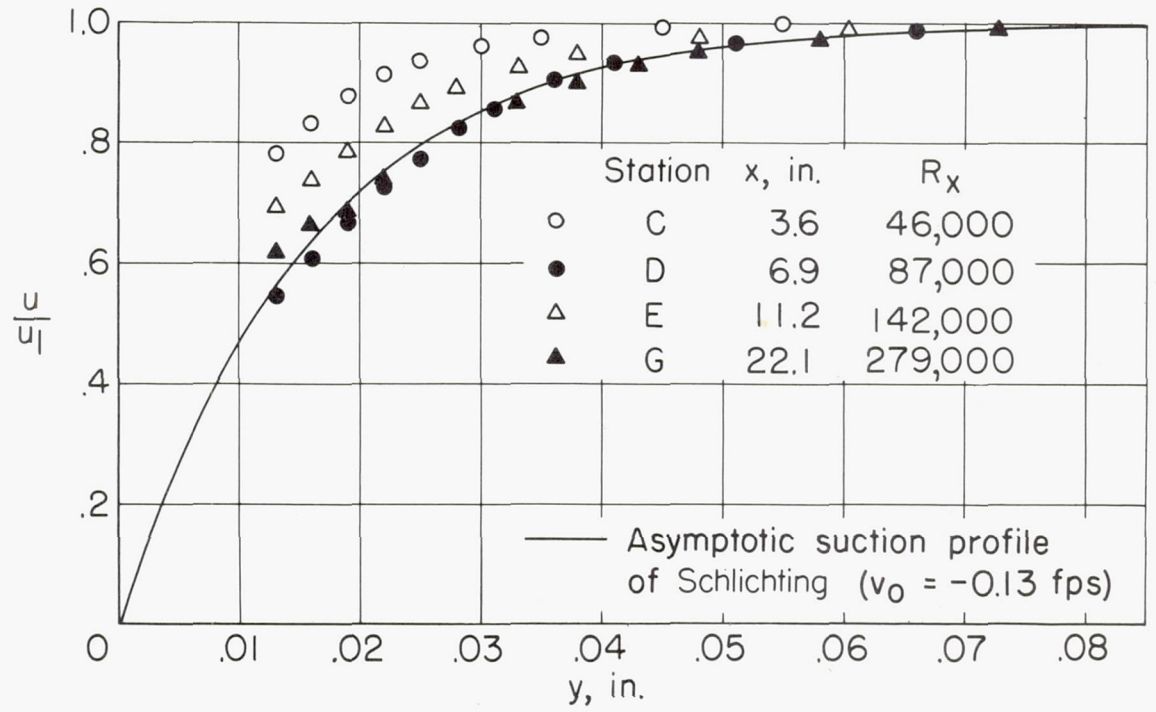

(b) Run V-8. u_1 = 25.7 fps; v_o = -0.13 fps.

Figure 15.- Mean velocity profiles in laminar regime with uniform suction.

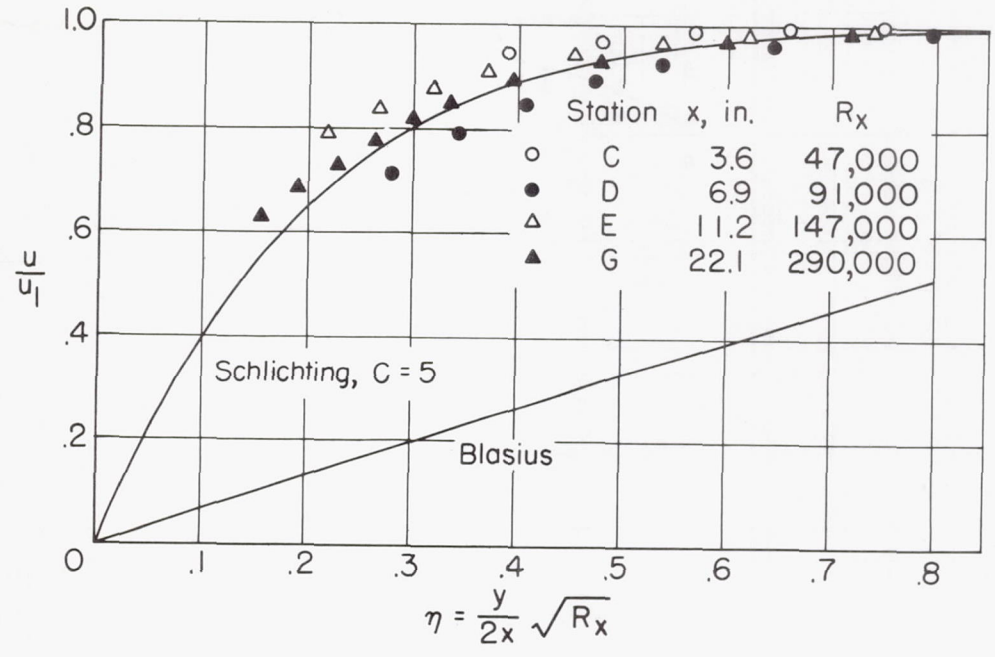

(a) Run V-9. $u_1 = 26.7$ fps; $C = \frac{-2v_o}{u_1}\sqrt{R_x} = 5.0$.

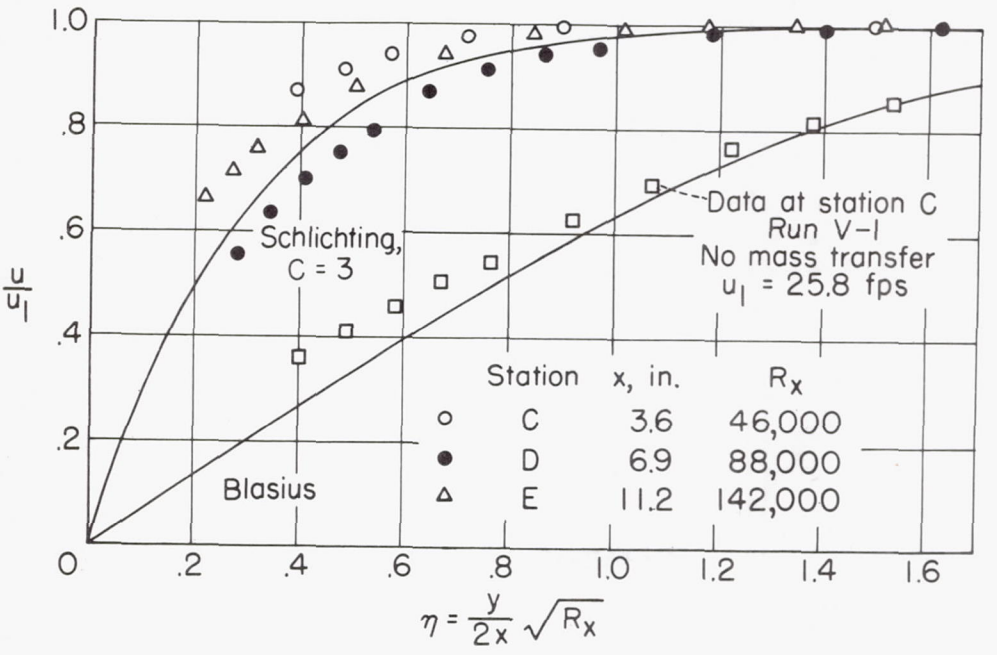

(b) Run V-10. $u_1 = 25.9$ fps; $C = \frac{-2v_o}{u_1}\sqrt{R_x} = 3.0$.

Figure 16.- Mean velocity profiles in laminar regime with inverse square-root suction distribution.

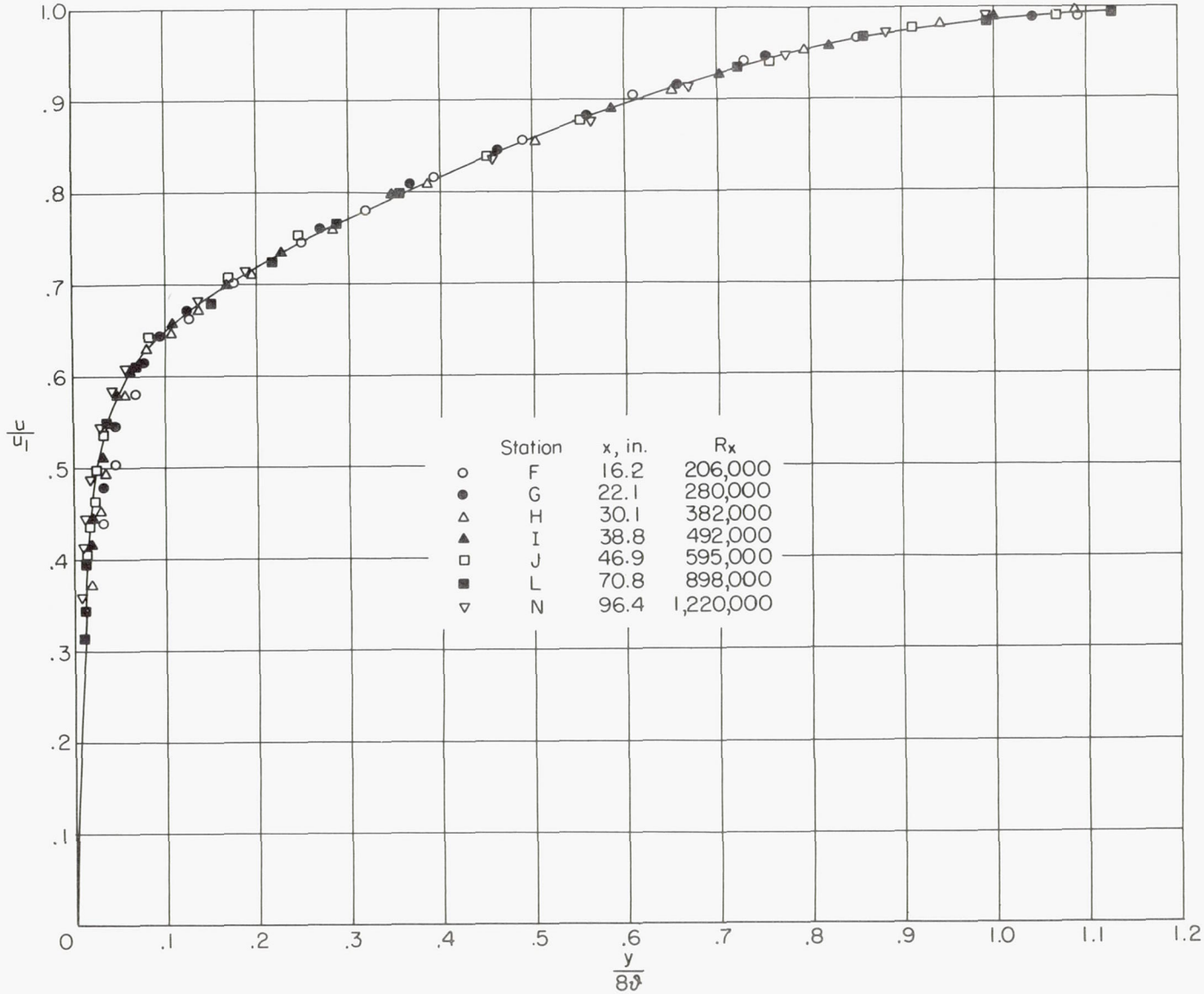

Figure 17.- Turbulent mean velocity profiles of run V-1 compared on dimensionless basis. No mass transfer; u_1 = 25.8 fps.

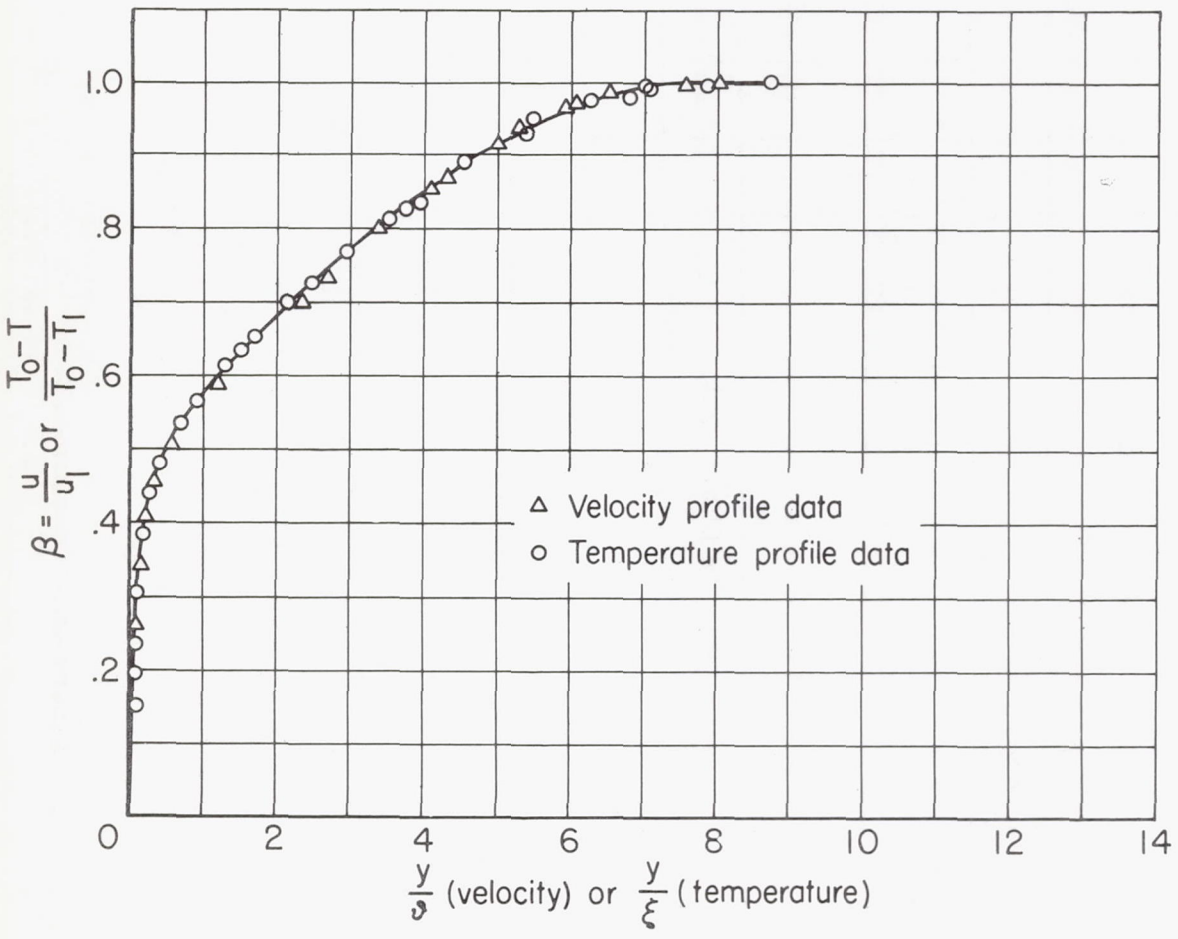

(a) Run H-8, stations G, J, and M. Blowing with $\phi_H = 1.2$; $u_1 = 19.6$ fps.

Figure 18.- Turbulent velocity and temperature profiles compared on dimensionless basis.

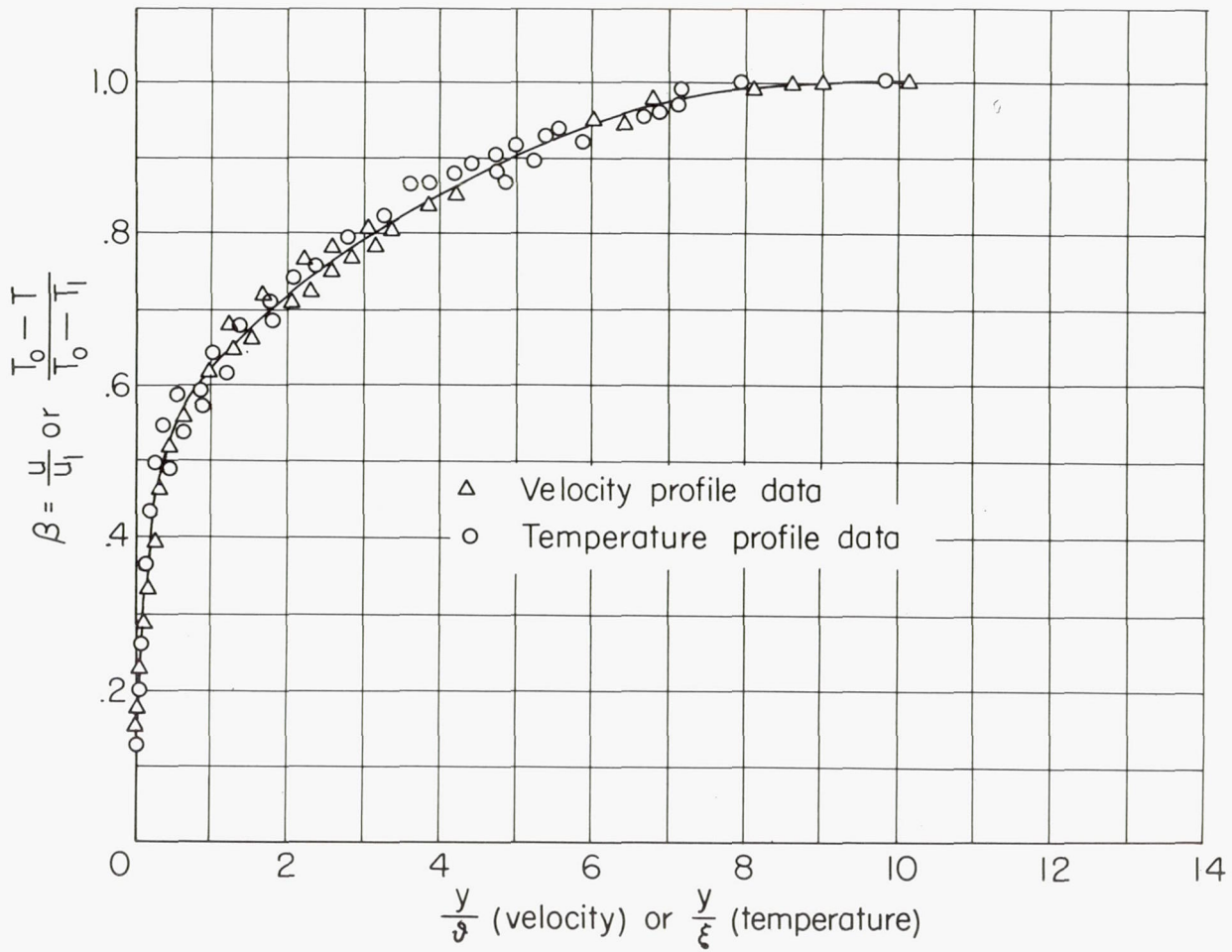

(b) Run H-17a, stations E, G, I, K, and M. Uniform blowing v_o = 0.04 fps; u_1 = 20.0 fps.

Figure 18.- Concluded.

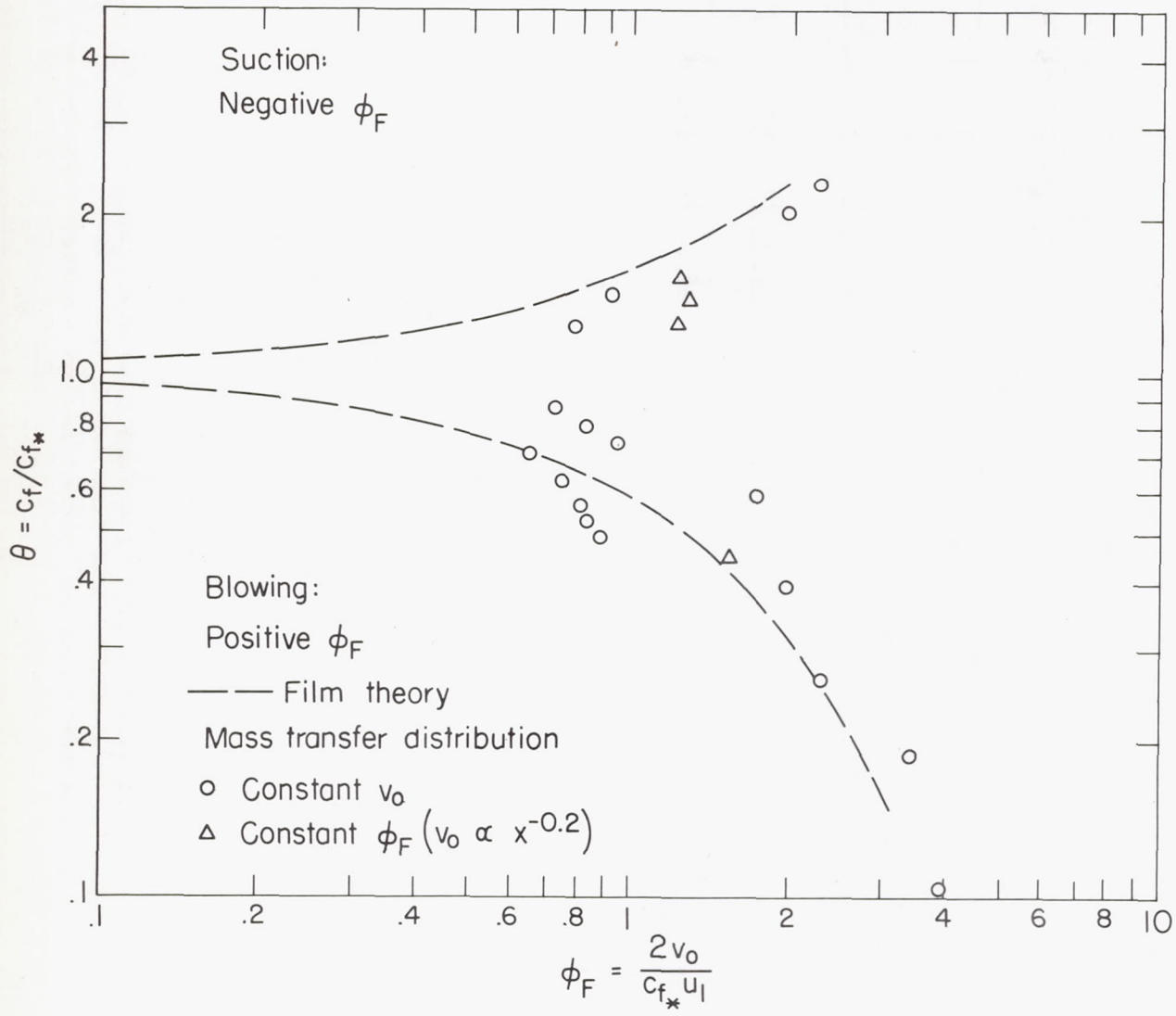

Figure 19.- Turbulent friction coefficients compared with film theory.

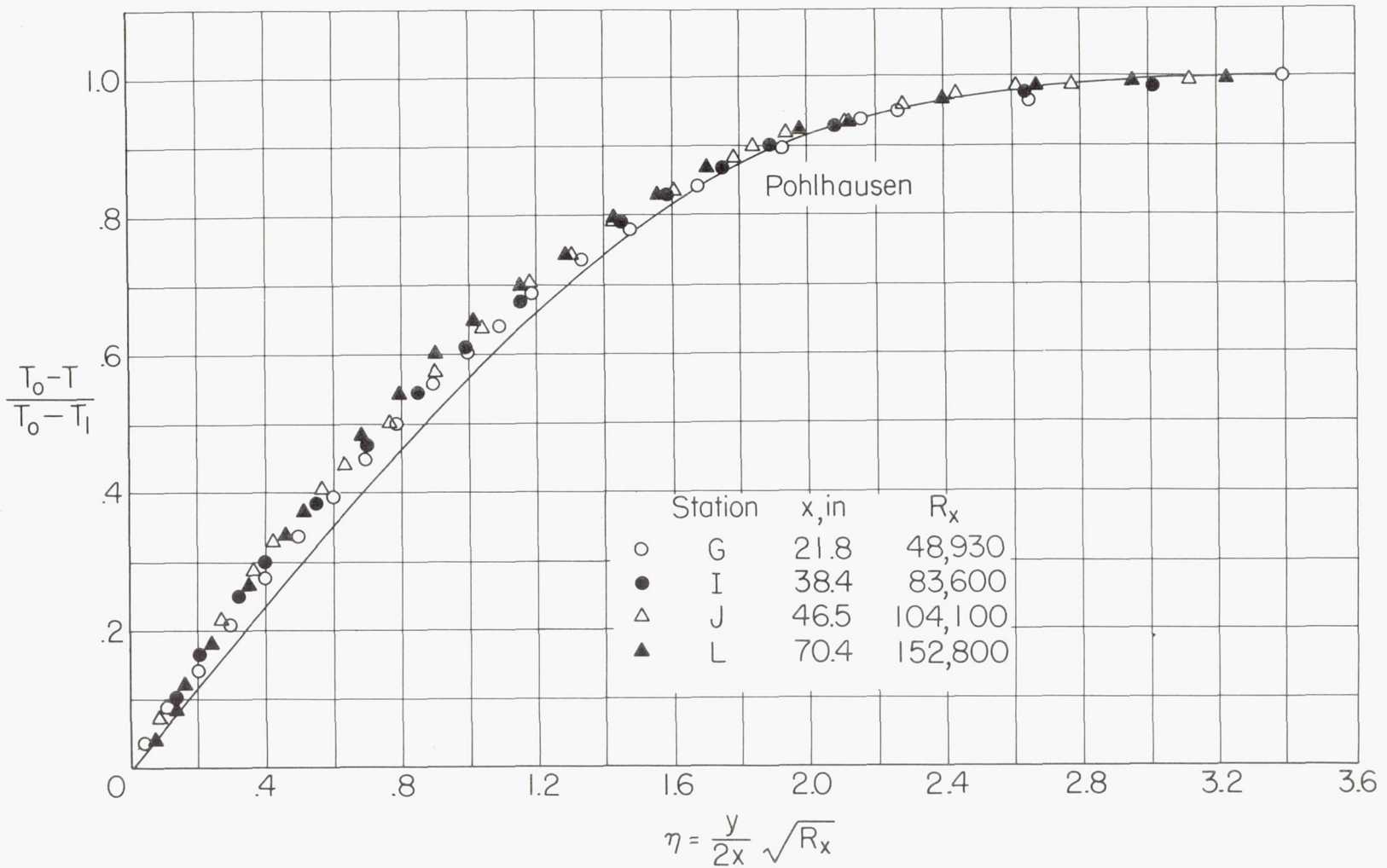

(a) Run H-1. No mass transfer; u_1 = 4.4 fps.

Figure 20.- Temperature profiles of laminar regime compared with theory.

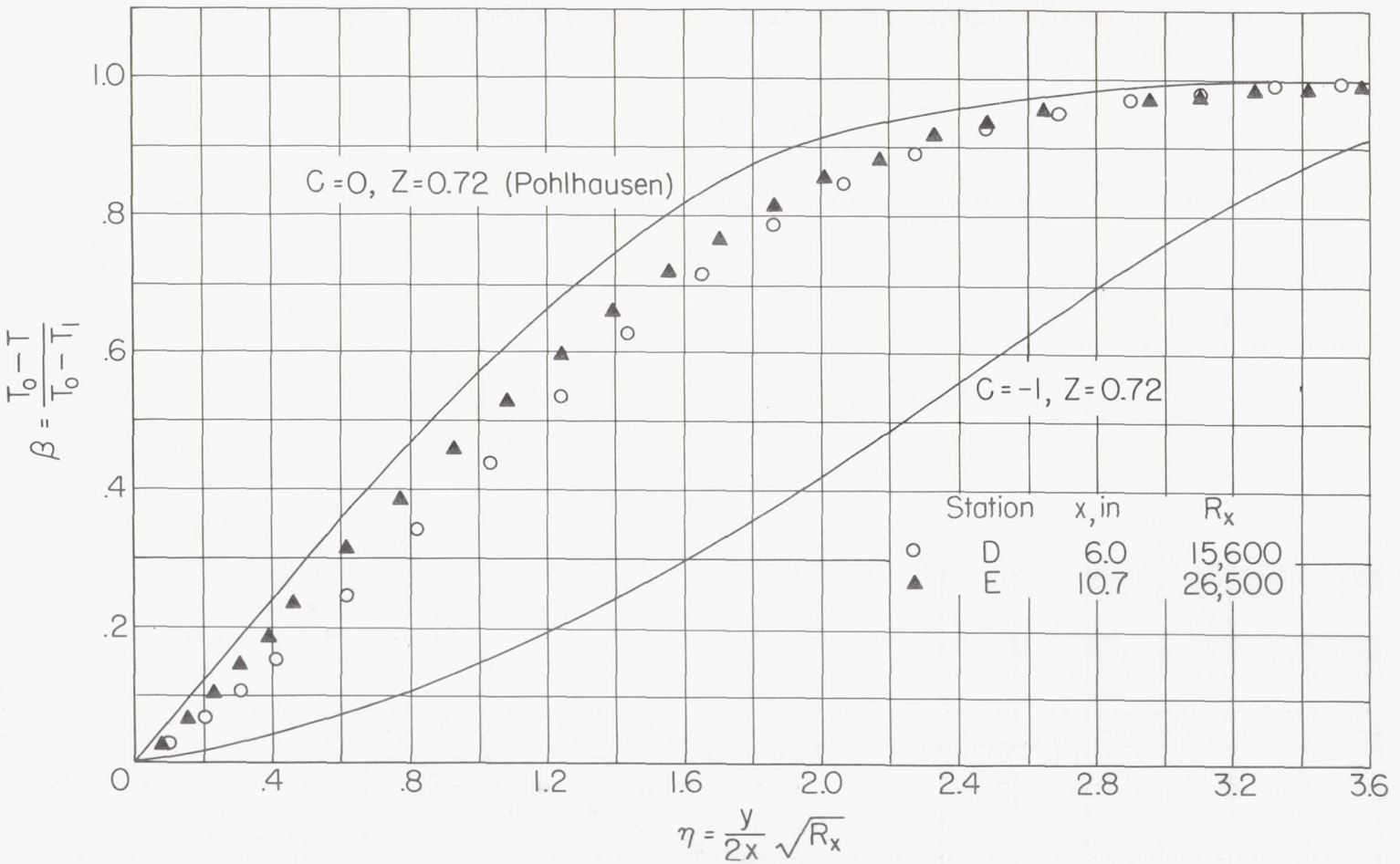

(b) Run H-10. Inverse square-root blowing distribution with $\phi_H = 1.2$; $u_1 = 5.3$ fps; $C = \frac{-2v_o}{u_1}\sqrt{R_x} = -0.97$.

Figure 20.- Continued.

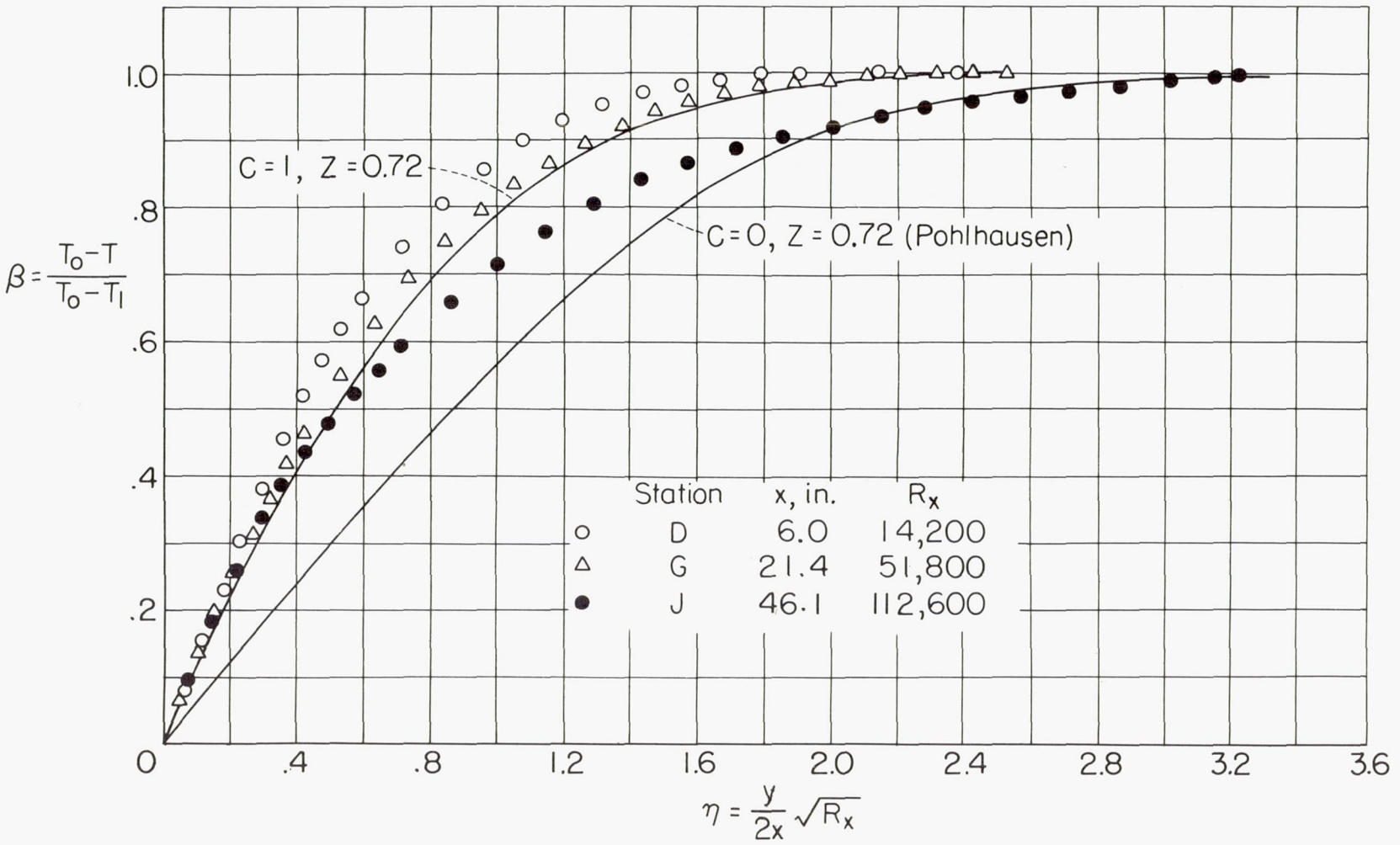

(c) Run H-11. Inverse square-root suction distribution with $\phi_H = -1.2$; $u_1 = 4.8$ fps; $C = \frac{-2v_o}{u_1}\sqrt{R_x} = 1.0$.

Figure 20.- Concluded.

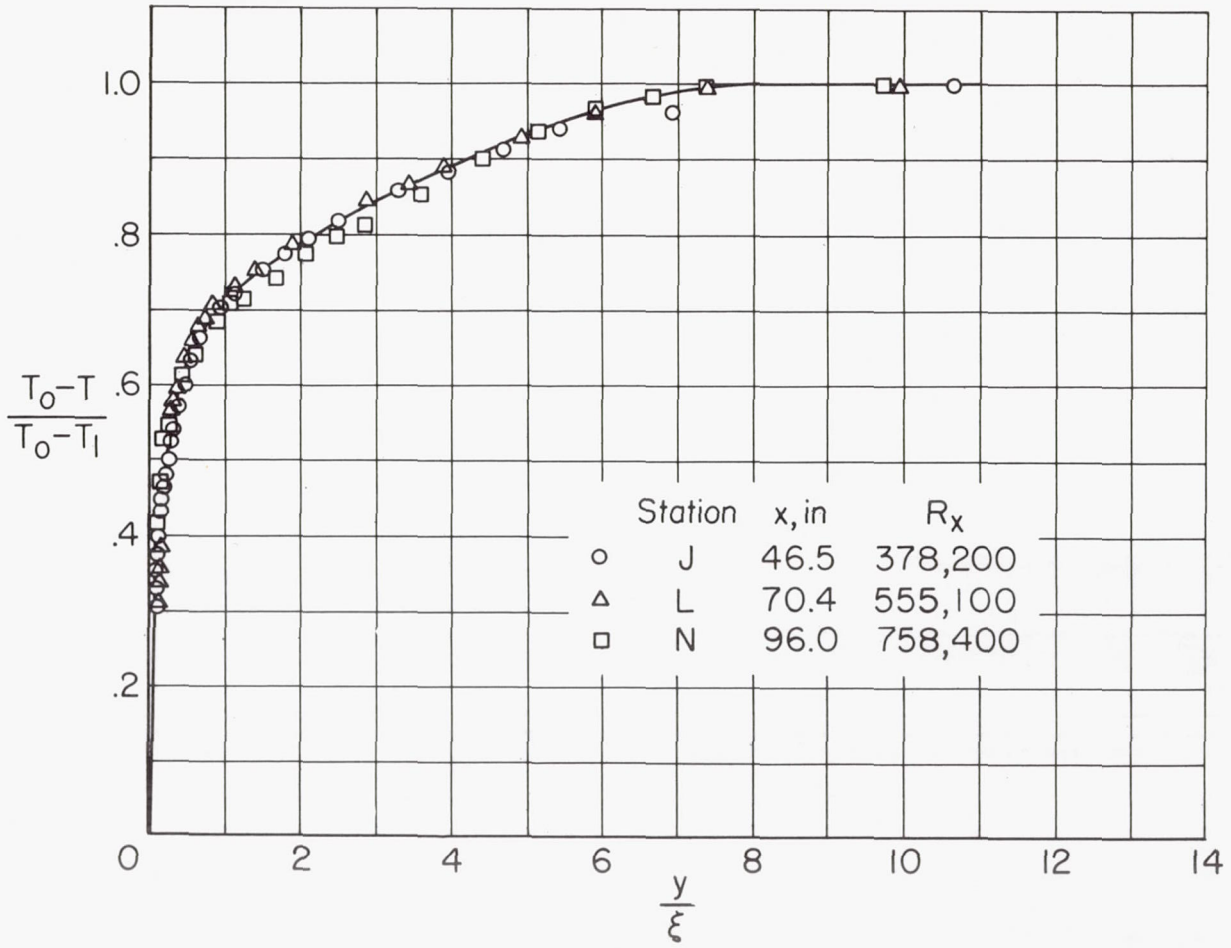

Figure 21.- Turbulent temperature profiles of run H-2 compared on dimensionless basis. No mass transfer; u_1 = 16.2 fps.

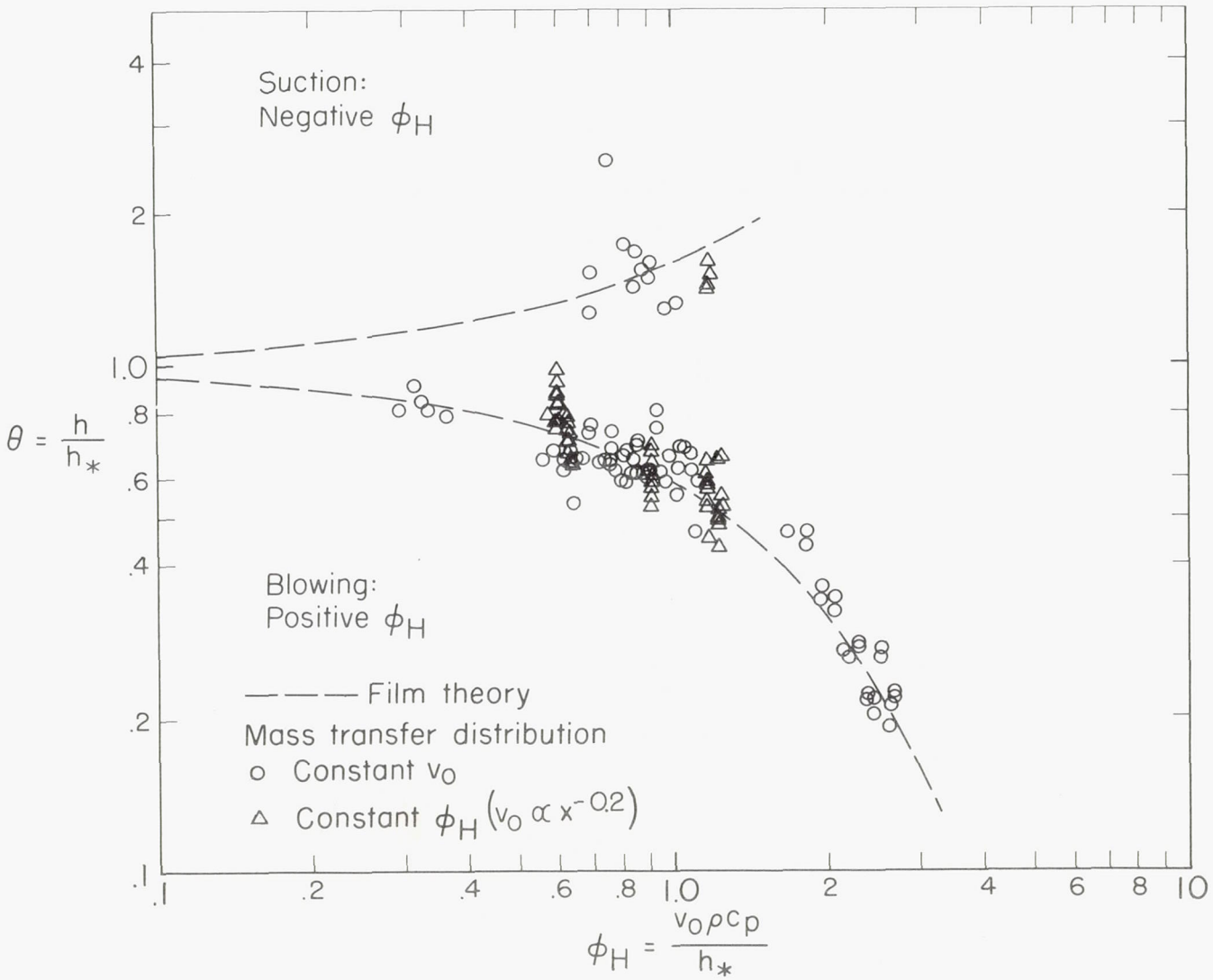

Figure 22.- Turbulent heat transfer coefficients compared with film theory.

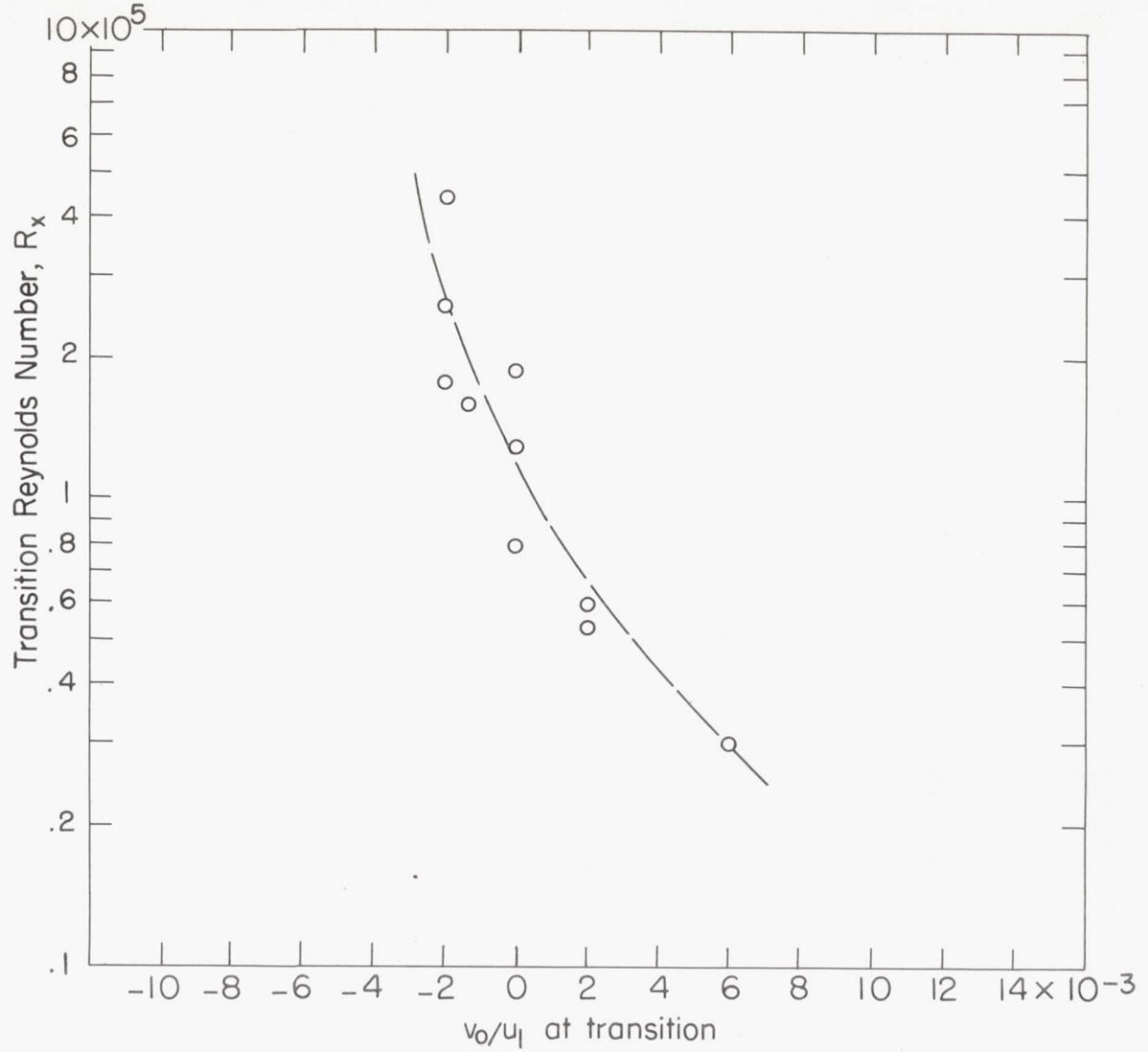

Figure 23.- Variation of transition Reynolds number with mass transfer rate.

NACA-Langley - 7-20-54 - 1000